Deep Divergence: Phylogeny and Age Estimates of Deep-water Chondrichthyes

Etmopterus granulosus, Chile, South East Pacific

Dissertation

zur Erlangung des Doktorgrades

der Fakultät für Biologie

der Ludwig-Maximilians-Universität München

Vorgelegt von

Nicolas Straube, München, 2011

Erklärung:

Diese Dissertation wurde im Sinne von § 12 der Promotionsordnung von Prof. Dr. Gerhard Haszprunar betreut. Ich erkläre hiermit, dass die Dissertation nicht einer anderen Prüfungskommission vorgelegt worden ist und dass ich mich nicht anderweitig einer Doktorprüfung ohne Erfolg unterzogen habe.

Ehrenwörtliche Versicherung:

Ich versichere hiermit ehrenwörtlich, dass die vorgelegte Dissertation von mir selbständig und ohne unerlaubte Hilfe angefertigt wurde.

_____

Nicolas Straube, München, den 09.02.2011

1. Gutachter: Prof. Dr. Gerhard Haszprunar
2. Gutachter: Prof. Dr. Dirk Metzler

Tag der mündlichen Prüfung: 07.06.2011

Content

Article I

STRAUBE N., IGLÉSIAS S. P., SELLOS D. Y., KRIWET J. & SCHLIEWEN U. K. (2010) Molecular Phylogeny and Node Time Estimation of Bioluminescent Lantern Sharks (Elasmobranchii: Etmopteridae). *Molecular Phylogenetics & Evolution*, 56, 905–917. doi:10.1016/j.ympev.2010.04.042

Article II

STRAUBE N., KRIWET J., SCHLIEWEN U. K. (2011) Cryptic diversity and species assignment of large Lantern Sharks of the *Etmopterus spinax* clade from the Southern Hemisphere (Squaliformes, Etmopteridae). *Zoologica Scripta*, 40 (1), 61-75.doi 10.1111/j.1463-6409.2010.00455.x

Article III

STRAUBE N., DUHAMEL G., GASCO N., KRIWET J. AND SCHLIEWEN U.K. (in revision) Description of a new deep-sea Lantern Shark *Etmopterus "viator"* sp. nov. (Squaliformes: Etmopteridae) from the Southern Hemisphere. Submitted to *Cybium*.

Article IV

IGLÉSIAS S. P., **STRAUBE N.** & SELLOS D. Y. (in preparation). Species level molecular phylogeny of Chimaeriformes and age estimates of extant Chimaeriform diversity. Intended to be submitted to *Molecular Phylogenetics & Evolution*.

Supplementary Material

Compact disc including online support material of Articles I & II, full specimen list, conference presentations, and pdf-files of publications.

1 Introduction

1.1 General Introduction

General knowledge on major questions dealing with the evolution and biology on cartilaginous fishes, i.e. sharks, rays, and chimaeras (Chondrichthyes), is relatively poor despite the huge public interest in shark attacks on humans. Chondrichthyes represent the oldest extant gnathostome vertebrate lineage that originated at least as early as the Late Silurian, and since these ancient times makes up a dominant component of earth´s marine ecosystems (Zhu *et al*. 2009). Today however, many cartilaginous fishes are suffering from the huge impacts of expanding commercial fisheries and are partially driven close to extinction. Therefore, scientists studying extant Chondrichthyans are in a rush.

Especially deep-water Chondrichthyes are suspected to be highly vulnerable to commercial deep-sea fisheries due to their extreme longevity, slow growth rate, late maturation, and small litter sizes (Forrest & Walters 2009, IUCN Red List 2010). Assessment of species-specific monitoring and management strategies is difficult, as fisheries and conservation efforts are usually focused on commercially targeted, valuable, and productive teleost fishes (Bonfil 1994, Devine *et al*. 2006, Forrest & Walters 2009). Many deep-water cartilaginous fishes are taken as by-catch, which is discarded in most cases before landing or species are landed under insufficient identification names such as “black shark” (Kyne & Simpfendorfer 2007). This vernacular name comprises species of at least four elasmobranch families (Hudson & Knuckey 2007). It has been suggested that 50 % of the world's catch of Chondrichthyans is taken as by-catch with an unknown number of unrecorded catch rates. Kyne & Simpfendorfer (2007) calculated that continuously increasing global deep-water Chondrichthyan production rose from 18245 tons in 1950 to 30304 tons in 2004. Uncertain taxonomic backgrounds aggravate the problem of insufficient landing information of deep-water Chondrichthyes, which is soundly demonstrated in Iglésias *et al*. (2009).

The aforementioned situation reflects difficulties of extant deep-sea cartilaginous fishes, but very little is known on phylogenetics and evolution, distribution and life history as well as population structure of most deep-water Chondrichthyans in general. Therefore, the main focus of this study is one of the largest deep-water shark families, the Lantern Sharks (Etmopteridae). The family comprises luminescent sharks of the order Squaliformes (Dogfish Sharks), which are not directly targeted by commercial fisheries, but are a significant by-catch component of deep-sea fisheries (Clarke *et al*. 2005, Compagno *et al*. 2005, Jakobsdottir 2001, Kyne & Simpfendorfer 2007, Wetherbee 1996, 2000). Although Etmopterids represent the largest family of Squaliformes, it is one of the least studied among the order, probably due to the lack of commercial interest. Despite being caught “only” as by-catch, benthic and bentho-pelagic Etmopterids are likely strongly affected by deep-sea fisheries (Forrest & Walters 2009; Wetherbee 1996).

Lantern Sharks are a highly diverse family with at least 43 species in five genera, i.e. *Trigonognathus*, *Aculeola*, *Centroscyllium*, *Miroscyllium*, and speciose *Etmopterus* (Compagno *et al.* 2005, Schaaf da Silva & Ebert 2006). The family includes the smallest known sharks, *E. perryi* and *E. carteri*, which mature at 16 to 19 cm total length. Even the largest member *Centroscyllium fabricii* reaches a total length of 107 cm only. Members of the family are distributed panoceanic at continental shelves, seamounts, and insular slopes. The average depth range of most species is 200 to 1500 meters (Compagno *et al*. 2005). Lantern Sharks are more or less densely covered with specific hook-like or conical dermal denticles. Some species had been known only from few specimens as e.g. *Trigonognathus* and *Miroscyllium*, but increased deep-sea fisheries yielded additional specimens of some rare species as well as from several undescribed species, highlighting both, the diversity and the vulnerability of the family. Etmopterids are long living and slowly reproducing ovoviviparous sharks, which give birth to only 6 to 14 pups per litter (Compagno *et al*. 2005).

Most detailed studies published to this point concentrate on a single Atlantic and Mediterranean species, *Etmopterus spinax* (Claes & Mallefet 2008, 2009a, 2009b, 2010a, 2010b, 2010c; Coelho & Erzini 2008a, 2008b; Klimpel *et al*. 2003; Neiva *et al*. 2006) analyzing its ecology and ability to emit light via photophores. Bioluminescence is a wide-spread phenomenon among inhabitants of the subphotic zone, but its occurrence is limited among sharks to only two Squaliform families, the Dalatiidae and Etmopteridae. The function and evolution of shark luminescence is still poorly understood. Photophores of Etmopterids are concentrated on the dark ventral region and on more or less prominent and often species specific flank and tail markings. Claes and Mallefet (2008) suggest a function of camouflage by counter-illumination for the numerous ventral photophores in *E. spinax*. Further studies suggest the flank and tail markings to function for intraspecific signaling i.e. as schooling aid and/ or for cooperative hunting strategies (Reif 1985; Claes & Mallefet 2009a, 2010a, 2010b, 2010c).

Generally, Etmopterid genera are characterized and diagnosed by specific dentitions. Dentition types in Etmopterids vary largely. *Etmopterus* and juvenile *Miroscyllium sheikoi* show a “cutting-clutching type” dentition, whereas the one of *Centroscyllium*, *Aculeola*, and adult *Miroscyllium sheikoi* is of the “clutching type”. The “tearing type” is restricted to *Trigonognathus* (Adnet *et al*. 2006). These unique types of dentitions also allow identification of extinct *Etmopteridae* to genus level but provide little or often ambiguous information on species level differentiation due to mostly unexplored ontogenetic and sexual dimorphisms (Straube *et al*. 2008). Consequently, identification, classification, and phylogenetics of the most speciose Lantern Shark genus *Etmopterus* (approx. 34 species; Compagno *et al*. 2005; Schaaf da Silva & Ebert 2006) are based mainly on the shape of

bioluminescent flank markings and the arrangement and morphology of dermal denticles (e.g. Compagno *et al*. 2005; Last *et al*. 2002; Schaaf da Silva & Ebert 2006; Shirai & Nakaya 1990a).

Several species groups within the genus *Etmopterus* had been postulated based on external morphological synapomorphies: the "*Etmopterus lucifer* group" (Yamakawa *et al*. 1986), the "*Etmopterus pusillus* group" (Shirai & Tachikawa 1993), and the "*Etmopterus splendidus* group" (Last *et al*. 2002).

The monotypic etmopterid genera *Trigonognathus*, *Miroscyllium* and *Aculeola* each display genus-specific morphological features, such as highly protrudable jaws armed with characteristically shaped, single-cusped teeth (*Trigonognathus*), small and slender erect teeth in both jaws (*Aculeola*), or a combination of a "cutting-clutching type" dentition in sub adults, and a "clutching type" dentition in adults (*Miroscyllium*). *Centroscyllium* includes seven described species with a dignathic homodont dentition, displaying multicuspid teeth in both jaws.

The fossil record of Squaliformes appears to be very good for some stratigraphic stage ages, but in fact is rather incomplete with respect to the full timeframe of squaliform appearances. Ghost-lineages, representing gaps in the fossil record, range from 5.5 to 100 million years (Klug & Kriwet 2010). Articulated fossils of Etmopterids are unknown and fossilized single teeth represent the only direct window of information to their past. Thus, the fossil record of Etmopteridae is comparatively poor and the phylogenetic assignment of extinct species is often difficult. For example, fossils such as *Eoetmopterus*, *Proetmopterus* and *Microetmopterus* have been assigned to Etmopteridae based on their tooth morphology (Müller & Schöllmann 1989, Siverson 1993), but rather show only minor or generalized similarities, which cannot be ranked as unambiguous etmopterid autapomorphies. These species went extinct by the end of the Cretaceous (Adnet *et al*. 2006) and seem to have occurred in shallow waters compared to extant Etmopterids, which may imply that extant forms have adapted to deep-water biota only along with or after the C/T boundary mass extinction event 65 Ma ago. The unambiguously oldest fossil teeth of Etmopteridae are known from the Eocene (Lutetian 48.6 – 40.4 Ma) and strongly resemble those of extant species (Adnet 2006, Adnet *et al*. 2008, Cappetta & Adnet 2001, Cigala 1986, Ledoux 1972).

Not only the lack of articulated fossils, but also the low density of phylogenetically informative morphological characters has prevented a detailed phylogenetic investigation of the family. Additional practical limitations have arisen due the scarcity of specimens available, which has rendered sampling efforts extremely difficult for some key taxa, as for example the availability of the Viper Dogfish *Trigonognathus kabeyai*.

First efforts to understand the intrarelationships of Etmopteridae were carried out by Shirai and Nakaya (1990b) based on 15 morphological characters of 14 species representing four genera (Fig.1). They established a new genus *Miroscyllium* for *Centroscyllium sheikoi* based on morphological

characters that are exhibited by both genera, *Etmopterus* and *Centroscyllium*. The sample size was increased to 19 described species in Shirai's Squalean phylogeny (1992) also including *Trigonognathus*. This latter study confirmed the monophyly of the four analyzed etmopterid genera within Squaliformes as previously suggested by Compagno (1973, 1984) and Cadenat and Blache (1981) and placed *Trigonognathus* as sister to *Aculeola* and *Centroscyllium*. Although being an important progress, further intragroup relationships, especially with regard to the speciose genus *Etmopterus* could not be resolved and re-examinations of Shirai's dataset (1992) by Carvalho and Maisey (1996) and Adnet and Cappetta (2001) led to different results (Adnet *et al*. 2006). Therefore, this study aims to apply modern molecular techniques to a new and extensive sampling of Etmopteridae to analyse taxonomy and evolution in detail.

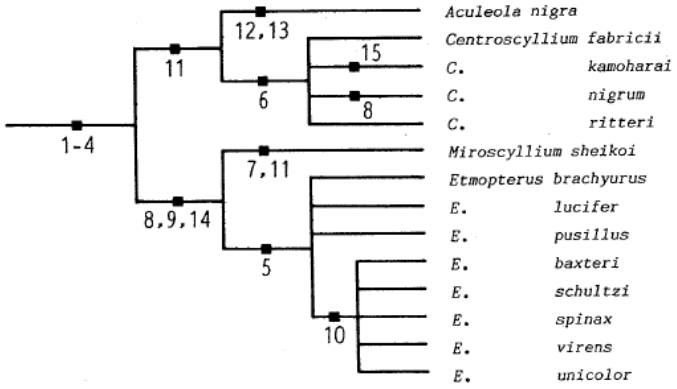

Figure 1: Proposed intrarelationships of Etmopterinae in Shirai and Nakaya (1990b). Numbers below branches indicate morphological apomorphies.

The second part of this study deals with the phylogenetic relationships of the sister group of all Neoselachii (i.e. modern sharks and rays), the Chimaeriformes. Mostly deep-sea inhabiting Chimaeriformes share several biological characters with Lantern Sharks and are exposed to the same human impacts. The Chondrichthyan subclass Holocephali comprises the extant Chimaeriformes as well as a number of extinct taxa. Interestingly, the extant Holocephalan diversity does not reflect a bit of their largest diversity in earth's history. Holocephali are already known from the Silurian (Benton & Donoghue 2007, Inoue *et al*. 2010) and the largest diversity is noted for the Carboniferous (Helfman *et al*. 2009). It appears that the Permian mass extinction event erased large parts of the Holocephalan diversity and surviving species may have adapted to the deep-sea (Grogan & Lund 2004). Holocephalan fossils dated back to 375 Ma already share distinct morphological characters with living forms (Venkatesh *et al*. 2007). This implies that Chimaeriformes are in fact living fossils with an evolutionary history of an estimated 420 Ma representing one of the oldest vertebrate lineages.

Chimaeriformes constitute a rather small group of marine holocephalan vertebrates and are sister to sharks and rays (Neoselachii). The sister group relationship of Neoselachians and Chimaeriforms is undisputed and supported by the most recent molecular phylogenies based on total

mitochondrial genomes (Inoue *et al*. 2010). Today, Chimaeriformes comprise three families (Callorhynchidae, Rhinochimaeridae, and Chimaeridae) and overall 44 species (Eschmeyer & Fricke 2010). The different species mostly inhabit bathyal ocean regions occurring at continental shelves, seamounts, insular slopes, and are also recorded from abyssal plains (Last & Stevens 2009). They are oviparous and generally feed on benthic crustaceans and molluscs, reaching sizes up to 2 meters in total length.

Monogeneric Callorhynchidae (Elephant Fishes or Plownose Chimaeras) contains three species which are restricted to the Southern Hemisphere. External morphological characteristics include serrated first dorsal fin spines, a heterocercal tail, and, most strikingly, “hoe-shaped” snouts (Last & Stevens 2009). Callorhynchidae is considered to be the most plesiomorphic family of Chimaeroids (Didier 1995). Members of the family Rhinochimaeridae (Spookfishes, Rabbitfishes, or Longnose Chimaeras) are also characterized by their snout morphology, which is broadly elongated. Spookfishes comprise three genera (*Rhinochimaera*, *Harriotta*, and *Neoharriotta*) and currently eight species occurring panoceanic in the deep-sea of temperate and tropical waters. The Chimaeridae (Shortnose Chimaeras or Ratfishes) display the largest diversity of Chimaeriforms. The family contains two genera only, *Chimaera* and *Hydrolagus*, with an estimated diversity of at least 35 species (Eschmeyer & Fricke 2010). Contrasting the other Chimaeriform families, Chimaeridae are characterized by short snouts, which are rounded or feebly pointed (Last & Stevens 2009). The number of species from this family has recently increased (Didier 2008, Didier *et al*.2008, Kemper *et al*. 2010a, 2010b, Luchetti *et al*. in press) due to expanding deep-sea fisheries surfacing rare and unknown species. Similar to Etmopteridae, some Chimaeriforms are a by-catch component, leading to significant catch-rate reduction as e.g. in North Atlantic *Chimaera monstrosa*, which today is categorized as ”near threatened” in the IUCN Red List of Threatened Species (2010).

1.2 Aims of this study

Due to the large and continuously increasing species number of deep-water Chondrichthyans in recent years as well as a large number of unresolved questions related to their taxonomy and evolution, this study applies DNA based molecular techniques and morphological analyses to material, that is new and based on an extensive worldwide sampling of Etmopterids and Chimaeroids.

The major aim of the first part of this study is the establishment of a robust molecular phylogeny of Etmopteridae. To infer phylogenetic interrelationships, a multilocus DNA dataset was analyzed to identify the sister-group of Etmopteridae among Squaliformes, to test for the monophyly of Etmopteridae, to test for the independent development of bioluminescence within Squaliformes, and to test for the monophyly of each of the two polytypic etmopterid genera *Etmopterus* and *Centroscyllium*. The recovered molecular phylogeny was compared to results based on morphological

analyses to identify candidate morphological autapomorphies for Etmopteridae, etmopterid genera, and intrageneric species clades. The sequence data were further used for estimating the age of Etmopteridae. Relaxed molecular clock approaches are applied to test for a Lower Eocene origin of Etmopteridae as indicated by the fossil record and to analyze sequential versus rapid speciation in the course of the etmopterid radiation. A possible correlation of estimated etmopterid diversification ages is discussed with major events in earth's history.

Further, a population genetic approach was applied to an extended sample of species from a particular difficult *Etmopterus* sub clade, which phylogeny could not be resolved with the sequence dataset. This study attempts to distinguish between populations of single species and cryptic species within this clade. Hitherto, this is the first approach to identify population structure in Etmopterids. The data are further compared to results from sequences of the "barcode" gene COI to test COI for its species-specificity in *Etmopterus*.

The final part of the present work on Etmopterids deals with a previously unrecognized *Etmopterus* species, which is identified with all applied molecular approaches. Specimens of this cryptic species were analyzed morphologically to verify its species status from the morphological perspective and in order to formally describe it as a new species.

In its second part, this thesis aims to extend the etmopterid phylogenetic study to another deep-water Elasmobranch group, i.e. the comparative analysis of a comprehensive Chimaeriform molecular dataset. A previous Chimaeriform dataset focused on the phylogenetic position and evolution of Chimaeriformes in the overall vertebrate phylogeny (Inoue *et al*. 2010). Consequently, the study presented here was designed to further resolve the phylogeny of extant Holocephalans, focusing on genus and species level by analyzing a larger species sampling compared to Inoue *et al*.'s studies (2010). Further, the monophyly of the two most speciose Chimaeroid genera *Hydrolagus* and *Chimaera* is specifically tested. A refined node age estimate for major extant Chimaeriform lineages is provided with respect to the hypothesis that the extant diversity represents surviving relicts of the Permian mass extinction event. Finally, this work compares molecular results with those of a morphological cladistics study by Didier (1995) characterizing the different families, genera, and species of Chimaeriformes on the basis of putative morphological synapomorphies.

2 Sampling

Global sampling efforts to recover fresh Lantern Shark material were extremely difficult due to the scarcity and endemism of several key taxa, the overall difficult-to-sample hostile deep-sea environment of Etmopterids, and the different conditions and logistics in visited countries. Tissue samples of all shark species included in the analyses were obtained from museum tissue-collections or were recently collected during deep-sea commercial fisheries, or during fishery-monitoring

programs. The study includes for the first time the very rare *Trigonognathus kabeyai* (Viper Dogfish), the Hooktooth Dogfish *Aculeola nigra* (known only from the Middle East Pacific) as well as the scarce *Miroscyllium sheikoi*, known only from few specimens off the coasts of Taiwan and Okinawa, for molecular analyses. To accomplish that sampling, the initial groundwork for this study was predominantly devoted to accumulating samples of Squaliform sharks (focusing on Etmopterids) from different parts of the world, which required travelling to Japan, France, New Zealand, Chile, and South Africa, i.e. all Squaliform diversity hotspots. Parallel efforts focused on contacting universities, fisheries institutes, and natural history collections worldwide, to request tissue samples (Fig. 2). Further, marine ichthyology conferences in Europe and the USA were attended, not only to present first results, but also to expand the list of colleagues willing to share samples.

All specimens collected overseas were deposited in the Bavarian State Collection of Zoology (ZSM) as reference specimens, resulting in more than 200 additional shark individuals in the ichthyological collection. Overall, 389 tissue samples with extracted DNA were deposited in the ZSM's DNA Bank (www.dnabank-network.com/ dnabank@zsm.mwn.de) (see Support CD-Rom).

The sampling of Chimaeriformes was conducted by S. P. Iglésias employed at the Museum of Natural History, Paris, France. Sampling areas for chimaeroids mostly cover the North West Atlantic. Further sampling was accomplished in the Indian Ocean and in the North and South West Pacific. The dataset was enriched with hitherto missing taxa by adding sequences deposited in Genbank.

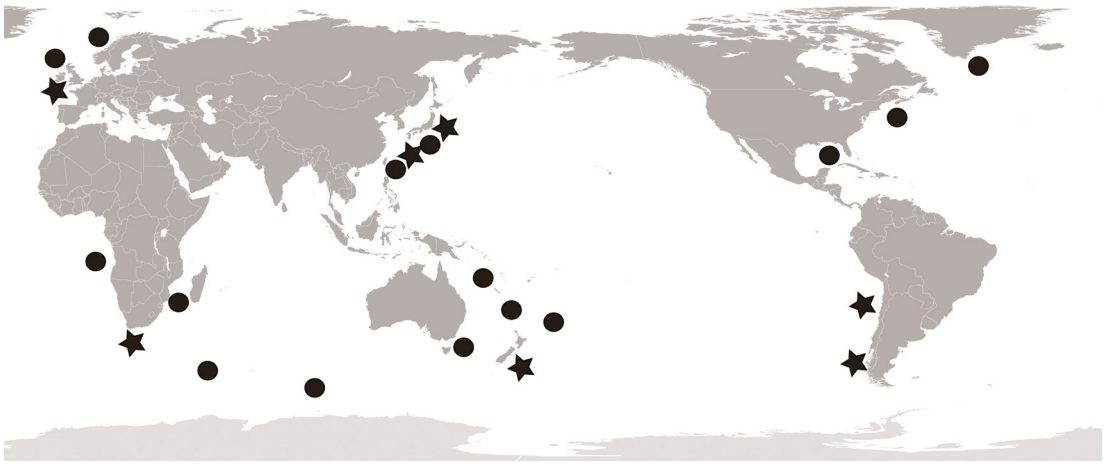

Figure 2: Sampling sites for the study on Etmopteridae. Stars mark visited sampling sites; filled circles mark locations of provided samples.

3 Material & Methods

3.1 Material & Methods Article I

STRAUBE N., IGLÉSIAS S. P., SELLOS D. Y., KRIWET J. & SCHLIEWEN U. K. (2010) Molecular Phylogeny and Node Time Estimation of Bioluminescent Lantern Sharks (Elasmobranchii: Etmopteridae). *Molecular Phylogenetics & Evolution*, 56, 905–917. doi:10.1016/j.ympev.2010.04.042.

For phylogenetic analyses of Etmopteridae, the sampling covers 26 of the extant 43 Etmopterid species plus 13 samples with no, or preliminary identification (highlighting taxonomic uncertainties). The sampling includes all five genera traditionally assigned to Etmopteridae, and all previously morphologically identified species groups within *Etmopterus*. In addition, representatives of the remaining five squaliform families Centrophoridae, Oxynotidae, Somniosidae, Dalatiidae, and Squalidae as well as Echinorhinidae were included in the analyses. *Odontaspis ferox* (Lamnidae), *Apristurus longicephalus* (Pentanchidae) and *Chimaera* sp. (Chimaeridae) were chosen as Chondrichthyan outgroups. Total genomic DNA was extracted from all samples. Thereafter, five loci were amplified using PCR techniques following the protocol of Iglésias *et al*. (2005). The final dataset comprised sequences of a portion of the nuclear RAG1 gene (1454 bp), portion of the mitochondrial gene cytochrome oxidase I (COI, 655 bp), partial $tRNA_{Phe}$, the full 12S rRNA, and partial 16S rRNA including the Valine tRNA (2606 bp when aligned). Cycle sequencing was performed at the sequencing service of the Department of Biology of the Ludwig-Maximilians-University (Munich). For a list of primers used see Table 1 in Straube *et al*. (2010). The combined dataset provides sufficient phylogenetic signals for both, ancient and more recent divergence in elasmobranchs as demonstrated in Iglésias *et al*. (2005), Maisey *et al*. (2004), Naylor *et al*. (2005), Ward *et al*. (2005, 2007), and White *et al*. (2008).

Sequences were edited with BioEdit v.7.0.9 (Hall 1999) and aligned with muscle v.3.6 (Edgar 2004). Non-coding mtDNA regions ($tRNA_{Phe}$, 12S rRNA, 16S rRNA, and $tRNA_{VAL}$) were checked for ambiguous alignment positions using Aliscore v.2.0 (Misof & Misof 2009). A check of RAG1 and COI sequences against nuclear pseudogene status was done by searching for stop codons in the translation of sequences into amino acids. Phylogenetic analyses were conducted on the smallest resulting sequenced fragments homologous to all taxa, resulting in an overall sequence size of 4685 bp per specimen when sequences of single loci were combined. Subsequent phylogenetic analyses were performed employing Maximum Parsimony using PAUP* (Swofford 2003), Maximum Likelihood (ML) using RaXML v.7.0.3 (Stamatakis 2006), and Bayesian phylogenetic inferences (BI) using MRBAYES v.3.1.2 (Huelsenbeck & Ronquist 2001). Testing for suitable substitution models and corresponding data partition, a Bayes Factor test was performed using MRBAYES and Tracer 1.4 (http://beast.bio.ed.ac.uk). Resulting data partitioning was applied to ML and BI analyses as well as node age reconstruction.

For estimating node ages, softwares BEAST v.1.4.7 (Bayesian approach, Drummond & Rambaut 2007) and r8s (Penalized Likelihood approach, Sanderson 2002, 2003) were applied to the dataset. Both methods make use of a relaxed molecular clock approach, which can be applied to several gene regions, allowing for different substitution rates. Further, multiple fossil calibration points can be implemented, which reduces errors in calibration (Renner 2005). In both approaches, the same five

calibration points and the Bayesian majority consensus tree from previous phylogenetic analyses were used as priors for calculating chronograms (Table 2, Straube *et al*. 2010). The resulting chronograms were now implemented as starting trees in further BEAST analyses under the assumption of an exponential prior, explaining the data more efficiently, because absolute dates can hardly be given in terms of calibrations using fossils. In contrast, the exponential prior assumes the taxon to be present some time before the occurrence of the fossil, which most probably does not represent the first occurrence, but rather its minimum age. Zero-offsets adopted node ages reconstructed from the pre-dating analyses. Exponential means were chosen to cover the age of stratigraphic ranges of fossil findings of used calibration points. Here, two identical runs were performed lasting 30 million MCMC generations each, which were subsequently combined. The attained r8s chronogram was implemented for reassessing results from both, Penalized Likelihood and Bayesian node age reconstructions (Hardman & Hardman 2008). Finally, analyses were re-run differing in applied calibration points to obtain a measure for the influence of calibration points on results. Further runs including mt- or nDNA-sequence data only were performed to test for cytonuclear discordance within the full dataset and to get a measure of the phylogenetic signal provided by the different loci constituting the concatenated dataset.

3.1.1 Contribution of authors Article I:

N. Straube designed and conducted the main part of sampling and laboratory work, all phylogenetic analyses, node age reconstructions, figure development, provision of sequences to Genbank, and wrote the manuscript. S. Iglésias collected samples of 23 of 75 samples used for the study and provided sequences of those 23 samples, which were gathered by D. Y. Sellos in the laboratory of the Marine Station of the Museum of Natural History, Concarneau, France. The cooperation with S. Iglésias was crucial for the enrichment of the dataset with sequences of geographically restricted species (New Caledonia). J. Kriwet financed the study through the DFG grant KR 2307-4, provided literature for calibration points, and gave useful comments on the manuscript. UK Schliewen co-designed and supervised the laboratory work and phylogenetic analyses, corrected the manuscript and financed the laboratory work through the DFG grant SCHL 567-3.

3.2 Material & Methods Article II

STRAUBE N., KRIWET J., SCHLIEWEN U. K. (2011) Cryptic diversity and species assignment of large Lantern Sharks of the *Etmopterus spinax* clade from the Southern Hemisphere (Squaliformes, Etmopteridae). *Zoologica Scripta*, 40 (1), 61-75. doi 10.1111/j.1463-6409.2010.00455.x.

As results from Article I recovered a monophyletic clade, which was insufficiently resolved, a population genetic approach was applied to an enhanced sample of this clade. It was newly defined

as "*E. spinax* clade" in Straube *et al*. 2010 (Clade II, Fig. 3) and comprises a number of closely related Lantern Shark species, displaying a highly similar morphology. This phenomenon already resulted in several taxonomic studies dealing with synonymization of species (e.g. Yano 1997, Tachikawa *et al*. 1989), which were partially not accepted in more recent literature (e.g. Compagno *et al*. 2005, Last & Stevens 2009) resulting in uncertain validity of species. Previous phylogenetic analyses could not clarify, if specimens assigned to *E. granulosus*, *E. baxteri*, *E.* cf. *baxteri*, and *E*. cf. *granulosus* are cryptic species or different populations of a single species, or a combination both. As an approach to further analyze the cryptic diversity and population structure among the "*E. spinax* clade", fragment length polymorphisms were amplified (AFLPs, Vos *et al*. 1995, Meudt & Clark 2007) as a basis for model based clustering methods and assignment of individuals to genotypic clusters.

DNA extracts were tested for suitability for AFLP analyses. Methods for AFLP genotyping (restriction / ligation / primary amplification) follow Herder *et al*. (2008). Twenty restrictive primer combinations were amplified, based on the core sequences provided in Vos *et al*. (1995). Capillary electrophoresis was conducted on an ABI 3130 Genetic Analyzer with an internal size standard (ROX 500 XL) at the ZSM laboratories. Automated peak scoring (binning) performed in the Genemapper® Software v4.0 enabled exportation of binary character matrices from each primer combination. Each single matrix was further corrected following Albertson *et al*. (1999). The final matrix comprised 2655 loci. Thereafter, several analyzing methods were applied to the AFLP dataset. A neighbor-joining network using the software Splitstree4 v.4.10 (Huson & Bryant 2006) was computed. PAST v1.94b (Hammer *et al*. 2001) allowed visual inspection of principal components after principal component analysis (PCA). For phylogenetic inferences based on neighbor-joining distances of AFLP data the software package TreeCon v1.3b (Van de Peer 1994) was used with subsequent bootstrapping comprising 1000 replicates.

Accepting *E. granulosus* as synonym to New Zealand *E. baxteri* based on previous results, the software package Arlequin v3.5 (Excoffier *et al*. 2005) was employed to conduct analyses of molecular variance (AMOVA) to evaluate the amount of population genetic structure of *E. granulosus* between the two sampling locations New Zealand and Chile and to estimate pairwise F_{ST} values. Further, AFLP data of *E. granulosus* was analyzed with BAYESCAN (Foll & Gaggiotti 2008) to identify loci with strong impact on population structuring.

STRUCTURE v2.2.3 (Pritchard *et al*. 2000, Falush *et al*. 2003) was used to calculate model based genotypic clusters and to assign individuals to genotypic clusters (populations). To detect population structure according to a hierarchical model, the methodology of Evanno *et al*. (2005) was followed. A second analysis focused on a smaller dataset including only specimens assigned to *E. granulosus* from Chile and *E. baxteri* from New Zealand, as no population structure was detected between the two sampling locations within the full dataset (as e.g. in Warnock *et al*. 2009). The smaller dataset

removes part of the variance of the full dataset, which may reveal subtle population structure. All STRUCTURE runs were repeated twice, ex- and including prior location information as informative prior settings (Hubisz *et al*. 2009).

Further, the data were used to test, if *E. granulosus* specimens previously assigned to *E. baxteri,* sampled off South Africa, and *E. princeps* show mixed ancestry. All three species are morphologically highly similar and have a potential Northern Hemisphere origin (Fig. 4, Straube *et al*. 2011). Therefore, STRUCTURE v2.3.2 *beta* was applied to analyze patterns of mixed ancestry among individuals of these three groups. The option allowing for implementation of prior information on population origin and a defined number of past generations (GENSBACK subpackage) were used. Here, the implemented model translates into the assumption that the largest part of individuals assigned to *E. baxteri* from South Africa is genotypically differentiable and that a small portion of individuals may have mixed ancestry from the species specific genotypes of *E. granulosus* and/ or *E. princeps* (Falush *et al*. 2007).

For comparing results from AFLP analyses, COI sequences from all samples used for AFLP analyses were attained. COI sequencing methodically follow 3.1. The software NETWORK v4.5.1.6 (fluxus-engineering.com) was applied to the smallest resulting sequenced fragments homologous to all taxa. The final alignment had 659 bp and was used as the basis to reconstruct most parsimonious phylogenetic networks (Bandelt *et al*. 1999). The network was calculated using the median joining algorithm (allowing for multistate data) under default settings. Pairwise Φ_{ST} values were computed in Arlequin including two separate groupings to explore differentiation of *E. granulosus* from Chile and New Zealand.

3.2.1 Contribution of authors Article II:

N. Straube conducted all sampling, laboratory work, phylo-and populationgenetic analyses, figure development, provision of sequences to Genbank, and wrote the manuscript. J. Kriwet financed the study through the DFG grant KR 2307-4 and provided manuscript corrections. UK Schliewen co-designed and supervised the laboratory work and all analyzing approaches, corrected the manuscript and financed the laboratory work through the DFG grant SCHL 567-3.

3.3 Material & Methods Article III

STRAUBE N., DUHAMEL G., GASCO N., KRIWET J. AND SCHLIEWEN U.K. (in revision) Description of a new deep-sea Lantern Shark *Etmopterus "viator"* sp. nov. (Squaliformes: Etmopteridae) from the Southern Hemisphere. Submitted to *Cybium*.

The description of the new species in Article III focuses on specimens included in previous analyses of Articles I & II, namely *Etmopterus* cf. *granulosus*. The species firstly appeared in literature in Duhamel *et al*. (2005) as *E.* cf. *granulosus* due to its similar morphological appearance to *E.*

granulosus. Genetic analyses show that it is indeed not *E. granulosus*, but a sister to a species mentioned in the literature as *Etmopterus* sp. B (Last & Stevens 1994), which today is accepted as a synonym to *E. unicolor* (Yano 1997). In all previous analyses, *E*. cf. *granulosus* forms a distinct clade or cluster. However, this species was assumed to be a cryptic species, which was unrecognized so far. A multidisciplinary approach comprising molecular and morphological data was applied to specimens of *E*. cf. *granulosus*, which identified several characters separating this cryptic species from its congeners in the Southern Hemisphere.

Specimens of the new species were collected around the Kerguelen Plateau in the years 2002, 2003, 2004, and 2007 during cruises of French commercial fishing vessels in the Southern Indian Ocean. A total number of 63 specimens from the Kerguelen Plateau were analyzed. In 2009, 24 tissue samples for "DNA-barcoding" were available enriching the sampling used in previous analyses in Straube *et al*. (2010, 2011). Morphological analyses dealt with the classical characters used in literature for identifying *Etmopterus* species, i.e. the morphology and arrangement of dermal denticles, morphometric and meristic analyses as well as "barcoding" as a very recent approach. Four ratios discussed in Kotlyar (1990) and Yano (1997) as potential species specific characters were used to identify differences and species specific characters: head length vs. interdorsal distance (HL/ID), distance of the snout tip to the first dorsal fin spine insertion vs. the interdorsal distance (PFDL/ ID), head length vs. the interorbital distance (HL/ IOD), and total length vs. the height of the first dorsal fin (TL/HFDF). After testing for homogeneity of error variances, a multi-factorial ANOVA was conducted. To test for significant differentiation of the new species with respect to three ratios, a LSD post-hoc test was performed. Statistical analyses were conducted with the software package SPSS v. 11.5.1 and visualization of resulting box-plots was accomplished in PAST v1.94b (Hammer *et al.* 2001).

The total number of vertebrae was analyzed as a frequently used meristic character in sharks. X-ray images of 38 specimens of the new species and of two paratypes of *E. litvinovi* (ZMH-24994; ZMH-24993) were available. Data were compared with published values for *E. granulosus* and *E.* sp. B (Yano 1997).

Shape, density, and arrangement of dermal denticles of the new species, *E. granulosus* and *E*. sp. B were investigated using a defined area below the 2nd dorsal fin with a dissecting microscope. For representative visualization of dermal denticles, a LEO 1430 VP scanning electron microscope (SEM) was used. To obtain a quantitative correlate for differences in dermal denticle morphology, the length of the dorsal part of dermal denticles below the 2nd dorsal fin was measured and statistically analyzed. Finally, the number of denticles in 3 mm^2 was counted by applying a 3 mm side-length frame to the SEM images of two specimens each.

For DNA barcoding, all available samples of members of the *E. spinax* clade (Clade II, Fig. 3) were used, following methodically chapter 3.1 concerning DNA extraction and further analyses. In addition, five COI sequences of *E*. cf. *unicolor* (Indonesia) and two COI sequences of *E. granulosus* (Tasman Sea) were included in the preliminary alignment downloaded from Genbank. A most parsimonious network was re-calculated from sequences as in Article II with the inclusion of additional samples of the new species using the software NETWORK v4.5.1.6 (Bandelt *et al.* 1999; fluxus-engineering.com).

3.3.1 Contribution of authors Article III:

N. Straube conducted all measurements and subsequent morphometrics, all laboratory work, phylogenetic analyses, SEM imaging and subsequent statistical analyses, figure development, provision of sequences to Genbank, and wrote the manuscript. Samples of the new species, images of the holotype, and x-ray images were provided by G. Duhamel. N. Gasco provided all ecological and biological data collected during his work as a fisheries observer at the Kerguelen Plateau. J. Kriwet partially financed the study through the DFG grant KR 2307-4 and provided manuscript corrections. UK Schliewen co-designed and supervised the study, corrected the manuscript and financed the laboratory work through DFG grant SCHL 567-3. The study received further support from the SYNTHESYS Project http://www.synthesys.info, which is financed by European Community Research Infrastructure Action under the FP6 "Structuring the European Research Area Programme."

3.4 Material & Methods Article IV

IGLÉSIAS S. P., **STRAUBE N.** & SELLOS D. Y. (in preparation). Species level molecular phylogeny of Chimaeriformes and age estimates of extant Chimaeriform diversity. Submission planned to *Molecular Phylogenetics & Evolution*.

The sampling covers 19 of the extant 44 described species and additionally include four samples with no species-level identification. All three Chimaeriform families Callorhynchidae, Rhinochimaeridae, and Chimaeridae are represented in the dataset. Outgroup selection comprises four representatives of Neoselachian orders, i.e. Lamniformes, Carcharhiniformes, Squaliformes, and Rajiformes. Total genomic DNA was extracted from fin clips and muscle tissues. Five mtDNA loci (portion of cytochrome oxidase I (COI, 655 bp), partial $tRNA_{Phe}$, the full 12S rRNA and partial 16S rRNA including the Valine tRNA (2606 bp)) were amplified using PCR technique following Iglésias *et al*. (2005) and subsequently sequenced on an ABI 3130 Genetic Analyzer (PE Applied Biosystems, Foster City, CA, USA) in the laboratory of the Marine Station of Concarneau, France. For amplifying loci, primers were used as in Iglésias *et al*. (2005) and Straube *et al*. (2010). Again, COI sequences were checked against nuclear pseudogene status by translating sequences into amino acids and scanned for stop codons. Aliscore v.2.0 was applied to the aligned non-coding loci, to identify

ambiguous alignment positions. The final concatenated alignment comprised 3413 characters. MRBAYES and Tracer were used to perform a Bayes Factor Test (BFT) to rule out unsuitable substitution models and data partitioning. Phylogenies were attained by applying three different tree reconstruction approaches to the dataset, i.e. ML using RaXML, BI using MRBAYES, and neighbor-joining analyses (NJ) using Treecon. Bootstrapping with 1000 bootstrap replicates was performed for NJ and ML analyses to attain node support in trees and to compare to posterior probabilities from BI.

Additional analyses were performed on a smaller dataset including sequence information of the rare species *Neoharriotta pinnata* to gather information on the placement of the genus in the overall Chimaeriform phylogeny. The smaller alignment comprised fragments of COI (653 bp) and partial 16S rRNA (559 bp) only, but underwent the same phylogenetic analyzing procedures as the larger dataset of 3413 bp.

The relaxed molecular clock approach was conducted in BEAST and was applied to the larger dataset only, since node-support values for the placement of *N. pinnata* in between Rhinochimaeridae and Chimaeridae was very low in all analyzing approaches. Estimated node ages from Inoue *et al*. (2010) and Straube *et al*. (2010) were used to calibrate the relaxed molecular clock (secondary calibration, Table 2, Article IV). The tree showing best likelihood scores from ML analyses was applied as starting tree in BEAST. As in Straube *et al*. (2010), settings were used to run BEAST under normal distribution prior settings for calibrated node ages. Means and standard deviations were adopted from 95% confidence intervals computed for node ages in Inoue *et al*. (2010) and Straube *et al*. 2010. Thereafter, the resulting chronogram was implemented in a further run as starting tree using exponential prior distributions for calibration points, choosing minimum ages as zero offsets with means covering the error bar ranges adopted from secondary calibration points (Table 2, Article IV). Appropriate run length (30 million MCMC generations) was indicated by suitable ESS values checked in Tracer. Posterior likelihoods were normally distributed.

3.4.1 Contribution of authors Article IV:

This work is a cooperative follow-up project of the Lantern Shark phylogeny with French colleagues Samuel P. Iglésias and Daniel Y. Sellos from the Marine Station Concarneau of the Museum of Natural History, Paris, France. S. Iglésias designed the study, collected all samples, and provided the full mtDNA alignment. N. Straube performed all phylogenetic analyses, node age reconstructions, figure development, and wrote the manuscript. D. Sellos amplified and sequenced all loci at the laboratory of the Marine Station of Concarneau, France.

4 Results & Discussion

4.1 Molecular phylogeny of Etmopteridae

An extensive DNA dataset was compiled to estimate the first molecular phylogeny of Etmopteridae. Phylogenetic inferences yielded consistent and well supported hypotheses. The multilocus dataset was analyzed with Maximum Likelihood (ML), Maximum Parsimony (MP), and Bayesian phylogenetics (BI). All three approaches recovered widely congruent tree topologies with regard to the well-supported monophyly of Squaliformes and Etmopteridae and for major etmopterid intrarelationships. Figure 3 provides an overview of obtained trees on the basis of the Bayesian consensus dendrogram with posterior probabilities and statistical node support from bootstrapping after ML and MP analyses. Most important results are summarized and discussed as follows: With regard to ancient splits within Squaliformes only the basal split of *Squalus* (Squalidae) from the remaining Squaliformes is strongly supported, whereas most relationships within Dalatiidae, Etmopteridae, Somniosidae, Centrophoridae, and Oxynotidae are only weakly or not supported, resulting in para- and polyphyletic higher taxa.

The sister family of Etmopteridae among Squaliformes could not be identified. Within Etmopteridae, nine major clades with strong node support are recovered. The concatenated nDNA and mtDNA dataset reveals *Trigonognathus kabeyai* (clade I, Fig. 3) as sister to *Etmopterus* comprising clades II, III, IV, V, VI, and VII (Fig. 3). Further, the monophyly of the most speciose genus *Etmopterus* is strongly supported. The genus *Etmopterus* is further split into two major sister clades. The first monophylum comprises two clades, the mostly panoceanic temperate *E*. *spinax* clade, previously unrecognized (clade II, Fig. 3), and the *E*. *gracilispinis* clade, also previously unrecognized (clade III, Fig. 3). Clade II represents a quite recently evolved and diverse clade. In contrast to the remaining *Etmopterus* sub clades, this clade comprises several morphologically highly similar species with an unresolved taxonomy. For a detailed re-analyses of the *E. spinax* clade see 4.3. The four species of the *E*. *gracilispinis* clade (clade III, Fig. 3) are confined to the Atlantic Ocean – a pattern of restricted endemism contrasting with the wide distribution range of the *E. spinax* clade. The second major monophylum comprises four clades, including *Miroscyllium sheikoi* (clade IV, Fig. 3), the paraphyletic traditional *Etmopterus lucifer* group, split into clades V and VI (Fig. 3), and the panoceanic *E*. *pusillus* clade (clade VII, Fig. 3). *Miroscyllium sheikoi* (clade IV, Fig. 3) renders the genus *Etmopterus* paraphyletic. The *E*. *lucifer* clade (clades IV, V, and VI, Fig. 3) represents a monophylum which is sister to clade VII. It was named *E. lucifer* clade, because it comprises the most species of the "*E*. *lucifer* species group" as defined by Yamakawa *et al*. (1986).

Centroscyllium (clade VIII, Fig. 3) is identified with strong support as the sister group of *Aculeola* (clade IX, Fig. 3) and forms two geographically characterizable subclades. Clades VIII and IX are basal sister clades to all remaining Etmopterids.

Morphological characters support *Etmopterus* species clades described above, but reveal several conflicts on the higher level etmopterid interrelationships. Seventeen of 27 morphological apomorphies described by Shirai (1992) and some external morphological characteristics used for species identifications are in concordance with the molecular tree topology, i.e. the morphology and arrangement of dermal denticles as well as the shape of flank markings within *Etmopterus*. This allows a preliminary assignment of species, which were not included in the analyses, to define species clades. A summary of morphological characters which are in concordance with results from molecular phylogenetics is given in Table 5 in Straube *et al*. (2010).

Shirai's analyses (1992) reveal *Trigonognathus* to be sister to basal genera *Aculeola* and *Centroscyllium*. The combined dataset conversely identifies *Trigonognathus* well-supported as sister genus to *Etmopterus* whereas the analyses of the nuclear RAG1 data alone support Shirai's hypothesis (Shirai 1992). Morphological evidence does not favor either topology (Adnet *et al*. 2006; Shirai 1992). Apparently, only substantially more nuclear data might reveal, whether alternative topologies favored by data in this study are due to unambiguous cytonuclear discordance or due to insufficient nuclear character sampling.

Molecular analyses further confirm Shirai and Nakaya´s (1990b) and Shirai´s (1992) analysis and place *Aculeola* and *Centroscyllium* as sister taxa to each other and both as basal sister taxa to *Etmopterus*. In contrast to Shirai and Nakaya´s (1990b) and Shirai´s (1992) morphological analysis, results in this study show *Miroscyllium* (clade IV, Fig. 3) to belong to the *E*. *lucifer* clade rendering *Etmopterus* paraphyletic with respect to *Miroscyllium*. Shirai and Nakaya (1990b) established the genus *Miroscyllium* based on the mosaic morphological character set of *Etmopterus* and *Centroscyllium*. However, the adult dentition of *Miroscyllium* is interpretable as a *Centroscyllium*-convergent dentition secondarily derived from an *Etmopterus* dentition since sub adult specimens of *M*. *sheikoi* show a dentition similar to that of *Etmopterus*. This is ontogenetically not necessarily contradicting a placement of *M. sheikoi* within *Etmopterus*. Further, monophyly of *Etmopterus* and *Miroscyllium* is morphologically evidenced by an apparently synapomorphic short eye-stalk (Shirai 1992). Consequently, *Miroscyllium sheikoi* should be transferred to *Etmopterus*.

In summary, this study displays a higher resolution of phylogenetic interrelationships of Etmopteridae and reveals so far unrecognized results, i.e. the morphologically characterizable subclades within *Etmopterus*, which allow fast assignment of species to subclades. Therefore, results represent a disinct progress in understanding the etmopterid taxonomy, but were not sufficient to attain new insights into the overall Squaliform phylogeny.

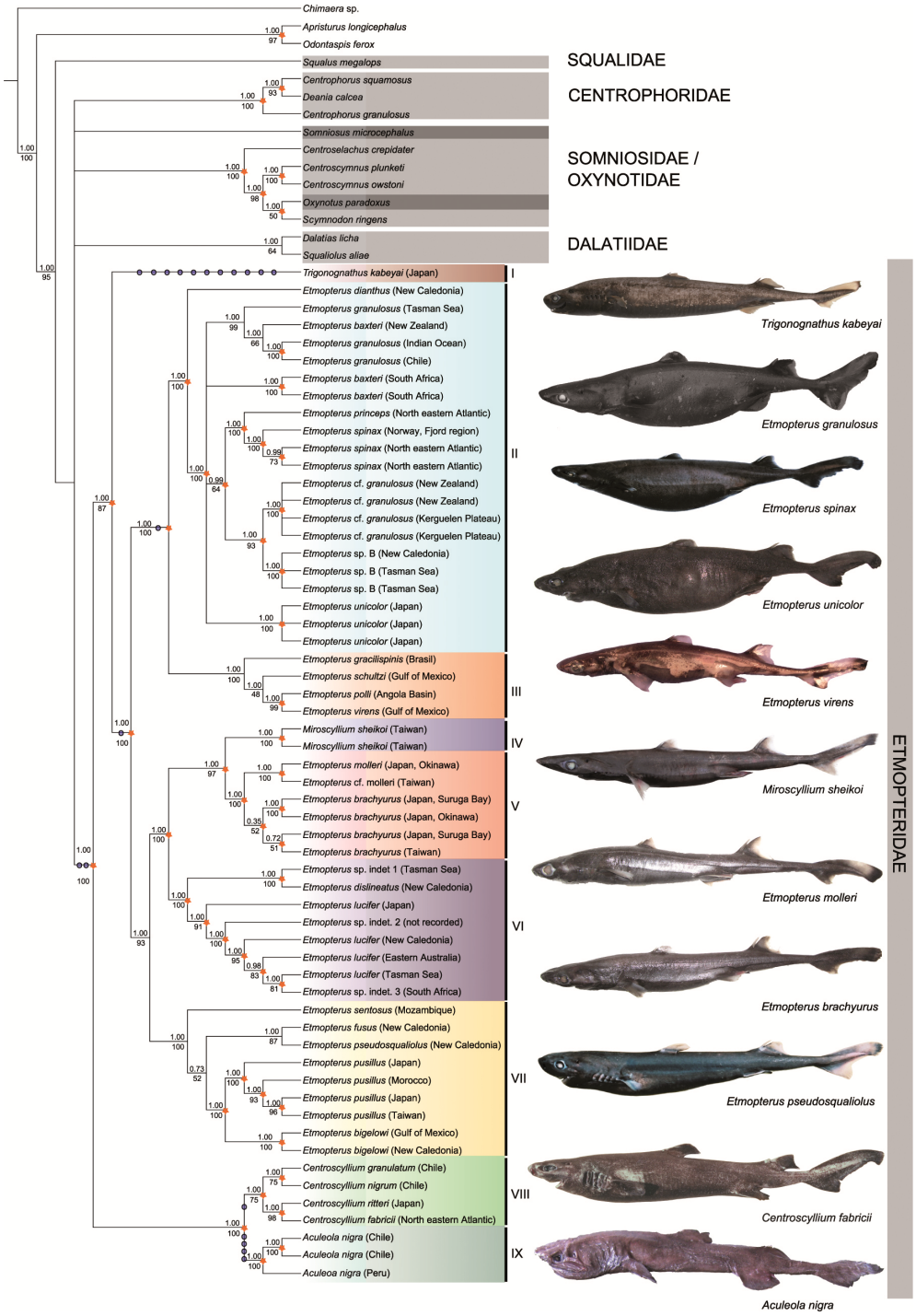

Figure 3: Dendrogram of phylogenetic relationships of Etmopteridae as constructed with Bayesian inference. Widely congruent topologies were attained with ML and MP analyses. Numbers above internal nodes indicate posterior probabilities (PPs) from Bayesian analyses, numbers below branches display bootstrap scores attained from ML search strategies. Orange asterisks refer to nodes found in MP analysis with a bootstrap support > 50%. Nodes displaying PPs and bootstrap scores < 0.95 (PP) and < 50% (bootstrap support) were collapsed. Blue circles refer to synapomorphic morphological character states found by Shirai (1992) which are in congruence with the tree topology (see Table 5 in Straube *et al*. 2010). Roman numerals refer to nine major clades resulting from phylogenetic analyses. Among the speciose genus *Etmopterus*, four clades can be identified, partially morphologically characterizable: *E*. *spinax* clade (Clade II), *E*. *gracilispinis* clade (Clade III), *E*. *lucifer* clade (clades IV, V and VI), and *E*. *pusillus* clade (Clade VII): *Etmopterus* sp. indet. 1: preliminary identified as *Etmopterus* cf. *molleri*; *Etmopterus* sp. indet. 2: preliminary identified as *E*. *lucifer*; *Etmopterus* sp. indet. 3: preliminary identified as *Etmopterus* cf. *brachyurus*. Dark grey colors mark taxa differing from traditional Squaliform families (light gray). Adopted from Straube *et al*. (2010).

4.2 Age and evolution of Etmopteridae

Estimation of node ages from sequence data was performed to explicitly test for a Lower Eocene origin of extant Etmopteridae as indicated by the fossil record, and to test for sequential versus rapid speciation in the course of the etmopterid radiation. Results from both analyzing approaches (Penalized Likelihood and Bayesian node age reconstruction) for reconstructing node ages of the etmopterid phylogeny are largely congruent and summarized in Figure 4. Penalized likelihood analyses generally estimate splittings to have occurred earlier, but estimates fall into confidence intervals computed from the Bayesian approach implemented in BEAST.

Alignments comprising either nuclear or mitochondrial data only differed in resolving power: mitochondrial sequences revealed more phylogenetic details on species level and therefore allowed to estimate more precise divergence dates as compared to the RAG1 dataset. In addition, BEAST node age reconstructions differing in the number of calibration points, revealed a differential effect on node time estimates: runs calibrated with only four vs. five calibration points had a larger effect on mean node ages and error bars compared to runs with identical calibration points, but only a subset of data, i.e. mtDNA only.

The split of Squaliformes from Carcharhiniformes and Lamniformes is estimated to 170 (218–133) Ma; this splitting is estimated by Penalized Likelihood analysis to 337.1 Ma, much older than estimated from the Bayesian approach and much older as expected from the fossil record. Therefore, the node age estimated in r8s seems inappropriate. After implying the attained r8s chronogram as starting tree in BEAST, the newly estimated age of node 2 falls into the error bar computed in previous BEAST analyses. The age of Squaliformes is estimated to 128 (130–127) Ma. The age of origin of the squaliform families Centrophoridae is 71 (74–69 Ma), Dalatiidae 67 (68–67 Ma), and Somniosidae 69 (70–67 Ma) are estimated to have occurred shortly before the C/T boundary. The hypothesis that bioluminescence has evolved twice independently, as suggested previously by several authors (Claes & Mallefet 2008, Hubbs *et al*. 1967, Reif 1985), is supported, since all squaliform families form monophyletic clades including the only other luminescent family Dalatiidae. Support for this scenario is provided by the fact that morphology of photophores and wavelengths of emitted light differs between both groups and, in addition, most probably serves different functions (Claes & Mallefet 2009c).

Age of extant Etmopteridae, as deduced from this analysis, is estimated to the end of the Cretaceous and beginning of the Paleocene (C/T boundary) and dates back substantially earlier than the first unambiguous etmopterid fossils from deep-water Eocene sediments (*Etmopterus bonapartei, E. acutidens, E. cahuzaci, Trigonognathus virginiae, Miroscyllium*, and *Paraetmopterus* (Adnet 2006; Adnet *et al*. 2008; Cappetta & Adnet 2001; Cigala 1986; Ledoux 1972)). Only the predominantly shallow water Squalidae, i. e. the sister group to all deep-water squaliform sharks, as

well as all ambiguously identified and now extinct etmopterid lineages (*Eoetmopterus, Microetompterus,* and *Proetmopterus*) are known from substantially before the C/T boundary (Adnet *et al*. 2006, Kriwet & Benton 2004, Siverson 1993, Cappetta & Siverson 2001, Underwood & Mitchell 1999). Nevertheless, their former habitat is debated, but they may not have been inhabitants of the bathyal environment adopted by extant species of Etmopteridae (Adnet *et al*. 2006). This pattern indicates that the extinction event at the C/T boundary affected squaliform sharks in different ways.

Node age estimates imply that extant forms, which are all bathyal species, have adapted to deep-water refugia in the subsequent recovery phase of the Eocene, possibly as a consequence of the end Cretaceous mass extinction event. This is further supported by the fact that *Eoetmopterus*, a potential shallow water species, is included in Etmopteridae based on phylogenetic analyses using odontological characters (Klug & Kriwet 2010).

An adaptive radiation well after the C/T boundary event is suggested by the fact, that the four major etmopterid lineages are distinguished by specific dental characters indicating that trophic specialization played an important role in the first radiation during the mid Eocene, evolving into the ecologically different etmopterid genera *Etmopterus*, *Trigonognathus*, *Aculeola*, and *Centroscyllium*.

Possibly, the Eocene recovery phase allowed the diversification of Etmopterids into the extant genera due to increased ecological opportunity after C/T extinction event along with the evolution of increased prey diversity in the Eocene (Kriwet & Benton 2004, Lindberg & Pyenson 2007). The most important radiation within *Etmopterus* occurred at the Oligocene/Miocene boundary continuing into the middle Miocene, i.e. roughly at the same time as a climatic shift from Palaeogene greenhouse conditions to icehouse conditions at the Eocene/Oligocene transition. This resulted in expanding antarctic ice shields, the establishment of the Circum Antarctic Current, and subsequent chilling of the deep-sea (Eldrett *et al*. 2009, Lear *et al*. 2008). In other words, the radiation and diversification within *Etmopterus* may be correlated with the impacts of these dramatic climatic changes. Results are further supported by analogous time estimates for the diversification of beaked whales (Ziphiidae), which have a similar depth penetration and prey spectrum as Etmopteridae (Dalebout *et al*. 2008).

Although the specific clutching-crushing type dentition of *Etmopterus* (including the juvenile phase of *Miroscyllium*; Adnet *et al*. 2006) is unique among Etmopteridae, the limited phenotypic diversity of tooth shapes within the genus cannot fully explain the evolution of more than 30 species in *Etmopterus*. The other distinct characteristics of *Etmopterus* are the complex bioluminescent organs. *Etmopterus* displays very diverse photophore patterns, which may serve several functions. Ventrally located photophores may provide counter illumination to serve as camouflage against residual sunlight when viewed from below (Claes & Mallefet 2008, Reif 1985, Widder 1998), whereas species-specific bioluminescent flank and tail markings may serve for species recognition and

possibly as schooling aid for cooperative hunting strategies (Claes & Mallefet 2008, 2009c, Reif 1985). Therefore, it is hypothesized that species specific diversity of social functions of the bioluminescent organ diversity may relate to selective forces that have influenced the evolutionary origin of species-richness in *Etmopterus*. In line with this argument, the shape of clade specific flank markings may also serve as candidate autapomorphy to identify the four species clades found within *Etmopterus* with molecular phylogenetics (Straube *et al*. 2010).

In summary, molecular phylogenetics and node age estimates allowed a detailed investigation of the evolution of this remarkably speciose shark family for the first time. General knowledge on the evolution of Etmopteridae in a time-window, spanning from the end of the Cretaceous to the Mid-Eocene, is substantially improved.

		BEAST		r8s
node #	node description	node age	height 95% HPD	node age
1	Root age	367.7	366.33 – 370.4	369.51
2	Split Squaliformes	170.23	133.37 – 218.42	337.1
3	Split *Squalus*	128.15	127.27 – 129.94	129.14
4	Split Centrophoridae	71.26	69.28 – 74.18	70.6
5	Split Etmopteridae & *Somniosus* from Somniosidae & Dalatiidae	68.78	67.06 – 70.89	-
6	Split Somniosidae / Dalatiidae	67.42	66.87 – 68.49	70.6
7	Split *Somniosus* / Etmopteridae	61.38	52.79 – 68.71	59.85
8	Split clades *Aculeola* & *Centroscyllium* from *Trigonognathus* and *Etmopterus*	43.89	41.26 – 48.46	56.81
9	Split *Aculeola* / *Centroscyllium*	22.7	12.48 – 38.78	40.78
10	Split *Trigonognathus* / *Etmopterus*	40.67	35.70 – 46.02	44.25
11	Split of clades II & III from IV, V & VI	36.48	31.55 – 41.36	34.24
12	Split clades II & III	29.65	21.67 – 36.29	30.34
13	Split clades IV, V & VI from VII	32.88	27.10 – 38.72	32
14	Split of *E. lucifer* species group in clades IV, V and VI	24.26	17.18 – 31.52	19.08
15	Split *Miroscyllium*	19.06	11.36 – 26.59	15.02

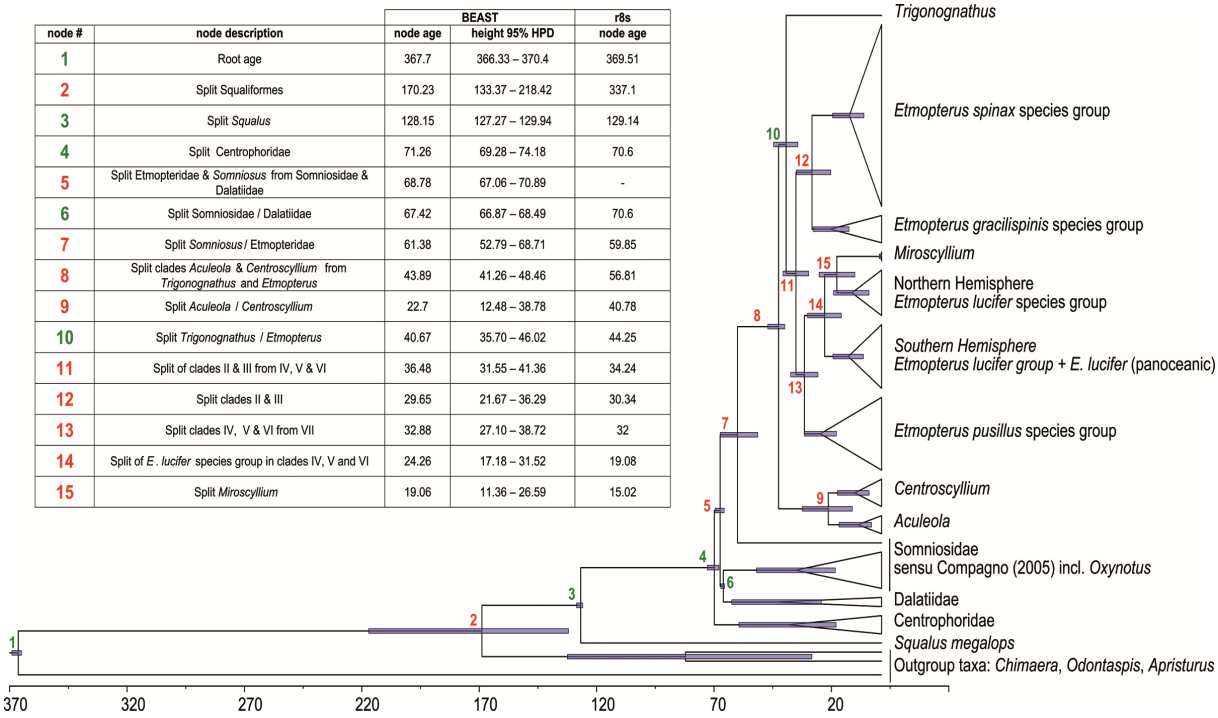

Figure 4: Estimated divergence times attained from Bayesian (BEAST) and penalized likelihood (r8s) analyses using relaxed molecular clock approaches. Red numbers refer to node numbers given in the table, which include node descriptions, mean node ages of both approaches and confidence intervals of BEAST analyses. Green numbers mark calibration points from fossils. Origin of Etmopteridae in between 53 and 69 Ma, origin of *Etmopterus* in between 36 and 48 Ma with further radiation events from 36 to 14 Ma. R8s appears to estimate older node ages, which are mostly congruent with estimated error bars from BEAST analyses. Modified from Straube *et al*. (2010).

4.3 The *E. baxteri* problem: re-evaluation of the *E. spinax* clade.

The overall etmopterid phylogenetic hypothesis revealed that the newly defined *E. spinax* clade (clade II, Fig. 3) contains multiple occurrences of species level paraphyly (e.g. *E. granulosus* and *E. baxteri*) indicating either misidentifications or previously undetected cryptic diversity (e.g. *Etmopterus* sp. B and *Etmopterus* cf. *granulosus*). Differentiation within *E. granulosus* and *E. baxteri* from diverse locations appears to be recent and not unambiguous with regard to species assignment,

i.e. with the limited sample size and number of analyzed loci in Straube *et al*. (2010), the question of paraphyly of *E. baxteri* cannot be resolved. Further, specimens included in the analyses as *E*. *unicolor* and *Etmopterus* sp. B are not monophyletic, suggesting that *E*. *unicolor* (NW Pacific) is specifically distinct from the undescribed *Etmopterus* sp. B (SW Pacific, Last & Stevens 1994). This contradicts recent morphological analyses (Yano 1997), which had suggested synonymy of *E*. *unicolor* with *Etmopterus* sp. B, which was subsequently accepted in current literature (Compagno *et al*. 2005, Last & Stevens 2009). Specimens of *E*. cf. *granulosus* (Duhamel *et al*. 2005) from the Kerguelen Plateau form another sub clade within clade II (Fig. 3) which appeared as sister to the *Etmopterus* sp. B sub clade. This species is similar to *E*. *unicolor* and *Etmopterus* sp. B in morphology and arrangement of dermal denticles, but also resembles *E*. *granulosus* in its flank mark shape suggesting these three species as cryptic species.

Therefore, the phylogenetic interrelationships of the *E. spinax* clade (clade II, Fig. 3) were re-analyzed with a substantially better specimen and locus selection, focusing on morphologically similar Southern Hemisphere representatives of this clade.

Results of this analysis reveal a complicated pattern of inter-and intraspecific relationships within the *E. spinax* clade (Fig. 4, Straube *et al*. 2011) that is not fully compatible with results from molecular phylogenetics in Straube *et al*. (2010). The phylogenetic hypothesis based on AFLP data reveals *E. spinax* (NE Atlantic) as the basal taxon to a clade comprising morphologically similar Lantern Sharks (*E. princeps*, *E. granulosus*, *E*. cf. *granulosus*, South African *E. baxteri*, and *E*. sp. B) with high bootstrap support. *Etmopterus princeps* (NE Atlantic) appeared as well-supported sister taxon to a clade comprising morphologically similar species from the Southern Hemisphere only (Fig. 4, Straube *et al*. 2011). This newly recovered phylogenetic hypothesis suggests that the origin of the *E. spinax* clade is in the Atlantic, because both basal members of the clade are sampled in the North Atlantic and display their main distribution there. Phylogenetically younger species of the *E. spinax* clade are distributed in the Southern Hemisphere. Origin and subsequent Southern Hemisphere diversification of the *E. spinax* clade occurred 36 – 22 Ma ago (Straube *et al*. 2010) and follows the Eocene/Oligocene climatic change from greenhouse to icehouse conditions (Eldrett *et al*. 2009; Lear *et al*. 2008). Therefore, it is not unlikely that a species closely related to *E. princeps* dispersed into the Southern Hemisphere and gave rise to the South Pacific and Indian Ocean taxa. Interestingly, a recent study of the global population structure of another squaloid shark, the Spiny Dogfish, *Squalus acanthias,* identified an analogous southward dispersal pathway from a putative Northern Hemisphere origin (Verissimo *et al*. 2010).

Further results contradict a synonymy of *E*. sp. B with *E. unicolor*, because specimens of *E. unicolor* included in the sample form a clearly distinct cluster differentiated from *E*. sp. B as being sister to a clade including North Atlantic and Southern Hemisphere species only. The samples of

E. unicolor were collected in the NW Pacific (Japan) close to the type locality. However, diagnostic morphological characters for *Etmopterus* sp. B remain unidentified, rendering a barcoding approach to be promising for monitoring and conservation of cryptic members of the *E. unicolor* species complex, as the "barcoding" locus COI identifies *E*. sp. B as a distinct cluster (Fig.2, Straube *et al*. 2011).

On the other hand, results from AFLP based assignment tests conducted with the STRUCTURE software package (Fig. 6A) strongly suggest that *E. baxteri* sampled off New Zealand is synonymous with *E. granulosus* sampled off Chile as suggested by Tachikawa *et al*. (1989). This argues in favor of a wide distribution in the Southern Hemisphere of *E. granulosus* and against an endemic distribution off southern South America (Compagno *et al*. 2005). Conversely, specimens sampled off South Africa, which had tentatively been assigned to *E. baxteri sensu* Compagno *et al*. (2005), as well as *E.* cf. *granulosus sensu* Duhamel *et al*. (2005), and *Etmopterus sp.* B *sensu* Last & Stevens (1994), form distinct clades representing most likely cryptic species, which support the hypothesis of three cryptic *E. granulosus*-like species in the Southern Hemisphere.

Since the two sampling locations New Zealand and Chile are roughly 7000 km apart, suggesting the possibility of additional population differentiation, further investigations were performed to test for the existence of population structure and phylogeography within *E. granulosus.* F_{ST} and Φ_{ST} values of the AFLP and mtDNA data, respectively, identify weak but nevertheless significant genetic differentiation of populations (Tab. 1, Straube *et al*. 2011). This is supported by AMOVA results, indicating that the vast majority of nuclear variation resides among and not within the two samples. A search for AFLP loci under divergent selection correlating with population differentiation (see 3.3) yielded only two candidate loci whose allele frequencies in the two samples might have been shaped by strong selection. Different STRUCTURE analyzing approaches did not detect further population structure between the two sampling locations (Fig. 6B). In summary, the two sampling sites for *E. granulosus* (Chile and New Zealand) are geographically distant but show unexpectedly low levels of population differentiation.

The modest level of population differentiation could either be indicative of an isolation-by-distance scenario or may be triggered by a very recent cessation of gene flow of these populations. Isolation-by-distance would require the existence of intermediate populations allowing for connectivity between Chile and New Zealand. The few COI haplotypes of specimens identified as *E.* cf. *baxteri* (Amsterdam Island) and *E. granulosus* (NE of the Kerguelen Plateau) from the Indian Ocean and *E. granulosus* from the Southeast Pacific (Australia) fall into the *E. granulosus* network cluster (Fig. 1, Straube *et al*. 2011). This supports their identity as *E. granulosus* and the close connectivity of populations separated by several thousand kilometers along the subantarctic ecoregion rather than a species-level distinction of populations. Such connectivity may be facilitated

by the Circum Antarctic Current passing all known sampling locations of *E. granulosus*. An explanation of a very recent separation of now reproductively isolated populations appears less likely given that regional faunal diversity, differentiating the two areas, has evolved in other species into phylogenetically distinct species assemblages. This has even lead to the designation of differentiated bathyal species ecoregions, i.e. New Zealand, Kermadec, and Nazcaplatensis ecoregions (UNESCO 2009). This is not reflected in the analysed *Etmopterus* species and suggests ongoing gene flow. In addition, population genetic differentiation was already detected between pelagic Southern Australian dolphins (*Delphinus delphis*) over a distance of 1500 km, supporting the regional differentiation hypothesis for non-Etmopterid faunal differentiation even beyond the bathyal realm (Bilgmann *et al*. 2008). Nevertheless, the ultimate test for these alternative hypotheses with regard to *Etmopterus* would be a classical tagging experiment allowing tracking of migration of individuals over large distances. So far, available data on migration behavior of Etmopterids in general is limited, because tagging studies do not exist (Forrest & Walters 2009).

Yet another explanation for a subtle population differentiation between distant *E. granulosus* populations is a response to natural selection acting divergently between e.g. the New Zealand and Chile sample sites. Chilean *E. granulosus* occur in shallow depths from 200 to 637 m (IUCN Red List 2010, and NS pers. obs.), compared to specimens of the same species from New Zealand, which on average occur much deeper, between 850 to 1200 m (Bass *et al*. 1986, Garrick 1960, Wetherbee 1996, NS pers. obs.). In this context, it must remain speculative, whether the two possible candidate loci identified in the AFLP genome scan relate to physiological characters under divergent selection for adaptations to different depths.

However, the distribution range of *E. granulosus* is most likely circumglobally along the Southern Hemisphere, and reports off Sierra Leone (Golovan & Pukhorukov 1986) need confirmation. Therefore, this study rather provides hints that *E. granulosus* is a migratory rather than a resident species. Evidence for sex and size-related aggregations in Etmopterids (Jakobsdottir 2001, Wetherbee 1996) might be related to socially induced migration for mating or schooling purposes (Claes & Mallefet 2008, 2009a, Reif 1985). Future population genetic analyses of the *E. granulosus* species group should comprise additional samples of potentially existing intermediate populations especially with regard to validation of the hypothesis of migration versus isolation-by-distance.

In summary, this study is the first population genetic approach applied to Etmopterids and yields first evidence that Etmopterids may be capable of covering large distances. Effective monitoring and management efforts of by-catch species should consider that the *E. granulosus* population is huge and there is the need to identify potential mating grounds and to collect further detailed data on distribution of sexes and different ontogenetic stages in the whole Southern Hemisphere.

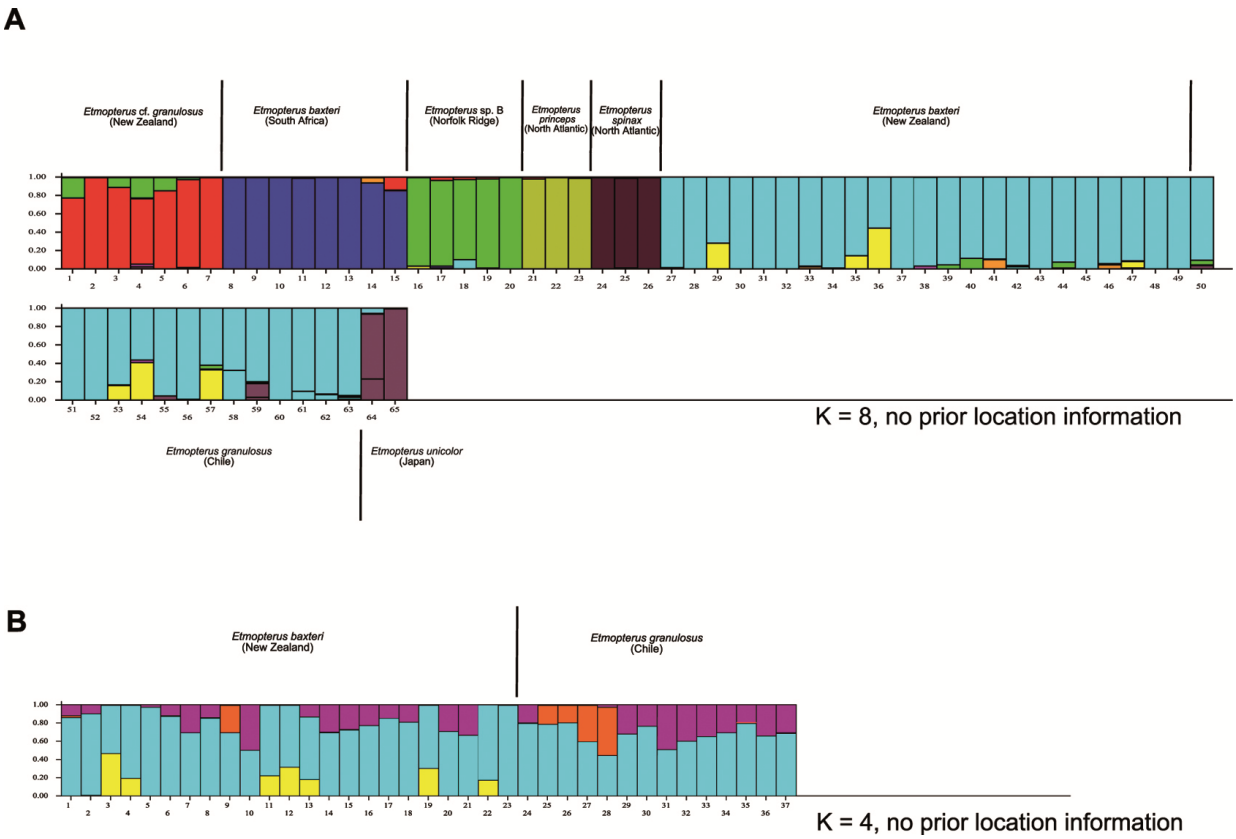

Figure 5: Bar plots of hierarchical STRUCTURE analysis displaying population assignments for the full AFLP dataset (A) and a downsized dataset (B) focusing on sampling sites Chile (*Etmopterus granulosus*) and New Zealand (*E. baxteri*). Each bar represents an individual on the x-axis, the y-axis displays the likelihood of assignment for K = 8 (A) and K = 4 (B). Adopted from Straube *et al*. (2011).

4.4 *Etmopterus* "*viator*" sp. nov.

(This document is not to be considered as published in the sense of the International Code of Zoological Nomenclature, and statements made herein are not made available for nomenclatural purposes)

In addition to results presented in Articles I and II of this thesis, which all group *E.* cf. *granulosus sensu* Duhamel *et al*. (2005) as a distinct clade or cluster, morphological analyses conducted in Article III support the existence of a previously unrecognized species, which is described in one paper out of this thesis as *Etmopterus* "*viator*" sp. nov.. The new species differs significantly from all Southern Hemisphere congeners in several characters.

Within the genus *Etmopterus*, *E. "viator"* sp. nov. is identified as member of the *E. spinax* clade *sensu* Straube *et al.* (2010) based on flank mark shape. Within the *E. spinax* clade, it can be distinguished from *E. spinax*, *E. compagnoi* and *E. dianthus* by a uniform coloration without an abrupt transition of a light dorsal to a black ventral side. It differs from *E. princeps* in geographical occurrence (Southern Hemisphere vs. North Atlantic), depth distribution range, maximum body size, and size at maturity. It differs from North Pacific *E. unicolor* in its dermal denticle shape: *E. unicolor* displays dense and bristle-like denticles similar to *E*. sp. B. (Article III, Fig. 1), while the new species displays less dense and hook-like denticles. Further, *E. unicolor* matures at larger body sizes (53 cm TL

for male *E. unicolor* (Compagno *et al*. 2005) versus 46 cm TL for male *E*. "*viator*" sp. nov.). Southern Hemisphere congeners are *E*. sp. B (*sensu* Last & Stevens 1994), *E. granulosus*, *E*. cf. *granulosus* (South Africa), and *E. litvinovi*. *Etmopterus "viator"* sp. nov. differs from all closely related congeners in smaller total lengths and smaller sizes at maturity. It specifically differs from *E*. sp. B in possessing less denser dermal denticles per area (3 mm^2 below the 2^{nd} dorsal fin: 23-40 vs >100) and in the combination of four ratios calculated from body measurements (TL/HFDF; PFDL/ID; HL/ID; HL/IOD; Fig. 1, Article III). South African *E*. cf. *granulosus* can be distinguished from *E*. *"viator"* sp. nov. by comparing the same four ratios (Fig. 1, Article III). The new species differs from *E. granulosus* in having fewer dermal denticles per area (3 mm^2 below 2^{nd} dorsal fin: 23-40 vs. 34-58), in the length of dermal denticles, and in the combination of the two ratios: PFDL/ID and HL/ID (Article III, Figs 1 & 2).

The most conspicuous difference between *E. "viator"* sp. nov. and *E. litvinovi* is the absence of any photophore markings. The body color differs between the two species. *E. litvinovi* displays a dark black body coloration while the new species is distinctly brown in adults. Further, *E*."*viator*" sp. nov. has distinct caudal peduncle and upper tail fin lobe markings as well as flank markings, which are absent in *E. litvinovi*. It further differs from *E. litvinovi* in the ratio HL/IOD and the total number of vertebrae (Article III, Fig. 1).

Results from barcoding support findings from morphological analyses. Figure 4 in Article III shows a monophyletic lineage clearly separating *E. "viator"* sp. nov. from its congeners, i.e. the barcode approach readily allows the identification of *E. "viator"* sp. nov.. It is most closely related to *E*. sp. B and *E*. cf. *unicolor*. *Etmopterus granulosus* and *E.* cf. *granulosus* (South Africa) form distinct clusters, which are rather distant with regard to the new species. Specimens sampled off New Zealand, preliminarily assigned to *E. granulosus*, are included in the new species´ cluster based on COI sequences, suggesting conspecifity of the Kerguelen and New Zealand populations. Interestingly, morphometric analyses also confirm *E. "viator"* sp. nov. to be present off South Africa as well, indicating the new species to be wide ranging in the Southern Hemisphere similar to the distribution range of *E. granulosus* (Straube *et al*. 2011).

Detailed biological data on *E. "viator"* sp. nov. are available from French fisheries surveys at the Kerguelen Plateau. It is ovoviviparous and gives birth to 2 to 10 pups per litter. Maturity is reached at approximately 50 cm TL in females and 46 cm TL in males. The largest specimen is a female measuring 577.2 mm (MNHN-20081900). Males are on average smaller than females. Duhamel *et al.* (2005) report the species to feed on myctiphids, euphausiids, and squid.

In summary, morphological as well as molecular data support the validity of the new species. Based on these findings, the new Lantern Shark species is described as *Etmopterus "viator"* sp. nov.. The new species was named after the Latin word "viator" (the traveler).

The species is caught in high numbers off the Kerguelen Plateau in longline and trawl fisheries, but these specimens were so far identified incorrectly as *E.* cf. *granulosus*. The description of the new species will have a direct effect on its monitoring, since fisheries observers are now able to distinguish between *E. granulosus* and *E. "viator"* sp. nov..

Figure 6: *Etmopterus* "*viator*" sp. nov. Holotype MNHN-20081899, adult female, formalin preserved.

4.5 Molecular phylogeny and node age reconstruction of Chimaeriformes

The DNA dataset of Chimaeriformes was compiled to provide detailed insights into phylogenetic interrelationships on genus and species levels. All three applied phylogenetic inferences recovered consistent phylogenetic hypothesis showing well supported nodes. The mtDNA dataset was analysed with Maximum Likelihood (ML), Neighbor-joining phylogenetics (NJ), and Bayesian inferences (BI). All three approaches recovered widely congruent tree topologies with regard to the well-supported monophyly of Chimaeriformes as sister group to Neoselachii. Figure 7 displays an overview of the most likely tree topology recovered from ML analyses.

Major nodes are recovered as in Inoue *et al*. (2010) implying correct sampling and adequate data acquisition. Further results reveal monophyletic Chimaeriformes as sister to Neoselachians (sharks and rays included as outgroup taxa) and are split into two major clades. Callorhynchidae is sister to all remaining Chimaeriforms (node 1, Fig. 7) and is confirmed as most basal family (Didier 1995, Inoue *et al*. 2010).

The next major splitting separates Rhinochimaeridae from Chimaeridae (node 5, Fig. 6). Within Rhinochimaeridae, *H. raleighana* from the South West Pacific appears as basal sister to the North Atlantic and North Pacific *Rhinochimaera* species and may hint to a Southern Hemisphere origin of the family.

Chimaeroid genera *Hydrolagus* and *Chimaera* appear paraphyletic. The clade containing *H. mirabilis*, *H. mitsukurii*, two specimens of *Ch. phantasma*, and *H. lemures* (Fig. 7) is well supported but the radiation of the clade into different species is not, rendering both genera already paraphyletic here. *Hydrolagus* and *Chimaera* are morphologically distinguished by two autapomorphies, i.e. the presence (*Chimaera*) and absence (*Hydrolagus*) of an anal fin, but experts report on the large variability of this character (Kemper *et al*. 2010a) which even can differ within

one species (Last & Stevens 2009). A taxonomic revision of the family Chimaeridae seems appropriate to validate its two genera and define adequate apomorphies.

The recovered phylogenetic tree further displays *H. mitsukurii*, *H. mirabilis*, and *H. lemures* in a clade with two specimens of *Ch. phantasma* splitting from the remaining *Hydrolagus* and *Chimaera* species (node 8, Fig. 7). Subsequently, North East Atlantic *Ch. monstrosa* constitutes a monophyletic, well-supported clade, which is sister to the remaining *Hydrolagus* and *Chimaera* species indicating the species to be distinct (node 9, Fig. 7). The following clade comprises *H. purpurescens*, *H. affinis*, and *H. pallidus* (node 11, Fig. 7). *Hydrolagus purpurescens* and *H. pallidus* are sister species to *H. affinis* (node 15, Fig. 7). The splitting of North East Atlantic *H. pallidus* into two well-supported subclades indicates unknown cryptic diversity.

Opposite to this *Hydrolagus* clade, a clade is recovered, which comprises *Ch. fulva*, *Chimaera* sp. 2, and *Ch. opalescens* as well as *Hydrolagus* sp. and *Chimaera* sp. 1 (node 21, Fig. 7). *Chimaera* sp. 1 & 2 sampled in the Indian Ocean likely represent still undescribed species and will be described elsewhere. Unknown cryptic diversity is not astonishing since a large number of species of the family has only recently been described (e.g. Didier 2008; Didier *et al*.2008; Kemper *et al*. 2010a, 2010b; Luchetti *et al*. in press).

As aforementioned for Rhinochimaeridae, Southern Hemisphere Chimaeriformes are strikingly often basal to Northern Hemisphere ones, i.e. Indian Ocean *H. purpurescens* is basal sister to North Atlantic *H. affinis*, Southern Hemisphere *Chimaera* sp. 1, *Ch. fulva*, and *Chimaera* sp. 2 are sister to North West Pacific *Hydrolagus* sp. and North East Atlantic *Ch. opalescens*. This may further indicate a Southern Hemisphere origin of extant Northern Hemisphere Chimaeriforms.

In addition, morphological (anatomical) characters provided by Didier (1995) were plotted on the molecular phylogeny to provide information on the congruence or inconsistency of morphological and molecular data. Didier (1995) altogether described 55 synapomorphies characterizing the different taxonomic levels in Chimaeroids. All synapomorphies introduced by Didier (1995) are in congruence with the molecular tree presented herein (Table 5 in Article IV).

As expected, node age estimates are in line with estimates from Inoue *et al*. (2010). Additional information is provided on genus and species level due to the higher number of Chimaeriform taxa included in the sampling. Results show that Chimaeriformes originated some 430 Ma ago in the Silurian and further radiated at two major events 177 and 123 Ma ago (nodes 3 & 4, Fig.3 and Table 4 in Article IV) into families Callorhynchidae, Rhinochimaeridae and Chimaeridae. Figure 3 in Article IV shows early secession of families (nodes 3 & 4, Fig. 3, Table 4 in Article IV) but rather recent radiations of taxa within families (nodes 7 to 20, Fig. 3 Table 4 in Article IV), i.e. a timeline of undetectable cladogenesis of approximately 40 Ma before the different families radiated into genera and species.

The radiation into extant species clades is estimated to have occurred in a time window of 59 to 18 Ma after the terminal Cretaceous mass extinction event. Diversification of Chimaeroids into extant species diversity comprises nodes 9 to 18 (Fig. 3, Table 4 in Article IV) that apparently evolved from the late Palaeogene on and lasting until the Quaterny with a diversification peak in the Neogene.

Analogously to the scenario described in Straube *et al*. (2011) for Lantern Sharks (Etmopteridae), a deep-sea ecosystem recovery phase in the Palaeogene may have induced diversification: nodes 23 and 24 (Fig. 3 and Table 4 in Article IV) mark the splitting of *Trigonognathus* from *Etmopterus* and further radiation within *Etmopterus* and also fall into the timeframe extrapolating radiation events in Chimaeriforms (see also Straube *et al*. 2010). These results further align with the radiation of Ziphiidae (Beaked Whales) which show analogous radiation ages (Dalebout *et al*. 2008) and partially overlap in ecological characters with Chimaeriforms. Therefore, it is speculated for Chimaeriformes as well, that the Eocene recovery phase in general may have been the beginning of deep-water colonization events of prey organisms which were followed by its predators including a wide range of marine vertebrates. Molecular clock estimates are a powerful tool to provide a first and often necessary step for the inference of the impact of natural disasters on past biodiversity for taxa without a complete fossil record.

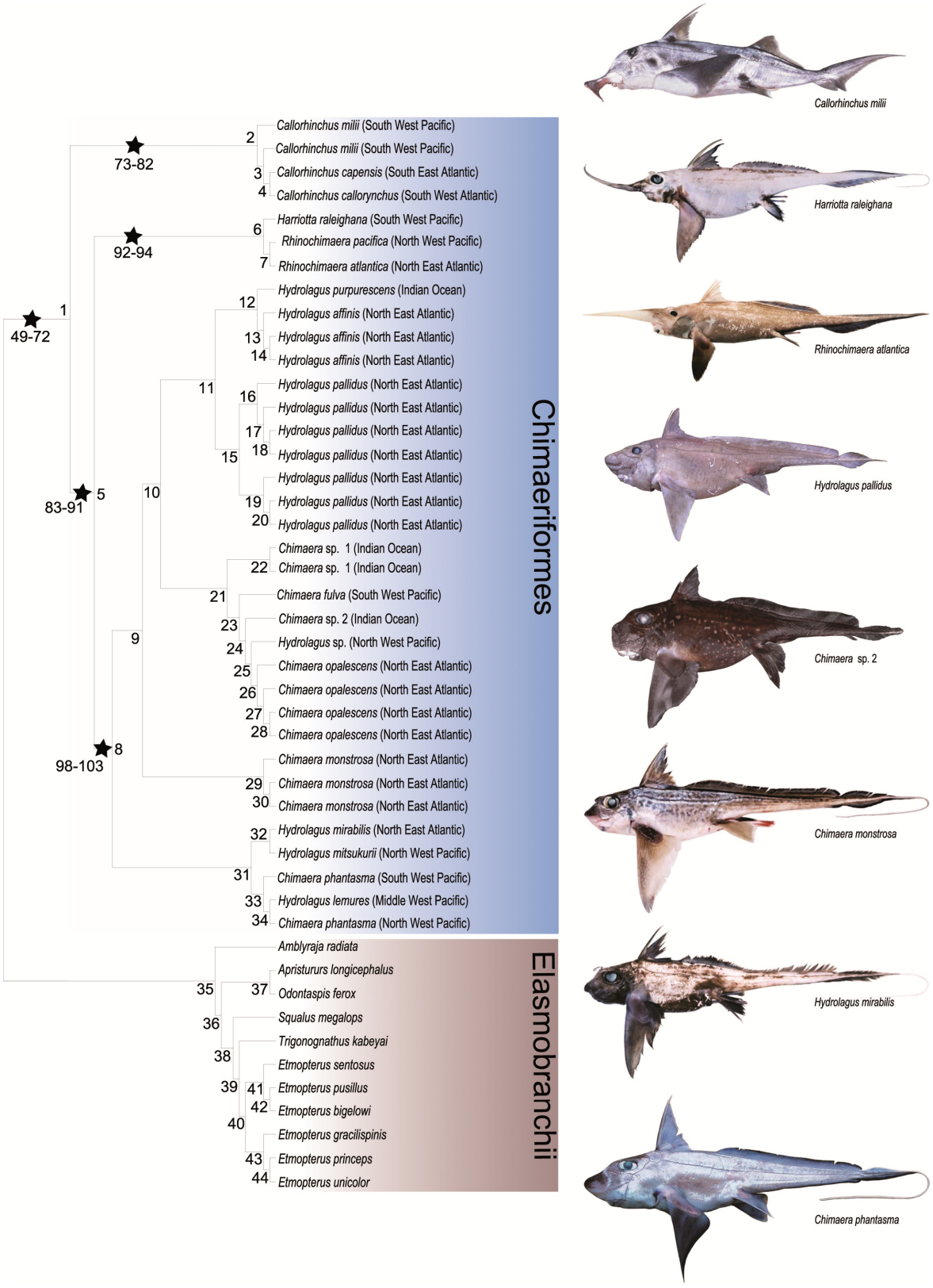

Figure 7: Phylogenetic tree reconstruction of Chimaeriformes based on five mtDNA loci and Maximum Likelihood analysis. Numbers above nodes refer to node numbers given in Table 3, Article IV, which provides node support values from bootstrapping of Maximum Likelihood and Neighbor-joining analyses as well as Bayesian posterior probabilities. Stars mark morphological synapomorphies introduced by Didier (1995) and refer to Table 4, Article IV.

5 Future perspectives

Analyses presented herein have revealed several interesting results, which are new to science, but other questions remain un-answered. Therefore, a re-analyses of the overall Chondrichthyan phylogeny (all sharks, skates, rays, and chimaeras) based on a continuative and larger nuclear locus sampling (>100 single copy protein coding nuclear exons) will be conducted in a post-doctoral project due to the severe lack of knowledge on interrelationships and evolution of a whole class of vertebrates. Studies will be performed at the Charleston University, Charleston, SC, USA in the working group of Professor Gavin Naylor applying next generation sequencing techniques to 500+ Chondrichthyan species. The dataset will allow detailed analyses of the overall Chondrichthyan phylogeny as part of the Tree of Life Project (CarTOL) and further node time estimates for analysing origin, evolution and radiation of the extant Chondrichthyan diversity.

Further, Etmopteridae still yield a high number of cryptic species, which need to be analyzed and described in the near future. A better understanding of taxonomy, distribution and population structure is crucial to enable the effective establishment of by-catch monitoring and management strategies, especially with regard to the potential vulnerability of deep-sea shark populations as recently estimated by Forrest and Walters (2009). Therefore, a collaborative project with South African and US shark experts will focus on the description of a number of unknown shark species present off South Africa, generally a diversity hotspot of deep-water Chondrichthyes.

6 Summary (German)

In der vorliegenden Dissertation wird über die Anwendung phylogenetischer Methoden an bisher relativ wenig bekannten und schwer zugänglichen tiefseebewohnenden Knorpelfischen berichtet.

Die Laternenhaie (Etmopteridae) sind eine der größten Haifamilien und zunehmend dem Druck der Überfischung ausgesetzt, obwohl bisher kaum etwas zu ihrer Lebensweise und Biologie bekannt ist. In der vorliegenden Studie werden Sequenzinformationen eines nukleären sowie von fünf mitochondrialen Genen zur phylogenetischen Rekonstruktion der Verwandtschaftsverhältnisse innerhalb der Etmopteridae sowie zwischen nah verwandten Familien genutzt. Die mit verschiedenen Methoden (Maximum Likelihood, Bayesian Phylogenetics und Maximum Parsimony) errechnete Phylogenie der Laternenhaie erlaubt eine detaillierte Analyse der bisher zur Arterkennung verwendeten morphologischen Merkmale und identifiziert eine Reihe von bisher unbekannten Gruppierungen innerhalb des artenreichsten Genus *Etmopterus*.

Weiter werden die Daten verwendet, um Abspaltungsereignisse in der Etmopteridenphylogenie mithilfe einer relaxierten molekularen Uhr abzuschätzen. Die Kalibrierung der molekularen Uhr erfolgt mithilfe fossiler Belege von Laternenhaien sowie sinnvollen Außengruppen, d.h. nahverwandte Familien innerhalb der Dornhaie, einzelne Stellvertreter anderer Haiordnungen sowie eine Chimärenart wurden als Außengruppen gewählt. Um möglichst genaue Verzweigungsalter

schätzen zu können, wurden zwei unterschiedliche Methoden angewandt, Penalized Likelihood und Bayesian Node Age Reconstruction. Die Ergebnisse zeigen, dass die rezenten Etmopteriden sehr wahrscheinlich nach der Kreide/Tertiärgrenze entstanden sind, die rezente Artenvielfalt des Genus *Etmopterus* jedoch relativ jung ist. *Etmopterus* radiierte an der Oligozän/Miozän Grenze in die gegenwärtige hohe Artenvielfalt, was interessanterweise bei anderen Wirbeltiergruppen mit ähnlicher Ökologie gleichfalls gezeigt werden konnte.

Eine, nach der phylogenetischen Rekonstruktion, im taxonomischen Sinne unzufriedenstellend aufgelöste Gruppierung, der „*E. spinax* clade“, innerhalb des Genus *Etmopterus* wurde mit Hilfe populationsgenetischer Methodik, der sogenannten AFLP-Genotypisierung, erneut analysiert, um die phylogenetischen Verhältnisse besser klären und kryptische Arten identifizieren zu können. Die AFLP Daten wurden mit mitochondrialen Sequenzdaten des Barcoding Gens COI verglichen. Aufgrund übereinstimmender Ergebnisse konnten eine Reihe taxonomischer Fragen geklärt werden, welche die Beschreibung einer unbekannten Haiart erlauben, *Etmopterus „viator“* sp. nov.. Zur Artabgrenzung wurden zusätzlich zu den akkumulierten DNS Sequenzdaten eine Reihe von morphologischen, morphometrischen und meristischen Merkmalen untersucht, die eindeutig belegen, dass es sich hier um eine bisher unbeschriebene Art handelt.

Die erlernten Methoden wurden in einem Folgeprojekt in Kooperation mit französischen Kollegen an einem weiteren Sequenzdatensatz tiefseelebender Knorpelfische angewendet. Hierbei handelt es sich um die erdgeschichtlich alte Gruppe der Chimären, der Schwesterngruppe aller Haie und Rochen. Die rekonstruierten phylogenetischen Verhältnisse bestätigen einerseits bereits bekannte Abspaltungen, andererseits erlauben unsere Daten einen tieferen Einblick in die Phylogenie der Chimaeriformes auf Artebene. So scheinen die Genera *Hydrolagus* und *Chimaera* innerhalb der größten Familie der Chimären paraphyletisch zu sein und sollten deshalb einer detaillierten Revision unterzogen werden. Weiter können zwei kryptische Arten aus dem Indischen Ozean identifiziert werden. Die phylogenetische Position des seltenen Genus *Neoharriotta* bleibt ungeklärt und kann wahrscheinlich nur mit einem erweiterten Sequenzdatensatz ausreichend untersucht werden. Der Vergleich morphologischer Merkmale mit molekularen Daten erlaubt einige Merkmale als Apomorphien, die die einzelnen taxonomischen Ebenen innerhalb der Chimären charakterisieren, auszuschließen, andere hingegen werden von den phylogenetischen Analysen gut unterstützt.

Die zeitliche Abschätzung von Abspaltungsereignissen innerhalb der Seekatzen zeigt, dass die rezente Diversität, vergleichbar der der Laternenhaie, nach der Kreide/ Tertiärgrenze entstanden ist und es sich bei den rezenten Formen, nicht wie ursprünglich angenommen, um Reliktarten handelt, die sich nach dem Massensterben am Ende des Perms in die Tiefsee zurückgezogen haben, sondern um wesentlich jüngere Arten.

7 Acknowledgements

First of all, I would like to express my sincere thanks to my supervisors Prof. G. Haszprunar, Dr. U. Schliewen, and Prof. J. Kriwet for their help, critics and encouragement during my work.

Further, I would like to thank my colleagues at the ZSM for useful comments on my manuscripts, help with diverse softwares needed for adequate analyses, and their nice characters creating a friendly working atmosphere: M. Geiger, J. Schwarzer, A. Dunz, I. Stöger, A. Cerwenka, J. Wedekind, H. Wedekind, B. Ruthensteiner, T. Lehmann, D. Neumann, R. Melzer, E. Lodde, T. Knebelsberger, H. Schütz. P. and F. Dawes are acknowledged for manuscript improvements.

All people organizing and sharing samples need to be mentioned here, since their help actually made my studies possible: S. Tanaka, T. Horie (Tokai University, Japan), S. Iglésias, G. Duhamel, B. Serét, N. Gasco, P. Pruvost (Muséum National d'Histoire Naturelle), A. Loerz, K. Schnabel, D. Tracey, M. Watson, P. McMillan (NIWA, New Zealand); A. Stewart (Te Papa Tongarewa, New Zealand), D. Bray (Victoria Museum Melbourne, Australia), K. Matsuura, G. Shinohara (Museum of Nature and Science, Japan), G. Johnston (Marine Institute Rinville, Ireland), F. Concha (Universidad de Valparaíso, Chile), R. Leslie (Marine and Coastal Management, South Africa). A. Verissimo, C. Cotton (Virginia Institute of Marine Science); K. Sato (Churaumi Aquarium, Japan); M. Grace, J. Carter (NOAA USA); M. McGrouther (Australian Museum Sydney, Australia); O. Gon, M. Mwale, P. and E. Heemstra (SAIAB South Africa), S. Hernandez (Victoria University of Wellington, New Zealand); J. Lamilla (Universidad Austral de Chile, Chile); D. Zaera (Institute of Marine Research, Norway); F. Burns (Fisheries Research Services, Great Britain); F. Herder (Zoologisches Museum Alexander König Bonn, Germany); M. Harris (Florida, USA); T. Tomita (University of Tokyo, Japan), T. Sasaki (University of Tokyo, Japan), Y. Chimura (Chiba Aquarium, Japan); S. Raredon (USNM, USA).

Finally, I especially thank my girlfriend Stephi and my family for their love and support.

8 References

Adnet, S. (2006). Two new selachian associations (Elasmobranchii, Neoselachii) from the Middle Eocene of Landes (South-West of France). Implication for the knowledge of deep-water selachian communities. *Palaeo Ichthyologica*, 10, 5-128.

Adnet, S. & Cappetta, H. (2001). A palaeontological and phylogenetical analysis of squaliform sharks (Chondrichthyes: Squaliformes) based on dental characters. *Lethaia*, 34, 234-248.

Adnet, S., Cappetta, H. & Nakaya, K. (2006). Dentition of etmopterid shark *Miroscyllium* (Squaliformes) with comments on the fossil record of Lantern Sharks. *Cybium*, 30 (4), 305-312.

Adnet, S., Cappetta, H. & Reynders, J. (2008). Contribution of Eocene sharks and rays from southern France to the history of deep-sea selachians. *Acta Geologica Polonica*, 58 (2), 257-260.

Albertson, R. C., Markert, J. A., Danley, P. D. & Kocher, T. D. (1999). Phylogeny of a rapidly evolving clade: the cichlid fishes of Lake Malawi, East Africa. *Proceedings of the National Academy of Sciences*, 96, 5107-5110.

Bandelt, H. J., Forster, P. & Rohl, A. (1999). Median-joining networks for inferring intraspecific phylogenies. *Molecular Biology and Evolution*, 16, 37-48.

Bass, A. J., Compagno, L. J. V. & Heemstra, P. C. (1986). Squalidae. In: M. M. Smith, P. C. Heemstra (eds.) *Smith's Sea Fishes*. Berlin: Springer Verlag, pp. 49-62

Benton, M. J., Donoghue, P. C. J. (2007). Paleontological Evidence to Date the Tree of Life. Molecular *Biolology and Evolution*, 24 (1), 26-53.

Bilgmann, K., Möller, L. M., Harcourt, R. G., Gales, R. & Beheregaray, L. B. (2008). Common dolphins subject to fisheries impacts in Southern Australia are genetically differentiated: implications for conservation. *Animal Conservation*, 11, 518-528.

Bonfil, R. (1994). Overview of world elasmobranch fisheries. *FAO Fisheries Technical Paper* 341. Food and Agricultural Organisation of the United Nations (FAO), Rome, Italy.

Cadenat, J. & Blache, J. (1981). Requins de Mediterranee et d'Atlantique (plus particulierement de la Coze occidentale d'Afrique). *Faune Tropicale*, 21, pp. 1-330.

Cappetta, H. & Adnet, S. (2001). Discovery of the recent genus *Trigonognathus* (Squaliformes: Etmopteridae) in the Lutetian of Landes (southwestern France). Remarks on the teeth of the recent species *Trigonognathus kabeyai*. *Paläontologische Zeitschrift*, 74 (4), 575-581.

Cappetta, H., Siverson, M. (2001). A skate in the lowermost Maastrichtian of southern Sweden. *Palaeontology*, 44, 431-445.

Carvalho, M.R. de & Maisey, J.G. (1996). Phylogenetic relationships of the Late Jurassic shark *Protospinax* Woodward 1919 (Chondrichthyes: Elasmobranchii). In: Arratia, G., Viohl, G. (eds.). *Mesozoic Fishes–Systematics and Paleoecolog*y, Verlag Pfeil, München, pp. 9-46

Cigala Fulgosi, F. (1986). A deep-water elasmobranch fauna from the Pliocene outcropping (North Italy). Proceedings of the 2nd Conference of Indopacific fishes. Uyeno, T., Arai, R., Taniuchi, T., Matsuura, K. (eds.). Ichthyological Society of Japan, pp. 133-139.

Claes, J. M. & Mallefet, J. (2008). Early development of bioluminescence suggests camouflage by counter-illumination in the velvet belly Lantern Shark *Etmopterus spinax* (Squaloidea: Etmopteridae). *Journal of Fish Biology*, 73, 1337-1350.

Claes, J. M. & Mallefet, J. (2009a). Ontogeny of photophore pattern in the velvet belly Lantern Shark, *Etmopterus spinax*. *Zoology*, 112, 433-441.

Claes, J. M. & Mallefet, J. (2009b). Hormonal control of luminescence from Lantern Shark (*Etmopterus spinax*) photophores. *Journal of Experimental Biology*, 212, 3684-3692.

Claes, J. M. & Mallefet, J. (2009c). Bioluminescence of sharks-a first synthesis. In: V. B. Meyer-Rochow (ed.) *Bioluminescence in focus-a collection of illumniating essays*, Trivandrum: Research Signpost, pp. 51-65.

Claes, J. M. & Mallefet, J. (2010a). Functional physiology of Lantern Shark (*Etmopterus spinax*) luminescent pattern: differential hormonal regulation of luminous zones. *Journal of Experimenatl Biology*, 213, 1852-1858.

Claes, J. M. & Mallefet, J. (2010b). The Lantern Shark's light switch: turning shallow water crypsis into midwater camouflage. *Biology Letters*, 6 (5), 685-687.

Claes, J. M., Aksnes, D. L. & Mallefet, J. (2010c). Phantom hunter of the fjords: Counterillumination in a shark, *Etmopterus spinax*. *Journal of Experimental Marine Biology and Ecology*, 388, 28-32.

Clarke, M. W., Borgess, L. & Officer, R. A. (2005). Comparisons of Trawl and Longline Catches of Deep-water Elasmobranchs West and North of Ireland. *Journal of Northwestern Atlantic Fisheries Science*, 35, 429-442.

Coelho, R. & Erzini, K. (2008a). Identification of deep-water Lantern Sharks (Chondrichthyes: Etmopteridae) using morphometric data and multivariate analysis. *Journal of the Marine Biological Association UK*, 88 (1), 199-204.

Coelho, R. & Erzini, K. (2008b). Life History of a wide-ranging deep-water Lantern Shark in the north-east Atlantic, *Etmopterus spinax* (Chondrichthyes: Etmopteridae), with implications for conservation. *Journal of Fish Biology*, 73, 1419-1443.

Compagno, L. J. V. (1973). Interrelationships of living elasmobranchs. In: Greenwood, P. H. *et al*. (eds.) *Interrelationships of fishes*. London: Academic Press, pp. 15-61.

Compagno, L. J. V. (1984). FAO species catalogue. Vol. 4. Sharks of the world. An annotated and illustrated catalogue of sharks species known to date. Part 1. Hexanchiformes to Lamniformes. *FAO Fisheries Synopsis*, 125 4 (1), pp. 1-249.

Compagno, L. J. V., Dando, M. & Fowler, S. (2005). A field guide to the Sharks of the World. London: Collins, pp 1-368.

Dalebout, M. L., Steel, D & Baker, S. (2008). Phylogeny of the Beaked Whale Genus *Mesoplodon* (Ziphiidae: Cetacea) Revealed by Nuclear Introns: Implications for the Evolution of Male Tusks. *Systematic Biology*, 57 (6), 857-875.

Devine, J. A., Baker, K. D. & Haedrich, R.L. (2006). Deep-sea fishes qualify as endangered. *Nature*, 439, 29.

Didier, D.A., 1995. Phylogenetic Systematics of Extant Chimaeroid Fishes (Holocephali, Chimaeroidei). American Museum Novitates, 3119, 1-86.

Didier, D.A., 2008. Two new species of the genus *Hydrolagus* Gill (Holocephali: Chimaeridae) from Australia. In: Last, P.R., White, W.T., Pogonoski, J.J. (eds.). *Descriptions of new Australian Chondrichthyans*. Hobart: CSIRO Publishing. pp. 349–356.

Didier, D.A., Last, P.R. & White, W.T., 2008. Three new species of the genus *Chimaera* Linnaeus (Chimaeriformes: Chimaeridae) from Australia. In: Last, P.R., White, W.T., Pogonoski, J.J. (eds.). *Descriptions of new Australian Chondrichthyans*. Hobart: CSIRO Publishing, pp. 327–340.

Drummond, A. J. & Rambaut, A. (2007). BEAST: Bayesian evolutionary analysis by sampling trees. *BMC Evolutionary Biology*, 7, 214.

Duhamel, G., Gasco, N. & Davaine, P. (2005). *Poissons des iles Kerguelen et Crozet. Guide regional de l'ocean Austral*, Paris: Museum national d'Histoire naturelle, pp. 62-64

Edgar, R. C. (2004). 'MUSCLE': multiple sequence alignment with high accuracy and high throughput. *Nucleic Acids Research*, 32, 1792-1797.

Eschmeyer, W.N. & Fricke, R. (eds.) (2010). Catalog of Fishes electronic version*:* http://research.calacademy.org/ichthyology/catalog/fishcatsearch.

Evanno, G., Regnaut, S. & Goudet, J. (2005). Detecting the number of clusters of individuals using the software STRUCTURE: a simulation study. *Molecular Ecology*, 14, 2611–2620.

Eldrett, J. S., Greenwood, D. R., Harding, I. C. & Huber, M. (2009). Increased seasonality through the Eocene to Oligocene transition in northern high latitudes. *Nature*, 459, 969-973.

Excoffier, L. G. L. & Schneider, S. (2005). Arlequin ver. 3.0: An integrated software package for population genetics data analysis. *Evolutionary Bioinformatics Online*, 1, 47-50.

Falush, D., Stephens, M. & Pritchard, J. K. (2003). Inference of population structure: Extensions to linked loci and correlated allele frequencies. *Genetics*, 164, 1567–1587.

Falush, D., Stephens, M. & Pritchard, J. K. (2007). Inference of population structure using multilocus genotype data: dominant markers and null alleles. *Molecular Ecology Notes*, 7, 574–578.

Foll, M. & Gaggiotti, O. E. (2008). A Genome-Scan Method to Identify Selected Loci Appropriate for Both Dominant and Codominant Markers: A Bayesian Perspective. *Genetics*, 180, 977-993.

Forrest, R. E. & Walters, C. J. (2009). Estimating thresholds to optimal harvest rate for long-lived, low-fecundity sharks accounting for selectivity and density dependence in recruitment. *Canadian Journal of Fish Aquatic Sciences*, 66, 2062-2080.

Garrick, J. A. F. (1960). Studies on New Zealand Elasmoranchii. Part XI. Squaloids of the genera *Deania*, *Etmopterus*, *Oxynotus* and *Dalatias* in New Zealand waters. *Transactions of the Royal Society of New Zealand*, 88, 489-517.

Golovan, G. A. & Pukhorukov, N. P. (1986). New Records of rare species of cartilaginous fishes. *Journal of Ichthyology*, 26, 117-120.

Grogan D. & Lund R. (2004). The origin and relationships of early Chondrichthyes. In: Carrier, J.C., Musick, J.A., Heithanus, M.R. (eds). *Biology of sharks and their relatives*. London: CRC Press, pp. 3–31.

Hall, T. A. (1999). BioEdit: a user-friendly biological sequence alignment editor and analysis program for Windows 95/98/NT. *Nucleic Acids Symposium Series*, 41, 95-98.

Hammer, Ø, Harper, D. A. T. & Ryan, P. D. (2001). PAST: Palaeontological Statistics software package for education and data analysis. *Palaeontologica Electronica*, 4 (1), 1-9.

Hardman, M. & Hardman, L. M. (2008). The Relative Influence of Body Size and Paleoclimatic Change as Explanatory Variables Influencing Lineage Diversification Rate: An Evolutionary Analysis of Bullhead Catfishes (Siluriformes: Ictaluridae). *Systematic Biology*, 57 (1), 116-130.

Helfman, G. S., Collette, B. B., Facey, D. E., Bowen, B. W. (2009). The diversity of fishes, 2nd ed. Oxford: Wiley-Blackwell.

Herder, F., Pfaender, J. & Schliewen, U. K. (2008). Adaptive sympatric speciation of polychromatic “roundfin” sailfin silverside fish in Lake Matano (Sulawesi). *Evolution*, 62, 2178-2195.

Hubbs, C. L., Iwai, T. & Matsubara, K. (1967). External and internal characters, horizontal and vertical distribution, luminescence, and food of the dwarf pelagic shark *Euprotomicrus bispinatus*. *Bulletin of the Scripps Institute of Oceanography of the University of California*, 10, 1-64.

Hubisz, M., Falush, D., Stephens, M. & Pritchard, J. (2009). Inferring weak population structure with the assistance of sample group information. *Molecular Ecology Resources*, 9, 1322-1332.

Hudson, R. & Knuckey, I. (2007). Estimates of the landed catch of mid-slope shark species 1992-2006. Paper presented to the Deep-water Shark Workshop, AFMA.

Huelsenbeck, J. P. & Ronquist, F. (2001). MRBAYES: Bayesian Inference of phylogenetic trees. *Bioinformatics*, 17, 754-755.

Huson, D. H. & Bryant, D. (2006). Application of Phylogenetic Networks in Evolutionary Studies. *Molecular Biology and Evolution*, 23, 254-267.

Iglésias, S. P., Lecointre, G. & Sellos, D. Y. (2005). Extensive paraphylies within sharks of the order Carcharhiniformes inferred from nuclear and mitochondrial genes. *Molecular Phylogenetics & Evolution*, 34, 569-583.

Iglésias, S. P., Toulhoat, L. & Sellos, D. Y. (2009). Taxonomic confusion and market mislabeling of threatened skates: important consequences for their conservation status. *Aquatic Conservation: Marine and Freshwater Ecosystems*, 20 (3), 319-333.

Inoue, J. G., *et al*. (2010). Evolutionary Origin and Phylogeny of the Modern Holocephalans (Chondrichthyes: Chimaeriformes): A Mitogenomic Perspective. *Molecular Biology and Evolution*, 27 (11), 2576-2586.

IUCN (2010). IUCN Red List of Threatened Species. Version 2010.1. www.iucnredlist.org.

Jakobsdottir, K. B. (2001). Biological aspects of two deep-water squalid sharks: *Centroscyllium fabricii* (Reinhardt, 1825) and *Etmopterus princeps* (Collett, 1904) in Icelandic waters. *Fisheries Research*, 51, 247-265.

Kemper, J. M., Ebert, D., Didier D. A. & Compagno L. J. V. (2010a). Description of a new species of chimaerid, *Chimaera bahamaensis* from the Bahamas (Holocephali: Chimaeridae). *Bulletin of Marine Science*, 86 (3), 649-659.

Kemper, J. M., Ebert, D., Compagno L. J. V. & Didier D. A. (2010b). *Chimaera notafricana* sp. nov. (Chondrichthyes: Chimaeriformes: Chimaeridae), a new species of Chimaera from Southern Africa. *Zootaxa*, 2532, 55-63.

Klimpel, S., Palm, H. W. & Seehagen, A. (2003). Metazoan parasites and food composition of juvenile *Etmopterus spinax* (L. 1758) (Dalatiidae, Squaliformes) from the Norwegian Deep. *Parasitological Research*, 89, 245-251.

Klug, S. & Kriwet, J. (2010). Timing of deep-sea adaptation in dogfish sharks: insights from a supertree of extinct and extant taxa. *Zoologica Scripta* 39, 331-342.

Kotlyar, A. N. (1990). Dogfish sharks of the genus *Etmopterus* Rafinesque from the Nazca and Sala y Gomez Submarine Ridges. *Trudy Instituta Okeanologii*, 125, 127-147.

Kriwet J. & Benton, M. (2004). Neoselachian (Chondrichthyes, Elasmobranchii) diversity across the C/T boundary. *Palaeogeography, Palaeoclimatology, Palaeoecology*, 214, 181–194.

Kyne, P.M. & Simpfendorfer, P. A. (2007). A collation and summarization of available data on deep-water Chondrichthyans: biodiversity, life history, and fisheries. A report prepared by the IUCN SSC Shark Specialist Group for the Marine Conservation Biology Institute, pp. 1-136.

Last, P.R., Burgess, G.H. & Séret B. (2002). Description of six new species of Lantern Sharks of the genus *Etmopterus* (Squaloidea: Etmopteridae) from the Australasian region. *Cybium*, 26, 203-223.

Last, P. R. & Stevens, J. D. (1994). Sharks and Rays of Australia. Hobart: CSIRO Publishing, pp. 1-513.

Last, P. R. & Stevens, J. D. (2009). Sharks and Rays of Australia. Cambridge: Harvard University Press, 2nd edition, pp. 1-554.

Lear, C. H., Bailey, T. R., Pearson, P. N., Coxall, H. K. & Rosenthal, Y. (2008). Cooling and ice growth across the Eocene-Oligocene transition. *Geology*, 36, 251-254.

Ledoux, J. C. (1972). Les Squalidae (Euselachii) miocenes des environs d'Avignon (Vaucluse). *Documents des Laboratoires de Geologie de la Facult des Sciences de Lyon, Notes et Memoires*, 52, 133-175.

Lindberg, D. R. & Pyenson, N. D. (2007). Things that go bump in the night: evolutionary interactions between cephalopods and cetaceans in the tertiary. *Lethaia*, 40, 335-343.

Luchetti, E. A., Iglésias, S. P. & Sellos, D. Y. (in press). *Chimaera opalescens* n. sp., a new chimaeroid (Chondrichthyes : Holocephali) from the Northeastern Atlantic. *Journal of Fish Biology*.

Maisey, J. G., Naylor G. J. P. & Ward, D. J. (2004). Mesozoic elasmobranchs, neoselachian phylogeny and the rise of modern elasmobranch diversity. In: Arratia G., Tintori A. (eds.), *Mesozoic Fishes 3– Systematics, Palaeoenvironments and Biodiversity*. Munich: Verlag Dr. Friedrich Pfeil, pp. 17-56.

Meudt, H. M. & Clarke, A. C. (2007). Almost forgotten or latest practice? AFLP applications, analyses and advances. *TRENDS in Plant Science*, 12, 106-117.

Misof, B. & Misof, K. (2009). A Monte Carlo approach successfully identifies randomness of multiple sequence alignments: A more objective means of data exclusion. *Systematic Biology*, 58, 21-34.

Müller, A. & Schöllmann L. (1989). Neue Selachier (Neoselachii, Squalomorphii) aus dem Campanium Westfalens (NW-Deutschland). *Neues Jahrbuch für Geologie und Paläontologie*, *Abhandlungen*, 178, 1-35.

Naylor, G. J. P., Ryburn J. A., Fedrigo O. & Lopez A. (2005). Phylogenetic Relationships among the Major Lineages of Modern Elasmobranchs. In: Hamlett, W. C. (ed.) *Reproductive Biology and Phylogeny of Chondrichthyes; sharks, batoids, and chimaeras*. Enfield: Science Publishers Inc., pp. 1-25.

Neiva, J., Coelho, R. & Erzini, K. (2006). Feeding habits of the velvet belly Lantern Shark *Etmopterus spinax* (Chondrichthyes: Etmopteridae) off the Algarve, southern Portugal. *Journal of the Marine Biological Association of the United Kingdom*, 86, 835–841.

Pritchard, J. K., Stephens, M. & Donnelly, P. (2000). Inference of population structure using multilocus genotype data. *Genetics*, 155, 945–959.

Reif, W. E. (1985). Functions of Scales and Photophores in Mesopelagic Luminescent Sharks. *Acta Zoologica-Stockholm*, 66 (2), 111–118.

Renner, S. (2005). Relaxed molecular clocks for dating historical plant dispersal events. *TRENDS in Plant Science*, 10 (11), 550-558.

Sanderson, M. J. (2002). Estimating absolute rates of molecular evolution and divergence times: A penalized likelihood approach. *Molecular Biology and Ev*olution, 19, 101–109.

Sanderson, M. J. (2003). r8s: inferring absolute rates of molecular evolution and divergence times in the absence of a molecular clock. *Bioinformatics*, 19, 301-302.

Schaaf da Silva, J. A. & Ebert D. (2006). *Etmopterus burgessi* sp. nov., a new species of Lantern Shark (Squaliformes: Etmopteridae) from Taiwan. *Zootaxa*, 1273, 53-64.

Shirai, S. (1992). Squalean Phylogeny. A new framework of “squaloid” sharks and related taxa. Hokkaido: Hokkaido University Press, pp. 1 – 151.

Shirai, S. & Nakaya, K. (1990a). A new squalid species of the genus *Centroscyllium* from the Emperor Seamount Chain. *Japanese Journal of Ichthyology*, 36, 391–398.

Shirai, S. & Nakaya, K. (1990b). Interrelationships of the Etmopteridae (Chondrichtyes, Squaliformes). In: Pratt H.L. JR., Gruber S.H., Taniuchi T. (eds.). Elasmobranchs as Living Resources: Advances in Biology, Ecology, Systematics and the status of the fisheries. *NOAA Technical report*, 90, 347-356.

Shirai, S., & Tachikawa H. (1993). Taxonomic resolution of the *Etmopterus pusillus* species group (Elasmobranchii, Etmopteridae) with description of *E. bigelowi*, n. sp.. *Copeia,* 2, 483-495.

Siverson, M. (1993). Maastrichthian squaloid sharks from southern Sweden. *Palaeontology*, 36 (1), 1-19.

Stamatakis, A. (2006). RAxML–VI-HPC: Maximum Likelihood-based phylogenetic analyses with thousands of taxa and mixed models. *Bioinformatics*, 22 (21), 2688-2690.

Straube N., Iglésias S. P., Sellos D. Y., Kriwet J. & Schliewen U. K. (2010) Molecular Phylogeny and Node Time Estimation of Bioluminescent Lantern Sharks (Elasmobranchii: Etmopteridae). *Molecular Phylogenetics & Evolution*, 56, 905–917.

Straube N., Kriwet J. & Schliewen U. K. (2011). Cryptic diversity and species assignment of large Lantern Sharks of the *Etmopterus spinax* clade from the Southern Hemisphere (Squaliformes, Etmopteridae). *Zoologica Scripta*, 40 (1), 61-75

Straube, N., Schliewen, U. K. & Kriwet, J. (2008). Dental Structure of the Giant Lantern Shark, *Etmopterus baxteri* (Chondrichthyes: Squaliformes) and its taxonomic implications. *Environmental Biolology of Fishes*, 82, 133-141.

Swofford, D. L. (2003). PAUP*. Phylogenetic analysis Uing Parsimony (*and Other Methods). Version 4. Sinauer Associates, Sunderland, Massachusetts.

Tachikawa, H., Taniuchi, T. & Ryoichi, A. (1989). *Etmopterus baxteri*, a junior synonym of *E. granulosus* (Elasmobranchii, Squalidae). *Bulletin of the Natural Science Museum of Tokyo*, 15, 235-241.

Underwood, C. J. & Mitchell, S. F. (1999). Albian and Cenomanian selachian assemblages from North-east England. *Special Papers in Palaeontology*, 60, 9-56.

UNESCO (2009). Global Open Oceans and Deep Seabed (GOODS) bioregional classification. In M. Vierros, I. Cesswell, B. E. Escobar, J. Rice & J. Ardron (eds) *UNESCO-IOC, IOC Technical Series,* pp. 84-89.

Van de Peer, Y. & De Wachter, R. (1994). TREECON for Windows: a software package for the construction and drawing of evolutionary trees for the Microsoft Windows environment. *Computer Applications in the Biosci*ences, 10, 569-570.

Venkatesh, *et al*. (2007). Survey sequencing and comparative analysis of the elephant shark (*Callorhinchus milii*) genome. PLoS Biology 5 (4): e 101. doi: 10.1371/journal.pbio.0050101.

Verissimo, A., MacDowell, J. & Graves, J. E. (2010). Global population structure of the spiny dogfish *Squalus acanthias*, a temperate shark with an antitropical distribution. *Molecular Ecology*, 19, 1651-1662.

Vos, P. *et al*. (1995). AFLP: a new technique for DNA fingerprinting. *Nucleic Acids Research*, 23, 4407-4414.

Ward, R. D., Zemlak, T. S., Innes, B. H., Last, P. R. & Hebert, D. N. (2005). DNA barcoding Australia's fish species. *Philosophical Transactions of the Royal Society of London - Series B: Biological Sciences*, 360, 1847-1857.

Ward, R. D., Holmes, B. A., Zemlak, T. S. & Smith, P. J. (2007). Part 12-DNA barcoding discriminates spurdogs of the genus *Squalus*. In: Last, P. R., White, W. T., Pogonoski J. J. (eds.). Descriptions of new dogfishes of the genus *Squalus* (Squaloidea: Squalidae). *CSIRO Marine and Atmosspheric Research Paper,* 14, 114-130.

Warnock, W. G., Rasmussen, J. B. & Taylor, E. B. (2009). Genetic clustering methods reveal bull trout (*Salvelinus confluentus*) fine-scale population structure as a spatially nested hierarchy. *Conservation Genetics*, 11 (4), 1421-1433.

Wetherbee, B. M. (1996). Distribution and reproduction of the southern Lantern Shark from New Zealand. *Journal of Fish Biology*, 49, 1186-1196.

Wetherbee, B. M. (2000). Assemblage of deep sea sharks on Chatham Rise, New Zealand. *Fish Bulletin*, 98, 189-198.

White, W. T., Ebert, D. A. & Compagno, L. J. V. (2008). Description of two new species of gulper sharks, genus *Centrophorus* (Chondrichthyes: Squaliformes: Centrophoridae) from Australia. In: P. R. Last, W. T. White & J. J. Pogonoski (eds.) *Descriptions of New Australian Chondrichthyans*. CSIRO Marine and Atmospheric Research Paper, 22, 1-22

Widder, E. (1998). A predatory use of counter illumination by the squaloid shark, *Isistius brasiliensis*. *Environmental Biology of Fishes*, 53, 267-273.

Yamakawa, T., Taniuchi, T. & Nose, Y. (1986). Review of the *Etmopterus lucifer* Group (Squalidae) in Japan. In: Uyeno T., Arai R., Taniuchi T. & Matsuura K. (eds.), Indo-Pacific Fish Biology: Proceedings of the Second International Conference on Indo-Pacific fishes. Ichthyological Society of Japan, Tokyo, 197-207.

Yano, K. (1997). First record of the Brown Lantern Shark, *Etmopterus unicolor*, from the waters around New Zealand, and comparison with the Southern Lantern Shark, *E. ganulosus*. *Ichthyological Research*, 44, 61-72.

Zhu, M., Zhao, W., Jia, L., Lu, J., Qiao, T. & Qu, Q. (2009). The oldest articulated osteichthyan reveals mosaic gnathostome characters. *Nature*, 458, 469-474.

9 Curriculum Vitae

Personal Details:

Prename: Nicolas
Surname: Straube

Professional background:

11.2006 – 01.2010:	Graduate assistant in the research project "**Evolution and adaptive radiation of Dogfish Sharks (Chondrichthyes, Squaliformes)**"
05.2005 – 01.2006:	Diploma thesis "**Statistical and shape analyses of dental characters of the deep-sea shark *Etmopterus baxteri* (Chondrichthyes, Squaliformes) with comments on its taxonomic status**"
10.2000 – 04.2005:	Study of Biology at the LMU, Munich, Germany.

10 Appendix

Article I

STRAUBE N., IGLÉSIAS S. P., SELLOS D. Y., KRIWET J. & SCHLIEWEN U. K. (2010) Molecular Phylogeny and Node Time Estimation of Bioluminescent Lantern Sharks (Elasmobranchii: Etmopteridae). *Molecular Phylogenetics & Evolution*, 56, 905–917. doi:10.1016/j.ympev.2010.04.042

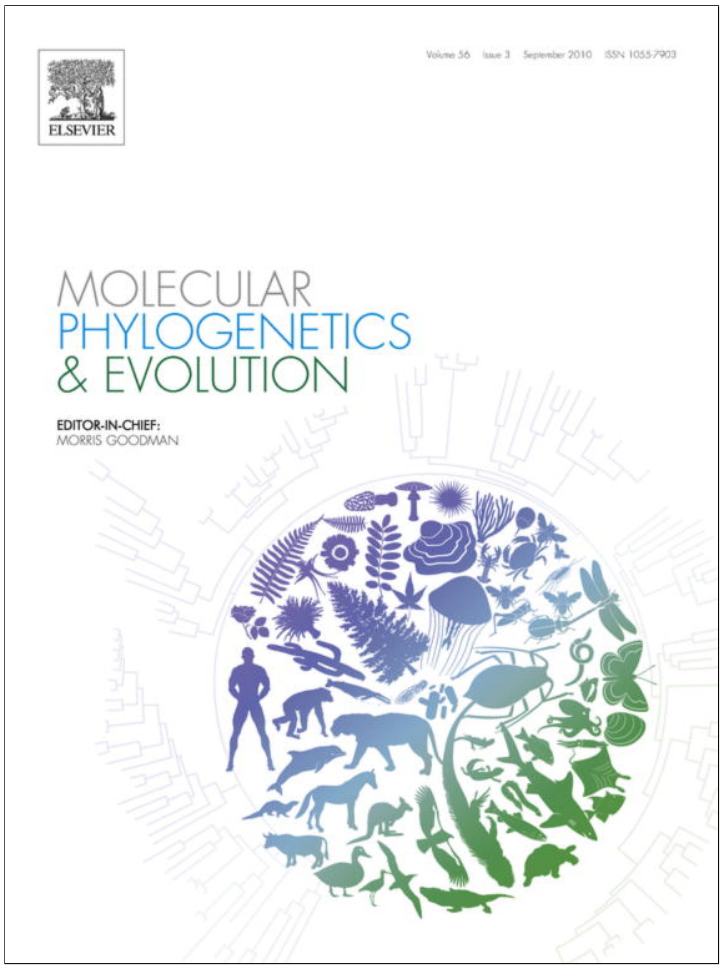

Molecular Phylogenetics and Evolution 56 (2010) 905–917

Contents lists available at ScienceDirect

Molecular Phylogenetics and Evolution

journal homepage: www.elsevier.com/locate/ympev

Molecular phylogeny and node time estimation of bioluminescent Lantern Sharks (Elasmobranchii: Etmopteridae)

Nicolas Straube [a,*], Samuel P. Iglésias [c], Daniel Y. Sellos [c], Jürgen Kriwet [b], Ulrich K. Schliewen [a]

[a] Zoologische Staatssammlung München, Sektion Ichthyologie, Münchhausenstraße 21, 81247 München, Germany
[b] Staatliches Museum für Naturkunde Stuttgart, Sektion Paläontologie, Rosenstein 1, 70191 Stuttgart, Germany
[c] Muséum national d'Histoire Naturelle, Département Milieux et Peuplements aquatiques, USM 0405, Station de Biologie Marine de Concarneau and UMR 7208 CNRS/MNHN/IRD/UPMC, Biologie des Organismes et Ecosystèmes Aquatiques, 29182 Concarneau cedex, France

ARTICLE INFO

Article history:
Received 15 October 2009
Accepted 20 April 2010
Available online 10 May 2010

Keywords:
Squaliformes
Phylogenetics
Molecular clock
Cryptic diversity
Deep-sea

ABSTRACT

Deep-sea Lantern Sharks (Etmopteridae) represent the most speciose family within Dogfish Sharks (Squaliformes). We compiled an extensive DNA dataset to estimate the first molecular phylogeny of the family and to provide node age estimates for the origin and diversification for this enigmatic group. Phylogenetic inferences yielded consistent and well supported hypotheses based on 4685 bp of both nuclear (RAG1) and mitochondrial genes (COI, 12S-partial 16S, tRNAVal and tRNAPhe). The monophyletic family Etmopteridae originated in the early Paleocene around the C/T boundary, and split further into four morphologically distinct lineages supporting three of the four extant genera. The exception is *Etmopterus* which is paraphyletic with respect to *Miroscyllium*. Subsequent rapid radiation within *Etmopterus* in the Oligocene/early Miocene was accompanied by divergent evolution of bioluminescent flank markings which morphologically characterize the four lineages. Higher squaliform interrelationships could not be satisfactorily identified, but convergent evolution of bioluminescence in Dalatiidae and Etmopteridae is supported.

1. Introduction

Lantern Sharks (Etmopteridae) are a highly diverse family of poorly known bioluminescent deep-sea elasmobranchs with 43 species in five genera (Compagno et al., 2005; Schaaf da Silva and Ebert, 2006). Although they represent the largest family of Squaliformes or Dogfish Sharks, it is one of the least studied among the order and very few data on their biology, life history, conservation and phylogenetics have been gathered. Etmopterids are rather small sharks including the smallest known shark, *Etmopterus perryi* (20 cm). The largest member *Centroscyllium fabricii* reaches a total length of 107 cm. Members of the family are distributed panoceanic in depths between 50 and 4500 m at slope regions. Their body is more or less densely covered with etmopterid specific hook-like or conical dermal denticles. Quite a few species had been known only from few specimens, but increased deep-sea fisheries recently yielded additional specimens of some rare species as well as from several undescribed species highlighting both the diversity of the family as well as the vulnerability of these longliving and slowly reproducing ovoviviparous sharks, which give birth to only 6–14 pups per litter (Compagno et al., 2005). Most detailed biological studies that have been published until now concentrate on a single Atlantic species, *Etmopterus spinax* (Claes and Mallefet, 2008, 2009; Coelho and Erzini, 2008a,b; Klimpel et al., 2003; Neiva et al., 2006).

Bioluminescence is a wide-spread phenomenon among inhabitants of the subphotic zone, but its occurrence is limited among sharks to only two squaliform families, the Dalatiidae and Etmopteridae. Photophores of etmoperids are concentrated on the dark ventral region and on more or less prominent and often species specific dark flank and tail markings. Claes and Mallefet (2008) suggest a function of camouflage by counter illumination for the numerous ventral photophores in *E. spinax*. Further studies suggest the elaborate flank and tail markings to function for intraspecific signalling i.e. as schooling aid (e.g. Reif, 1985; Claes and Mallefet, 2009).

The fossil record of Etmopteridae is comparatively poor and the phylogenetic assignment of extinct species is often difficult. The reason is, that articulated fossils of etmopterids are unknown so far and fossilized single teeth represent the only direct window of information to their past. The unambiguously oldest fossil teeth of Etmopteridae are known from the Eocene (Lutetian 48.6–40.4 Ma) and strongly resemble those of extant species (Adnet, 2006; Adnet et al., 2008; Cappetta and Adnet, 2001; Cigala, 1986; Ledoux, 1972). Fossils such as *Eoetmopterus* (Müller and Schöllmann, 1989), *Proetmopterus* (Siverson, 1993) and *Microetmopterus*

* Corresponding author. Fax: +49(0)898107300.
E-mail addresses: straube@zsm.mwn.de (N. Straube), Iglesias@mnhn.fr (S.P. Iglésias), sellos@mnhn.fr (D.Y. Sellos), kriwet.smns@naturkundemuseum-bw.de (J. Kriwet), schliewn@zsm.mwn.de (U.K. Schliewen).

1055-7903/$ - see front matter © 2010 Elsevier Inc. All rights reserved.
doi:10.1016/j.ympev.2010.04.042

(Siverson, 1993) have been assigned to Etmopteridae based on their tooth morphology, but nevertheless show only minor or very generalized similarities, respectively, to extant species' tooth morphologies. These species apparently went extinct by the end of the Cretaceous (Adnet et al., 2006). Their former habitat is debated, but interestingly they may not have been inhabitants of the bathyal environment adopted by extant species of Etmopteridae (Adnet et al., 2006). Therefore, and because the systematic assignment of these extinct species is not soundly demonstrated, the phylogenetic position of the latter within Squaliformes and especially their unambiguous assignment to Etmoperidae remains to be tested.

Not only the limitation of the fossil record to teeth, but also the low density of phylogenetically informative morphological characters (including tooth characters) have prevented a detailed phylogenetic investigation of the family. Additional practical limitations have arisen due to the scarcity of specimens available, which renders sampling efforts extremely difficult, e.g. availability of *Trigonognathus*.

Alternative characteristic dentition types of Etmopteridae have helped diagnosing genera rather than elucidating inter- and intrageneric phylogenetic relationships. Dentitions in etmopterids include a wide array of types. *Etmopterus* and juvenile *Miroscyllium sheikoi* are characterized by a "cutting–clutching type", whereas the dentition of *Centroscyllium, Aculeola* and adult *Miroscyllium sheikoi* is of the "clutching type". The "tearing type" dentition within etmopterids is restricted to *Trigonognathus* (Adnet et al., 2006). These unique types of dentition also allow identification of extinct Etmopteridae to genus level but provide little or often ambiguous information for species identification due to ontogenetic and sexual dimorphisms (Straube et al., 2008). Consequently, identification, classification and partially phylogenetics of the most speciose Lantern Shark genus *Etmopterus* (approx. 32 species (Compagno et al., 2005)) are based mainly on the shape of flank markings and the arrangement and shape of placoid scales (e.g. Compagno et al., 2005; Last et al., 2002; Schaaf da Silva and Ebert, 2006; Shirai and Nakaya, 1990a). Their characterists diagnose several species groups within the genus, i.e. (1) the "*Etmopterus lucifer* group" (Yamakawa et al., 1986), including all species with rows of hook-like denticles, (2) the "*Etmopterus pusillus*" group comprising *E. bigelowi* and *E. pusillus* displaying conical dermal denticles (Shirai and Tachikawa, 1993), and the (3) "*Etmopterus splendidus*" group, consisting of species, which show similarities in the shape of flank markings as well as arrangement of dermal denticles (Last et al., 2002). The monotypic etmopterid genera *Trigonognathus, Miroscyllium* and *Aculeola* each display genus-specific morphological features, such as highly protrudable jaws armed with characteristically shaped, single-cusped teeth without lateral cusplets (*Trigonognathus*), small and slender erect teeth in both jaws (*Aculeola*), or a combination of a "cutting–clutching type" dentition in subadults, and a "clutching type" dentition in adults (*Miroscyllium*). *Centroscyllium* includes seven described species with a dignathic homodont dentition, displaying morphologically highly similar teeth in both jaws. Further characters are differently shaped and sparsely spaced dermal denticles, and no conspicuous flank markings with the exception of *Centroscyllium ritteri*.

First efforts to understand the intrarelationships of Etmopteridae were carried out by Shirai and Nakaya (1990b) based on 15 osteological and myological characters of 14 species representing four genera. In this study, the authors defined the new genus *Miroscyllium* for *Centroscyllium sheikoi* based on morphological characters that combine both genera, *Etmopterus* and *Centroscyllium*. The sample size was increased to 19 described species in Shirai's Squalean phylogeny (1992) now also including the rare *Trigonognathus*. This latter study confirmed the monophyly of the four analyzed etmopterid genera within Squaliformes as previously suggested by Compagno (1973, 1984) and Cadenat and Blache (1981) and placed *Trigonognathus* as sister to *Aculeola* and *Centroscyllium*. Although being an important step forwards, further intragroup relationships especially with regard to the speciose genus *Etmopterus* could not be resolved and re-examinations of Shirai's dataset (1992) by Carvalho and de Maisey (1996) and Adnet and Cappetta (2001) led to different results (Adnet et al., 2006).

The large and continuously increasing species number within Etmopteridae, one of the most diverse families within Chondrichthyes, as well as a number of unresolved questions related to their biology and radiation provoked us to apply DNA based molecular phylogenetics to a new and extensive worldwide sampling of etmopterids to provide 20 years after Shirai and Nakaya's (1990b) initial study new insights into the taxonomy and evolution of these still poorly known family of bioluminescent deep-sea sharks. Specifically, we compiled an extensive DNA dataset to (1) identify the sister-group of Etmopteridae among Squaliformes, to (2) test for the monophyly of Etmopteridae and for the (3) independent development of bioluminescence within Squaliformes, to (4) test for the monophyly of each of the two polytypic etmopterid genera, to (5) test for a Lower Eocene origin of Etmopteridae as indicated by the fossil record, to (6) analyse sequential versus rapid speciation in the course of the speciose etmopterid radiation and (7) compare our molecular phylogeny with results based on morphological analyses.

2. Material and methods

2.1. Taxon sampling

Tissue samples were obtained from museum tissue collections or recently collected during deep-sea commercial fisheries or during fisheries monitoring programs and represent 26 of the extant 43 etmopterid species plus 13 samples being either unidentified or identification is preliminary. Species missing for a complete taxon sampling of extant Etmopteridae were too difficult to attain, since they are only known from very few specimens and remote locations (e.g. Springer and Burgess, 1985; Kotlyar, 1990). However, our sampling includes all five genera traditionally assigned to Etmopteridae and all previously identified species groups are well represented. In addition, representatives of the remaining five squaliform families Centrophoridae, Oxynotidae, Somniosidae, Dalatiidae, and Squalidae as well as Echinorhinidae were included in our analyses. *Odontaspis ferox* (Lamnidae), *Apristurus longicephalus* (Pentanchidae as defined in Iglésias et al., 2005) and *Chimaera* sp. (Chimaeridae) were chosen as chondrichthyan outgroups. For a list of all included species, specimen vouchers and Genbank Accession Numbers see Supplementary Material 1.

2.2. DNA-extraction, locus sampling, PCR and sequencing

Total genomic and mitochondrial DNA was extracted from muscle tissue or fin clips either preserved in 96% ethanol or 20% DMSO salty solution using the QIAmp tissue Kit (Qiagen®, Valencia, CA).

We targeted partial fragments of one nuclear gene and four mitochondrial loci, which provide sufficient phylogenetic signals for both ancient and more recent divergence in elasmobranchs (compare Iglésias et al., 2005; Maisey et al., 2004; Naylor et al., 2005; Ward et al., 2005; Ward et al., 2007): a portion of the nuclear RAG1 gene (1454 bp), portion of the mitochondrial gene Cytochrome Oxidase I (COI, 655 bp) which is established as potential "barcoding gene" for identifying species of sharks (e.g. Ward et al., 2005; Ward et al., 2007), partial tRNA-Phe, the full 12S rRNA and partial 16S rRNA including the Valine tRNA (2606 bp when aligned). All loci were amplified using PCR following the protocol of Iglésias et al. (2005). PCR products were cleaned using the

QIAquick PCR Purification Kit (Qiagen®, Valencia, CA) after the manufacturer's protocol. Cycle sequencing was performed using ABI Big Dye 3.1 chemistry (PE Applied Biosystems®, Foster City, CA). If necessary, internal sequencing primers were designed for attaining sequences from problematic samples. A summary of primers used in this study is given in Table 1.

2.3. Phylogenetic analyses

2.3.1. Alignment

Sequences were edited using the BioEdit software version 7.0.9 (Hall, 1999) and aligned with MUSCLE 3.6 (Edgar, 2004). Aliscore v.0.2 was used to check aligned single loci for ambiguous alignment positions (Misof and Misof, 2009). All loci were aligned separately and combined afterwards with BioEdit. For analysing homogeneity of base frequencies a X^2-test was performed with PAUP* v4b10 (Swofford, 2003). Phylogenetic analyses were conducted on the smallest resulting sequenced fragments homologous to all taxa which match an overall sequence size of 4685 bp per specimen. The first 1437 bp are portion of the RAG1 gene, following 2594 bp representing non-protein coding mtDNA fragments and the last 654 bp of the concatenated multigene alignment were attained from the coding mitochondrial COI gene. Confirmation of aligned single loci for coding RAG1 and COI was done by translating sequences into amino acids. Ambiguous sites in sequences, attributed to double peaks in the electropherogram were coded referring to IUB symbols. Transition and transversion rates (ts–tv) among third codon positions of coding gene regions were examined by comparing absolute distances in PAUP* (Swofford, 2003).

2.3.2. Maximum parsimony (MP)

MP analyses were carried out using PAUP* and the heuristic search option using the tree bisection reconnection branch swapping algorithm (tbr), which adds sequences of taxa randomly. A limit of 100 rearrangements was set, parsimony uninformative characters were excluded from the analyses, gaps were treated as missing data and characters were not weighted. We performed non-parametric bootstrapping with 1000 bootstrap replicates and 10 random additions.

2.3.3. Model selection using Bayes' factor test (BFT)

To test our dataset for suitable substitution models and corresponding partitioning avoiding over-parameterisation, a Bayes' Factor Test was conducted with MRBAYES (v3.1.2 Huelsenbeck and Ronquist, 2001; Nylander et al., 2004). Eight different partition strategies were tested for their best-fitting model or model combinations, respectively. Bayes' factors were computed calculating harmonic means with 100 bootstrap replicates. Analyses of likelihoods attained with MRBAYES were performed with Tracer v1.4

Table 1
Primers used for amplification and sequencing.

Primer	Sequence 5′–3′	Length (bp)	Forward/reverse	PCR	Sequencing	Site of fixation	Area
Chon-Mito-S003[a]	TCTCTGTGGCAAAAGAGTGG	20	F	X	X	1421–1440	Non-coding mtDNA
Chon-Mito-S005[a]	AGGCAAGTCGTAACATGGTAAG	22	F	X	X	0988–1009	Non-coding mtDNA
Chon-Mito-R008[a]	CCACTCTTTTGCCACAGAGA	20	R		X	1421–1440	Non-coding mtDNA
Chon-Mito-S009[a]	CACGAGAGTTTAACTGTCTCT	21	F		X	2158–2178	Non-coding mtDNA
Chon-Mito-R010[a]	TAGAGACAGTTAAACTCTCGT	21	R		X	2159–2179	Non-coding mtDNA
Chon-Mito-S014[a]	AGTGGGCCTAAAAGCAGCCA	20	F		X	1665–1684	Non-coding mtDNA
Chon-Mito-R017[a]	ATCCAACATCGAGGTCGTAAACC	23	R		X	2526–2548	Non-coding mtDNA
Chon-Mito-S032[b]	AAG(CT)AT(AG)GCACTGAAGATGCTA	22	F	X	X	0020–0041	Non-coding mtDNA
Chon-Mito-S033[b]	ACTAGGATTAGATACCCTACTATG	24	F	X	X	0505–0528	Non-coding mtDNA
Chon-Mito-R034[b]	CGCCAAGTCCTTTGGGTTTTAAGC	24	R	X	X	0596–0619	Non-coding mtDNA
Chon-Mito-R035[b]	(CT)CCGGTCCTTTCGTACTAGG	20	R		X	2670–2689	Non-coding mtDNA
Chon-Mito-S037[b]	TGACCGTGC(AG)AAGGTAGCGTAATC	24	F		X	2098–2121	Non-coding mtDNA
Chon-Mito-R038[b]	TCTTC(CT)C(AC)CTCTTTTGC(AC)ACAGAG	24	R		X	1422–1445	Non-coding mtDNA
Chon-Mito-R039[b]	CAG(AG)TGGCTGCTT(CT)TAGGCC(CT)ACT	24	R		X	1665–1688	Non-coding mtDNA
Chon-Mito-R041[b]	(CT)CCGGTCCTTTCGTACT(AG)GG	20	R	X	X	2670–2698	Non-coding mtDNA
Chon-Mito-S043[b]	AGACGAGAAGACCCTATGGAGCTT	24	F		X	2233–2256	Non-coding mtDNA
Chon-Mito-R044[b]	AAGCTCCATAGGGTCTTCTCGTCT	24	R		X	2233–2256	Non-coding mtDNA
Fish F2 Barcode[c]	TCGACTAATCATAAAGATATCGGCAC	26	F	X	X	6448–6474	mtDNA, COI
Fish R2 Barcode[c]	ACTTCAGGGTGACCGAAGAATCAGAA	26	R	X	X	7152–7127	mtDNA, COI
S0156 Barcode[b]	TAGCTGATGAATCTGACCGTGAAAC	25	F	X	X	5458–5491	mtDNA, COI
R084 Barcode[b]	TGAACGCCAGATTTCATAGCGTTC	24	R	X	X	6177–6204	mtDNA, COI
Chon-Rag1-S018[a]	ACAGTCAAAGCTACTAC(AG)GGGA	22	F	X	X	2576–1597	nDNA, RAG1
Chon-Rag1-S019[a]	TGGCAGATGAATCTGACCATGA	22	F	X	X	2096–2117	nDNA, RAG1
Chon-Rag1-S020[a]	TGTGAACTGAT(CT)CCATCTGAAG	22	F		X	2719–2740	nDNA, RAG1
Chon-Rag1-R021[a]	AATATTTTGAAGTGTACAGCCA	22	R		X	3094–3115	nDNA, RAG1
Chon-Rag1-R022[a]	CTGAAACCCCTTTCACTCTATC	22	R		X	2440–2461	nDNA, RAG1
Chon-Rag1-R023[a]	CCCATTCCATCACAAGATTCTT	22	R		X	1904–1925	nDNA, RAG1
Chon-Rag1-S024[a]	CAGATCTTCCAGCCTTTGCATGC	23	F	X	X	1600–1622	nDNA, RAG1
Chon-Rag1-R025[a]	TGATG(CT)TTCAAAATG(CT)CTTCCAA	23	R		X	3070–3092	nDNA, RAG1
Chon-Rag1-S026[a]	TTCC(TA)GCCTTTGCA(CT)GCACTCCG	23	F	X	X	1606–1628	nDNA, RAG1
Chon-Rag1-S027[a]	GAGA(CT)TCTCAGAGAGTTAATGCA	23	F		X	2749–2771	nDNA, RAG1
Chon-Rag1-R028[a]	GT(CT)TCATGGTCAGATTCATC(CT)GC	23	R		X	2098–2120	nDNA, RAG1
Chon-Rag1-R029[a]	AGTGTACAGCCA(AG)TGATG(CT)TTCA	23	R	X	X	3083–3105	nDNA, RAG1
Chon-Rag1-S030[a]	GTGAG(AG)TATTCCTT(CT)AC(AC)ATCATG	24	F		X	1975–1998	nDNA, RAG1
Chon-Rag1-S031[a]	GA(AG)CGCTATGAAAT(CT)TGGCGTTCA	24	F		X	2383–2406	nDNA, RAG1
Chon-RAG1-S-trigo[d]	GTGTAAGTGTGATGAATGA	19	F		X	1666–1684	nDNA, RAG1
Chon-RAG1-R-trigo[d]	ACATAGCGTTCCAAGTTCTC	20	R		X	2374–2393	nDNA, RAG1
Chon_RAG1-R019[d]	TCATGGTCAGATTCATCTGCCA	22	R	X	X	2096–2117	nDNA, RAG1

[a] Primers from Iglésias et al. (2005).
[b] The position of the primers refers to the 5′–3′ position in the complete mitochondrial genome sequence of *Amblyraja radiata* (GenBank Accession No. NC_000893.1).
[c] Primers from Ward et al. (2005).
[d] Internal PCR and sequencing primers designed for this study.

(http://beast.bio.ed.ac.uk). Bayes' factors favoured a partition of the data for ML and Bayesian phylogenetic analyses into (1) a single partition for RAG1, (2) a single partition for the large ribosomal mitochondrial fragment encompassing tRNA-Phe, 12S rRNA, 16S rRNA and the valine tRNA, and (3) two further partitions for COI, one for a combined 1st and 2nd position and one for the third codon position. For RAG1 and 3rd codon position of COI, the HKY Gamma substitution model revealed highest likelihood scores, whereas for the large ribosomal fragment and COI 1st and 2nd positions the GTR Gamma model was favoured.

2.3.4. Maximum likelihood (ML)

ML analyses were performed using RaxML ver. 7.0.3 (Stamatakis, 2006). A hill-climbing algorithm is used for analyses using the GTR Gamma nucleotide substitution model. Several runs were conducted to avoid local maxima in the space of trees. The partition scheme follows results attained from the Bayes' Factor test (see Section 2.3.3). Initially, runs were carried out using the RaxML option of automatically generated MP starting trees. Maximum likelihoods of fixed initial rearrangement settings were compared with likelihoods obtained from automatically generated settings. Rate category number was set to 25 after testing values of 10–55 in steps of five rate categories as recommended in the RaxML manual. For attaining support values for nodes in the ML tree, bootstrapping was performed with 150 bootstrap replicates after assessment of a reasonable number of bootstrap replicates (Pattengale et al., 2009) using the option to search for an adequate number of bootstrap replicates implemented in RaxML v7.1.0. Branches showing bootstrap support below 50% were collapsed. Analyses were performed for single loci, nuclear versus mitochondrial, and combined datasets.

2.3.5. Bayesian phylogenetic analyses

MRBAYES v3.1.2 software was used for Bayesian phylogenetic reconstruction under a partitioning scheme as described under Section 2.3.3. Two independent analyses were performed under the option of random starting trees and four simultaneous Markov Chains (three heated and one cold chain). Trees were sampled every 1000 generations in an overall run of 10.000.000 generations. After checking the likelihood values with the plot option of MRBAYES, the first 25% of generations were discarded as burn-in and a 50% majority rule consensus tree was computed from trees showing likelihoods of stationarity. Again, analyses were performed for single loci, nuclear versus mitochondrial and concatenated datasets.

2.3.6. Node age reconstruction based on fossil calibration points

Several problems appear when searching for suitable fossils as calibration points for implementing a meaningful molecular clock approach in an etmopterid phylogeny. On the one hand fossil remains of etmopterids comprise fossilized teeth only and few studies exist dealing with the identification of general morphological tooth characteristics for identifying genera (Adnet and Cappetta, 2001; Kriwet and Klug, 2010; Straube et al., 2008). On the other side, dating of geological strata including fossil remains of Etmopteridae are partially debatable (Adnet et al., 2006). Therefore we used only a set of five comparatively undebatable fossil calibration points. The five calibration points are stated in the following as mean ages of stratigraphic ranges and represent minimum ages. Our first point provides a minimum age for the root of the tree using the first unambiguous chimaeroid fossil dated to 374.5 Ma in the late Devonian (Venkatesh et al., 2007; Benton and Donoghue, 2007). Further, we restricted the minimum age of Squaliformes to a time window of 130–125 Ma ago in the early Cretaceous, as indicated by fossil findings of teeth of *Protosqualus* (Cappetta, 1987), apparently the oldest known representative of Squaliformes suggested by its tooth root morphology (Kriwet and Klug, 2010) and assuming that *Protospinax* is not a squaliform shark (Kriwet and Klug, 2004). Further calibration points within Squaliformes comprise the minimum age of *Centroscymnus* ranging from 83.5 to 70.6 Ma (Thies and Müller, 1993) and *Centrophoridae* with 70.6 to 65.5 Ma referring to articulated fossils from Sahel Alma, Lebanon (Cappetta, 1987) displaying the desired clear linkage to extant species. Finally, the age of *Trigonognathus/Etmopterus* was set to a mean minimum age of 44.5 Ma in the Eocene as indicated by fossil teeth of *Trigonognathus virginiae*, which are morphologically highly similar to teeth of the extant *Trigonognathus kabeyai* (Cappetta and Adnet, 2001).

Node age reconstruction was performed in using the penalized likelihood approach implemented in r8s (Sanderson, 2002; Sanderson, 2003) as well as the Bayesian approach implemented in BEAST (v.1.4.7 Drummond and Rambaut, 2007). In both cases, all five calibration points and the Bayesian majority consensus tree topology in the Newick format were used as starting points for calculating chronograms.

For estimating unknown node ages in r8s, non-parametric rate smoothing was conducted via cross-validation and resulted in a smoothing parameter of 1.6e + 02. Our five calibration points were assumed as constrained node ages, allowing r8s to estimate divergence times. Minimal and maximal age constraints were set to cover stratigraphic ranges of fossil findings (Table 2). A bootstrapping procedure was conducted with the help of the r8s-bootstrap Kit (Eriksson, 2007) to attain confidence intervals on parameters. Here, we reproduced 100 pseudo replicates from the original alignment with Seqboot implemented in Phylip v3.6.7 (Felsenstein, 2005). For each replicate, a cross-validation analysis was performed to find optimal smoothing parameters. Thereafter, confidence intervals were calculated.

For estimating node ages with Bayesian inferences, the BEAST programme package (Drummond and Rambaut, 2007) was used. We created XML files with BEAUti containing a starting tree and calibration points. Node ages of calibration points were implemented assuming different prior distributions. The analyses assumed a relaxed molecular clock approach under the assumption of an uncorrelated lognormal model (UCLN Drummond et al., 2006) and the substitution models and data partitioning following the results of the BFT (see Section 2.3.3). The Yule speciation process was chosen as tree prior, assuming a constant speciation rate per lineage (Drummond and Rambaut, 2007), and a Markov Chain lasting 30 million generations. Tracer v.1.4 was used for checking performed runs for reaching stationarity regarding the posterior probabilities and confirming adequate effective sample sizes (ESS) in final runs. A burn-in of 25% of all sampled trees was discarded. Log-Combiner was employed to combine trees and log files attained from several identical runs, which were combined afterwards to decrease computational times. TreeAnnotator allowed to create consensus trees and FigTree v.1.1.2 enabled the visualization of the attained chronograms. We used three strategies to attain reliable node age estimates. First, we performed a run assuming a normal distribution as prior settings for calibration points. Means and standard deviations of calibration point ages were chosen to cover the range of stratigraphic stage ages where fossils used as calibration points were discovered. This run was conducted to roughly pre-date the tree for further runs with a Markov Chain lasting one million generations only. In a second step, the resulting chronogram from our first run was implemented as starting tree for a re-run with BEAST since the node ages from our pre-dating run fell into the time ranges of our calibration points. This time, the fossil calibration points were used under the assumption of an exponential prior, explaining the data more efficiently, because absolute dates can hardly be given in terms of calibration with fossils in contrast to an exponential prior

Table 2
Fossil calibration points used for node age estimation.

Calibration point	Age (mya)	Stage	References
Chimaeriformes	374.5–359.2	Upper Devonian, Fammenian	Benton and Donoghue (2007), Venkatesh et al. (2007)
Squaliformes	130.0–125.0	Lower Cretaceous, Barremian	Cappetta (1987)
Somniosidae	83.5–70.6	Upper Cretaceous, Campanian	Thies and Müller (1993)
Centrophoridae	70.6–65.5	Upper Cretaceous, Maastrichtian	Cappetta (1987)
Splitting *Trigonognathus*/*Etmopterus*	44.5–40.4	Palaeogen, Middle to Upper Lutetian	Cappetta and Adnet (2001)

assuming the genus to be present some time before the occurrence of the fossil which most probably does not represent the first occurrence. Zero-offsets adopted node ages reconstructed from the pre-dating analyses using normally distributed prior settings and exponential means were chosen, as in our first run, to cover the age of stratigraphic ranges of fossil findings of used calibration points. Here, two identical runs were performed lasting 30 million generations each, which subsequently were combined.

In a third step, we implemented the attained r8s chronogram as starting tree in BEAST following Hardman and Hardman (2008) for reassessing results from both, ML and Bayesian node age reconstructions. This step was conducted to obtain an independent measure for the accuracy of our node age estimation. The run lasted 30 million generations.

Finally, the same procedure was conducted again, only differing in calibration points to get a measure for the influence of calibration points on node age reconstructions. In additional runs operated in BEAST, we eliminated either the node age calibration of Centrophoridae or Somniosidae to obtain insights into the variability of results. Performed runs which were not calibrated with fossils displayed older node ages and larger confidence intervals as expected. See Table 2 for fossil calibration points used in this study.

3. Results

3.1. Sequence characteristics and phylogenetic signal

The sequenced portion of the RAG1 gene shows 925 constant characters, of which 265 are parsimony non-informative and 247 parsimony informative. As expected, RAG1 displays a smaller number of parsimony informative characters compared to the mtDNA dataset (constant characters = 1933, variable parsimony non-informative = 422 and parsimony informative = 1007). The X^2-test revealed equally distributed base frequencies for all loci (df = 216, all $p > 0.9$). For empirical base frequencies of single loci see Table 3. Translation of coding genes RAG1 and COI into amino acids showed no stop codons or improbable frame shifts. Inspection of transition–transversion rates (ts–tv) showed no saturation for third codon positions of coding genes.

3.2. Phylogenetic analyses

ML, Bayesian and MP analyses yielded almost identical phylogenetic hypotheses with regard to the well supported monophyly of Squaliformes and Etmopteridae as well as for major etmopterid intrarelationships, but failed to unambiguously identify the sistergroup of Etmopteridae. Fig. 1 provides an overview of obtained tree topologies as a BI dendrogram with statistical support values for ML and BI. Supplementary Materials 2 and 3 supply BI and MP phylograms with bootstrap or posterior probability values.

Table 3
Empirical base frequencies.

Area	Pi (A)	Pi (G)	Pi (T)	Pi (C)
RAG1	0.323437	0.243525	0.256767	0.176271
CM	0.346216	0.176951	0.270659	0.206174
COI	0.259488	0.168938	0.332910	0.238664

Within Squaliformes only the basal split of *Squalus* (Squalidae) from the rest of Squaliformes is strongly supported, whereas most relationships within other families of Squaliformes were not supported with high support values. However, all analyses render Somniosidae sensu Compagno et al. (2005) to be paraphyletic with respect to Oxynotidae (represented here by *Oxynotus paradoxus*). In addition, separate analyses of the RAG1 dataset including *Echinorhinus brucus* (Echinorhinidae) and *Isistius brasiliensis* (Dalatiidae) strongly suggest that these are not the sister-clades of Etmoperidae, although the full sequence dataset including mitochondrial loci could not be amplified for these taxa (Fig. 3).

Intrafamilial relationships of Etmopteridae identify nine major clades, each supported with 99–100% bootstrap support in ML and MP analyses or 1.00 posterior probabilities in BI (Fig. 1). Interrelationships of these clades are not always well supported. In combined mtDNA and RAG1 analyses, *Trigonognathus kabeyai* (clade I) is sister to *Etmopterus*, whereas employing RAG1 alone identifies *Trigonognathus* as sister to the *Aculeola*/*Centroscyllium* clade (clades VIII and IX, Fig. 1). *Aculeola* (clade IX, Fig. 1), a monotypic genus endemic to the southeastern Pacific, is identified with strong support as the sistergroup of *Centroscyllium* (clade VIII, Fig. 1), a genus comprising seven species, four of which could be sampled in our dataset. *Centroscyllium* mainly occurs in temperate southern ocean basins. The rarely caught *Miroscyllium sheikoi*, another monotypic genus known from southern Japan and Taiwan only, occurs in all analyses within the *Etmopterus lucifer* clade (clades IV, V and VI, Fig. 1), and thus renders *Etmopterus* paraphyletic.

Etmopterid intrageneric phylogenetic analyses of the speciose genera *Etmopterus* and *Centroscyllium* partially revealed multiple and previously undetected hypotheses with high support values in all analyses. *Etmopterus* is not monophyletic with regard to *Miroscyllium* (see above) and is split into two major sister clades. The first monophylum comprises two clades, the mostly panoceanic temperate *E. spinax* clade, previously unrecognised (clade II, Fig. 1) and named after the type species of the genus *Etmopterus* Rafinesque 1810, and the (sub-) tropical Atlantic *E. gracilispinis* clade, previously unrecognised (clade III, Fig. 1). The second major monophylum comprises four clades, including *Miroscyllium sheikoi* (clade IV, Fig. 1), the paraphyletic traditional *Etmopterus lucifer* group, split into clades V and VI (Fig. 1) and the panoceanic *E. pusillus* clade (clade VII, Fig. 1). The *E. lucifer* clade (clades IV, V, and VI, Fig. 1) represents a monophylum which is sister to clade VII. Interestingly, *Miroscyllium* is sistergroup to clade V, part of the *E. lucifer* clade comprising specimens from the northern hemisphere only. Most terminal taxon-relationships at species level were resolved with high statistical support. However, we detected multiple occurrences of species level paraphyly indicating either misidentifications or previously undetected cryptic diversities, e.g. within the *E. spinax* clade (*Etmopterus unicolor*, *Etmopterus* sp. B, *Etmopterus* cf. *granulosus*). For phylogenetic placement and geographic origin of terminal taxa, see Fig. 1 and Supplementary Material 1.

The second comparatively species rich etmopterid genus *Centroscyllium* is represented by four species in our analyses (out of seven described): *C. fabricii* (Northern Atlantic) and *C. ritteri* (Japan)

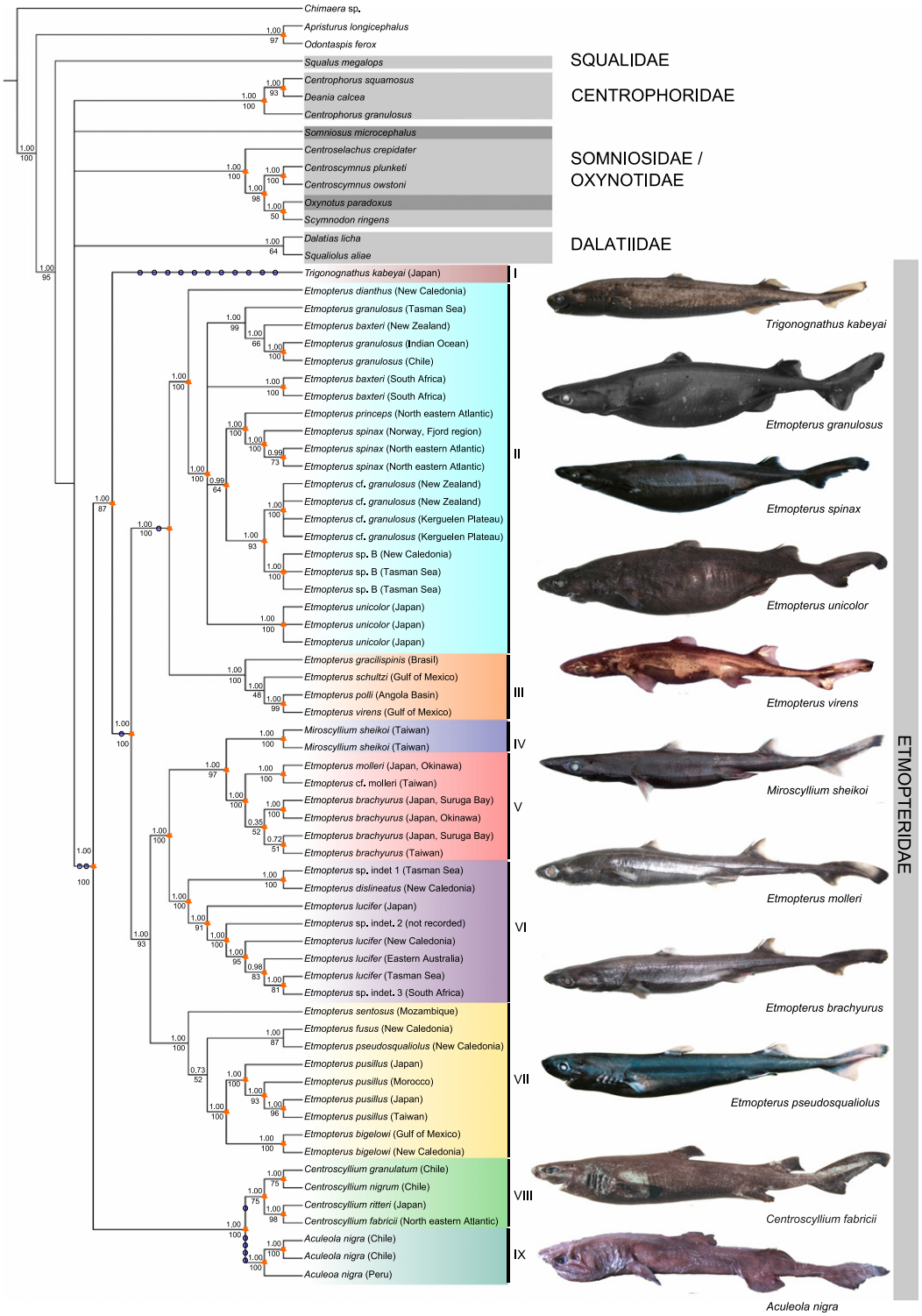

Fig. 1. Dendrogram displaying phylogenetic relationships of Etmopteridae, reconstructed with Bayesian inference. Widely congruent topologies were attained with ML and MP analyses. Numbers above internal nodes indicate posterior probabilities (PPs) from Bayesian analyses, numbers below branches bootstrap scores attained from ML search strategies. Orange asterisks refer to nodes found in MP analysis with a bootstrap support >50%. Nodes displaying PPs and bootstrap scores <0.95 (PP) and <50% (bootstrap support) were collapsed. Blue circles refer to synapomorphic morphological character states found by Shirai (1992) which are in congruence with our tree topology (see Table 5). Roman numerals refer to nine major clades resulting from phylogenetic analyses. Among the speciose genus *Etmopterus*, four clades can be identified, partially morphologically characterizable: *E. spinax* clade (clade II), *E. gracilispinis* clade (clade III), *E. lucifer* clade (clades IV, V and VI), and *E. pusillus* clade (clade VII): Etmopterus sp. indet. 1: preliminary identified as *Etmopterus* cf. *molleri*; *Etmopterus* sp. indet. 2: preliminary identified as *E. lucifer*; *Etmopterus* sp. indet. 3: preliminary identified as *Etmopterus* cf. *brachyurus*. Dark grey colours mark taxa differing from traditional squaliform families (light gray).

forming a subclade opposite to the South American endemics *C. nigrum* and *C. granulatum*. The monophyly of the genus is significantly supported (Fig. 1).

Seventeen of 27 morphological synapomorphies described by Shirai (1992) are in concordance with our molecular tree topology (Fig. 1, Table 5).

3.3. Node age reconstruction

Our partitioned Bayesian estimates of node ages using the BEAST program package were largely congruent with results attained using the penalized likelihood approach as implemented in r8s (Fig. 2 and Table 4). We based our analysis on the Bayesian tree (see Supplementary Material 2), but refer here only to well supported nodes as shown in Fig. 1. With regard to outgroups of Squaliformes, the early split of monophyletic Squaliformes from Lamniform and Carcharhiniform lineages (*Odontaspis* and *Apristurus*, respectively), occurred some 170 (218–133) Ma ago, and the split between *Apristurus* from *Odontaspis* is stated to 84 (134–30) Ma, but confidence intervals for these nodes are large. In contrast, the age of Squaliformes is estimated comparatively precisely around 128 (130–127) Ma, and the age of origin of the squaliform families Centrophoridae is 71 (74–69 Ma), Dalatiidae 67 (68–67 Ma) and Somniosidae 69 (70–67 Ma; excluding *Somniosus*). Although sister-family relationships among Squaliformes could not be satisfactorily resolved and resulted in a polytomy (Fig. 1), the different families form monophyla, whose minimum ages can be estimated using fossil calibration points, i.e. Centrophoridae and Somniosidae. *Somniosus* is not included in Somniosidae sensu Compagno et al. (2005) but support values are weak. Therefore the branch was collapsed and treated as a separate monophyletic group neighbouring remaining squaliform families. Intrafamilial diversification of the respective families stated at 45 (64–26) Ma for Dalatiidae, 40 (61–19) Ma for Centrophoridae and Somniosidae (without *Somniosus*) are dated to 37 (53–20) Ma. Confidence intervals are large but broadly overlapping.

The age of our focus group Etmopteridae is dated as the splitting between *Somniosus* and etmopterids and must have occurred at the end of the Cretaceous or beginning of the Paleocene, about 61 (69–53) Ma ago. We highlight here, that the sister-group relationship between *Somniosus* and Etmopteridae as depicted on the basis of the Bayesian phylogenetic hypothesis (Fig. 1, Supplementary Material 2), is only weekly supported and therefore the precise age of origin remains questionable. With Etmoperidae, the major divergence of the *Aculeola*/*Centroscyllium* clade from the remaining clades is estimated to be ca. 44 (48–41) Ma ago, and further divergence of *Aculeola* from *Centroscyllium* to 23 (39–12) Ma ago. Taxon sampling of *Centroscyllium* is incomplete preventing an age estimate for the genus. However, *Aculeola* with only one known species to date seems to be comparatively old with a split age of 11 (18–4) Ma ago for the Peruvian and Chilean samples. The age of the next split within Etmopteridae is the divergence between *Trigonognathus* and the *Etmopterus*/*Miroscyllium* – lineage, which is dated to 41 (46–36) Ma based on the calibration point using the *T. virginiae* fossils. The early steps of the *Etmopterus*/*Miroscyllium* radiation into multiple subgroups (clade II-*E. spinax* clade, III-*E. gracilispinis* clade, IV, V and VI-*E. lucifer* clade, and VII-*E. pusillus* clade) apparently took place in a comparatively narrow time window between 31 and 40 Ma. As the taxon sampling for the *Etmopterus* radiation is fairly complete, we assume that time estimates for subgroup origins are close to real group diversification ages, but age estimates are nevertheless overlapping. The divergence of the two major etmopterid clades (clades II + III sister to clades IV, V, VI, and VII) containing two subclades each date to 36 (42–32) Ma. The *E. spinax* clade (clade II) separates from the *E. gracilispinis* clade (clade III) around 30 (36–22) Ma ago, a similar age as compared to the *E. lucifer* clade (clades IV, V, and VI) and *E. pusillus* clade (clade VII, ca. 33 (39–27) Ma). The youngest subgroup is apparently the *E. spinax* clade (clade II), which radiated some 14 (21–8) Ma ago. The *E. gracilispinis* clade (clade III) shows an older radiation age, which is dated to 22 (29–14) Ma. clades IV, V, VI and VII on average evolved 33 (39–27) Ma ago, displaying radiation dates for the *E. lucifer* clade 24 (32–17) Ma ago, but for *Miroscyllium* of only 19 (27–11) Ma ago. Radiation events of clades V and VI (the Northern and Southern Hemisphere species of the *E. lucifer* clade)

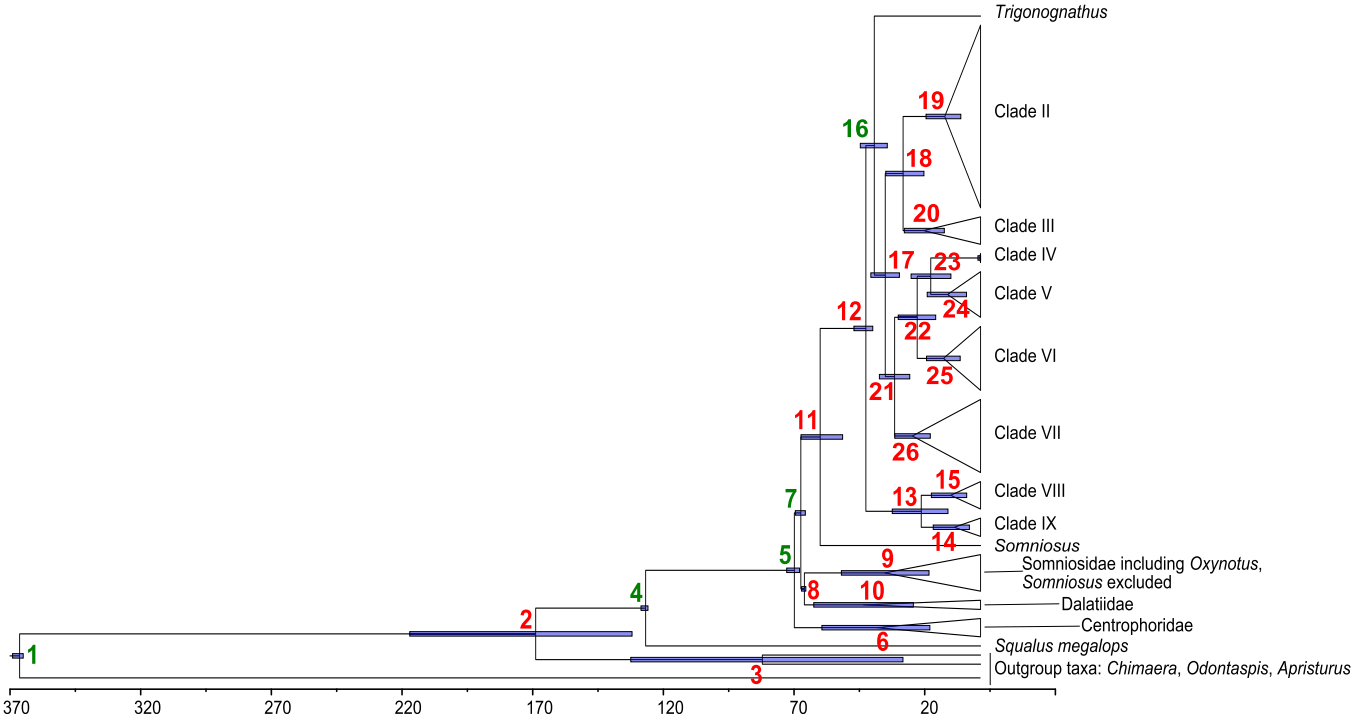

Fig. 2. Estimated divergence times attained from Bayesian and Penalized Likelihood methods. Red numbers refer to node numbers given in Table 4 including node descriptions, mean node ages and confidence intervals of both analysing approaches. Green numbers indicate applied calibration points attained from fossils. Origin of Etmopteridae in between 69 and 53 Ma, origin of genus *Etmopterus* in between 48 and 36 Ma with further radiation events from 14 to 36 Ma. (For interpretation of references to color in this figure legend, the reader is referred to see the web version of this article.)

Fig. 3. Maximum likelihood based phylogram of RAG1 data, additionally including *Echinorhinus brucus* and *Isistius brasiliensis*. Red-coloured species represent additional taxa not included in the concatenated dataset and *Trigonognathus* controversial placement in analyses using RAG1 data only. (For interpretation of references to color in this figure legend, the reader is referred to see the web version of this article.)

also occurred comparatively recently with age estimates of 13 (20–5) and 14 (21–8) Ma, respectively. In contrast, the oldest clade, the *Etmopterus pusillus* clade (clade VII), started separation and diversification already 26 (33–19) Ma ago. The inferred confidence intervals were partially in concordance with ages calculated with the Bayesian tree as starting tree in r8s, but some confidence intervals

Table 4
Mean node ages and confidence intervals attained with different analysing approaches.

Node #	Node description	Age estimates BEAST		Age estimates r8s	
		Node age	Height 95% HPD	Node age	Height 95% HPD
1	Root age	367.70	366.33–370.4	369.51	366.33–370.52
2	Split Squaliformes	170.23	133.37–218.42	337.10	134.77–229.87
3	Split *Odontaspis* & *Apristurus*	83.51	29.70–133.85	241.72	40.64–144.29
4	Split *Squalus*	128.15	127.27–129.94	129.14	127.27–129.76
5	Split Centrophoridae	71.26	69.28–74.18	70.6	69.28–74.35
6	Radiation Centrophoridae	39.75	19.41–60.72	43.08	19.42–58.31
7	Split Etmopteridae & *Somniosus* from Somniosidae & Dalatiidae	68.78	67.06–70.89	–	67.04–70.99
8	Split Somniosidae/Dalatiidae	67.42	66.87–68.49	70.6	66.87–68.48
9	Radiation Somniosidae	36.64	19.73–53.26	37.83	20.80–54.211
10	Radiation Dalatiidae	44.83	25.73–63.83	62.34	21.59–64.84
11	Split *Somniosus*/ Etmopteridae	61.38	52.79–68.71	59.85	53.57–68.72
12	Split clades VIII & IX from clades I and II-VII	43.89	41.26–48.46	56.81	41.26–48.94
13	Split clades VIII & IX	22.70	12.48–38.78	40.78	15.47–39.90
14	Radiation clade IX	10.60	4.29–18.11	25.67	4.93–18.05
15	Radiation clade VIII	11.43	5.32–18.81	21.85	5.08–20.42
16	Split clades I & II–VII	40.67	35.70–46.02	44.25	36.26–47.70
17	Split up of clades II & III from IV, V & VI	36.48	31.55–41.36	34.24	31.67–42.76
18	Split clades II & III	29.65	21.67–36.29	30.34	22.88–37.17
19	Radiation clade II	13.71	7.57–20.87	23.59	7.64–20.12
20	Radiation clade III	21.80	13.88–29.17	29.54	14.02–29.68
21	Split clades IV, V & VI from VII	32.88	27.10–38.72	32.00	27.77–39.11
22	Splitting up of clades IV, V and VI	24.26	17.18–31.52	19.08	18.21–31.43
23	Split IV	19.06	11.36–26.59	15.02	11.72–26.88
24	Radiation clade V	12.63	5.38–20.42	7.73	5.89–19.91
25	Radiation *E. lucifer*, split *E. dislineatus* & *E.* sp. indet. 1	14.19	7.80–20.68	16.80	7.94–21.53
26	Radiation clade VII	26.07	19.24–32.85	18.69	19.32–33.97

displayed biases revealing unreasonable large confidence intervals, which can be explained by low likelihood scores of ML trees attained from the bootstrapped alignment. Using the chronogram attained with the Penalized Likelihood method in r8s as starting tree in BEAST aligns with results attained from the Bayesian tree as starting setting. A summary of node age estimations is provided in Fig. 2 and Table 4.

4. Discussion and conclusions

Phylogenetic reconstruction of extant Lantern Sharks (Etmopteridae), has been restricted to two studies primarily based on 27 osteological and myological characters up to now (Shirai, 1992; Shirai and Nakaya, 1990b). Additionally, several studies on elasmobranch interrelationships incorporated a single or few Lantern Shark species providing information about the sister-clade of Etmopteridae among Squaliformes (Compagno, 1973; Compagno, 1977; Maisey et al., 2004; Shirai, 1992). Our study is based both on more etmopterid taxa and significantly more characters and provide evidence for monophyly of Etmopteridae which comprise four major intrafamilial lineages (clades I–IX) corresponding largely but not fully to the four morphologically well diagnosable genera *Aculeola, Centroscyllium, Trigonognathus* and the highly diverse genus *Etmopterus* (Fig. 1).

4.1. Age and origin of Lantern Sharks

Our age estimate for the origin of Etmopteridae, which corresponds to the (not strongly supported) divergence between Etmopteridae and *Somniosus* (Figs. 2 and 3, Supplementary Material 2), agrees with the end of the Cretaceous and beginning of the Paleocene (Cretaceous/Tertiary boundary), respectively, and dates back substantially earlier than the first unambiguous etmopterid fossils from deep-water Eocene sediments (*Etmopterus bonapartei, E. acuticens, E. cahuzaci, Trigonognathus virginiae, Miroscyllium*, and *Paraetmoperus* (Adnet, 2006; Adnet et al., 2008; Cappetta and Adnet, 2001; Cigala, 1986; Ledoux, 1972)). According to our node age estimates as well as to the fossil record, all other squaliform deep-water inhabitants, i.e. Somniosidae, Centrophoridae, and Dalatiidae also originate around or shortly before the C/T boundary. Only the predominantly shallow water Squalidae, the sister-group to all deep-water squaliform sharks, as well as all ambiguously identified and now extinct "etmopterid" lineages from shallow waters (*Eoetmopterus, Microetmopterus* and *Proetmopterus*) are known from substantially before the C/T boundary (Adnet et al., 2006; Kriwet and Benton, 2004; Siverson, 1993; Cappetta and Siverson, 2001; Underwood and Mitchell, 1999). This pattern indicates that the major biotic crisis at the C/T boundary affected squaliform sharks in different ways. However, this interpretation has to be treated with caution, because the ML based age estimate for the *Somniosus*/Etmopteridae split displays large error bars and because a sister-clade relationship of Etmopteridae and *Somniosus* is not supported with high confidence in all our analyses. Further, it remains to be substantiated, that squaliform teeth fossils from the Turonian (93.5–89.3 Ma) are indeed a *Centrophorus* (Cappetta, 1987), which would invalidate our C/T boundary deep-water colonization hypothesis.

The four major etmopterid lineages differ mostly in specific dental characters indicating that trophic specialization played an important role for the early radiation of the group. According to our molecular clock estimates, this trophic radiation took place in the late Palaeocene/early Eocene between 48 and 41 Ma ago (Table 4). Subsequent evolution leading to the extant diversity of etmopterid genera occurred in the Middle Eocene to Early Miocene, approximately 45–15 Ma ago. Taking into account that this period (Palaeogene) is considered to represent the recovery phase after the extinction crisis at the C/T boundary (Kriwet and Benton, 2004; Stanley, 2009), the evolution of specialized dentitions in etmopterids may be the result of increased ecological opportunity after C/T extinction events as well as of the evolution of increased prey diversity in the post C/T boundary recovery phase, which e.g. led to a diversification of cephalopods (Lindberg and Pyenson, 2007), which form a major part of extant etmopterid diet (Klimpel et al., 2003; Neiva et al., 2006).

Table 5
Preliminary classification of Etmopteridae based on results of this study. *E. villosus* is not shown due to missing informations and samples for the present study. Morphological characteristics list synapomorphies diagnosed by Shirai (1992), which are in concordance with our molecular tree topology and general flank mark shapes of *Etmopterus* clades found in this study.

Genus	Clade	Morphological characteristics
Aculeola		– secundary loss of fossa for rectus externus – double-pointed expansion of basihyal – double-pointed expansion of puboisschiadic bar – loss of the primary calcification of the centrum with a cylindrical notochordal sheath interrupted by a transverse septum
Centroscyllium		– subnasal stay present
Trigonognathus		– profundus canal present – suborbital keel-process lost secondarily – basibranchial copula very reduced (*Trigonognathus*-lype) – anterior basi-branchial absent – suborbitalis absent; constructor dorsalis arising from a seam of connective tissue at the middorsal line – posterior part of the intermandibularis inserting on ceratohyal – posterior slip of arcualis dorsalis lost secundarily – subspinalis externus present – pectoral propterygium fused with mesopterygium
Etmopterus		– short eye-stalk, not reaching eye-ball
	***E. spinax* & *E. gracilispinis* clades**	– adductor mandibularis ß present
	***E. spinax* clade** (**clade II, Fig. 1**) *E. baxteri, E. dianthus, E. granulosus, E. litvinovi*. E. princeps. E. hillianus*, E. spinax. E. unicolor*. E. sp. B	– flank mark shape (if present) displaying long thin linear, anterior branches, and no or only weak posterior branches 
	***E. gracilispinis* clade** (**clade III, 1, Fig. 1**) *E. gracilispinis, E. perryi*, E. polli, E. robinsi*, E. schultzi, E. virens*	– flank mark shape displaying long, thick, and curved anterior branches and short to medium thick posterior branches 
	***E. lucifer* clade** (**clades IV, V, VI Fig. 1**) *E. brachyurus, E. burgessi*. E. bullisi*, E. decacuspidatus, E. dislineatus, E. evansi*, E. lucifer, E. molleri, E. pycnolepis** (*excluding E. sheikoi*)	– flank mark shapes displaying long thin anterior branches and long thin, linear posterior branches exceeding anterior branch lengths 
	***E. pusillus* clade** (**clade VII, Fig. 1**) *E. bigelowi, E. carteri*, E. caudistigmus*, E. fusus, E. pseudosqualiolus, E. pusillus, E. sentosus, E. splendidus**	– flank mark shapes displaying short, thick anterior branches and no or only weak posterior branches 

*Species not included in molecular analyses.

According to our analyses, intrageneric diversification within *Etmopterus* commenced at the Oligocene/Miocene boundary and continued well into the middle Miocene. It is interesting in this context, that a climatic shift from Palaeogene greenhouse conditions to icehouse conditions at the Eocene/Oligocene transition resulted in expanding Antarctic ice shields, the establishment of the circum-Antarctic current and subsequent chilling of the deep-sea (Eldrett et al., 2009; Lear et al., 2008). This coherence might indicate that the *Etmopterus* radiation was correlated with this significant climate change that established cooler temperatures which prevail until today. The cooling event allowed for the formation of eutrophic conditions at the seafloor, as known for example from palaeo-ecological studies from the western Tethys (Alegret et al., 2008). Cooling in coherence with steep continental slopes favours fast downslope transfer of organic material and consequently a rich benthic fauna especially of this part of the bathyal zone (Türkay, 2002). This establishment of nutritious food webs on the slopes is a prerequisite for rich feeding grounds for species ranking higher in food webs such as etmopterid sharks, or beaked whales (Cetacea: Ziphiidae). Interestingly, beaked whales with a similar depth penetration spectrum as Etmopteridae radiated roughly at the Oligocene/Miocene boundary, too (Dalebout et al., 2008).

4.2. Bioluminescence and the Etmopterus radiation

Our phylogenetic analyses of portions of the RAG1 gene place the bioluminescent dalatiid *Isistius brasiliensis* within a monophyletic group alongside with bioluminescent species *Dalatias licha* and *Squaliolus aliae* (Fig. 3). Although the sister-family relationships of Etmopteridae could not be clarified in our study, these results show that a monophyletic clade Dalatiidae evolved independently from Etmopteridae supporting the hypothesis that bioluminescence has evolved twice independently as suggested previously by several authors (Claes and Mallefet, 2008; Hubbs et al., 1967; Reif, 1985).

The reasons for the rapid and massive diversification of *Etmopterus* generating the most speciose clade of Squaliformes and one of the largest groups within Neoselachii may be discussed controversially. Trophic diversification based on alternatively adapted dentitions might be one reason. However, although the specific clutching–crushing type dentition of *Etmopterus* is unique among Etmopteridae the limited phenotypic diversity of tooth shapes within the genus cannot explain the evolution of more than 30 species. In addition, this type of dignathic heterodonty (cuspid teeth in the upper jaw, blade-like, overlapping teeth in the lower jaw) evolved in Centrophoridae, Dalatiidae and Somniosidae, too, but

without producing increased species richness. In contrast, the ability to emit light via photophores (bioluminescence) is limited among sharks to Dalatiidae and Etmopteridae. Here, bioluminescence may serve several functions: first, ventrally located photophores may provide counter illumination to serve as camouflage against residual sunlight when viewed from below (Claes and Mallefet, 2008; Reif, 1985; Widder, 1998).

Second, species specific bioluminescent flank markings may be interpreted as visual cues enabling species recognition, and, in combination with social interactions as schooling. Those flank markings are not present in bioluminescent Dalatiidae, *Aculeola*, and most *Centroscyllium* species, but they are highly diverse within *Etmopterus*. In *Etmopterus* it has even been hypothesized to aid cooperative hunting in closely interacting conspecific packs (Claes and Mallefet, 2008, 2009; Reif, 1985). The latter behaviour is assumed both for *E. virens* (Springer, 1967) and for *E. spinax* (Macpherson, 1980). Stomach food content analyses of *E. spinax* revealed very large prey chunks, but may be explained by scavenging behaviour instead of cooperative hunting of large prey (Neiva et al., 2006). In the case of sympatry, markings may enhance the efficiency of alternative and species specific social foraging strategies using a high level visual interaction. This bioluminescent diversity may ultimately explain the evolutionary origin of species richness in *Etmopterus*. Obviously, this hypothesis is currently difficult to test, but improved possibilities both for direct observation in the deep-sea or in aquaria may be possible in the near future. Our phylogenetic analysis shows, that flank markings among (roughly) sympatric congeners may differ substantially, i.e. sympatric occurrence of clades V, VI, and VII (Fig. 1).

4.3. Phylogenetic implications

4.3.1. Trigonognathus

Clade I includes only a single extant species, *Trigonognathus kabeyai*. Shirai's analyses (1992) reveal *Trigonognathus* to be sister of *Aculeola* and *Centroscyllium*. Our combined dataset conversely identifies *Trigonognathus* well supported as sister genus to *Etmopterus* whereas the analyses of the nuclear RAG1 alone supports Shirai's hypothesis (Shirai, 1992) (Fig. 3). Morphological evidence does not favour either topology (Adnet et al., 2006; Shirai, 1992). Currently, only more nuclear data can reveal, whether alternative topologies favoured by our datasets are due to unambigous cytonuclear discordance or due to insufficient nuclear character sampling. Osteological and myological autapomorphies as identified by Shirai (1992) for *Trigonognathus* (Table 5) are numerous and are mapped on Fig. 1.

4.3.2. Placement of Aculeola, Centroscyllium and Miroscyllium sheikoi

Our molecular analyses confirm Shirai and Nakaya's (1990b) as well as Shirai's (1992) analysis and place *Aculeola* and *Centroscyllium* as sistertaxa to each other and both as sister taxon to *Etmopterus*. In contrast to their morphological analysis, our results show *Miroscyllium* (clade IV) to belong to the *E. lucifer* clade rendering *Etmopterus* paraphyletic with respect to *Miroscyllium*. Shirai and Nakaya (1990b) established the genus *Miroscyllium* for *Centroscyllium sheikoi* based on the mosaic morphological characterset of *Etmopterus* and *Centroscyllium*, i.e. a number of synapomorphies, a *Centroscyllium*-dentition of adults and flank markings as in *Etmopterus*. However, since subadult specimens of *M. sheikoi* show a dentition similar to that of *Etmopterus*, the adult dentition is interpretable as a *Centroscyllium*-convergent dentition secondarily derived from an *Etmopterus* dentition, and ontogenetically is not necessarily contradicting a placement of *M. sheikoi* within *Etmopterus*. Further, monophyly of *Etmopterus* and *Miroscyllium* is morphologically evidenced by an apparently synapomorphic short eyestalk (Shirai, 1992). Consequently, *Miroscyllium sheikoi* should be transferred to *Etmopterus*. However, its flank mark shape indicates a closer relationship between *Miroscyllium* and clade VII, rather than between *Miroscyllium* and clade V (as in our study).

4.3.3. Phylogenetic structure within Etmopterus

Within *Etmopterus*, we identified six monophyla including *Miroscyllium*. Those six clades are partitioned into two major monophyla, one comprising the *E. spinax* clade (II) and the *E. gracilispinis* clade (III), and the other one comprising *Miroscyllium*, two sisterclades within the major *E. lucifer* clade and *E. pusillus* clade (Fig. 1). In Shiraís analysis (1992) the first major monophylum (*E. spinax* and *E. gracilispinis* major clade) is morphologically supported (Table 5), but not all taxa analysed herein were represented in their dataset, i.e. morphological evidence needs to be substantiated with increased taxon sampling. There is currently no morphological support for our second major monophylum (clades IV–VII).

Clade II comprises the *E. spinax* clade, which had not been identified before. This group represents a quite recently evolved and diverse clade. Members of this group are distributed worldwide from subantarctic and – arctic zones to the tropics. Unfortunately, diagnostic morphological characters for the *E. spinax* clade are difficult to identify. External morphological characters traditionally used for species identification display much variation ranging from conspicuous flank markings with thin anterior and short and thick posterior branches (e.g. *E. granulosus, E. spinax*) to complete lack of flank markings (*E. princeps*), fine bristle-like hooked denticles irregularly arranged (*E. unicolor, E. spinax*) to rough textured denticles partially defined in rows (*E. granulosus*). More detailed morphological analyses have to be conducted to clearly separate species forming identified subclades within this group. The *E. spinax* clade is further partitioned into five well supported subclades. Here, *E. dianthus* is the sister taxon to a clade comprising the remaining five species (Supplementary Material 2). Differentiation within *E. granulosus* and *E. baxteri* from diverse locations appears to be recent and not unambiguous with regard to species assignment, i.e. with our limited sample the question of paraphyly of *E. baxteri* cannot be resolved but is subject to an ongoing study. Surprisingly, specimens included in our analyses identified as *E. unicolor* and *Etmopterus* sp. B are not monophyletic, suggesting that *E. unicolor* from close to the type locality in North East Pacific (Japan), is specifically distinct from *Etmopterus* sp. B (Last and Stevens, 1994) – specimens from New Caledonia. This contradicts recent morphological analyses (Yano, 1997), which had suggested conspecificity of specimens of *E. unicolor* with *Etmopterus* sp. B from southern Australia which was subsequently accepted in current literature (Last and Stevens, 2009). Specimens of *E.* cf. *granulosus* (Duhamel et al., 2005) from the Kerguelen Plateau form another subclade within clade II which is sister taxon to the *Etmopterus* sp. B subclade including specimens from New Zealand. This suggests that this undescribed species is wide spread throughout the Southern Hemisphere (NS, pers. obs.). This species is similar to *E. unicolor* and *Etmopterus* sp. B (shape and arrangement of dermal denticles) and *E. granulosus* (similar flank markings) suggesting these three species as cryptic species. It is most probably closely related to *E. litvinovi* (Kotlyar, 1990) and to another undescribed species from South Africa, *Etmopterus* sp. (Bass et al., 1986). This species will be described in a separate publication.

The four species of our *E. gracilispinis* clade (clade III) are confined to the Atlantic Ocean (incl. the Carribean) and southern Africa (*E. gracilispinis*) – a pattern of restricted endemism contrasting with the wide distribution range of the *E. spinax* clade (II). Shared external morphological characters within this group are hook-like denticles, never forming rows and flank markings displaying a short posterior (except *E. polli* and *E. robinsi*) but conspicuous anterior branch with a thinning of the dark area accumulating photophores at the basis of the marking (Table 5). According to these

characters, the rare Caribbean *E. perryi* belongs to this group, too (NS, pers. obs.). A remarkable aspect of this small marine elasmobranch species-flock is, that the intragroup heterogeneity of biolumiscent flank mark shapes is conspicuously larger than in other more widely distributed clades. Possibly, this diversity indicates that species recognition through diversification of flank marks helped establishing reproductive isolation among diverging tropical Atlantic Etmopteridae (see also Section 4.2).

Clades IV (*Miroscyllium*), V and VI represent a monophylum, which we name *E. lucifer* clade, because it comprises most species of the "*E. lucifer* species group" as defined by Yamakawa et al. (1986). However, our results partially contradict, because *E. granulosus* appears not to be a member of the *E. lucifer* clade and *Miroscyllium sheikoi* is a member of it. Yamakawa et al. (1986) diagnosed the group using the arrangement of dermal denticles in longitudinal rows along the flanks and included seven nominal species in this group: *E. lucifer, E. villosus, E. brachyurus, E. bullisi, E. abernethyi* (synonym of *E. lucifer* according to Last and Stevens, 1994), *E. molleri* and *E. granulosus*. In recent years, five newly described species were assigned to the "*E. lucifer* species group" (*E. burgessi* (Schaaf da Silva and Ebert, 2006), *E. decacuspidatus* (Chan, 1966), *E. dislineatus, E. evansi* (Last et al., 2002), and *E. pycnolepis* (Kotlyar, 1990)). Using flank mark shapes as potentially diagnostic characters instead of longitudinal rows of dermal denticles as diagnostic character for the *E. lucifer* clade, we find increased consistency of molecular results and morphology. Then, the *E. lucifer* clade is predominantly characterized by flank markings displaying conspicuous anterior and posterior branches, which are similar to those of *E. lucifer* (Yamakawa et al., 1986; Last et al., 2002; Schaaf da Silva and Ebert, 2006). This character would be suitable to identify all members of the molecularly identified *E. lucifer* clade except *M. sheikoi*. Based on results of this study, we remove *E. granulosus* from the traditional "*E. lucifer* species group" (Yamakawa et al., 1986), as it does not share the aforementioned flank mark characteristics and simultaneously is placed with the *E. spinax* clade using molecular characters. Nevertheless, we suggest to test the intrageneric placement of *M. sheikoi* along with the evolution of flank marks within *Etmopterus* using additional nuclear markers from several genomic regions. In summary, we suggest to re-define the "*E. lucifer* species group" as *E. lucifer* clade to comprise *E. brachyurus, E. bullisi, E. burgessi, E. decacuspidatus, E. dislineatus, E. evansi, E. lucifer, E. molleri, E. pycnolepis*, and possibly *M. sheikoi*.

Clade VII is herein referred to as the *E. pusillus* clade. Morphological analyses had identified an "*E. pusillus* species group" mainly characterized by conical, block-like dermal denticles (Shirai and Tachikawa, 1993). However, their analysis included only *E. bigelowi* and *E. pusillus*, which indeed form a monoyphyletic subclade with the *E. pusillus* clade. Here, we include in an *E. pusillus* clade species, which were previously included into a tentative "*E. splendidus* species group" namely *E. pseudosqualiolus* and *E. fusus* (Last et al., 2002). These do not share the conical denticles of *E. bigelowi* and *E. pusillus* but exhibit hook-like denticles in rows (Last et al., 2002). In summary, all species of our molecularly defined *E. pusillus* clade cannot be characterized by a uniform shape of denticles but by a very similar shape of flank markings which are characterised by an high and elongated anterior branch and no or only slightly visible posterior branches (Table 5). Our analyses did not include *E. carteri*, a dwarf species very similar to *E. pseudosqualiolus*. Images of the holotype of this rare species, reveal not only a similar body shape but also flank markings as in *E. pseudosqualiolus* (NS, pers. obs.). We therefore tentatively place this taxon with the *E. pusillus* clade.

Acknowledgments

This work would not have been possible without the help of all the people organizing and sharing samples: Tokai University, Japan: S. Tanaka, T. Horie; Virginia Institute of Marine Science: A. Verrissimo, C. Cotton; Churaumi Aquarium, Japan: K. Sato; Muséum National d'Histoire Naturelle, France: G. Duhamel, P. Janvier; NIWA, New Zealand: A. Loerz, K. Schnabel, D. Tracey, M. Watson, P. McMillan; Te Papa Tongarewa, New Zealand: A. Stewart; NOAA USA: M. Grace, J. Carter; Australian Museum Sydney, Australia: M. McGrouther; Victoria Museum Melbourne, Australia: D. Bray; Museum of Nature and Science, Tokyo: K. Matsuura, G. Shinohara; SAIAB South Africa: O. Gon, M. Mwale, P. and E. Heemstra; School of Biological Sciences, Victoria University of Wellington, New Zealand: S. Hernandez; Universidad Austral de Chile: J. Lamilla; Institute of Marine Research, Norway: D. Zaera; Marine Institute Rinville, Ireland: G. Johnston; Fisheries Research Services, Great Britain: F. Burns; Universidad de Valparaíso, Chile: F. C. Toro; Marine and Coastal Management, South Africa: R. Leslie; Zoologisches Museum Alexander König Bonn, Germany: F. Herder. We further thank S. Socher, J. Schwarzer, M. Geiger, A. Dunz, D. Neumann, T. Moritz, M. Harris, T. Tomita, T. Sasaki, and Y. Chimura for providing images and a sample of *Trigonognathus*, and S. Raredon for providing images of holotypes of *Etmopterus* housed in the USNM. This study was financed by Grants of the German Research Foundation D.F.G. to J. Kriwet (KR 2307-4) and to U. Schliewen (SCHL 567-3). This research received further support from the SYNTHESYS Project http://www.synthesys.info/ which is financed by European Community Research Infrastructure Action under the FP6 "Structuring the European Research Area" Programme." The study was also supported in part by the PPF «Etat et structure phylogénétique de la biodiversité actuelle et fossile».

Appendix A. Supplementary data

Supplementary data associated with this article can be found, in the online version, at doi:10.1016/j.ympev.2010.04.042.

References

Adnet, S., 2006. Two new selachian associations (Elasmobranchii, Neoselachii) from the Middle Eocene of Landes (south–west of France). Implication for the knowledge of deep-water selachian communities. Palaeo Ichthyologica 10, 5–128.

Adnet, S., Cappetta, H., 2001. A palaeontological and phylogenetical analysis of squaliform sharks (Chondrichthyes: Squaliformes) based on dental characters. Lethaia 34, 234–248.

Adnet, S., Cappetta, H., Nakaya, K., 2006. Dentition of etmopterid shark *Miroscyllium* (Squaliformes) with comments on the fossil record of Lantern Sharks. Cybium 30 (4), 305–312.

Adnet, S., Cappetta, H., Reynders, J., 2008. Contribution of Eocene sharks and rays from southern France to the history of deep-sea selachians. Acta Geol. Pol. 58 (2), 257–260.

Alegret, L., Cruz, L.E., Fenero, R., Molina, E., Ortiz, S., Thomas, E., 2008. Effects of the Oligocene climatic events on the formainiferal record from Fuente Caldera section (Spain, western Tethys). Palaeogeogr. Palaeolocl. 269, 94–102.

Bass, A.J., Compagno, L.J.V., Heemstra, P.C., 1986. Squalidae. In: Smith, M.M., Heemstra, P.C. (Eds.), Smith's Sea Fishes. Springer Verlag, Berlin, pp. 49–62.

Benton, M.J., Donoghue, P.C.J., 2007. Paleontological evidence to date the tree of life. Mol. Biol. Evol. 24 (1), 26–53.

Cadenat, J., Blache, J., 1981. Requins de Mediterranee et d'Atlantique (plus particulierement de la Coze occidentale d'Afrique). Faune Trop. 21, 330.

Cappetta, H., 1987. Les sélaciens du Crétacé supérieur du Liban. I. Requins. Palaeontographica A 168, 69–229.

Cappetta, H., Adnet, S., 2001. Discovery of the recent genus *Trigonognathus* (Squaliformes: Etmopteridae) in the Lutetian of Landes (southwestern France). Remarks on the teeth of the recent species *Trigonognathus* kabeyai. Paläontol. Z. 74 (4), 575–581.

Cappetta, H., Siverson, M., 2001. A skate in the lowermost Maastrichtian of southern Sweden. Palaeontology 44, 431–445.

Carvalho, M.R., de Maisey, J.G., 1996. Phylogenetic relationships of the Late Jurassic shark *Protospinax* Woodward 1919 (Chondrichthyes: Elasmobranchii). In: Arratia, G., Viohl, G. (Eds.), Mesozoic Fishes – Systematics and Paleoecology. Verlag Pfeil, München, pp. 9–46.

Chan, W.L., 1966. New Sharks from the South China Sea. J. Zool. 148, 218–237.

Cigala Fulgosi, F., 1986. A deep-water elasmobranch fauna from the Pliocene outcropping (North Italy). In: Proceedings of the 2nd Conference of Indopacific fishes. Uyeno, T., Arai, R., Taniuchi, T., Matsuura, K. (Eds.). Ichthyological Society of Japan, pp. 133–139.

Claes, J.M., Mallefet, J., 2008. Early development of bioluminescence suggests camouflage by counter-illumination in the velvet belly lantern shark *Etmopterus spinax* (Squaloidea: Etmopteridae). J. Fish Biol. 73, 1337–1350.

Claes, J.M., Mallefet, J., 2009. Ontogeny of photophore pattern in the velvet belly lantern shark, *Etmopterus spinax*. Zoology, doi:10.1016/j.zool.2009.02.003.

Coelho, R., Erzini, K., 2008a. Identification of deep-water Lantern Sharks (Chondrichthyes: Etmopteridae) using morphometric data and multivariate analysis. J. Mar. Biol. Assoc. UK 88 (1), 199–204.

Coelho, R., Erzini, K., 2008b. Life history of a wide-ranging deep-water Lantern Shark in the north–east Atlantic, *Etmopterus spinax* (Chondrichthyes: Etmopteridae), with implications for conservation. J. Fish Biol. 73, 1419–1443.

Compagno, L.J.V., 1973. Interrelationships of living elasmobranchs. In: Greenwood, P.H. et al. (Eds.), Interrelationships of Fishes. Academic Press, London, pp. 15–61.

Compagno, L.J.V., 1977. Phyletic relationships of living sharks and rays. Am. Zool. 17, 303–322.

Compagno, L.J.V., 1984. FAO species catalogue. Vol. 4. Sharks of the world. An annotated and illustrated catalogue of sharks species known to date. Part 1. Hexanchiformes to Lamniformes. FAO Fish Synop. vol. 1254(1), pp. 1–249.

Compagno, L.J.V., Dando, M., Fowler, S., 2005. A Field Guide to the Sharks of the World. Collins, London. pp. 1–368.

Dalebout, M.L., Steel, D., Baker, S., 2008. Phyogeny of the beaked whale Genus Mesoplodon (Ziphiidae: Cetacea) revealed by nuclear introns: implications for the evolution of male tusks. Syst. Biol. 57 (6), 857–875.

Drummond, A.J., Ho, S., Philipps, M., Rambaut, A., 2006. Relaxed phylogenetics and dating with confidence. PloS Biol. 4, 88.

Drummond, A.J., Rambaut, A., 2007. BEAST: Bayesian evolutionary analysis by sampling trees. BMC Evol. Biol. 7, 214.

Duhamel, G., Gasco, N., Davaine, P., 2005. Poissons des iles Kerguelen et Crozet. Guide regional de l'ocean Austral. Museum national d'Histoire naturelle, Paris. pp. 62–64.

Edgar, R.C., 2004. MUSCLE: multiple sequence alignment with high accuracy and high throughput. Nucleic Acids Res. 32 (5), 1792–1797.

Eldrett, J.S., Greenwood, D.R., Harding, I.C., Huber, M., 2009. Increased seasonality through the Eocene to Oligocene transition in northern high latitudes. Nature 459, 969–973.

Eriksson T., 2007. r8s bootstrap kit. Published by the author.

Felsenstein, J., 2005. PHYLIP. Phylogeny Inference Package (Version 3.6.7). Distributed by the author. Department of Genome Sciences, University of Washington, Seattle, USA.

Hall, T.A., 1999. BioEdit: a user-friendly biological sequence alignment editor and analysis program for Windows 95/98/NT. Nucl. Acids. Symp. Ser. 41, 95–98.

Hardman, M., Hardman, L.M., 2008. The relative influence of body size and paleoclimatic change as explanatory variables influencing lineage diversification rate: an evolutionary analysis of bullhead catfishes (Siluriformes: Ictaluridae). Syst. Biol. 57 (1), 116–130.

Hubbs, C.L., Iwai, T., Matsubara, K., 1967. External and internal characters, horizontal and vertical distribution, luminescence, and food of the dwarf pelagic shark *Euprotomicrus bispinatus*. Bull. Scripps Inst. Oceanogr. Univ. Calif. 10, 1–64.

Huelsenbeck, J.P., Ronquist, F., 2001. MRBAYES: Bayesian inference of phylogenetic trees. Bioinformatics 17, 754–755.

Iglésias, S.P., Lecointre, G., Sellos, D.Y., 2005. Extensive paraphyllis within sharks of the order Carcharhiniformes inferred from nuclear and mitochondrial genes. Mol. Phylogenet. Evol. 34, 569–583.

Klimpel, S., Palm, H.W., Seehagen, A., 2003. Metazoan parasites, food composition of juvenile *Etmopterus spinax* (L. 1758) (Dalatiidae, Squaliformes) from the Norwegian Deep. Parasitol. Res. 89, 245–251.

Kotlyar, A.N., 1990. Dogfish Sharks of the genus *Etmopterus* Rafinesque from the Nazca and Sala y Gomez Submarine Ridges. Trudy Instituta Okeanologii 125, 127–147.

Kriwet, J., Benton, M., 2004. Neoselachian (Chondrichthyes, Elasmobranchii) diversity across the K/T boundary. Palaeogeogr. Palaeocl. 214, 181–194.

Kriwet, J., Klug, S., 2004. Late Jurassic Selachians (Chondrichthyes: Elasmobranchii) from Southern Germany: re-evaluation on taxonomy and diversity. Zitteliana A44, 67–95.

Kriwet, J., Klug, S., 2010. Timing of deep-sea adaptation in dog-fish sharks: insights from a supertree of extinct and extant taxa. Zoologica Scripta, doi:10.1111/j.1463-6409.2010.00427.x.

Last, P.R., Burgess, G.H., Seret, B., 2002. Description of six new species of Lantern-Sharks of the genus *Etmopterus* (Squaloidea: Etmopteridae) from the Australasian region. Cybium 26, 203–223.

Last, P.R., Stevens, J.D., 1994. Sharks and Rays of Australia. CSIRO Australia, pp. 1–513.

Last, P.R., Stevens, J.D., 2009. Sharks and Rays of Australia, 2nd ed. Harvard University Press, Cambridge, pp. 1–554.

Lear, C.H., Bailey, T.R., Pearson, P.N., Coxall, H.K., Rosenthal, Y., 2008. Cooling and ice growth across the Eocene–Oligocene transition. Geology 36, 251–254.

Ledoux, J.-C., 1972. Les Squalidae (Euselachii) miocenes des environs d'Avignon (Vaucluse). Doc. Lab. Geol. Fac. Sci. Lyon, Notes Mem 52, 133–175.

Lindberg, D.R., Pyenson, N.D., 2007. Things that go bump in the night: evolutionary interactions between cephalopods and cetaceans in the tertiary. Lethaia 40, 335–343.

Macpherson, E., 1980. Régime alimentaire de Galeus melastomus Rafinesque, 1810, *Etmopterus spinax* (L., 1758) et Schymnorhinus licha (Bonnaterre 1788) en Méditerranée occidentale. Vie et Milieu 30, 139–148.

Maisey, J.G., Naylor, G.J.P., Ward, D.J., 2004. Mesozoic elasmobranchs, neoselachian phylogeny and the rise of modern elasmobranch diversity. In: Arratia, G., Tintori, A. (Eds.), Mesozoic Fishes 3-Systematics. Palaeoenvironments and Biodiversity. Verlag Dr. Friedrich Pfeil, Munich, pp. 17–56.

Misof, B., Misof, K., 2009. A Monte Carlo approach successfully identifies randomness of multiple sequence alignments: a more objective means of data exclusion. Syst. Biol. 58 (1), 21–34.

Müller, A., Schöllmann, L., 1989. Neue Selachier (Neoselachii, Squalomorphii) aus dem Campanium Westfalens (NW-Deutschland). Neues Jahrb. Geol. Palaeontol., Abh. 178, 1–35.

Naylor, G.J.P., Ryburn, J.A., Fedrigo, O., Lopez, A., 2005. Phylogenetic relationships among the major lineages of modern elasmobranchs. In: Hamlett, W.C. (Ed.), Reproductive Biology and Phylogeny of Chondrichthyes; Sharks. Batoids and Chimaeras. Science Publishers Inc., Enfield, pp. 1–25.

Neiva, J., Coelho, R., Erzini, K., 2006. Feeding habits of the velvet belly lanternshark *Etmopterus spinax* (Chondrichthyes: Etmopteridae) off the Algarve, southern Portugal. J. Mar. Biol. Assoc. UK 86, 835–841.

Nylander, J.A.A., Ronquist, F., Huelsenbeck, J.P., Nieves-Aldrey, J.L., 2004. Bayesian phylogenetic analysis of combined data. Syst. Biol. 53 (1), 47–67.

Pattengale, N.D., Alipour, M., Bininda-Edmonds, O.R.P., Moret, B.M.E., Stamatakis, A., 2009. How many Bootstrap replicates are necessary? Presented at: International Conference on Research in Computers. Molecular Biology RECOMB. Tucson. In: Proceedings of the 13th International Conference on Research in Computational Molecular Biology RECOMB. 2009, Springer 2009. Lecture Notes in Computer Science. Online Pre-print: http://lcbb.epfl.ch/bootstrapping.pdf.

Reif, W.E., 1985. Functions of scales and photophores in Mesopelagic Luminescent Sharks. Acta Zool.-Stockholm 66 (2), 111–118.

Sanderson, M.J., 2002. Estimating absolute rates of molecular evolution and divergence times: a penalized likelihood approach. Mol. Biol. Evol. 19, 101–109.

Sanderson, M.J., 2003. R8s: inferring absolute rates of molecular evolution and divergence times in the absence of a molecular clock. Bioinformatics 19, 301–302.

Schaaf da Silva, J.A., Ebert, D., 2006. *Etmopterus burgessi* sp. Nov., a new species of lantern shark (Squaliformes: Etmopteridae) from Taiwan. Zootaxa 1273, 53–64.

Siverson, M., 1993. Maastrichthian squaloid sharks from southern Sweden. Palaeontology 36 (1), 1–19.

Shirai, S., Nakaya, K., 1990a. A new squalid species of the genus *Centroscyllium* from the Emperor Seamount Chain. Jpn. J. Ichthyol. 36, 391–398.

Shirai, S., Nakaya, K., 1990b. Interrelationships of the Etmopteridae (Chondrichtyes, Squaliformes). In: Pratt, H.L. JR., Gruber, S.H., Taniuchi, T. (Eds.). Elasmobranchs as Living Resources: Advances in Biology, Ecology, Systematics and the status of the fisheries. NOAA Technical report 90, pp. 347–356.

Shirai, S., 1992. Squalean Phylogeny and Related Taxa. Hokkaido University Press. pp. 1–151.

Shirai, S., Tachikawa, H., 1993. Taxonomic resolution of the *Etmopterus pusillus* species group (Elasmobranchii, Etmopteridae) with description of *E. bigelowi*, n. sp.. Copeia 2, 483–495.

Springer, S., 1967. Social organization of shark populations. In: Gilbert, P.W., Mathewson, R.F., Rall, D.P. (Eds.), Sharks Skates and Rays. Johns Hopkins University Press, Baltimore, pp. 503–531.

Springer, S., Burgess, G.H., 1985. Two New Dwarf Dogsharks (*Etmopterus*, Squalidae), found off the Carribean Coast of Colombia. Copeia 3, 584–591.

Stamatakis, A., 2006. RAxML-VI-HPC: maximum Likelihood-based phylogenetic analyses with thousands of taxa and mixed models. Bioinformatics 22 (21), 2688–2690.

Stanley, M., 2009. Earth system history. In: Raymond, V., Clench, W., Thorne, A. (Eds.). W.H. Freeman and Company, New York, USA. pp. 1–549.

Straube, N., Schliewen, U., Kriwet, J., 2008. Dental Structure of the Giant lantern shark, *Etmopterus baxteri* (Chondrichthyes: Squaliformes) and its taxonomic implications. Environ. Biol. Fish. 82, 133–141.

Swofford, D.L., 2003. PAUP*. Phylogenetic analysis Uing Parsimony (*and Other Methods). Version 4. Sinauer Associates, Sunderland, Massachusetts.

Thies, D., Müller, A., 1993. A neoselachian fauna (Vertebrata, Pisces) from the Late Cretaceous (Campanian) of Höver, near Hannover (NW, Germany). Paläontol. Z. 67, 89–107.

Tracer, v1.4. (http://beast.bio.ed.ac.uk/tracer).

Türkay, M., 2002. Die Tiefsee. In: Hofrichter (Ed.), Das Mittelmeer. Fauna, Flora, Ökologie. Band I: Allgemeiner Teil. Spektrum Akademischer Verlag Heidelberg, Berlin, pp. 416–423.

Underwood, C.J., Mitchell, S.F., 1999. Albian and Cenomanian selachian assemblages from north–east England. Spec. Pap. Palaeontol. 60, 9–56.

Venkatesh, B., Kirkness, E.F., Loh, Y.H., Halpern, A.L., Lee, A.P. et al., 2007. Survey sequencing and comparative analysis of the elephant shark (Callorhinchus milii) genome. PLoS Biology 5(4), e 101. doi:10.1371/journal.pbio.0050101.

Ward, R.D., Zemlak, T.S., Innes, B.H., Last, P.R., Hebert, D.N., 2005. DNA barcoding Australia's fish species. Phil. Trans. R. Soc. Lond. B 360, 1847–1857.

Ward, R.D., Holmes, B.A., Zemlak, T.S., Smith, P.J., 2007. Part 12-DNA barcoding discriminates spurdogs of the genus Squalus. In: Last, P.R., White, W.T., Pogonoski J.J. (Eds.), Descriptions of new dogfishes of the genus Squalus (Squaloidea: Squalidae). CSIRO Marine and Atmospheric Research Paper No. 14, pp. 114–130.

Widder, E., 1998. A predatory use of counter illumination by the squaloid shark, Isistius brasiliensis. Environ. Biol. Fish. 53, 267–273.

Yamakawa, T., Taniuchi, T., Nose, Y., 1986. Review of the *Etmopterus lucifer* Group (Squalidae) in Japan. In: Uyeno, T., Arai, R., Taniuchi, T., Matsuura, K. (Eds.), Indo-Pacific Fish Biology: Proceedings of the Second International Conference on Indo-Pacific fishes. Ichthyological Society of Japan, Tokyo, pp. 197–207.

Yano, K., 1997. First record of the brown lantern shark, *Etmopterus* unicolor, from the waters around New Zealand, and comparison with the southern lantern shark, *E. Ganulosus*. Ichthyol. Res. 44 (1), 61–72.

Article II

STRAUBE N., KRIWET J., SCHLIEWEN U. K. (2011) Cryptic diversity and species assignment of large Lantern Sharks of the *Etmopterus spinax* clade from the Southern Hemisphere (Squaliformes, Etmopteridae). *Zoologica Scripta*, 40 (1), 61-75.doi 10.1111/j.1463-6409.2010.00455.x

Zoologica Scripta

KUNGL. VETENSKAPS-AKADEMIEN
THE ROYAL SWEDISH ACADEMY OF SCIENCES

Cryptic diversity and species assignment of large lantern sharks of the *Etmopterus spinax* clade from the Southern Hemisphere (Squaliformes, Etmopteridae)

Nicolas Straube, Jürgen Kriwet & Ulrich Kurt Schliewen

Submitted: 30 April 2010
Accepted: 12 September 2010
doi:10.1111/j.1463-6409.2010.00455.x

Straube, N., Kriwet, J. & Schliewen, U. K. (2011). Cryptic diversity and species assignment of large lantern sharks of the *Etmopterus spinax* clade from the Southern Hemisphere (Squaliformes, Etmopteridae). — *Zoologica Scripta*, *40*, 61–75.

Many species of the speciose deep-sea shark family Etmopteridae (lantern sharks) are a regular by-catch component of deepwater trawl and longline commercial fisheries. As for many elasmobranchs, the low fecundity, late sexual maturation and extreme longevity of the lantern sharks increase their susceptibility to overfishing. However, the taxonomic uncertainty within etmopterids and the poorly known patterns of dispersal of these shark species hampers the establishment of reasonable monitoring efforts. Here, we present the first molecular approach to clarify the taxonomy and distribution of a morphologically uniform group of lantern sharks comprising *Etmopterus granulosus* and closely related congeners by using nucleotide sequence data from the mitochondrial DNA cytochrome oxidase I gene and amplified fragment length polymorphisms. Samples were collected from several locations in the Southern Hemisphere, where the species occur. Our analyses reveal a high level of cryptic diversity. *E. granulosus* is not endemic to Chile, but instead has a widespread distribution in the Southern Hemisphere being synonymous to New Zealand *Etmopterus baxteri*. Conversely, specimens previously assigned to *E. baxteri* from off South Africa apparently represent a distinct species. Our results provide the basis for the redescription of *E. granulosus* and *E. baxteri* which will help in the establishment of useful monitoring and management strategies.

Corresponding author: *Nicolas Straube*, *Zoologische Staatssammlung München*, *Sektion Ichthyologie*, *Münchhausenstrasse 21*, *81247 München*, *Germany*. *E-mail: straube@zsm.mwn.de*
Jürgen Kriwet, *Department of Paleontology*, *University of Vienna*, *Geozentrum*, *Althanstrasse 14*, *1090 Vienna*, *Austria*. *E-mail: juergen.kriwet@univie.ac.at*
Ulrich Kurt Schliewen, *Zoologische Staatssammlung München*, *Sektion Ichthyologie*, *Münchhausenstr. 21*, *81247 Munich*, *Germany*. *E-mail: schliewen@zsm.mwn.de*

Introduction

Deep-sea fishes in general, and deep-sea sharks in particular, are suspected to be highly vulnerable to recently expanding commercial deep-sea fisheries due to their extreme longevity, slow growth, late maturation and small litter sizes (Devine *et al.* 2006; Forrest & Walters 2009). Unfortunately, assessment of species-specific conservation needs is difficult as very little is known about the distribution and population genetics of deep-sea sharks, and because commercial fisheries and conservation efforts are usually focused on more valuable and productive teleost fishes (Bonfil 1994; Forrest & Walters 2009). The problem is made worse by the taxonomic uncertainty that often does not allow for the collection of accurate species-specific catch data. A recent study by Iglésias *et al.* (2009) has highlighted problems arising from the lack of accurate species identification of the commercially targeted skate species *Dipturus batis* and *Dipturus oxyrinchus*, whose landings data in fact comprises five distinct species. Mislabelling of specimens and hence incorrect monitoring data resulted in a dramatic decline of once common species increasing the risk of extinction (Iglésias *et al.* 2009). Deep-sea luminescent sharks of the squaliform genus *Etmopterus* are not directly targeted by commercial fisheries, but are a significant by-catch component of deep-sea fisheries (Clarke *et al.* 2005; Compagno *et al.* 2005; Jakobsdottir 2001; Wetherbee 1996, 2000). Despite being caught 'only' as by-catch, benthic and bentho-pelagic etmopterids are likely strongly affected by deep-sea fisheries targeting other species. Several lantern sharks are locally endemic to

small areas and hence may be especially vulnerable to overfishing. Another factor that has been shown to increase susceptibility to overfishing in the deep sea is that species are long-lived and late reproducing (Devine *et al.* 2006). Preliminary age estimates suggest *Etmopterus baxteri* to reach maturity between 10 and 20 years for males and 11.5 to 30 years for females (Irvine *et al.* 2006). In addition, several species are known to form sex and size specific aggregations (Jakobsdottir 2001; Wetherbee 1996). Some lantern sharks are only found regionally while others are distributed worldwide. For instance, the world's smallest shark species, *Etmopterus perryi* and *Etmopterus carteri*, are both considered endemic to a narrow stripe of the Caribbean coast of Colombia (Springer & Burgess 1985). In contrast, *Etmopterus pusillus* and *Etmopterus lucifer* are distributed almost circumglobally (Compagno *et al.* 2005). Contrary to highly migratory elasmobranchs such as *Isurus oxyrinchus* (Schrey & Heist 2003), *Rhincodon typus* (Castro *et al.* 2007), *Carcharodon carcharias* (Bonfil *et al.* 2005; Boustany *et al.* 2002) or the more closely related *Squalus acanthias* (McFarlane & King 2003; Verrissimo *et al.* 2010), lantern sharks are not known to undergo large scale migrations. However, migrations may occur to distinct spawning and mating grounds as indicated by the presence of size-related and sex-related aggregations (Forrest & Walters 2009; Jakobsdottir 2001; Wetherbee 1996). Consequently, assessment of by-catch impact for narrow endemics vs. wide spread and potentially migrating taxa need reliable data for correct species identification, which in turn allow to asses conservation relevant issues of their life history, ecology and distribution.

Among lantern sharks that are potentially most affected by deep-sea fisheries, the alpha-level taxonomy of the *Etmopterus spinax* clade (Straube *et al.* 2010) is particularly difficult. Species of this clade are distributed worldwide and comprise *E. spinax*, *Etmopterus princeps*, *Etmopterus dianthus*, *Etmopterus unicolor*, *Etmopterus granulosus*, and *E. baxteri*. Straube *et al.* (2010) further suggested the inclusion of *Etmopterus hillianus* and *Etmopterus litvinovi* as well as the undescribed *Etmopterus* sp. B. Although some species of the clade are morphologically distinguishable using the shape of bioluminescent flank markings such as *E. spinax*, and *E. dianthus*, others are not (e.g. *E. granulosus*, *E. unicolor*, *E. princeps*, and *E. baxteri*). The taxonomy and distribution of the Southern lantern shark, *E. granulosus* (Günther 1880), is controversial. The species is listed in the IUCN (2010) Red List of Threatened species as endemic to Chile. However, a very similar species described from New Zealand, *E. baxteri* (Garrick 1957), was synonymized with *E. granulosus* based on morphological data (Tachikawa *et al.* 1989). Despite Tachikawa *et al.* (1989) study, taxonomic uncertainty about the species status of different populations of lantern sharks broadly referable to either *E. granulosus* or *E. baxteri* has remained, as reflected in the inconsistent usage of both species names in the most recent taxonomic shark literature. For instance, *E. baxteri* and *E. granulosus* are either accepted as two distinct species (Compagno *et al.* 2005; Last & Stevens 2009) or mentioned as *E. granulosus* comprising different populations (Forrest & Walters 2009; Wetherbee 1996, 2000). Both species are considered as 'least concern' in the IUCN (2010) Red List of Threatened Species.

Catch records of *E. granulosus*-like specimens from off South Africa, South America, Australasia, New Zealand and the Kerguelen Plateau are doubtful with regard to correct species assignment, as cryptic diversity has not been analysed in detail so far (IUCN Red List 2010). Phylogenetic analyses based on nuclear and mitochondrial DNA sequences including several *E. granulosus*-like specimens from Chile, the Tasman Sea, New Zealand, South Africa and the Kerguelen Plateau did not provide a fine-grained resolution to the species status problem, but highlighted the paraphyly and cryptic diversity within the *E. spinax* clade (Straube *et al.* 2010).

Here, we provide the first phylo- and population-genetic analysis investigation of the cryptic diversity among a group of deep-sea sharks with a still unresolved taxonomic background that is potentially affected by fisheries targeting shrimp and Orange Roughy (Wetherbee 1996; IUCN 2010). We included all available *E. granulosus/E. baxteri*-like specimens from the Southern Hemisphere to critically test for sympatric and allopatric diversity among specimens recorded as *E. granulosus* or *E. baxteri*. We tested for assignation of all individuals to discernable genetic clusters, i.e. potential species or populations. The results are used to provide information on population structure of *E. granulosus*, which is the basis for adequate conservation measures and estimating the cryptic diversity among specimens assigned previously to *E. granulosus* and *E. baxteri*, respectively. We further used our data to re-analyse the phylogenetic interrelationships of the *E. spinax* clade for establishing an improved resolution of the clade.

Material and methods

Sampling

Tissue samples from fresh or frozen specimens from the Southern Hemisphere of *E. granulosus sensu* Compagno *et al.* 2005 (n = 13, Chile), *E. baxteri sensu* Last & Stevens 2009 (n = 24, New Zealand), *E. baxteri sensu* Compagno *et al.* (1991) (n = 8, South Africa), *E.* cf. *baxteri* (n = 1, Amsterdam Island), *E.* sp. B *sensu* Last & Stevens 1994 (n = 6, Norfolk Ridge), *E. granulosus* (n = 1, NE of the Kerguelen Plateau), and *E.* cf. *granulosus sensu* Duhamel *et al.* 2005 (n = 9, New Zealand and Kerguelen Plateau),

were preserved in 96% ethanol. In addition, cytochrome oxidase I (COI) sequences from Genbank [n = 5 specimens of *E.* cf. *unicolor sensu* Ward *et al.* 2008 from off Indonesia (accession numbers EU398778, EU398779, EU398780, EU398781, EU398782)] and n = 2 specimens of *E. granulosus sensu* (Ward *et al.* 2008) from the Tasman Sea (accession numbers DQ108226, DQ108216) were included. Further, samples from the Northern Hemisphere were analysed in order to test for refined phylogenetic resolution of the entire *E. spinax* clade *sensu* Straube *et al.* (2010), i.e. specimens of *E. unicolor* (n = 3, North-West Pacific), *E. princeps* (n = 3, North-East Atlantic), *E. spinax* (n = 3, North-East Atlantic), and *Etmopterus brachyurus* (n = 3, Japan, North-West Pacific). *E. brachyurus* was chosen as outgroup as it is the most closely related taxon to the *E. spinax* clade (Straube *et al.* 2010), for which high quality DNA was available. For a summary of all specimens analysed in this study see Supporting Information S1, for sampling locations see Fig. 1.

DNA extraction, sequencing and phylogenetics

Total genomic DNA was extracted from muscle tissues using the QIAmp tissue kit (Qiagen®, Valencia, CA, USA). The mitochondrial COI gene was sequenced (655 bp) as it is a well-established gene fragment for identification of shark species (Ward *et al.* 2005, 2007). The COI sequences were amplified using primers S0156 (5′-TAGCTGATGAATCTGACCGTGAAAC-3′) and R0084 (5′-TGAACGCCAGATTTCATAGCGTTC-3′) following the PCR protocol of Iglésias *et al.* (2005). The PCR products were cleaned using the QIAquick PCR Purification Kit (Qiagen®) following the manufacturer's protocol. Cycle sequencing was performed at the sequencing service of the Department of Biology of the Ludwig Maximilian University (Munich), using ABI Big Dye 3.1 chemistry (PE Applied Biosystems®, Foster City, CA. USA).

Sequences were edited using the BioEdit software version 7.0.9 (Hall 1999) and aligned with MUSCLE v3.6 (Edgar 2004). Check of COI sequences against nuclear pseudogene status was done by searching for stop codons and by translating sequences into amino acids. Ambiguous sites in nucleotide sequences, attributed to double peaks in the electropherogram, were coded referring to IUB symbols. The software NETWORK v4.5.1.6 (fluxus-engineering.com) was applied to the smallest resulting sequenced fragments homologous to all taxa. The final alignment had 659 bp and was used as the basis to reconstruct most parsimonious phylogenetic networks (Bandelt *et al.* 1999). The network was calculated using the median joining algorithm (allowing for multistate data) under default settings (weights = 10, epsilon = 0).

Genotyping and subsequent analyses

We genotyped amplified fragment length polymorphisms (AFLPs), (Vos *et al.* 1995; Meudt & Clarke 2007) as a basis for model based clustering methods and assignment of individuals to genotypic clusters. The AFLP dataset differs from the mtDNA data by the exclusion of 16 specimens [*E.* cf. *granulosus* (n = 3), *E.* cf. *baxteri* (n = 1), *E. granulosus* (n = 3), *E.* sp. B (n = 1), *E. brachyurus* (n = 3), *E. unicolor* (n = 1), *E.* cf. *unicolor* (n = 5)], which could not be amplified or for which highly genomic DNA was not available.

Methods for AFLP genotyping (restriction/ligation/primary amplification) follow Herder *et al.* (2008). The following restrictive primer combinations, based on the core sequences provided in Vos *et al.* (1995) (EcoRI: 5′-CTCGTAGACTGCGTACC; MseI: 5′-GAC

Fig. 1 Sampling sites of specimens used in this study.

GATGAGTCCTGAG), were used: EcoRI-AGG/MseI-CTG, EcoRI-ACA/MseI-CAA, EcoRI-ACA/MseI-CTG, EcoRI-ACT/MseI-CAA, EcoRI-AGG/MseI-CTC, EcoRI-ACC/MseI-CTA, EcoRI-ACT/MseI-CAG, EcoRI-ACC/MseI-CAT, EcoRI-AGG/MseI-CTA, EcoRI-ACA/MseI-CAT, EcoRI-ACT/MseI-CTG, EcoRI-ACC/MseI-CAG, EcoRI-ACT/MseI-CTT, EcoRI-AGC/MseI-CTC, EcoRI-AGG/MseI-CAA, EcoRI-AGC/MseI-CAC, EcoRI-AGG/MseI-CTT, EcoRI-AGC/MseI-CAG, EcoRI-ACT/MseI-CAC, EcoRI-ACC/MseI-CTC.

Capillary electrophoresis was conducted on an ABI 3130 Genetic Analyzer (PE Applied Biosystems, Foster City, CA, USA) with an internal size standard (ROX 500 XL). Binary character matrices were produced from each primer combination using automated peak scoring (binning) in the GeneMapper® Software v4.0 (PE Applied Biosystems, Foster City, CA, USA). Quality of runs were checked by eye and repeated if necessary. For each primer, a range of 50–499.5 bp was analysed. For optimizing automated AFLP scoring, peak height threshold was set to 50 relative fluorescent units (RFU), and bin width was set to 0.75 bp. The option of 'light' smoothing was chosen, the Local Southern Method was evaluated as size calling method and common alleles were deleted from the matrix. Each run included six replicate samples to detect and delete inconsistently produced fragments. Each single matrix resulting from the 20 different primer combinations was further corrected by removing all pairs of neighbouring bins in which the minimum distance between them was less than 0.25 bps, as well as those bins containing fragments differing by more than 0.65 bps in size (Albertson *et al.* 1999). For comparison with the mtDNA sequence data, a neighbor-joining network was calculated using the software Splitstree4 v4.10 (Huson & Bryant 2006). PAST v1.94b (Hammer *et al.* 2001) allowed visual inspection of principal components after principal component analysis (PCA) of the combined data set. For phylogenetic inferences based on neighbor-joining distances of AFLP data we used the Link *et al.* (1995) algorithm as implemented in the software package TreeCon v1.3b (Van de Peer & De Wachter 1994) with a subsequent bootstrap analysis comprising 2000 replicates. The algorithm by Link *et al.* (1995) uses shared and present bands only, while absent bands are not included in analyses. This is important for AFLP data because the absence of a band in the final data matrix may have more reasons as compared with the presence of a band.

Adopting results of previous analyses and hence accepting *E. granulosus* being a synonym to New Zealand *E. baxteri*, the software package Arlequin v3.5 (Excoffier & Schneider 2005) was employed to conduct analyses of molecular variance (AMOVA) to evaluate the amount of population genetic structure of *E. granulosus* between the two sampling locations New Zealand and Chile and to estimate pairwise F_{ST} values. The AFLP data set of *E. granulosus* was further analysed with BAYESCAN (Foll & Gaggiotti 2008) to identify loci which are under selection and are therefore strongly affecting population structuring. Subsequently, the AMOVA was re-run without the loci identified by BAYESCAN as contributing the most for the population structure to test for changes in the percentage variation and pairwise F_{ST}. For comparison, pairwise Φ_{ST} values were computed in Arlequin for the mtDNA (COI) sequence data including two separate groupings to explore differentiation of *E. granulosus* from Chile and specimens from New Zealand with 10 000 permutations and a significance level of 0.01 using haplotype frequencies only.

STRUCTURE v2.2.3 (Pritchard *et al.* 2000; Falush *et al.* 2003) was used to calculate model based genotypic clusters and to assign individuals to genotypic clusters (populations). We treated AFLP loci as either being present (i.e. di-allelic), or as missing as recommended by Falush *et al.* (2007) for dominant markers. To detect population structure according to a hierarchical model, we followed methodologically Evanno *et al.* (2005), testing numbers of populations from $K = 1$ to $K = 12$. Each test was performed 15 times with a burn-in of 75 000 generations and following 2 00 000 Markov chain Monte Carlo (MCMC) generations, respectively after exploratory preruns to estimate convergence of likelihoods with different burn-ins and MCMC generations. The allelic frequency was set to 1. We applied the admixture model and the allele frequency model assuming correlated allelic frequencies as recommended in the user's manual. The mean ln of likelihoods of 15 runs for each K was used to estimate the true number of K by computing ΔK following Evanno *et al.* (2005). A second analysis focused on a smaller dataset including only specimens assigned to *E. granulosus* from Chile and *E. baxteri* from New Zealand as no population structure was detected between the two sampling locations within the full dataset (as e.g. in Warnock *et al.* 2009). The smaller dataset removes part of the variance of the full dataset which may reveal subtle population structure. STRUCTURE v2.3.1 runs were repeated twice, excluding and including prior location information as informative prior settings (Hubisz *et al.* 2009).

Due to the high morphometric similarity of *E. granulosus* specimens with those previously assigned to *E. baxteri* sampled off South Africa and due to a potential Northern Hemisphere origin of the Southern Hemisphere *E. granulosus*, STRUCTURE v2.3.2 *beta* was used to test for a mixed ancestry of *E. princeps*, *E. granulosus* and specimens assigned to *E. baxteri* sampled off South Africa. To test for patterns of mixed ancestry among individuals of the three

groups, we used the program option using putative prior information on population origin and a defined number of past generations (GENSBACK subpackage of STRUCTURE). In our case, the implemented model translates into the assumption that the largest part of individuals assigned to *E. baxteri* from South Africa is genotypically differentiable and that a small portion of individuals may have a mixed ancestry of the species specific genotypes of *E. granulosus* and/or *E. princeps* from the North Atlantic (Falush *et al.* 2007). We did so by using settings of GENSBACK between two and four past generations and a fixed number of $K = 3$ as derived from our prior analyses, i.e. representing *E. granulosus* from off Chile and New Zealand, *E. princeps* from the North Atlantic, and specimens assigned to *E. baxteri* sampled off South Africa. MIGPRIOR was set to 0.001 using the admixture model as suggested by Falush *et al.* 2007, and 1 50 000 MCMC generations with a burnin of 50 000 generations for each run were performed.

Results

Phylogenetics

mt DNA. The COI alignment has 541 constant characters plus 17 variable characters, which are parsimony-uninformative and 101 characters which are parsimony-informative. Base frequencies are equally distributed in all positions (chi-square test: $\chi^2 = 34.42$, d.f. = 201, $P = 1.0$). Empirical base frequencies are 0.26 for A, 0.25 for C, 0.18 for G, and 0.31 for T. Altogether 63 haplotypes were

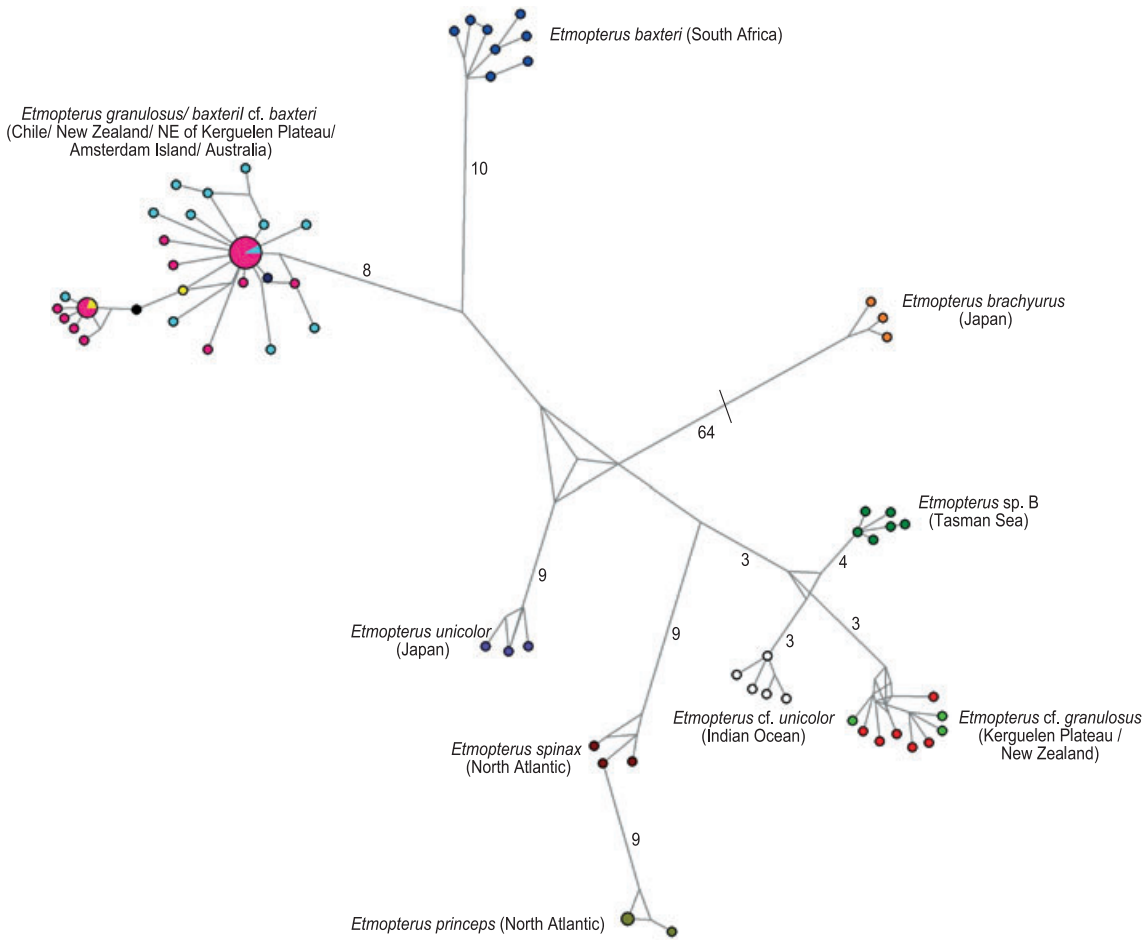

Fig. 2 Most parsimonious haplotype network structure attained from cytochrome oxidase I sequences (mitochondrial DNA). Numerals above branches indicate the number of mutated positions. Branches without numbers show two or less mutated positions. Pink = *Etmopterus baxteri* (New Zealand). Turquoise = *Etmopterus granulosus* (Chile). Yellow = *E. granulosus* (Tasman Sea). Black = *E.* cf. *baxteri* (Amsterdam Island). Blue = *E. baxteri* (South Africa). Purple = *Etmopterus unicolor* (Japan). Orange = *Etmopterus brachyurus* (Japan). Dark red = *Etmopterus spinax* (North Atlantic). Olive = *Etmopterus princeps* (North Atlantic). Dark green = *Etmopterus* sp. B (Norfolk Ridge). Red = *E.* cf. *granulosus* (New Zealand). Green = *E.* cf. *granulosus* (Kerguelen Plateau). White = *E.* cf. *unicolor* (Indian Ocean). Dark blue = *E. granulosus* (NE of Kerguelen Plateau).

detected, and the estimate for mutations steps for the shortest network is 328. The most parsimonious network identifies nine major monophyletic clusters, i.e. *E. spinax* (NE Atlantic), *E. princeps* (NE Atlantic), *E.* cf. *granulosus* (*sensu* Duhamel *et al.* 2005; Kerguelen Plateau & New Zealand), *E.* sp. B (*sensu* Last & Stevens 1994; Norfolk Ridge), *E. unicolor* (Japan), *E. brachyurus* (Japan), *E. baxteri* (*sensu* Compagno *et al.* 2005; South Africa), *E.* cf. *unicolor* (Ward *et al.* 2008; Indonesia), and *E. granulosus–E. baxteri* (Chile and New Zealand). Within the latter cluster there is no apparent lineage sorting between *E. granulosus* from Chile (close to the type locality of *E. granulosus*) and *E. baxteri* from New Zealand (close to the type locality of *E. baxteri*) according to location or preliminary species assignment. In contrast, specimens of *E. baxteri* sampled off South Africa form a distinct cluster (Fig. 2).

AFLP data. The AFLP scoring resulted in a binary matrix comprising 2655 loci in 68 specimens.

A neighbor-joining network calculation based on AFLP data (Fig. 3) identified the same eight major clusters retrieved by the network using mtDNA data (Fig. 2). The *E. baxteri* (New Zealand) and *E. granulosus* (Chile) cluster together. The *E. baxteri* (South Africa) forms a distinct cluster along with *E. spinax*, *E. princeps*, *E.* cf. *granulosus*, *E.* sp. B, *E. unicolor* and *E. brachyurus*.

For phylogenetic inferences of the *E. spinax* clade, a neighbor-joining tree was calculated from AFLP data. All specimens sampled in the Southern Hemisphere constitute a monophyletic group (Fig. 4). Its basal sister clade comprises specimens of *E. princeps* from the North Atlantic. *E. princeps* (NE Atlantic) and the Southern Hemisphere species are sister to *E. spinax* (NE Atlantic). The monophyletic lineage is sister to *E. unicolor* (NE Pacific). Again, there is no species delimitation between *E. baxteri* sampled off New Zealand and *E. granulosus* sampled off Chile, which are sister to *E.* cf. *granulosus* and *E.* sp. B. Specimens assigned to *E. baxteri* from South Africa form a distinct clade sister to a clade comprising *E. granulosus* (Chile)/*E. baxteri* (New Zealand), *E.* sp. B and *E.* cf. *granulosus*. Bootstrap support is high for all clades, lower bootstrap support values are found at nodes explaining the interrelationships of the Southern Hemisphere clade.

Population genetics

PCA. The PCA computed from the AFLP dataset reveals five clusters when plotting principal component (PC) 1 against PC2 (Fig. 5A), i.e. one for *E. granulosus* (Chile) and *E. baxteri* (New Zealand) and one for *E.* cf. *granulosus* and *E.* sp. B. Specimens assigned to *E. baxteri* from South Africa form a third cluster. Finally, the two specimens of *E. unicolor* from Japan and the *E. baxteri* specimens from South Africa each plot as separate but neighbouring groupings. *Etmopterus spinax* (NE Atlantic) and *E. princeps* (NE Atlantic) form additional clusters (Fig. 5A). The PCs 1 and 2 explain 22.9% of the total variance, the variance evenly decreases with increasing PCs. Plotting PCs 1 and 3, *E.* cf. *granulosus* and *E.* sp. B form distinct cluster (20.3% of variance explained, Fig. 5B). The same applies to comparison of PCs 2 and 3 (8.78% of variance explained), whereas *E. granulosus* and *E. baxteri* always broadly overlap independent of PC comparison. Subsequent plotting of PCs 1 & 2 (11.52% of total variance), 1 & 3 (10.77% of total variance), and 2 & 3 (9.49% of total variance) using AFLP data

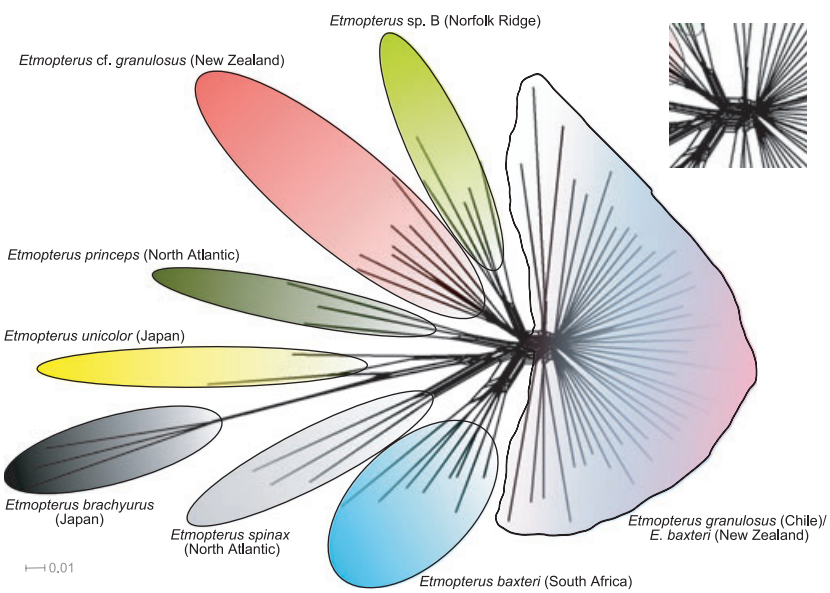

Fig. 3 Neighbor network structure attained from amplified fragment length polymorphism genotyping based on the algorithm by Link *et al.* (1995). Conflicting phylogenetic signal in the centre magnified top right.

of *E. granulosus* and *E. baxteri* showed again strong overlap of both species. Conversely, plotting PCs 1 and 2 (explaining 30.71% of total variance) of *E.* cf. *granulosus* against *E.* sp. B, specimens form distinct clusters (data not shown). There are no differences of *E. granulosus* (Chile) and *E. baxteri* (New Zealand), whereas specimens assigned to *E. baxteri* from South Africa form a distinct cluster, not overlapping with *E. baxteri* (New Zealand) and *E. granulosus* (Chile), respectively. The *E.* cf. *granulosus* and *E.* sp. B seem closely related, but form distinct clusters, if PCs 1 and 3 as well as PCs 2 and 3 are compared.

F-*statistics*. The F_{ST} value between *E. granulosus* (Chile) and *E. baxteri* (New Zealand) was estimated using AFLP data to assess the degree of genetic differentiation between the two groups. The percentage of variation is 2.43% among populations, whereas it is 97.57% within populations on a highly significant level ($P < 0.01$). Pairwise difference between both locations show a low but significant F_{ST} ($F_{ST} = 0.024$, $P < 0.01$) (Table 1).

BAYESCAN identified no loci as decisive factors for population structuring, assuming a posterior probability of 0.99 to 1.00 [Bayes factors (BF) = 99 and increasing] as threshold for identifying loci which are under strong selection and therefore cause population structuring. Decreasing the threshold to a posterior probability from of 0.99 to 0.72 (BF = 3) only reveals one locus as strongly selected. Further decreasing the posterior probability show a second locus at $P = 0.68$ ranging in the field of 'barely worth mentioning' loci under population shaping selection (Foll & Gaggiotti 2008). This indicates the absence of loci which account for population structure of the two locations New Zealand and Chile. Excluding those two loci and re-running an AMOVA in Arlequin slightly decreased the percentage of among population variation to 2.19%, and rose the variation within populations to 97.81%,

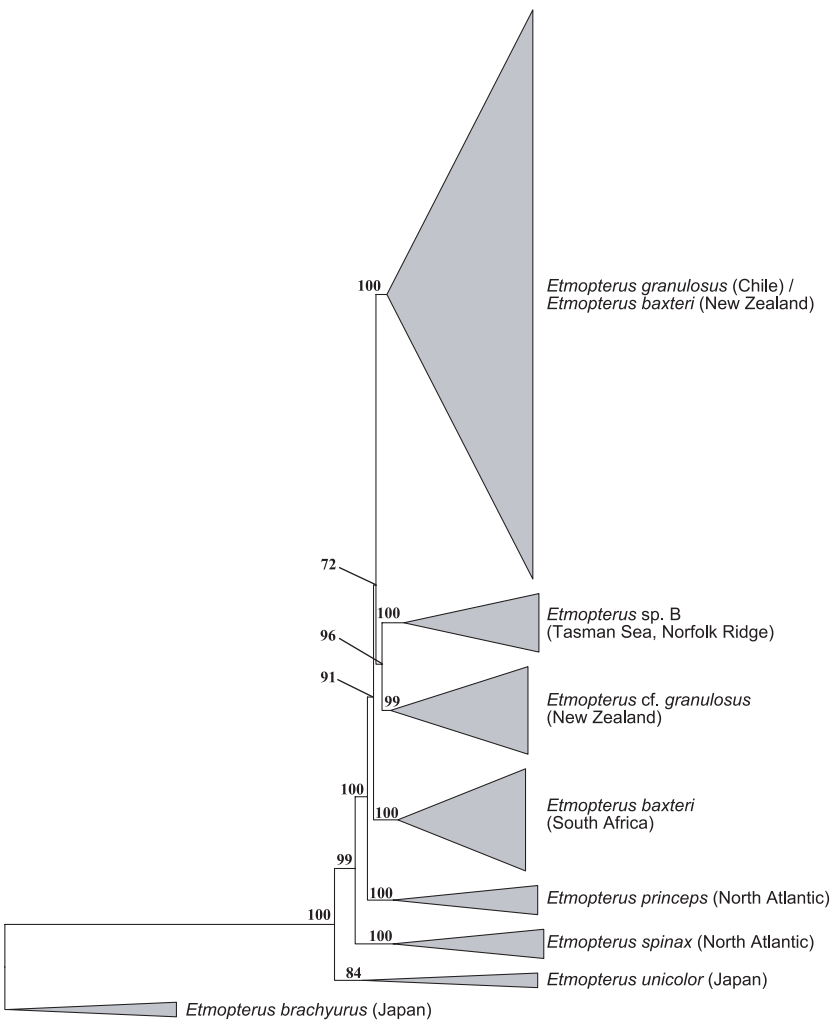

Fig. 4 Neighbor-joining tree calculated from amplified fragment length polymorphism data with bootstrap support values above nodes computed from 2000 bootstrap replicates. Main clusters are summarized to ease visualization.

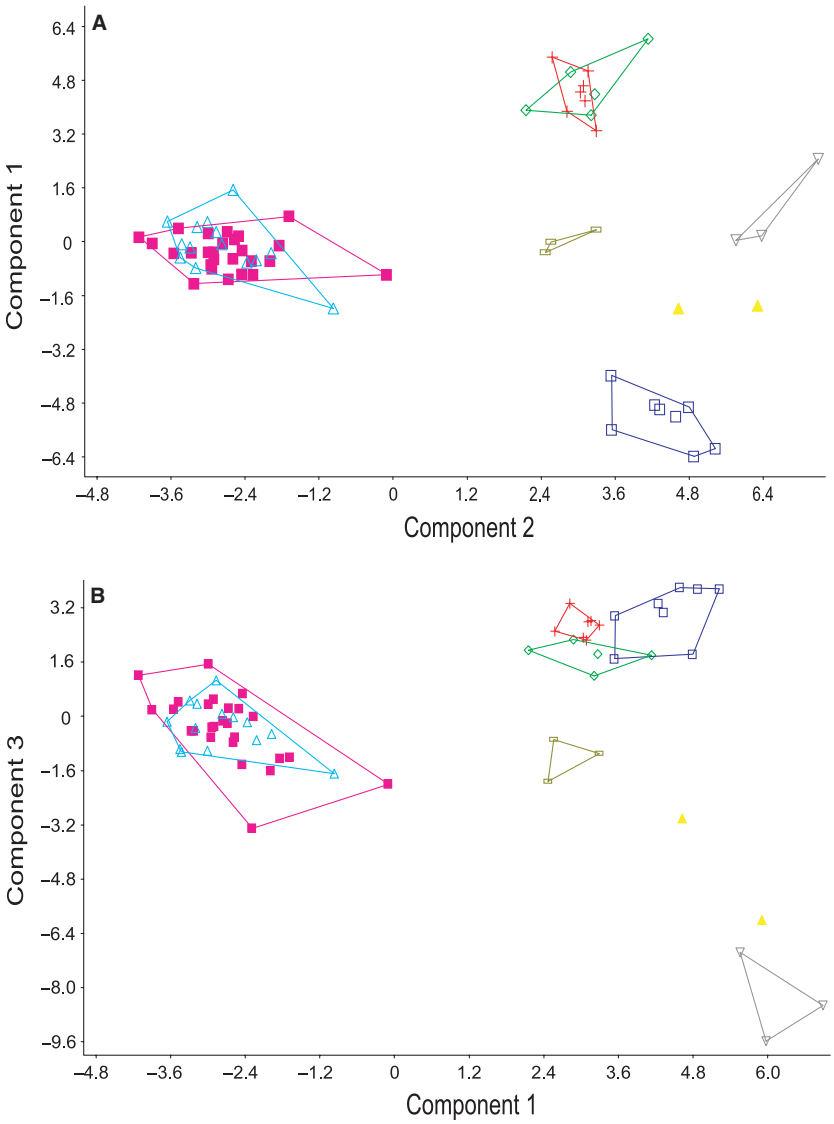

Fig. 5 Scatter plot from principal component (PC) analysis comparing PCs 1 & 2 (A) and PCs 1 & 3 (B) based on amplified fragment length polymorphism data. Filled squares = *Etmopterus baxteri* (New Zealand). Empty squares = *E. baxteri* (South Africa). Empty triangles = *Etmopterus granulosus* (Chile). Filled triangles = *Etmopterus unicolor* (Japan). Crosses = *E.* cf. *granulosus* (New Zealand). Diamonds = *Etmopterus* sp. B (Norfolk Ridge). Headstanding triangles = *Etmopterus spinax* (North Atlantic). Rectangles = *Etmopterus princeps* (North Atlantic).

Table 1 Percentage of molecular variation among (V_A) and within (V_W) two populations of *Etmopterus granulosus* from New Zealand and Chile and pairwise Φ_{ST} and F_{ST} estimates

	mtDNA	AFLP data	AFLP data after exclusion of population structuring loci
V_A	19.14	2.43	2.19
V_W	80.86	97.57	97.81
Φ_{ST}/F_{ST}	0.043*	0.024*	0.022*

*P-values highly significant ($P < 0.01$).
mtDNA, mitochondrial DNA; AFLP, amplified fragment length polymorphism.

which is in concordance with our expectations, since an exclusion of population structure giving loci should decrease the detected structuring of populations further indicating low to none population structure between sampling sites of *E. granulosus* in the SE (Chile) and SW Pacific Ocean (New Zealand).

The computed pairwise Φ_{ST} value for the two separate groupings *E. granulosus* (SW Pacific) and *E. baxteri* (SW Pacific) display a significant U_{ST} of 0.043 indicating the absence of population differences. For a summary of computed population variation and U_{ST}/F_{ST} estimates see Table 1.

Population assignment using STRUCTURE. Assignment of individuals to genotypic clusters primarily required an estimation of the true number of K populations. Estimates resulted in a proposed number of $K = 8$ ($\Delta K = 16.37$), i.e. referring broadly to the number of geographic groups,

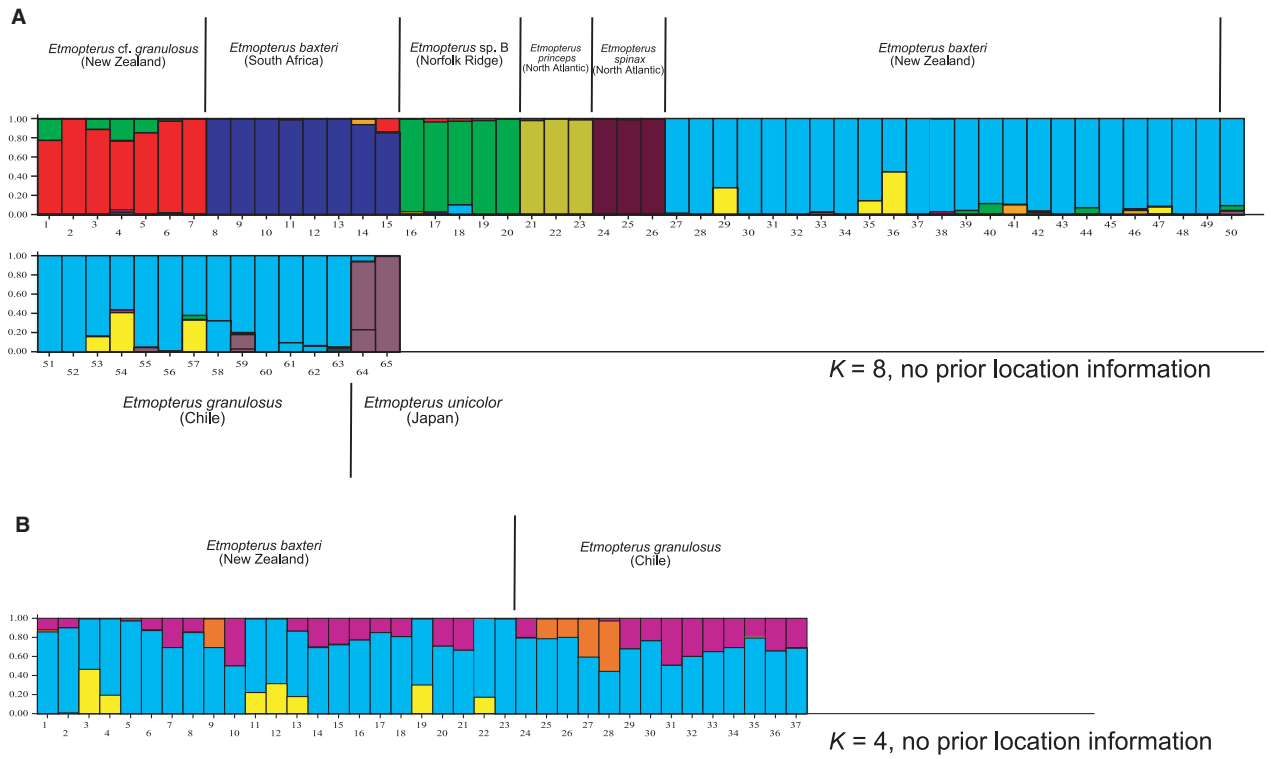

Fig. 6 Bar plots of hierarchical STRUCTURE analysis displaying population assignments for the full amplified fragment length polymorphism dataset (A) and a downsized dataset (B) focusing on sampling sites Chile (*Etmopterus granulosus*) and New Zealand (*Etmopterus baxteri*). Each bar represents an individual on the *x*-axis, the *y*-axis displays the likelihood of assignment for $K = 8$ (A) and $K = 4$ (B).

namely *E. granulosus* (Chile) plus *E. baxteri* (New Zealand), *E. baxteri* (South Africa), *E.* cf. *granulosus* (New Zealand), *E.* sp. B (Tasman Sea), *E. princeps* (NE Atlantic), *E. spinax* (NE Atlantic), and *E. unicolor* (NE Pacific). An eighth *K* was introduced due to variance within the largest cluster formed by *E. granulosus* (Chile) and *E. baxteri* (New Zealand) (Fig. 6A). As discussed by Evanno *et al.* (2005), $K = 2$ corresponds to the uppermost level of structuring ($\Delta K = 107.47$) (Supporting Information S2). The assignment test was run on the full dataset to test whether STRUCTURE detects differences between different species and to check for additional intraspecific population structure. Given no prior location information, STRUCTURE detected seven major clusters. There is no population structure for *E. granulosus* (Chile) and *E. baxteri* (New Zealand). Subsequent analyses including prior location information yielded no further structuring within the *E. granulosus* (Chile)/*E. baxteri* (New Zealand) cluster (Supporting Information S3).

For further investigation of population structuring, we analysed a smaller dataset including only samples of *E. granulosus* from Chile and New Zealand. Estimating the true number of *K* populations from specimens sampled at those two locations resulted in a proposed number of $K = 4$ ($\Delta K = 14.1$), given no prior population information. In this case, $K = 2$ ($\Delta K = 3.72$) does not correspond to the uppermost level of structuring. The proposed number of $K = 4$ shows no structuring referring to the two sampling locations New Zealand and Chile. Several individuals in the bar plot partially include different population information (Supporting Information S4).

Subsequently, we used prior location information to overcome the apparently weak information content of our dataset. Runs including prior location information also could not detect population structure. As in runs performed without any prior location information, increasing *K* increased the assignment of parts of single individuals as distinct populations, but did not reveal further population structure information which could be referred to the sampling locations New Zealand and Chile (Fig. 6B; Supporting Information S4). STRUCTURE detected the species assignment comparable to other applied methods to our AFLP dataset (Figs. 2–4). We could not detect population structure for the two sampling sites of *E. granulosus* in the SW (New Zealand) and SE Pacific (Chile).

Efforts to detect a mixed ancestry of *E. granulosus*, *E. princeps* and specimens assigned to *E. baxteri* from South Africa resulted in clear separation of the three clusters in all three analyzing runs differing in the assumed number of past generations. However, a fourth cluster including specimens of mixed ancestry was not detected (Supporting Information S5).

Discussion

Taxonomic confusion and conservation implications

Mitochondrial DNA-sequence ('barcoding') and high-resolution AFLP data presented herein demonstrate a complicated pattern of inter-specific and intraspecific relationships within etmopterid deep sea sharks (Figs. 2–6) that is not compatible with the current taxonomy. On the one hand, phylogenetic data strongly suggest that the taxon *E. baxteri* sampled off New Zealand is a synonym of *E. granulosus* sampled off Chile as suggested by Tachikawa *et al.* (1989). This argues in favour of a wide distribution in the Southern Hemisphere of *E. granulosus* and against an endemic distribution off southern South America (Fig. 6). On the other hand, specimens sampled off South Africa which have been tentatively assigned to *E. baxteri sensu* Compagno *et al.* (2005), as well as *E.* cf. *granulosus sensu* Duhamel *et al.* (2005) and *E.* sp. B *sensu* Last & Stevens (1994) form distinct clades representing most likely cryptic species. In combination, this strongly suggests the presence of two cryptic *E. granulosus*-like species in the Southern Hemisphere (Fig. 4). A third cryptic species of this Southern Hemisphere clade is *E.* sp. B, which according to our results branches as a distinct clade (Figs. 4 and 6A). Therefore, *E.* sp. B is not a synonym to *E. unicolor* from the NW Pacific as described in recent literature (Compagno *et al.* 2005; Last & Stevens 2009; Yano 1997).

This type of taxonomic confusion in combination with cryptic diversity may have profound effects on long term survival of species caught as by-catch of commercial fisheries. It is known from other shark genera, too, e.g. *Orectolobus* spp. off the Australian east coast, which exhibit also increased levels of cryptic diversity within a group of species with very similar morphological appearance (Corrigan *et al.* 2008).

However, there is still a limitation of available data on deep-sea sharks concerning behaviour (migration), spatial structuring of populations, taxonomy, and distribution. Considering that *E. granulosus* is widespread in the Southern Hemisphere, the species would require cooperative international efforts for conservation, whereas regional endemic species, such as specimens assigned to *E. baxteri* from off South Africa, need to be regionally managed (Ahonen *et al.* 2009). Forrest & Walters (2009) estimated the constant annual harvest rate (U_{MSY}) of several dogfish shark species including *E. granulosus* off Australia to be unsustainable indicating severe danger of overfishing if U_{MSY} is exceeded. Most likely, the same applies for the three cryptic species detected here, which inhabit the SW Pacific sympatrically with *E. granulosus*, and all of which are potential by-catch of increased deep-sea fisheries exploitation. Generally, there is a high level of unrecognized cryptic diversity among deep-sea sharks, which is also demonstrated by several recent publications on new species of deep-sea sharks especially within the order Squaliformes (e.g. Schaaf da Silva & Ebert 2006; Ward *et al.* 2005, 2007; White *et al.* 2008) and new information on patterns of dispersal of species (Nakaya *et al.* 2008; Oñate & Pequeño 2005; Reyes & Hüne 2006; Soto 2001). Results from our study reveal the existence of previously undescribed species and the problem of species misidentification in a group of sharks regularly caught as by-catch in commercial fisheries. Cryptic species need to be taxonomically described in order to make names and identification tools available for effective monitoring and conservation measures. Our study further highlights the necessity of taxonomically sound stock assessment analyses based on molecular data, not only for commercially targeted species but also for 'by-catch'.

Population structure and phylogeography of E. granulosus

For both sampling sites of *E. granulosus* (Chile and New Zealand) F_{ST} and Φ_{ST} values of the AFLP and mtDNA data, respectively, identify only extremely weak but nevertheless significant genetic differentiation of populations (Table 1). This is supported by AMOVA results indicating that the vast majority of nuclear variation resides among and not within the two samples (among population variation = 2.43%). A search for differentially segregating AFLP loci using the genome scan approach only yielded two candidate loci whose allele frequencies in the two samples might have been shaped by strong selection. However, removal of these two loci did only slightly affect population differentiation as measured by a lower but still significant pairwise F_{ST} value. Despite these low but significant values for population differentiation and despite an estimated number of populations within the *E. granulosus* sample of $K = 4$, STRUCTURE did not detect additional population structure between the two sampling locations. Instead, individuals within the New Zealand sample that were not unambiguously assignable to the large undifferentiated group of *E. granulosus*-like etmopterids, formed a separate cluster under $K = 4$ assumptions. In summary, the two sampling sites for *E. granulosus* (Chile and New Zealand) are separated by roughly 7000 km but show a very modest level of population differentiation only. The low level of population differentiation could either be indica-

tive for an isolation-by-distance scenario or by a very recent cessation of gene flow divergence of these populations. Isolation by distance would require the existence of intermediate populations allowing for connectivity between Chile and New Zealand. The few COI haplotypes of specimens identified as *E.* cf. *baxteri* (Amsterdam Island) and *E. granulosus* (NE of the Kerguelen Plateau) from the Indian Ocean and *E. granulosus* from off SE Australia [Tasman Sea, Genbank (accession numbers DQ108226, DQ108216)] fall into the *E. granulosus* network cluster (Fig. 2). This supports their identity as *E. granulosus* and the notion of close connectivity of populations separated by several thousands of kilometers along the subantarctic ecoregion. Such a connectivity may be facilitated by the circum-antarctic current passing all known sampling locations of *E. granulosus* (Fig. 1). A very recent separation of now reproductively isolated populations appears less likely given that overall regional diversity in the area has evolved into differentiated bathyal species ecoregions, i.e. New Zealand, Kermadec and Nazcaplatensis ecoregions are clearly discernable (UNESCO 2009). Genetic differentiation was already detected between pelagic Southern Australian dolphins (*Delphinus delphis*) over a distance of 1500 km, supporting the hypothesis of differentiated ecoregions in the Southern Hemisphere (Bilgmann *et al.* 2008). Nevertheless, the appropriate approach to test for these alternative hypotheses would be a classical tagging experiment allowing to track movements of individuals over large distances. So far, available data on migration behaviour of etmopterids in general is limited, because tagging studies do not exist (Forrest & Walters 2009).Yet another explanation for a subtle population differentiation between distant *E. granulosus* populations is a response to natural selection acting divergently between e.g. the New Zealand and Chile sample sites. Chilean *E. granulosus* occur in comparatively shallow depths from 200 to 637 m (IUCN 2010, and N. Straube personal observation), whereas the same species occurs off New Zealand on average much deeper between 850 and 1200 m (Bass *et al.* 1986; Garrick 1960; Wetherbee 1996; N. Straube personal observation). In this context, it must remain speculative, whether the two possible candidate loci identified in the AFLP genome scan relate to physiological characters under divergent selection for adaptations to different depths. However, the distribution range of *E. granulosus* is most likely circumglobally along the Southern Hemisphere, and reports off Sierra Leone (Golovan & Pukhorukov 1986) need confirmation.

Generally, our study supports the possibility of *E. granulosus* being a migratory rather than a resident species. Evidence for sex and size-related aggregations (Jakobsdottir 2001; Wetherbee 1996) might be related to socially induced migraton for mating or schooling purposes, too (Claes & Mallefet 2008, 2009).

Although the sample size of our study is limited, it represents the first population genetic approach applied to etmopterids, and it is based on a very large number of AFLP-loci, i.e. compensating partially unsatisfactory sample size by analyzing patterns of differentiation across the whole genome. Especially for comparatively low sample sizes, AFLPs are the appropriate method, because the AFLP technique often provides better resolution of population structure size than e.g. microsatellites (e.g. Cambpell *et al.* 2003; Evanno *et al.* 2005; Sønstebø *et al.* 2007). The robustness of analyses presented herein is supported by coherent results based on different analytical methods and on two different datasets (mtDNA and AFLPs). Obviously, future population genetic analyses of the *E. granulosus* species group should comprise additional samples of potentially existing intermediate populations especially with regard to validation of the hypothesis of migration versus isolation by distance. We anticipate that a larger sample size may further allow to confirm the presence of *E. granulosus* off South Africa.

Etmopterus spinax clade: biogeographic and alpha-level taxonomic implications

Results presented herein further resolve phylogenetic interrelationships of the *E. spinax* clade. Preliminary phylogenetic data of numerically limited samples had previously suggested the existence of hitherto undetected cryptic diversity and insufficient phylogenetic resolution among this morphologically uniform etmopterid group (*E. spinax* clade, *sensu* Straube *et al.* 2010). This study resulted in a polytomy displaying a weakly supported sister-relationship of NE Atlantic *E. spinax* and *E. princeps* to *E.* cf. *granulosus* and *E.* sp. B. The phylogenetic hypothesis based on AFLP data reveals *E. spinax* (NE Atlantic) as the basal taxon to a clade comprising morphologically similar large lantern sharks (*E. princeps*, *E. granulosus*, *E.* cf. *granulosus*, South African *E. baxteri*, and *E.* sp. B) with high bootstrap support. *E. princeps* (NE Atlantic) is the well-supported sister taxon to a clade comprising species from the Southern Hemisphere only (Fig. 4). This refined phylogenetic hypothesis suggests that the origin of the *E. spinax* clade is in the Atlantic, because both basal members of the clade are sampled in the North Atlantic and display its main distribution in the North Atlantic, whereas younger species are distributed in the Southern Hemisphere. Origin and subsequent Southern Hemisphere diversification of the *E. spinax* clade species occurred 36–22 Ma ago (Straube *et al.* 2010) and follow the Eocene/Oligocene climatic deterioration from greenhouse to icehouse condi-

tions (Eldrett *et al.* 2009; Lear *et al.* 2008). The climatic cooling and simultaneous ice sheet development on the Antarctic continent was connected to the final separation of Antarctica from the surrounding continents by opening of the Tasman and Drake passages. The development of these gateways initiated circumpolar circulations and the thermal isolation of the Antarctic continent and the Southern Ocean (Dingle & Lavelle 2000). Increased deepening of the Tasmanian and Drake passages at ca. 34 Ma resulted in enlarged Pacific throughflow and subsequent deeper Atlantic–Pacific connections close to the Eocene/Oligocene boundary (Sher & Martin 2006). Simultaneously, deep-sea temperatures decreased considerably from 12 to 4.5 °C (Zacho *et al.* 2001). We hypothesize that a species closely related to *E. princeps* dispersed into the Southern Hemisphere oceans through the deepend gateways and gave rise to the Pacific and Indian Ocean taxa. This interpretation also is supported by the fossil record of Southern Ocean sharks, which consists of a very diverse fauna prior to climatic cooling at the end of the Eocene including representatives of three squaliform sharks, *Centrophorus*, *Deania* and *Squalus*, but no etmopterid (Kriwet 2005). The gradual thermal isolation of the Southern Ocean, in which water temperatures finally dropped to below 0 °C barred sharks and most bony fishes from this hostile environment. The modern fish fauna is impoverished and striking in its low taxonomic diversity and sharks only sporadically intrude into the Southern Ocean (Long 1992a; Kriwet 2005). Only a few skates, which are assumed to have persisted since the Eocene, inhabit the Southern Ocean today (Long 1992b; Eastman 2005). Analogously, a recent study of the global population structure of another squaloid shark, the spiny dogfish, *Squalus acanthias*, identified a southward dispersal pathway from a putative Northern Hemisphere origin, which partially aligns with our results (Verrissimo *et al.* 2010).

Taxonomically useful information on the three cryptic molecular species identified herein is scarce. South African specimens assigned to *E. baxteri* by Compagno *et al.* (2005) and probably conspecific with our specimens assigned to *E. baxteri* sampled off South Africa, are reported to have a larger body size than *E. granulosus* (up to 85.5 cm in contrast to average 75 cm), but otherwise appear to be very similar to *E. granulosus sensu* lato (Ebert *et al.* 1992). Based on this similarity, we used the AFLP data set to test the hypothesis of mixed ancestry, that specimens assigned to *E. baxteri* from South Africa are of hybrid origin with *E. granulosus* (New Zealand & Chile) and *E. princeps* (NE Atlantic), but results did not indicate a hybrid origin of the specimens (Support Information S5). Haplotypes identified from mtDNA (COI) broadly refer to the different species, mixed haplotypes are only found among specimens assigned to *E. granulosus* from Chile, Australia, Amsterdam Island, NE of the Kerguelen Plateau and New Zealand.

Unfortunately, diagnostic morphological characters are still missing to separate the cryptic *E. baxteri* from South Africa from *E. granulosus*, but a DNA-barcoding approach would readily identify it. Monitoring etmopterid by-catch using DNA-barcoding would enable not only to study the distribution of this cryptic species, but might also allow to test for the existence of *E. granulosus* in waters off South Africa, which is not unlikely according to the presumed peri-antarctic distribution of this taxon as discussed.

Finally, specimens of *E.* cf. *granulosus* sensu Duhamel *et al.* (2005) from the Kerguelen Plateau and New Zealand appeared as a distinct clade in the AFLP and mtDNA phylogeny. Figure 2 reveals the species to be widespread as well, since specimens were sampled off New Zealand as well as in the Indian Ocean (Kerguelen Plateau). This species is not closely related to *E. granulosus* (as the name suggests), but is sister to the undescribed *E.* sp. B (Figs. 2–4), which was placed in synonymy with *E. unicolor* in recent publications (Last & Stevens 2009; Yano 1997). The results presented here and in a larger phylogenetic study of Etmoperidae (Straube *et al.* 2010) contradict a synonymy of *E.* sp. B with *E. unicolor*, because specimens of *E. unicolor* included in our sampling are clearly distinct from *E.* sp. B and unambiguously identified as *E. unicolor* using characters presented in the synonymisation of this species with Southern Hemisphere congeners (*E.* sp. B) by Yano (1997). In addition, our samples were collected in the NW Pacific (Japan) close to the type locality of *E. unicolor*. However, as in the previous species, diagnostic morphological characters for *E.* sp. B are still missing, rendering a barcoding approach to be promising for monitoring and conservation of cryptic members of the *E. unicolor* species complex. The mtDNA sequences further included in the analysis of specimens of *E.* cf. *unicolor* [Genbank (accession numbers EU398778, EU398779, EU398780, EU398781, EU398782)] from off Indonesia revealed a distinct clade as well, leading to the assumption of an even higher cryptic diversity among the *E. unicolor* species complex.

Acknowledgements

We would like to express our sincere thanks to S. Tanaka, T. Horie (Tokai University, Japan), G. Duhamel, Samuel Iglésias, Bernard Serét (Muséum National d'Histoire Naturelle), A. Loerz, K. Schnabel, D. Tracey, M. Watson, P. McMillan (NIWA, New Zealand); A. Stewart (Te Papa Tongarewa, New Zealand), D. Bray (Victoria Museum Melbourne, Australia), K. Matsuura, G. Shinohara (Museum of Nature and Science, Japan), G. Johnston (Marine Institute Rinville, Ireland), F. C. Toro (Universidad de Valparaíso, Chile), R. Leslie (Marine and Coastal Management, South

Africa); S. Socher, J. Schwarzer, A. Dunz, D. Neumann, M. Geiger and A. Verrissimo for useful comments on the manuscript. This study was financed by grants of the German Research Foundation DFG to J. Kriwet (KR 2307-4) and to U. Schliewen (SCHL 567-3). This research received further support from the SYNTHESYS Project http://www.synthesys.info/ which is financed by European Community Research Infrastructure Action under the FP6 "Structuring the European Research Area Programme."

References

Ahonen, H., Harcourt, R. G. & Stow, A. J. (2009). Nuclear and mitochondrial DNA reveals isolation of imperiled grey nurse shark populations (*Carcharias taurus*). *Molecular Ecology*, *18*, 4409–4421.

Albertson, R. C., Markert, J. A., Danley, P. D. & Kocher, T. D. (1999). Phylogeny of a rapidly evolving clade: the cichlid fishes of Lake Malawi, East Africa. *Proceedings of the National Academy of Sciences*, *96*, 5107–5110.

Bandelt, H. J., Forster, P. & Rohl, A. (1999). Median-joining networks for inferring intraspecific phylogenies. *Molecular Biology and Evolution*, *16*, 37–48.

Bass, A. J., Compagno, L. J. V. & Heemstra, P. C. (1986). Squalidae. In M. M. Smith & P. C. Heemstra (Eds) *Smith's Sea Fishes* (pp. 49–62). Berlin: Springer Verlag.

Bilgmann, K., Möller, L. M., Harcourt, R. G., Gales, R. & Beheregaray, L. B. (2008). Common dolphins subject to fisheries impacts in Southern Australia are genetically differentiated: implications for conservation. *Animal Conservation*, *11*, 518–528.

Bonfil, R. (1994). *Overview of world elasmobranch fisheries. FAO Fisheries Technical Paper* 341. Rome, Italy: Food and Agricultural Organisation of the United Nations (FAO).

Bonfil, R., Meyer, M., Scholl, M. C., Johnson, R., O'Brien, S., Oosthuizen, H., Swanson, S., Kotze, D. & Paterson, M. (2005). Transoceanic migration, spatial dynamics, and population linkages of white sharks. *Science*, *310*, 100–103.

Boustany, A. M., Davis, S. F., Pyle, P. *et al.* (2002). Expanded niche for white sharks. *Nature*, *415*, 35–36.

Cambpell, D., Duchesne, P. & Bernatchez, L. (2003). AFLP utility for population assignment studies: analytical investigation and empirical comparison with microsatellites. *Molecular Ecology*, *12*, 1979–1991.

Castro, A. L. F., Stewart, B. S., Wilson, S. G. *et al.* (2007). Population genetic structure of Earth's largest fish, the whale shark (*Rhincodon typus*). *Molecular Ecology*, *16*, 5183–5192.

Claes, J. M. & Mallefet, J. (2008). Early development of bioluminescence suggests camouflage by counter-illumination in the velvet belly lantern shark *Etmopterus spinax* (Squaloidea: Etmopteridae). *Journal of Fish Biology*, *73*, 1337–1350.

Claes, J. M. & Mallefet, J. (2009). Ontogeny of photophore pattern in the velvet belly lantern shark, *Etmopterus spinax*. *Zoology*, *112*, 433–441.

Clarke, M. W., Borgess, L. & Officer, R. A. (2005). Comparisons of trawl and longline catches of deepwater elasmobranchs west and north of Ireland. *Journal of Northwestern Atlantic Fisheries Science*, *35*, 429–442.

Compagno, L. J. V., Ebert, D. A. & Cowley, P. D. (1991). Distribution of offshore demersal cartilaginous fish (Class Chondrichthyes) off the west coast of southern Africa, with notes on their systematic. *South Africa Journal of Marine Science*, *11*, 43–139.

Compagno, L. J. V., Dando, M. & Fowler, S. (2005). *Sharks of the World*. Princeton: University Press.

Corrigan, S., Huveneers, C., Schwartz, T. S., Harcourt, R. G. & Beheregaray, L. B. (2008). Genetic and reproductive evidence for two species of ornate wobbegong shark *Orectolobus* spp. on the Australian east coast. *Journal of Fish Biology*, *73*, 1662–1675.

Devine, J. A., Baker, K. D. & Haedrich, R. L. (2006). Deep-sea fishes qualify as endangered. *Nature*, *439*, 29.

Dingle, R. V. & Lavelle, M. (2000). Antarctic Peninsula Late Cretaceous–Early Cenozoic palaeoenvironments and Gondwana palaeogeographies. *Journal of African Earth Sciences*, *31*, 91–105.

Duhamel, G., Gasco, N. & Davaine, P. (2005). *Poissons des iles Kerguelen et Crozet. Guide regional de l'ocean Austral* (pp. 62–64), Paris: Museum national d'Histoire naturelle.

Eastman, J. T. (2005). The nature of the diversity of Antarctic fishes. *Polar Biology*, *28*, 93–107.

Ebert, D. A., Compagno, L. J. V. & Cowley, P. D. (1992). A preliminary investigation of the feeding ecology of squaloid sharks off the west coast of southern Africa. *South Africa Journal of Marine Science*, *12*, 601–609.

Edgar, R. C. (2004). 'MUSCLE: multiple sequence alignment with high accuracy and high throughput. *Nucleic Acids Research*, *32*, 1792–1797.

Eldrett, J. S., Greenwood, D. R., Harding, I. C. & Huber, M. (2009). Increased seasonality through the Eocene to Oligocene transition in northern high latitudes. *Nature*, *459*, 969–973.

Evanno, G., Regnaut, S. & Goudet, J. (2005). Detecting the number of clusters of individuals using the software STRUCTURE: a simulation study. *Molecular Ecology*, *14*, 2611–2620.

Excoffier, L. G. L. & Schneider, S. (2005). Arlequin ver. 3.0: an integrated software package for population genetics data analysis. *Evolutionary Bioinformatics Online*, *1*, 47–50.

Falush, D., Stephens, M. & Pritchard, J. K. (2003). Inference of population structure: extensions to linked loci and correlated allele frequencies. *Genetics*, *164*, 1567–1587.

Falush, D., Stephens, M. & Pritchard, J. K. (2007). Inference of population structure using multilocus genotype data: dominant markers and null alleles. *Molecular Ecology Notes*, 7, 574–578.

Foll, M. & Gaggiotti, O. E. (2008). A genome-scan method to identify selected loci appropriate for both dominant and codominant markers: a bayesian perspective. *Genetics*, *180*, 977–993.

Forrest, R. E. & Walters, C. J. (2009). Estimating thresholds to optimal harvest rate for long-lived, low-fecundity sharks accounting for selectivity and density dependence in recruitment. *Canadian Journal of Fish Aquatic Sciences*, *66*, 2062–2080.

Garrick, J. A. F. (1957). Studies on New Zealand Elasmoranchii. Part VI. Two new species of *Etmopterus* from New Zealand. *Bulletin of the Museum of Comparative Zoology*, *116*, 170–190.

Garrick, J. A. F. (1960). Studies on New Zealand Elasmoranchii. Part XI. Squaloids of the genera *Deania*, *Etmopterus*, *Oxynotus*

and *Dalatias* in New Zealand waters. *Transactions of the Royal Society of New Zealand*, *88*, 489–517.

Golovan, G. A. & Pukhorukov, N. P. (1986). New Records of rare species of cartilaginous fishes. *Journal of Ichthyology*, *26*, 117–120.

Günther, A. (1880). Report on the shore fishes procured during the voyage of H.M.S. Challenger in the years 1873–1876. In: Report on the scientific results of the voyage of H.M.S. Challenger during the years 1873–1876. *Zoology*, *1*, 1–82.

Hall, T. A. (1999). BioEdit: a user-friendly biological sequence alignment editor and analysis program for Windows 95/98/NT. *Nucleic Acids Symposium Series*, *41*, 95–98.

Hammer, Ø., Harper, D. A. T. & Ryan, P. D. (2001). PAST: palaeontological statistics software package for education and data analysis. *Palaeontologica Electronica*, *4*, 9p.

Herder, F., Pfaender, J. & Schliewen, U. K. (2008). Adaptive sympatric speciation of polychromatic "roundfin" sailfin silverside fish in Lake Matano (Sulawesi). *Evolution*, *62*, 2178–2195.

Hubisz, M., Falush, D., Stephens, M. & Pritchard, J. (2009). Inferring weak population structure with the assistance of sample group information. *Molecular Ecology Resources*, *9*, 1322–1332.

Huson, D. H. & Bryant, D. (2006). Application of phylogenetic networks in evolutionary studies. *Molecular Biology and Evolution*, *23*, 254–267.

Iglésias, S. P., Lecointre, G. & Sellos, D. Y. (2005). Extensive paraphylies within sharks of the order Carcharhiniformes inferred from nuclear and mitochondrial genes. *Molecular Phylogenetics and Evolution*, *34*, 569–583.

Iglésias, S. P., Toulhoat, L. & Sellos, D. Y. (2009). Taxonomic confusion and market mislabeling of threatened skates: important consequences for their conservation status. *Aquatic Conservation: Marine and Freshwater Ecosystems*, *20*, 319–333.

Irvine, S. B., Stevens, J. D. & Laurenson, L. J. B. (2006). Comparing external and internal dorsal spine bands to interpret the age and growth of the giant lantern shark, *Etmopterus baxteri* (Squaliformes, Etmopteridae). *Environmental Biology of Fishes*, 77, 253–264.

IUCN 2010. IUCN Red List of Threatened Species. Ver. 2010.1. http://www.iucnredlist.org.

Jakobsdottir, K. B. (2001). Biological aspects of two deep-water squalid sharks: *Centroscyllium fabricii* (Reinhardt, 1825) and *Etmopterus princeps* (Collett, 1904) in Icelandic waters. *Fisheries Research*, *51*, 247–265.

Kriwet, J. (2005). Additions to the Eocene selachian fauna of Antarctica with comments on Antarctic selachian diversity. *Journal of Vertebrate Paleontology*, *25*, 1–7.

Last, P. R. & Stevens, J. D. (1994). *Sharks and Rays of Australia*. Australia: CSIRO Australia.

Last, P. R. & Stevens, J. D. (2009). *Sharks and Rays of Australia*. 2nd edn. Cambridge: Harvard University Press.

Lear, C. H., Bailey, T. R., Pearson, P. N., Coxall, H. K. & Rosenthal, Y. (2008). Cooling and ice growth across the Eocene-Oligocene transition. *Geology*, *36*, 251–254.

Link, W., Dixkens, C., Singh, M., Schwall, M. & Melchinger, A. E. (1995). Genetic diversity in European and Mediterranean faba bean germ plasm revealed by RAPD markers. *Theoretical and Applied Genetics*, *90*, 27–32.

Long, D. J. (1992a). Sharks from the La Meseta Formation (Eocene), Seymour Island, Antarctic Peninsula. *Journal of Vertebrate Paleontology*, *12*, 11–32.

Long, D. J. (1992b). Quaternary colonization or Paleogene persistence? Historical biogeography of skates (Chondrichthyes: Rajidae) in the Antarctic ichthyofauna. *Paleobiology*, *20*, 215–228.

McFarlane, G. A. & King, J. R. (2003). Migration patterns of spiny dogfish (*Squalus acanthias*) in the North Pacific Ocean. *Fisheries Bulletin*, *101*, 358–367.

Meudt, H. M. & Clarke, A. C. (2007). Almost forgotten or latest practice? AFLP applications, analyses and advances. *TRENDS in Plant Science*, *12*, 106–117.

Nakaya, K., Sato, K. & Iglésias, S. P. (2008). Occurrence of *Apristurus melanoasper* from the South Pacific, Indian and South Atlantic Oceans (Carcharhiniformes: Scyliorhinidae). In: P. R. Last, W. T. White & J. J. Pogonoski (Eds) *Descriptions of New Australian Chondrichthyans* (pp. 1–21). Australia: CSIRO Marine & Atmospheric Research Paper.

Oñate, J. & Pequeño, G. (2005). Etmopterus brachyurus Smith & Radcliffe, 1912 (Chondrichthyes, Dalatiidae): first record in eastern Pacific waters. *Revista de Biología Marina y Oceanografía*, *40*, 67–70.

Pritchard, J. K., Stephens, M. & Donnelly, P. (2000). Inference of population structure using multilocus genotype data. *Genetics*, *155*, 945–959.

Reyes, P. R. & Hüne, M. (2006). First record of the lantern shark *Etmopterus unicolor* (Engelhardt, 1912) off Valdivia, Chile (Chondrichthyes: Dalatiidae). *Investigaciones Marinas*, *34*, 137–142.

Schaaf da Silva, J. A. & Ebert, D. A. (2006). *Etmopterus burgessi* sp. nov., a new species of lantern shark (Squaliformes: Etmopteridae) from Taiwan. *Zootaxa*, *1273*, 53–64.

Schrey, A. W. & Heist, E. J. (2003). Microsatellite analysis of population structure in the shortfin mako (*Isurus oxyrinchus*). *Canadian Journal of Fisheries And Aquatic Sciences*, *60*, 670–675.

Sher, H. D. & Martin, E. E. (2006). Timing and climatic consequences of the opening of Drake Passage. *Science*, *312*, 428–430.

Sønstebø, J. H., Borgstrøm, R. & Heun, M. (2007). A comparison of AFLPs and microsatellites to identify the population structure of brown trout (*Salmo trutta* L.) populations from Hardangervidda, Norway. *Molecular Ecology*, *16*, 1427–1438.

Soto, J. M. R. (2001). First record of Southern lanternshark *Etmopterus granulosus* (Günther, 1880) (Squaliformes, Daatiidae) from the Brazilian coast. *Mare Magnum*, *1*, 7–10.

Springer, S. & Burgess, G. H. (1985). Two new dwarf dogsharks (*Etmopterus*, Squalidae), found off the Carribean coast of Colombia. *Copeia*, *3*, 584–591.

Straube, N., Iglésias, S. P., Sellos, D. Y., Kriwet, J. & Schliewen, U. K. (2010). Molecular phylogeny and node time estimation of bioluminescent lantern sharks (Elasmobranchii: Etmopteridae). *Molecular Phylogenetics and Evolution*, *56*, 905–917.

Tachikawa, H., Taniuchi, T. & Ryoichi, A. (1989). *Etmopterus baxteri*, a junior synonym of *E. granulosus* (Elasmobranchii, Squalidae). *Bulletin of the Natural Science Museum of Tokyo*, *15*, 235–241.

UNESCO (2009). Global Open Oceans and Deep Seabed (GOODS) bioregional classification. In M. Vierros, I. Cesswell,

B. E. Escobar, J. Rice & J. Ardron (Eds) *UNESCO-IOC, Technical Series 84* (pp. 84–89), Paris.

Van de Peer, Y. & De Wachter, R. (1994). TREECON for Windows: a software package for the construction and drawing of evolutionary trees for the Microsoft Windows environment. *Computer Applications in the Biosciences*, *10*, 569–570.

Verrissimo, A., MacDowell, J. & Graves, J. E. (2010). Global population structure of the spiny dogfish *Squalus acanthias*, a temperate shark with an antitropical distribution. *Molecular Ecology*, *19*, 1651–1662.

Vos, P. *et al.* (1995). AFLP: a new technique for DNA fingerprinting. *Nucleic Acids Research*, *23*, 4407–4414.

Ward, R. D., Zemlak, T. S., Innes, B. H., Last, P. R. & Hebert, D. N. (2005). DNA barcoding Australia's fish species. *Philosophical Transactions of the Royal Society B: Biological Sciences*, *360*, 1847–1857.

Ward, R. D., Holmes, B. A., Zemlak, T. S. & Smith, P. J. (2007). Part 12- DNA barcoding discriminates spurdogs of the genus *Squalus*. In: P. R. Last, W. T. White & J. J. Pogonoski (Eds) *Descriptions of New Dogfishes of the Genus Squalus (Squaloidea: Squalidae)* (pp. 114–130). Hobart: CSIRO Marine and Atmosspheric Research Paper, 14.

Ward, R. D., Bronwyn, H. H., White, W. T. & Last, P. R. (2008). DNA barcoding Australasian Chindrichthyans: results and potential uses in conservation. *Marine and Freshwater Research*, *59*, 57–71.

Warnock, W. G., Rasmussen, J. B. & Taylor, E. B. (2009). Genetic clustering methods reveal bull trout (Salvelinus confluentus) fine-scale population structure as a spatially nested hierarchy. *Conservation Genetics*, *11*, 1421–1433.

Wetherbee, B. M. (1996). Distribution and reproduction of the southern lantern shark from New Zealand. *Journal of fish biology*, *49*, 1186–1196.

Wetherbee, B. M. (2000). Assemblage of deepsea sharks on Chatham Rise, New Zealand. *Fish Bulletin*, *98*, 189–198.

White, W. T., Ebert, D. A. & Compagno, L. J. V. (2008). Description of two new species of gulper sharks, genus *Centrophorus* (Chondrichthyes: Squaliformes: Centrophoridae) from Australia. In: P. R. Last, W. T. White & J. J. Pogonoski (Eds) *Descriptions of New Australian Chondrichthyans* (pp 1–22). Hobart: CSIRO Marine and Atmospheric Research Paper, 22.

GenBank, http://www.ncbi.nlm.nih.gov/sites, [accession numbers EU398778, EU398779, EU398780, EU398781, EU398782, DQ108216, DQ108226]; (accessed January, 2010).

Yano, K. (1997). First record of the brown lantern shark, *Etmopterus unicolor*, from the waters around New Zealand, and comparison with the southern lantern shark, *E. ganulosus*. *Ichthyological Research*, *44*, 61–72.

Zacho, J., Pagani, M., Sloan, L., Thomas, E. & Billups, K. (2001). Trends, rhythms, and aberrations in global climate 65 Ma to Present. *Science*, *292*, 686–693.

Supporting Information

Additional Supporting Information may be found in the online version of this article:

Support Information S1. Samples used in this study with location information and Genbank Accession numbers for cytochrome oxidase I sequences.

Support Information S2. Estimation criteria for the number of genetic clusters in the amplified fragment length polymorphism (AFLP) data set. **A:** Evanno's model choice criterion 'ΔK' for the uppermost level of genetic structure computed from the full AFLP dataset. **B**: Evanno's model choice criterion 'ΔK' for the uppermost level of genetic structure computed from the downsized AFLP dataset including specimens of *Etmopterus granulosus* from Chile & New Zealand only.

Support Information S3. Bar plots of STRUCTURE analyses showing population assignments for $K = 8$. Each bar represents an individual on the *x*-axis, the *y*-axis displays the likelihood of assignment for *K*. **A**: not including prior location information. **B**: including prior location information.

Support Information S4. Bar plots of STRUCTURE analyses of a smaller dataset including samples of *Etmopterus granulosus* from the SE Pacific and *Etmopterus baxteri* from the SW Pacific ($K = 4$). Each bar represents an individual on the *x*-axis, the *y*-axis displays the likelihood of assignment for *K*. **A**: not including prior location information. **B**: including prior location information.

Support Information S5. Bar plots of STRUCTURE analyses of potential mixed ancestry of *Etmopterus baxteri* (South Africa) with *Etmopterus granulosus* (Chile)/*E. baxteri* (New Zealand) and *Etmopterus princeps* (North Atlantic) ($K = 3$). Each bar represents an individual on the *x*-axis, the *y*-axis displays the likelihood of assignment for *K*.

Please note: Wiley-Blackwell are not responsible for the content or functionality of any supporting materials supplied by the authors. Any queries (other than missing material) should be directed to the corresponding author for the article.

Article III

STRAUBE N., DUHAMEL G., GASCO N., KRIWET J. AND SCHLIEWEN U.K. (in revision) Description of a new deep-sea Lantern Shark *Etmopterus "viator"* sp. nov. (Squaliformes: Etmopteridae) from the Southern Hemisphere. Submitted to: *Cybium*.

Title: Description of a new deep-sea Lantern Shark *Etmopterus viator* sp. nov. (Squaliformes: Etmopteridae) from the Southern Hemisphere

Straube N., Duhamel G., Gasco N., Kriwet J. and Schliewen U.K.

Corresponding author: Straube Nicolas (NS)

Zoologische Staatssammlung München, Sektion Ichthyologie, Münchhausenstr. 21, 81247 Munich, Germany

straube@zsm.mwn.de **Tel. 0049(0)898107107 Fax 0049(0)898107300**

Duhamel Guy (GD)

Muséum national d'Histoire naturelle; Département MPA, UMR 5178, 43 rue Cuvier, Paris, France

Gasco Nicolas (NG)

Muséum national d'Histoire naturelle; Département MPA, UMR 5178, 43 rue Cuvier, Paris, France

Kriwet Jürgen (JK)

Department of Paleontology, University of Vienna, Geozentrum, Althanstrasse 14, A-1090 Vienna, Austria

Schliewen Ulrich K. (UKS)

Zoologische Staatssammlung München, Sektion Ichthyologie, Münchhausenstr. 21, 81247 Munich, Germany

Short Title: New deep-sea Lantern Shark

Abstract

Lantern Sharks (*Etmopterus* spp.) constitute regular by-catch in fisheries conducted at the north-eastern Kerguelen Plateau shelf in depths of 600 to 1700 m. Kerguelian Lantern Sharks are morphologically close to *E. granulosus*, *E*. sp. B, South African *E*. cf. *granulosus*, and *E. litvinovi*. However, molecular phylogenetic analyses support the hypothesis that they represent a distinct cryptic species, which is in line with morphological characters separating the species from its Southern Hemisphere congeners. The new species is described as *Etmopterus viator* sp. nov. and differs significantly from *E. granulosus*, *E*. sp. B, and South African *E*. cf. *granulosus* in body shape characters as well as shape and density of dermal denticles. The poorly known *E. litvinovi* differs from Kerguelian specimens of *E. viator* sp.nov. by lacking flank and tail markings. Flank mark shape and molecular phylogenetic analyses of the new species support its assignation to the recently defined *E. spinax* clade. The species is widespread in the Southern Hemisphere.

Key Words:

new species – deep-sea shark – barcoding – morphometrics – dermal denticles

1 Introduction

Lantern Sharks (Etmopteridae) are deep-water sharks inhabiting continental slope and seamount regions occurring almost globally in an average depth range of 200 to more than 2500 meters (Compagno *et al.*, 2005; Last and Stevens, 2009). With an estimated 42 species, Lantern Sharks constitute the largest family of Squaliformes or Dogfish Sharks (Compagno *et al.*, 2005). Within the family, the genus *Etmopterus* broadly exceeds, with 33 described *Etmopterus* species, the remaining three genera *Trigonognathus*, *Aculeola*, and *Centroscyllium* in species number (Compagno *et al.*, 2005; Schaaf da Silva and Ebert, 2005). The common name Lantern Shark refers to the hormone induced light emission ability, which is probably used in the social (schooling) and camouflage context (counter shading against residual sunlight) (Claes and Mallefet, 2008, 2009a, 2009b, 2010a, 2010b, 2010c). Their phylogeny, life-history, and ecology has recently become of increased interest in shark research (e.g. Coelho and Erzini, 2008a, 2008b; Neiva *et al.*, 2006; Klimpel *et al.*, 2003, Straube *et al.*, 2010, 2011). Many etmopterids are regular by-catch of commercial deep-sea fisheries (Clarke *et al.*, 2005; Jakobsdottir, 2001; Wetherbee, 1996; Kyne and Simpfendorfer, 2007).

Lantern Shark species are diagnosed based on classical characters used in shark systematics, i.e. body shape characters, morphology, density and arrangement of dermal denticles as well as tooth shape, and number of vertebrae (e.g. Garrick, 1957, 1960; Springer and Burgess, 1985; Yano, 1997; Yamakawa *et al.*, 1986). In addition, the shape and position of flank and tail markings forming fields of photophores is in many cases species or species-group specific (Yamakawa *et al.*, 1986; Last *et al.*, 2002). Recent molecular phylogenetic analyses revealed four major clades within *Etmopterus*, which are distinguishable based on their flank mark shapes, i. e. the *Etmopterus lucifer* clade, the *E. gracilispinis* clade, the *E. pusillus* clade, and the *E. spinax* clade (Straube *et al.*, 2010). The latter clade comprises at least three species, which are morphologically very similar (*Etmopterus granulosus* (Günther, 1880), *E. unicolor*

79 (Engelhardt, 1912), and *E. princeps* (Collett, 1904)), as well as a high number of cryptic species,
80 especially from the Southern Hemisphere, i. e. *E. baxteri* (Garrick, 1957) from South Africa and
81 New Zealand, *E*. cf. *granulosus* (Kerguelen Plateau), and *E. unicolor* (South East Pacific)
82 (Straube *et al.*, 2010, 2011). Morphologically similar Southern Hemisphere species within the
83 *E. spinax* clade comprise *E. granulosus* (including *E. baxteri* as synonym of *E. granulosus*
84 referring to Straube *et al*., 2011), *E*. cf. *granulosus* (i.e. the nominal *E. baxteri* from South Africa
85 in Straube *et al.*, 2010, 2011, and throughout Compagno *et al.*, 1991), and finally *E*. sp. B,
86 which is not synonymous to the North Pacific *E. unicolor* according to results from Straube *et*
87 *al.* (2010, 2011). In this study, we focus on the separation of *E*. cf. *granulosus sensu* Duhamel *et*
88 *al.* (2005) from its congeners in the Southern Hemisphere and provide a description of the
89 species. It is a new species of the *E. spinax* clade (Straube *et al.* 2010) based on distinct
90 morphological and molecular characters.

91 **2 Material and Methods**

92 **2.1 Taxon sampling**

93 Most specimens and samples of the new species were collected at the Kerguelen Plateau in
94 the years 2001, 2002, 2003, 2004 and 2007 during cruises of French commercial fishing vessels
95 in the Southern Indian Ocean. A total number of 63 specimens from the Kerguelen Plateau
96 were available, of which 24 were accompanied by tissue samples for “DNA-barcoding”.
97 Additional specimens and samples of the new species were obtained from off New Zealand
98 (tissue samples only, n = 7, collected by McMillan P., NIWA, New Zealand, 2007) and off South
99 Africa (measurements only, n = 2, collected by Anderson M. E., SAIAB, South Africa, 2001). For
100 comparison with closely related species, 27 specimens of *E. granulosus* sampled off Chile, New
101 Zealand, and the Indian Ocean (NE of Kerguelen Plateau and off Amsterdam Island) including
102 the holotype (BMNH-1879.5.14.460), 17 specimens of *E*. sp. B (*sensu* Last and Stevens, 1994)
103 and 16 specimens of *E.* cf. *granulosus* from South Africa were inspected. *E. litvinovi* (Kotlyar

and Parin, 1990) is only known from a few specimens from the Nasca and Sala-y-Gómez Ridges off Chile and is considered to be an endemic species of this region (Kotlyar, 1990). It is not unlikely that *E. litvinovi* is a member of the *E. spinax* clade consulting morphological features describing sub clades of *Etmopterus* in Straube *et al*. (2010). Therefore, we included as much information as possible for *E. litvinovi* to compare this species to the new species. However, only two paratypes (ZMH-24994; ZMH-24993) were available for studying the full set of measurements and number of vertebrae; the holotype was inspected from images, but tissue samples were not available for any of the types used in this study.

2.2 Morphology: morphometrics, meristics, and dermal denticles

Morphometrics: 31 body measurements of 50 specimens of the new species, 27 specimens of *E. granulosus*, 18 specimens of *E*. sp. B, and 16 specimens of *E.* cf. *granulosus sensu* Compagno *et al.*, 1991 (sampled off South Africa), formed the comparative basis for the species description. See tables I and II for measurements and their definitions. Out of these measurements, four ratios discussed in Kotlyar (1990) and Yano (1997) as potential species specific characters were used: head length vs. interdorsal distance (HL/ID), distance of the snout tip to the first dorsal-fin spine insertion vs. the interdorsal distance (PFDL/ID), head length vs. the interorbital distance (HL/IOD), and total length vs. the height of the first dorsal fin (TL/HFDF)). Ratio value variation was tested for deviation from a Gaussian distribution by compiling normal probability plots. After testing for homogeneity of error variances (Levene Test, $p > 0.05$ for TL/HFDF, PFDL/ID, and HL/ID; $p < 0.05$ for HL/IOD), a multi-factorial ANOVA was performed for those three variables, which showed homogeneity of error variance. To test for significant differentiation of the new species with respect to these three ratios, a LSD post-hoc test was conducted. For the fourth ratio (HL/IOD), homogeneity was rejected by the Levene Test ($p = 0.001$), which is the reason that Kruskal-Wallis and subsequent Dunnett post-hoc tests were performed under the assumption that homogeneity of error variance is not

given. Statistical analyses were conducted with the software package SPSS v. 11.5.1 and visualization of resulting box-plots was accomplished in PAST v1.94b (Hammer *et al.*, 2001).

Meristics: A meristic character frequently used for species identification in sharks is the total number of vertebrae. X-rays of 38 specimens of the new species and of two paratypes of *E. litvinovi* were available. Data were compared with published vertebrae numbers for *E. granulosus* and *E.* sp. B (Yano, 1997). Since means of total vertebrae numbers of *E. granulosus* and *E*. sp. B were adopted from Yano (1997), potential differences could only visualized by plotting means and standard deviations of species analysed. Data on the total number of vertebrae of *E.* cf. *granulosus* specimens sampled off South Africa were not available for this study.

Dermal denticles: Shape, density, and arrangement of dermal denticles of the new species and closest relatives *E. granulosus* and *E*. sp. B (n = 2 for each species) was investigated using a defined area below the 2nd dorsal fin with a dissecting microscope. For representative visualization a LEO 1430 VP scanning electron microscope (SEM) was used after skin samples were mounted on SEM stubs and coated with gold in a POLARON SEM Coating System for 80 seconds. To obtain a quantitative correlate for differences in dermal denticle morphology, the length of the dorsal part of dermal denticles below the 2nd dorsal fin was measured by calibrating a calliper in TPSDig v2.15 (Rohlf, 2010) with the included size indication provided by the SEM. The Levene Test rejected homogeneity of error variance between values of the three species ($p = 0.001$). Therefore, the non-parametric Kruskal-Wallis test was performed to test for significant differences between species and a subsequent Dunnett post-hoc test was conducted to test for significant pairwise differentiation. Finally, the number of denticles in 3 mm^2 was counted by applying a 3 mm side-length frame to the SEM images of two specimens each.

2.3 DNA-barcoding

154 Muscle or fin tissue samples preserved in 96 % ethanol p.a. were available for n = 31
155 specimens of the new species, for n = 26 specimens of *E. granulosus*, for n = 6 specimens of *E.*
156 sp. B, and for n = 8 specimens of *E.* cf. *granulosus* (South Africa). Total genomic DNA was
157 extracted using the QIAmp tissue kit (Qiagen®, Valencia, CA). A part of the mitochondrial
158 Cytochrome Oxidase I (COI) gene was amplified and sequenced from all available samples
159 following the PCR protocol of Iglésias *et al.* (2005). The COI locus is a well-established gene
160 fragment for identification of shark species (Ward *et al.*, 2005, 2007, 2008). PCR and
161 sequencing primers are S0156 (5' TAGCTGATGAATCTGACCGTGAAAC 3') and R0084 (5'
162 TGAACGCCAGATTTCATAGCGTTC 3'). PCR products were cleaned using the QIAquick PCR
163 Purification Kit (Qiagen®, Valencia, CA) after the manufacturer´s protocol. Cycle sequencing
164 was performed at the sequencing service of the Department of Biology at the Ludwig-
165 Maximilians-University (Munich), using ABI Big Dye 3.1 chemistry (PE Applied Biosystems®,
166 Foster City, CA). Obtained back and forward sequences of COI were edited using BioEdit v7.0.9
167 (Hall, 1999) and aligned with MUSCLE v3.6 (Edgar, 2004). In addition, five COI sequences of *E.*
168 cf. *unicolor* (Indonesia) and two COI sequences of *E. granulosus* (Tasman Sea) were included in
169 the preliminary alignment from Genbank (accession numbers EU398778, EU398779,
170 EU398780, EU398781, EU398782, DQ108216, DQ108226). Aliscore v.0.2 (Misof and Misof,
171 2009) was used to check the alignment for ambiguous alignment positions to confirm the
172 absence of nuclear inserts in the COI sequences, which were translated into amino acids. A
173 most parsimonious phylogenetic network using default settings (weights = 10, epsilon = 0) was
174 calculated using the median joining algorithm (allowing for multistate data) with the software
175 NETWORK v4.5.1.6 (Bandelt *et al.*, 1999; fluxus-engineering.com). The dataset comprised the
176 smallest resulting sequenced fragments homologous to all taxa (overall size: 655 base pairs).
177 COI sequences were submitted to Genbank.

178 **3 Results**

179 **3.1 Morphology: morphometrics, meristics, and dermal denticles**

180 **Morphometrics:** multifactorial ANOVA detected significant differences between the new
181 species, *E*. sp. B, *E*. cf. *granulosus* (South Africa), and *E. granulosus* with regard to the four
182 ratios (TL/FDFH; HL/IOD; PFDL/ID; HL/ID) analysed. Significant differences were found using
183 multifactorial ANOVA comparing the new species with *E*. sp. B in TL/HFDF, PFDL/ID, and HL/ID.
184 *E*. cf. *granulosus* (South Africa) differs significantly from the new species based on the same
185 three ratios (Fig. 1). Further significant differences were detected between the new species
186 and *E. granulosus* when comparing the ratio of distance from the snout tip to the first dorsal-
187 fin spine insertion and the interdorsal distance (PFDL/ID) as well as the ratio of head length
188 and the interdorsal distance (HL/ID), where *E. granulosus* displays significantly higher values
189 (Fig. 1). No significant differences were found between the new species and *E. litvinovi*, which
190 is most likely due to the small sample size of *E. litvinovi*. See Tables III and IV for a summary of
191 ANOVA results.

192 Multiple species comparisons of the ratio of head length and interorbital distance (HL/IOD)
193 displayed further significant differences, i. e. the new species differs significantly from *E*. sp. B
194 and *E*. cf. *granulosus* (South Africa) (Fig. 1 B; Tab. V). Differences to *E. litvinovi* are visualized in
195 Figure 1, but could not be statistically verified.

196 **Meristics:** The total number of vertebrae of the new species ranges between 75 and 84 (n=38).
197 The data was compared with *E. granulosus*, *E*. sp. B and *E. litvinovi* using data from Yano (1997)
198 and Kotlyar (1990). Figure 1 F visualizes means and standard deviations of total counts. This
199 result may read as a possible hint to species-specific differences, especially with regard to *E.*
200 *granulosus*, which appears to have on average a larger number of vertebrae. Krefft (1967)
201 counted 89 vertebrae in the holotype of *E. granulosus*.

202 **Dermal denticles:** The morphology of dermal denticles of the new species is hook-like and they
203 are densely covering the body with approximately 23- 40 denticles per 3 mm^2 counted below

204 the 2nd dorsal fin (Fig. 2 A, B) in adults. The shape of its dermal denticles strongly differs from
205 the bristle-like denticles of its molecularly identified sister taxon *E*. sp. B (Fig. 2 E, F). No
206 significant differences in the length of dermal denticles below the second dorsal fin between
207 the new species and *E.* sp. B were detected (Dunnett-test, mean difference = 0.258, p=0.149).
208 *E. granulosus* has significantly shorter denticles compared to the new species (mean
209 difference = 0.2303, p < 0.000) (Fig. 2 C, D). However, the number of dermal denticles is
210 significantly lower in the new species (23-40/3 mm^2) than in *E*. sp B (>100/ 3 mm^2) (Fig. 2). In
211 comparison with *E. granulosus*, the number of dermal denticles is lower (23-40/ mm^2 vs. 34 to
212 58/ mm^2), too. *E. granulosus* and the new species described herein additionally differ in the
213 degree of coverage of the 2nd dorsal fin with denticles, i.e. it is densely covered in adults of the
214 new species, but sparsely covered or even without any dermal denticles in *E. granulosus*. This
215 was already described by Yano (1997) for New Zealand specimens of *E. granulosus*. The new
216 species displays no shape differences between dermal denticles of males and females, adults,
217 sub adults and pups (Fig. 3).
218 *E. litvinovi* is very similar to the new species in having hook-like dermal denticles. However,
219 they are arranged in higher density in the two inspected paratypes (51/3 mm^2 ZMH-24993 and
220 57/ 3 mm^2 in ZMH-24994). *E. litvinovi* further differs in having dermal denticles arranged in
221 rows on the 2nd dorsal fin (holotype ZIN-49228) as compared to absence of denticle rows in the
222 new species. Unfortunately, the 2nd dorsal fins of both inspected paratypes seemed to be
223 abraded probably due to damages from fishing.
224 **3.2 DNA barcoding**
225 The mtDNA-alignment (COI) from all specimens has 541 constant, 17 variable but
226 parsimony-uninformative and 101 parsimony-informative characters. Base frequencies are
227 equally distributed in all positions (χ^2-test: χ^2 = 8.47, df = 267, p = 1.0). Empirical base
228 frequencies are 0.25 for A, 0.25 for C, 0.18 for G, and 0.32 for T. The most-parsimonious

network contains 55 haplotypes which are connected via estimated 137 mutations along the shortest tree. Five major clades are recovered among the Southern Hemisphere species (Fig.4). The new species unambiguously constitutes a distinct cluster, most closely connected to *E*. sp. B and *E*. cf. *unicolor*. *E. granulosus* and *E.* cf. *granulosus* form rather distant clusters with regard to the new species. Specimens sampled off New Zealand are included in the new species´ cluster suggesting conspecificity of the Kerguelen and New Zealand populations.

In summary, morphological as well as molecular data support the diagnosable distinctiveness of the new species. Based on this diagnosability, we describe the new Lantern Shark species as *Etmopterus viator* sp. nov..

4 *Etmopterus viator* new species Straube

Etmopterus cf. *granulosus* – Duhamel *et al.*, 2005

Holotype –MNHN-20081899, female, 525 mm TL, Kerguelen Plateau, 49°39' 29" S 72°45'0" E, 01.10.2006, longline fishing, depth 1111 – 1023 m, Genbank Accession number: HM998635

Paratypes - specimens from the Kerguelen Plateau, Southern Indian Ocean:

MNHN-20071666, female, 517 mm TL, Kerguelen Plateau, 46° 49' 03" S 70° 32' 32" E, 30.01.2007, longline fishing, depth 1091 – 1288 m Genbank Accession number: HM998638

MNHN-20071667, female, 350 mm TL, Kerguelen Plateau, 50° 1' 42" S 74° 0' 33" E, 01.11.2006, longline fishing, depth 807 – 1038 m, Genbank Accession number: HM998635

MNHN-20071668, pregnant female, 545 mm TL, Kerguelen Plateau, 50° 5' 13" S 73° 55' 59" E, 19.09.2006, longline fishing, depth 952 – 926 m, Genbank Accession number: GU130729

MNHN-20081900, female, 577 mm TL, Kerguelen Plateau, 49°39' 29" S 72°45'0" E, 01.10.2006, longline fishing, depth 1111 – 1023 m (Fig. 4 A). Genbank Accession number: HM998646.

ZSM-38530 (ref. MNHN-20081898), male, 362 mm TL, Kerguelen Plateau, 47°15' 36" S 71°49'26" E, 02.10.2006, longline fishing, depth 834 – 1052 m, Genbank Accession number: HM998645.

MNHN-20081896, male, 391 mm TL, Kerguelen Plateau, 47° 51' S -73°30' E, 04.11.2006, longline fishing, depth 1600 – 1509 m, Genbank Accession number: HM998637.

6 specimens from Chatham Rise, New Zealand, South West Pacific:

NMNZ P.42738, male, 357 mm TL, Genbank Accession number: HM998654; NMNZ P.42739, female, 400 mm TL, Genbank Accession number: HM998653; NMNZ P.42740, female, 340 mm TL, Genbank Accession number: GU130731; NMNZ P.42741, female, 296 mm TL, Genbank Accession number: HM998642; NMNZ P.42742, male, 378 mm TL, Genbank Accession number: GU130730; all specimens caught during a research cruise of RV Tangaroa. Station TAN 0709/ 119, Central northern slope of Chatham Rise, New Zealand; 42° 38.08' S, 179° 52.97' E to 42° 37.90' S, 179° 55.10' E; bottom trawl, depth 1573 – 1610 m, 25. 07. 2007.

4.1 Description

Diagnosis - A medium-sized *Etmopterus* species with the following combination of characters: Body fusiform, caudal peduncle short 0.1 (0.08 – 0.13) % of total length (TL). Moderately long interdorsal distance 0.19 (0.09 – 0.24) % TL, very long distance from first dorsal fin spine insertion to snout tip 0.36 (0.26 – 0.56) % TL. Head long 0.21 (0.19 – 0.72) % TL and broad 0.1 (0.09 – 0.16) % TL long, as long as caudal peduncle. Snout short 0.41 (0.13 – 0.53) % head length (HL) and broad 0.37 (0.12 – 0.48) % HL. Interorbital distance narrow 0.28 (0.11 – 0.51) % HL, shorter than snout width. Large oval eyes, eye length 0.26 (0.07 – 0.34) % HL. Eyes reflect greenish in fresh specimens. Large tear-drop shaped spiracles 0.05 (0.01 – 0.13) % HL. Mouth strongly arched and broad 0.4 (0.16 – 0.51) % HL with dignathic homodont dentition (details see below). Nostrils large and oblique 0.11 (0.03 – 0.19) % HL. Gill openings with distinct white margins. Pectoral fins rounded and white-edged with fringed ceratotrichia, moderate in size. Inner margin 0.04 (0.04 – 0.08) % TL, fin base short 0.05 (0.02 – 0.06) % TL. Dorsal fins densely covered with dermal denticles, 2nd dorsal fin significantly larger than 1st dorsal fin, height 0.09 (0.09 – 0.18) % TL compared to 0.03 (0.01 – 0.06) % TL in 1st dorsal fin. 2nd dorsal fin deeply

279 concave with drawn-out lower lobe. Both dorsal fins fringed, with strong fin spines. The 2nd
280 dorsal fin spine is larger than 1st (broken in the holotype) pointing posteriorly. 1st dorsal fin
281 origin distinctively behind the pectoral fin insertions whereas origin of 2nd dorsal fin only
282 slightly behind pelvic fin insertions (Fig. 5 A, B). Large heterocercal caudal fin 0.2 (0.18 – 0.27)
283 % TL with strong upper and weaker lower edged lobes, widely covered with dermal denticles.
284 Morphometric data for the holotype and variations in Kerguelian paratypes are presented in
285 Table I.
286 *Dermal denticles* - Stout, dense, single-cusped dermal denticles with a keel on the upper
287 surface, the basis of denticles displays four branches. Skin appears rough-textured, the number
288 of dermal denticles in a square of 3 mm^2 below the second dorsal fin ranges from 23 to 40
289 denticles in the Kerguelian paratypes, 39 in the holotype; arranged in short rows on the flanks
290 and the caudal peduncle. Denticles appear less curved and thorn-like on head and ventral side,
291 hook-like at flank and tail, on head less dense. Sub adults generally with a lower density of
292 denticles compared to the high coverage of denticles in adults.
293 *Markings* - Photophores most densely clustered on ventral side of the body, flanks, caudal
294 peduncle and caudal fin. Markings, especially flank markings, can differ substantially in their
295 distinctiveness. Flank markings are distinct in sub adults but may be inconspicuous in adults.
296 Indistinct triangular flank marking base below 2nd dorsal fin base. Posterior branch short, in
297 contrast to the long, drawn-out anterior branch extending the 2nd dorsal fin spine insertion.
298 Shape of the flank marking typical for the *E. spinax* clade (Straube *et al.*, 2010). Photophores
299 are possibly present in a distinct white bar on the upper eye-lid.
300 *Vertebrae* - Total number of vertebrae 79 ranging from 75 to 84 (n = 38 including
301 paratypes). 38 (38 to 68) precaudal vertebrae, 41 (34 to 51) caudal vertebrae.
302 *Dentition* - Upper teeth multicuspid with two lateral pairs of cusplets flanking a main cusp.
303 Lateral cusplets smaller than the central cusp. Most males have, at least in the majority of

upper teeth, only one pair of cusplets. Lower teeth single-cusped and interlocking (Fig. 5 C). Eight tooth rows in upper jaw with three functional rows and four replacement rows. Lower jaw with one functional tooth series and three replacement rows. 26 teeth in upper and 37 in the lower jaw. There are no symphyseal teeth.

Distribution - The species is bentho-pelagic inhabitant of the sub photic zone: records range from 830 to 1400 meters depth at the Kerguelen Plateau (Duhamel *et al.*, 2005) down to 1610 m from off New Zealand, suggesting it to be a rather deep-dwelling species of *Etmopterus*. The species has been collected at three geographically distant locations, i.e. South Africa, New Zealand, and the Kerguelen Plateau (Fig. 5 D). It was further confirmed for the Macquarie Ridge south of New Zealand (P. Last, pers. comm.). It hypothetically occurs in the whole Southern Hemisphere.

Biological notes - *E. viator* sp. nov. is ovoviviparous and gives birth to 2 to 10 pups per litter. Maturity is reached at approximately 50 cm TL in females and 46 cm TL in males (Duhamel *et al.*, 2005). Males are on average smaller than females, adult females reach at least 58 cm TL, adult males approx. 50 cm TL. Duhamel *et al.* (2005) report the species to feed on myctiphids, euphausiids, and squid.

Etymology - The species is named after the Latin word “viator” (the traveler), since the species is confirmed for geographically distant locations in the Southern Hemisphere.

The body color is blackish to brown in adult females. Sub adult specimens appear black. Preserved specimens mostly maintain original color. See Figure 5 for general appearance.

4.2 Remarks

Within the genus *Etmopterus*, *E. viator* sp. nov. is identified in previous studies (nominal *E.* cf. *granulosus* in these studies)as member of the *E. spinax* clade (Straube *et al.*, 2010, 2011) based on flank mark shapes displaying long and thin anterior branches and a weakly developed triangular posterior branches. It is hereby readily distinguished from all other remaining

329 *Etmopterus* clades. Among species of the *E. spinax* clade, *E. viator* sp. nov. can be distinguished
330 from *E. spinax* (Linnaeus, 1758), *E. compagnoi* (Fricke and Koch, 1990) and *E. dianthus* (Last *et*
331 *al*., 2002) by a uniform coloration without an abrupt transition of a light dorsal to a black
332 ventral side. It differs from *E. princeps* in geographical occurrence (Southern Hemisphere vs.
333 North Atlantic), depth distribution range (600 – 1600 m vs. 350 – 4500 m), and maximum total
334 length (57 cm vs. 75 cm). It differs from North Pacific *E. unicolor* in its dermal denticle shape. *E.*
335 *unicolor* displays dense and bristle-like denticles as in *E*. sp. B. Further, *E. unicolor* matures at
336 larger body sizes: 53 cm for male specimens (Compagno *et al*. 2005), which implies even larger
337 sizes at maturity for females.
338 Within the *E. spinax* clade, *E. viator* sp. nov. is a member of a group of morphologically
339 close species from the Southern Hemisphere. This group includes several cryptic species, which
340 have been preliminarily assigned to formally described species (Straube *et al*., 2011). Southern
341 Hemisphere congeners are *E*. sp. B (*sensu* Last & Stevens, 1994), *E. granulosus*, *E*. cf.
342 *granulosus* (South Africa), and *E. litvinovi*. *E. viator* sp. nov. differs from *E*. sp. B in having fewer
343 dermal denticles in a 3 mm^2 area below the 2^{nd} dorsal fin (23-40 vs >100) and in the
344 combination of the following body measurement ratios: ratio of TL/HFDF (0.42 – 0.82 vs. 0.44
345 – 0.98), PFDL/ID (0.01 – 0.03 vs. 0.01 – 0.02), HL/ID (1.21 – 2.37 vs 1.02 – 2.25), and HL/IOD
346 (0.01 – 0.07 vs 0.01 – 0.03). It differs from *E*. cf. *granulosus* (South Africa) in the ratios TL/HFDF
347 (0.42 – 0.82 vs. 0.52 – 0.62), PFDL/ID (0.01 – 0.03 vs 0.01 – 0.02), HL/ID (1.21 – 2.37 vs. 1.61 –
348 1.94), and HL/IOD (0.01 – 0.07 vs. 0.01 – 0.03). Further morphometric differences of *E. viator*
349 sp. nov. to *E. granulosus* are found comparing ratios PFDL/ID (0.01 – 0.03 vs. 0.01 – 0.08) and
350 HL/ID (1.21 – 2.37 vs. 0.17 – 2.17). *E. viator* sp. nov. has fewer dermal denticles in a 3 mm^2
351 area below the 2^{nd} dorsal fin (23 – 40 vs. 34 – 58) compared to *E. granulosus* and the two
352 species also differ in the length of dermal denticles (0.37 – 0.66 µm vs. 0.15 – 0.44 µm).
353 Although the density and size of dermal denticles differs between *E. granulosus* and *E. viator*

354 sp. nov., its shape is very similar. Sub adult specimens of *E. viator* sp. nov. strongly resemble
355 sub adults of *E. granulosus*, as the density of dermal denticles in sub adult *E. viator* sp. nov. is
356 much lower compared to adults. *E. granulosus* generally reaches a larger total length and
357 matures at larger body sizes. Maturity is reached at 55-60 cm TL for male *E. granulosus*, and at
358 64-69 cm in females (Compagno *et al.*, 2005), whereas male *E. viator* sp. nov mature at 46 cm
359 TL and female specimens at 54 cm TL. The situation is similar comparing *E*. sp. B, where males
360 mature around 50 cm TL and females at 60 cm TL (Last and Stevens, 2009), with *E. viator* sp.
361 nov..

362 The most striking difference between *E. litvinovi* and *E. viator* sp. nov. is the lack of any
363 markings in *E. litvinovi*, as described by Kotlyar (1990). Re-inspections of two paratypes of *E.*
364 *litvinovi* support this observation (NS, pers. obs.). *E. viator* sp. nov. shows a different
365 conspicuousness of its flank markings throughout ontogenetic stages, but markings at the
366 caudal peduncle as well as the upper lobe of the tail fin are always clearly visible. The body
367 colour of the preserved paratypes of two adult specimens of *E. litvinovi* is uniformly black.
368 Preserved as well as fresh specimens of *E. viator* sp. nov. appear rather brownish in adult
369 specimens. Although sub adult *E. viator* sp. nov are blackish in body color, specimens display
370 clearly visible flank markings. Potential morphometric and meristic differences are the ratio of
371 HL/IOD and the total number of vertebrae, but these results have to be verified analyzing a
372 larger sample of *E. litvinovi*. The density of dermal denticles is higher in *E. litvinovi* (> 50
373 denticles below the 2nd dorsal fin in *E. litvinovi* vs < 50 in *E. viator* sp. nov.).

374 Kotlyar (1990) discusses the similarity of *E. litvinovi* with a South African species shortly
375 described by Bass *et al.* (1986). We conclude that the *Etmopterus* sp in Bass *et al.* (1986) may
376 in fact be our newly described *E. viator* sp. nov., as its presence is confirmed off the coast of
377 South Africa. Generally, the usage of flank markings of *E. viator* sp. nov. as species-specific

character has to be treated with care, as *E. granulosus* displays flank markings of highly similar shape.

Results from mtDNA sequence analyses show a monophyletic lineage clearly separating *E. viator* sp. nov. from its congeners. The barcode approach readily allows identifying the new species. Interestingly, *E. viator* sp. nov. is distributed off New Zealand and morphometric analyses confirm its presence off South Africa as well, indicating *E. viator* sp. nov. to be a wide ranging species in the Southern Hemisphere (Fig. 5 D), which is comparable to the distribution range of *E. granulosus* (Straube *et al*., 2011). The *E. spinax* clade still yields a number of cryptic species, which need to be analysed and described in the near future.

Acknowledgements

We would like to express our sincere thanks to all the people who helped collecting samples and provided crucial information for the article. MNHN, France: S. Iglésias, D. Sellos B. Serét, P. Pruvost, R. Causse; NIWA, New Zealand: A. Loerz, K. Schnabel, D. Tracey, M. Watson, P. McMillan; Te Papa Tongarewa, New Zealand: A. Stewart, Victoria Museum Melbourne, Australia: D. Bray, Universidad de Valparaíso, Chile: F. Concha, Marine and Coastal Management, South Africa: R. Leslie; SAIAB, South Africa: M. Mwale, O. Gon, Zoologisches Museum Hamburg, Germany: R. Thiel, I. Eidus, Zoological Institute RAS St. Petersburg, Russia: A. Balushkin, V. Spodareva. We thank Peter Last for constructive critics on the manuscript. N. Straube thanks S. Socher, J. Wedekind, T. Lehmann, and M. Geiger for help and critics. This study was financed by grants of the German Research Foundation DFG to J. Kriwet (KR 2307-4) and to U. Schliewen (SCHL 567-3). This research received further support from the SYNTHESYS Project http://www.synthesys.info/ which is financed by European Community Research Infrastructure Action under the FP6 "Structuring the European Research Area Programme." This paper was supported (in part) by the NZ Foundation for Research, Science and Technology

through Te Papa Biosystematics of NZ EEZ Fishes subcontract within NIWA's Marine Biodiversity and Biosecurity OBI programme (contract C01X0502).

References:

BANDELT, H. J., FORSTER, P. AND ROHL, A., 1999.- Median-joining networks for inferring intraspecific phylogenies. *Mol. Biol. Evol*., 16: 37-48.

BASS, A. J., COMPAGNO, L. J. V. AND HEEMSTRA, P. C., 1986.- Squalidae. *In*: Smith's Sea Fishes (Smith M. M., Heemstra P. C. eds), pp. 49-62. Berlin: Springer Verlag.

CLAES, J. M., MALLEFET, J., 2008.- Early development of bioluminescence suggests camouflage by counter-illumination in the velvet belly Lantern Shark *Etmopterus spinax* (Squaloidea: Etmopteridae). *J. Fish Biol.*, 73: 1337-1350.

CLAES, J. M., MALLEFET, J., 2009a.- Ontogeny of photophore pattern in the Velvet Belly Lantern Shark, *Etmopterus spinax*. *Zoology*, 112: 433-441.

CLAES J. M., MALLEFET J., 2009b.- Hormonal control of luminescence from Lantern Shark (*Etmopterus spinax*) photophores*. J. Exp. Biol.*, 212: 3684-3692.

CLAES J. M., AKSNES, D. L., MALLEFET J., 2010a.- Phantom hunter of the fjords: Counterillumination in a shark, *Etmopterus spinax*. *J. Exp. Mar. Biol. Ecol.*, 388: 28-32.

CLAES J. M., MALLEFET J., 2010b.- Functional physiology of lantern shark (*Etmopterus spinax*) luminescent pattern: differential hormonal regulation of luminous zones. *J. Exp. Biol.*, 213: 1852-185.

CLAES, J. M., MALLEFET, J., 2010c.- The lantern shark's light switch: turning shallow water crypsis into midwater camouflage. *Biol. Lett*., 6 (5), 685-687

CLARKE, M. W., BORGESS, L. AND OFFICER, R. A., 2005.- Comparisons of Trawl and Longline Catches of Deepwater Elasmobranchs West and North of Ireland. *J. Northw. Atl. Fish. Sci*, 35: 429-442.

COELHO, R., ERZINI, K., 2008a.- Identification of deep-water lantern sharks (Chondrichthyes: Etmopteridae) using morphometric data and multivariate analysis. *J. Mar. Biol. Assoc*. UK 88 (1): 199-204.

427 COELHO, R., ERZINI, K., 2008b.- Life History of a wide-ranging deep-water lantern shark in the north-east
428 Atlantic, *Etmopterus spinax* (Chondrichthyes: Etmopteridae), with implications for conservation. *J. Fish*
429 *Biol.*, 73: 1419-1443.
430 COLLETT, R., 1904.- Diagnoses of four hitherto undescribed fishes from the depths south of the Faroe
431 Islands. Forhandlinger i Videnskabs-selskabet i Christiania, No. 9: 1-7.
432 COMPAGNO, L. J. V., DANDO, M. AND FOWLER, S., 2005.- Sharks of the world. 368 p. Princeton:
433 University Press.
434 COMPAGNO, L. J. V., EBERT, D. A. AND COWLEY, P. D., 1991.- Distribution of offshore demersal
435 cartilaginous fish (Class Chondrichthyes) off the west coast of southern Africa, with notes on their
436 systematic. *S. Afr. J. mar. Sci.*, 11: 43-139.
437 DUHAMEL, G., GASCO, N. AND DAVAINE, P., 2005.- Poissons des iles Kerguelen et Crozet. Guide régional
438 de l'océan Austral. 417 p. Paris: Muséum national d'Histoire naturelle.
439 EDGAR, R. C., 2004.- 'MUSCLE': multiple sequence alignment with high accuracy and high throughput.
440 *Nucleic Acids Research*, 32, 1792-1797.
441 ENGELHARDT, R., 1912.- Über einige neue Selachier-Formen. *Zoologischer Anzeiger*, 39, 643-648.
442 FRICKE, R., KOCH, I., 1990.- A new species of the lantern shark genus *Etmopterus* from southern Africa
443 (Elasmobranchii: Squalidae). *Stuttgarter Beiträge zur Naturkunde*, 450: 1-9.
444 GARRICK, J. A. F., 1957.- Studies on New Zealand Elasmobranchii. Part VI. Two new species of
445 *Etmopterus* from New Zealand. *Bull. Mus. Comp. Zool.*, 116: 170-190.
446 GARRICK, J. A. F., 1960.- Studies on New Zealand Elasmobranchii. Part XI. Squaloids of the genera
447 *Deania*, *Etmopterus*, *Oxynotus,* and *Dalatias* in New Zealand waters. *Trans. Roy. Soc. New Zealand*, 88:
448 489-517.
449 GENBANK, 2010.- http://www.ncbi.nlm.nih.gov/sites, [accession numbers EU398778, EU398779,
450 EU398780, EU398781, EU398782, DQ108216, DQ108226]; accessed January, 2010).
451 GÜNTHER, A., 1880.-Report on the shore fishes procured during the voyage of H. M. S. Challenger in the
452 years 1873-1876. In: Report on the scientific results of the voyage of H. M. S. Challenger during the years
453 1873-76. *Zoology*. Report on the shore fishes procured during the voyage of H. M. S. Challenger in the
454 years 1873-1876. v. 1 (pt 6): 1-82, Pls. 1-32.

455 HALL, T. A., 1999.- BioEdit: a user-friendly biological sequence alignment editor and analysis program for
456 Windows 95/98/NT. *Nucleic Acids Symposium Series*, 41, 95-98.
457 HAMMER, Ø, HARPER, D. A. T. AND RYAN, P. D., 2001.- PAST: Palaeontological Statistics software
458 package for education and data analysis. *Palaeontologica Electronica*, 4, 9pp.
459 IGLÉSIAS, S. P., LECOINTRE, G. AND SELLOS, D. Y., 2005.- Extensive paraphylies within sharks of the order
460 Carcharhiniformes inferred from nuclear and mitochondrial genes. *Mol. Phylogenet. Evol.*, 34, 569 - 583.
461 JAKOBSDOTTIR, K. B., 2001.- Biological aspects of two deep-water squalid sharks: *Centroscyllium fabricii*
462 (Reinhardt, 1825) and *Etmopterus princeps* (Collett, 1904) in Icelandic waters. *Fisheries Research*, 51,
463 247-265.
464 KLIMPEL, S., PALM, H. W., SEEHAGEN, A., 2003.- Metazoan parasites and food composition of juvenile
465 *Etmopterus spinax* (L. 1758) (Dalatiidae, Squaliformes) from the Norwegian Deep. *Parasitol. Res.*,
466 89:245-251.
467 KOTLYAR, A.N., 1990.- Dogfish sharks of the genus *Etmopterus* Rafinesque from the Nazca and Sala y
468 Gomez Submarine Ridges. *Trudy Instituta Okeanologii*, 125: 127-147.
469 KREFFT G., 1967.- Neue und erstmalig nachgewiesene Knorpelfische aus dem Archibenthal des
470 Südwestatlantiks, einschließlich einer Diskussion einiger *Etmopterus*-Arten südlicher Meere. *Archiv für*
471 *Fischereiwissenschaften*, XVIII, 1, 1-42.
472 KYNE, P.M. AND SIMPFENDORFER, P.A., 2007.- A collation and summarization of available data on
473 deepwater Chondrichthyans: biodiversity, life history, and fisheries. A report prepared by the IUCN SSC
474 Shark Specialist Group for the Marine Conservation Biology Institute, 1-136 p.
475 LAST, P. R. AND STEVENS, J. D., 1994.- Sharks and Rays of Australia. Australia. 1-513 p. CSIRO: Australia.
476 LAST, P. R., STEVENS, J. D., 2009.- Sharks and Rays of Australia. 1-554 p. Harvard University Press,
477 Cambridge, 2nd edition.
478 LAST, P.R., BURGESS, G.H., SERET B., 2002.- Description of six new species of Lantern-Sharks of the genus
479 *Etmopterus* (Squaloidea: Etmopteridae) from the Australasian region. *Cybium*, 26: 203-223.
480 LINNAEUS, C.**,** 1758.-Systema Naturae, Ed. X. (Systema naturae per regna tria naturae, secundum
481 classes, ordines, genera, species, cum characteribus, differentiis, synonymis, locis. Tomus I. Editio

482 decima, reformata.) Holmiae. Systema Naturae, Ed. X. v. 1: i-ii + 1-824. [Nantes and Pisces in Tom. 1, pp.
483 230-338.
484 MISOF, B., MISOF, K., 2009.- A Monte Carlo approach successfully identifies randomness of multiple
485 sequence alignments: A more objective means of data exclusion. *Syst. Biol.*, 58 (1): 21-34.
486 NEIVA, J., COELHO, R., ERZINI, K., 2006.- Feeding habits of the velvet belly lanternshark *Etmopterus*
487 *spinax* (Chondrichthyes: Etmopteridae) off the Algarve, southern Portugal. *J. Mar. Biol. Assoc*. UK 86:
488 835–841.
489 ROHLF, F.J., 2010.- TpsDig, digitize landmarks and outlines, version 2.15. Department
490 of Ecology and Evolution, State University of New York at Stony Brook.
491 SCHAAF DA SILVA, J. A. AND EBERT, D. A., 2006.- *Etmopterus burgessi* sp. nov., a new species of lantern
492 shark (Squaliformes: Etmopteridae) from Taiwan. *Zootaxa,* 1273, 53-64.
493 SPRINGER, S., BURGESS, G. H., 1985.- Two new dwarf Dogsharks (*Etmopterus*, Squalidae), found off the
494 Carribean Coast of Colombia. *Copeia*, 3, 584-591.
495 STRAUBE, N., IGLÉSIAS S. P., SELLOS D. Y., KRIWET, J. AND SCHLIEWEN, U. K. 2010.- Molecular Phylogeny
496 and Node Time Estimation of Bioluminescent Lantern Sharks (Elasmobranchii: Etmopteridae). *Mol.*
497 *Phylogenet. Evol*, 56, 905–917.
498 STRAUBE, N., KRIWET, J. AND SCHLIEWEN, U. K. 2011. – Cryptic diversity and species assignment of large
499 Lantern Sharks of the *Etmopterus spinax* clade from the Southern Hemisphere, (Squaliformes,
500 Etmopteridae). *Zoologica Scripta*, 40 (1): 61-75.
501 WARD, R. D., BRONWYN, H. H., WHITE, W. T., LAST, P. R., 2008.- DNA barcoding Australasian
502 Chondrichthyans: results and potential uses in conservation. *Mar. Freshwater Res.*, 59: 57-71.
503 WARD, R. D., HOLMES, B. A., ZEMLAK, T. S., SMITH, P. J., 2007.- Part 12- DNA barcoding discriminates
504 spurdogs of the genus *Squalus*. *In*: *Descriptions of new dogfishes of the genus Squalus (Squaloidea:*
505 *Squalidae)* (Last P. R., White W. T. and Pogonoski J. J., eds), CSIRO Marine and Atmospheric Research
506 Paper, 14, 114-130
507 WARD, R. D., ZEMLAK, T. S., INNES, B. H., LAST, P. R., HEBERT, D. N., 2005.- DNA barcoding Australia's
508 fish species. *Phil. Trans. R. Soc. B*, 360, 1847-1857.

509 WETHERBEE, B. M., 1996.- Distribution and reproduction of the southern lantern shark from New
510 Zealand. *J. Fish Biol.*, 49, 1186-1196.
511 YAMAKAWA, T., TANIUCHI, T., NOSE, Y., 1986.- Review of the *Etmopterus lucifer* Group (Squalidae) in
512 Japan. In: Indo- Pacific Fish Biology: Proceedings of the Second International Conference on Indo-Pacific
513 fishes (Uyeno T., Arai R., Taniuchi T. and Matsuura K., eds.). Ichthyological Society of Japan, Tokyo, 197-
514 207.
515 YANO, K., 1997.- First record of the brown lantern shark, *Etmopterus unicolor*, from the waters around
516 New Zealand, and comparison with the southern lantern shark, *E. granulosus*. *Ichthyological Research*,
517 44, 61-72.

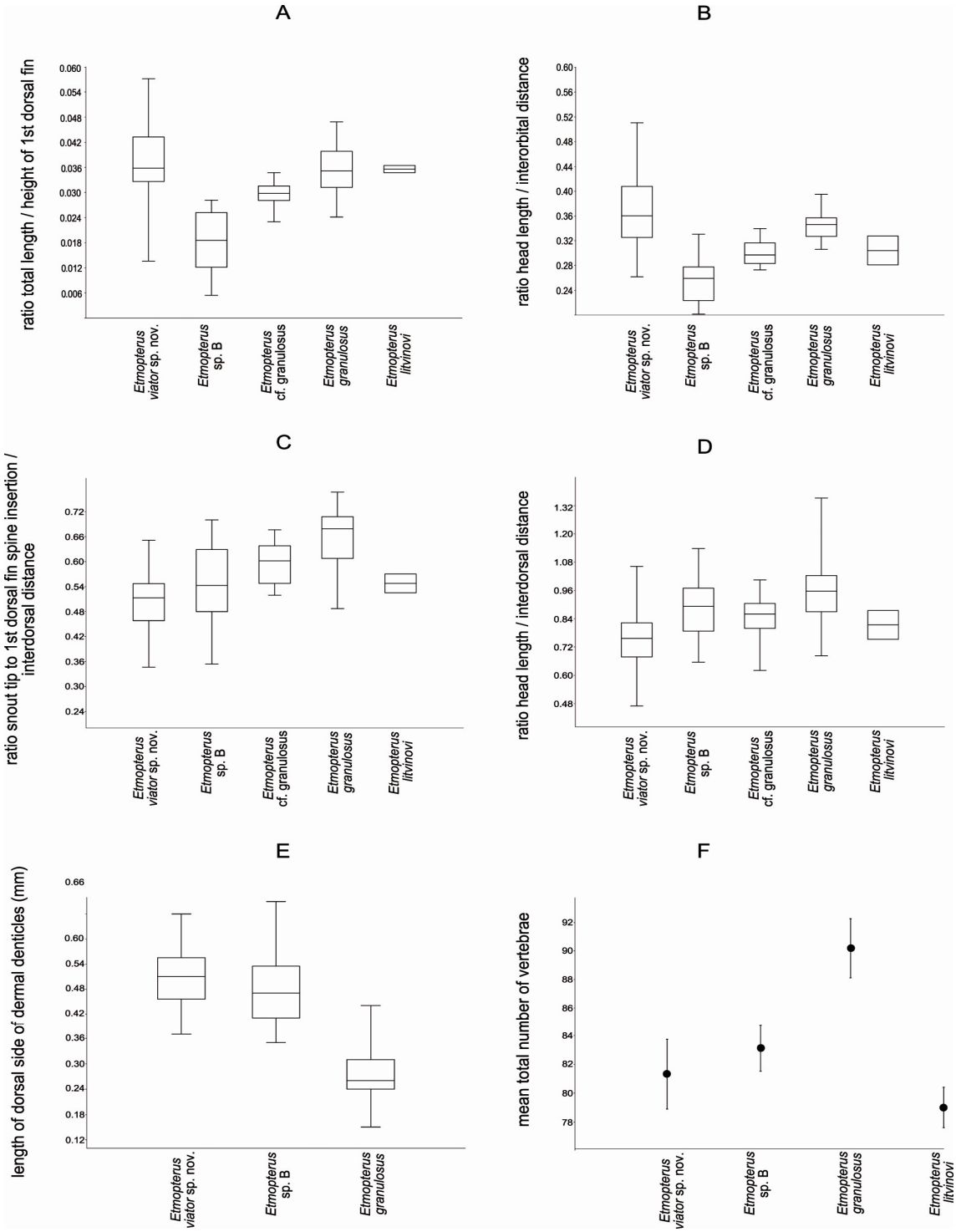

Figure 1: Overview of box-plots visualizing results from morphometric and meristic analyses.

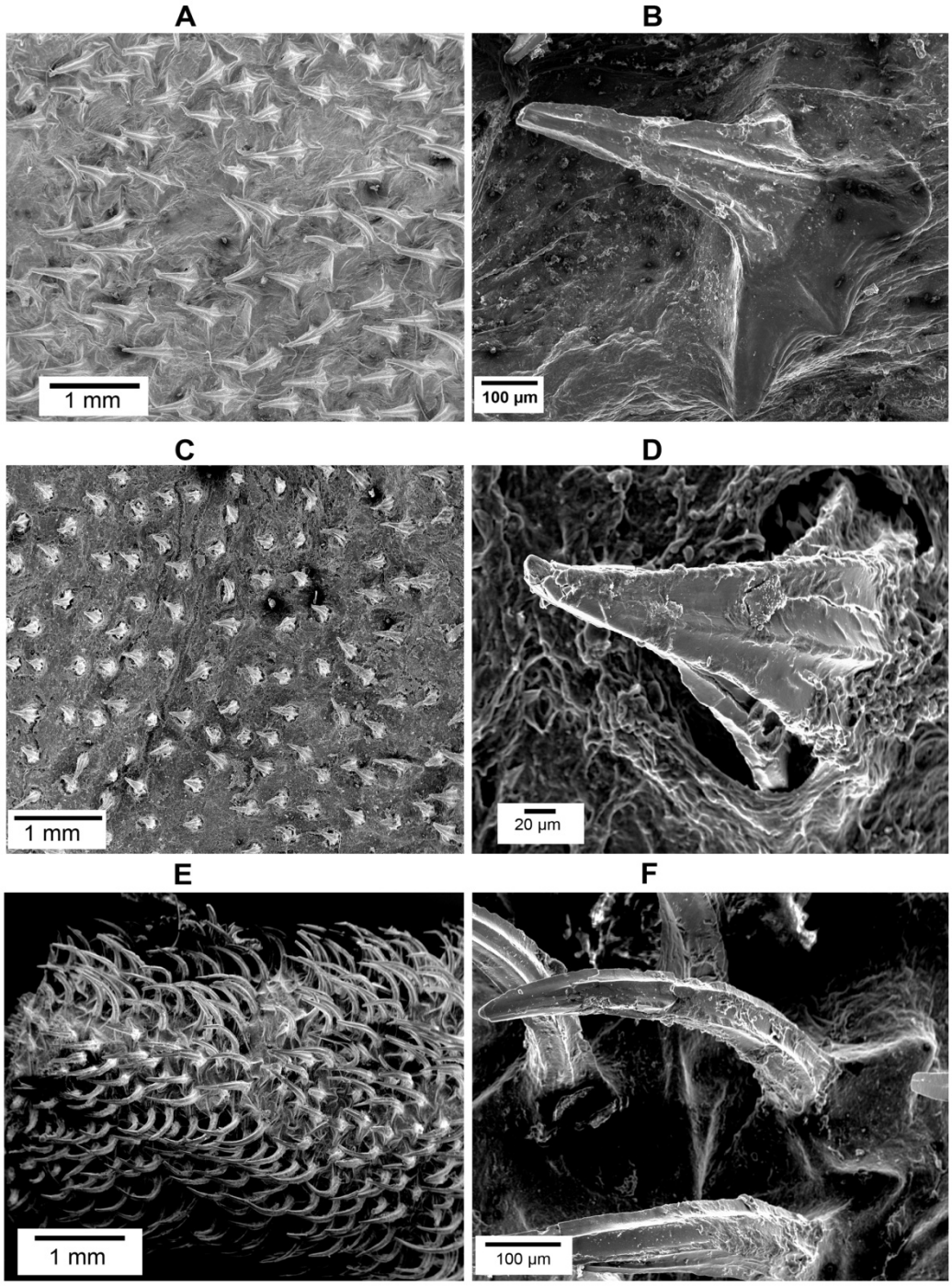

Figure 2: SEM images of dermal denticles of *Etmopterus viator* sp. nov. (A, B; holotype MNHN-20081899), *Etmopterus granulosus* (C, D; ZSM-37667), and *Etmopterus* sp. B (E, F; MNHN-20052703). A, C, and E show the arrangement of dermal denticles below the 2nd dorsal fin on the right lateral side of specimens. B, D, and F display enlarged images of single dermal denticles.

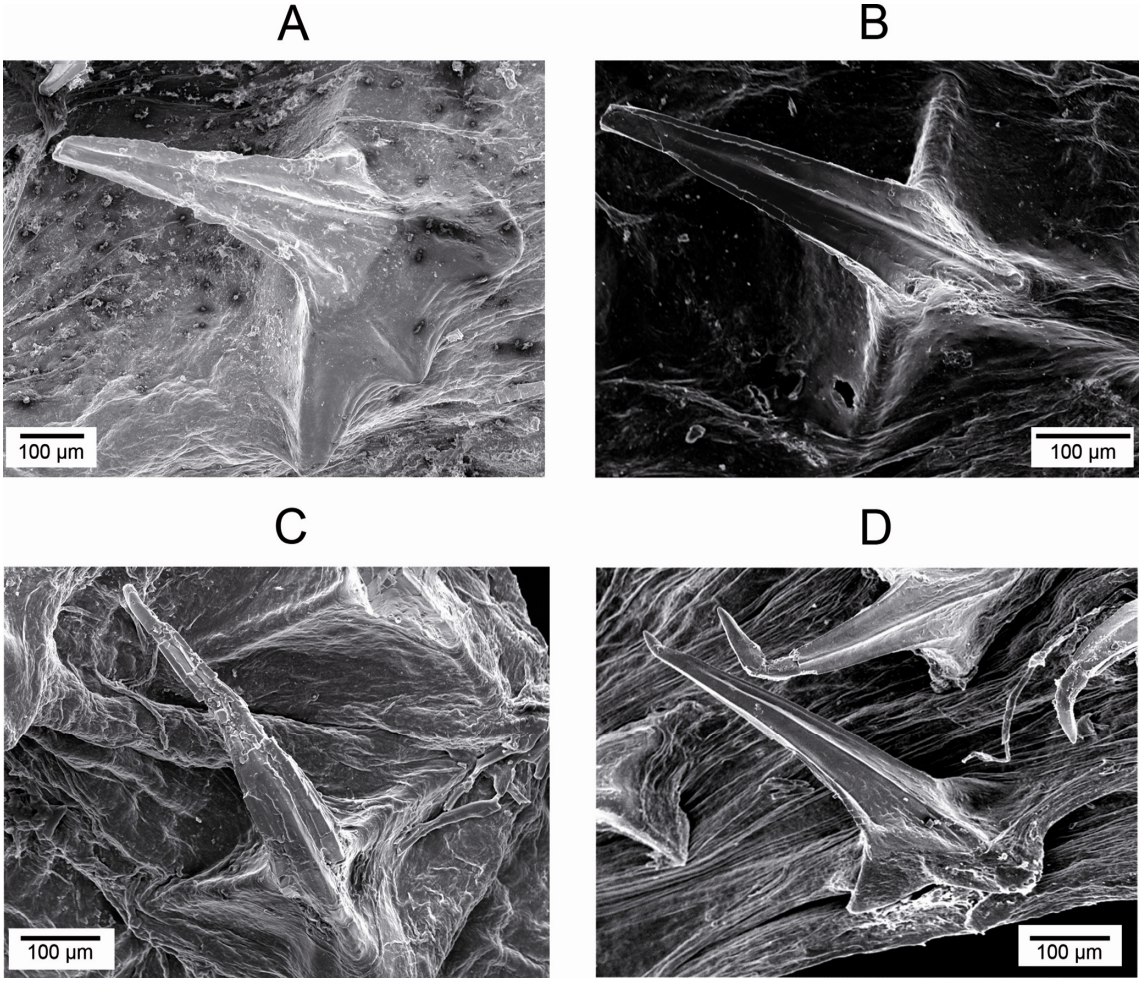

Figure 3: SEM images of different ontogenetic stages in *Etmopterus viator* sp. nov. A= adult female, holotype, MNHN-20081899; B= adult male, paratype, MNHN-20081898; C= sub adult male, ZSM-37614; D= almost ready to be born embryo extracted from holotype.

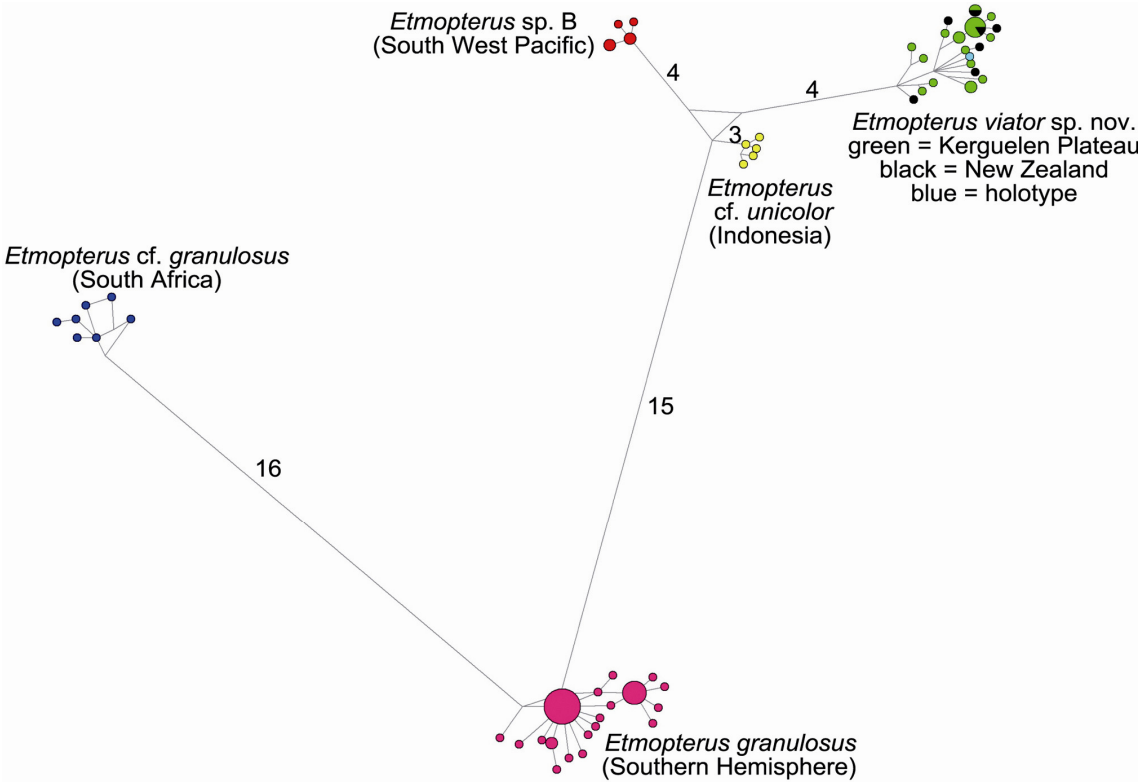

Figure 4: Most parsimonious haplotype network structure attained from COI sequences (mtDNA). Numerals above branches indicate the number of mutated positions. Branches without numbers show 2 or less mutated positions.

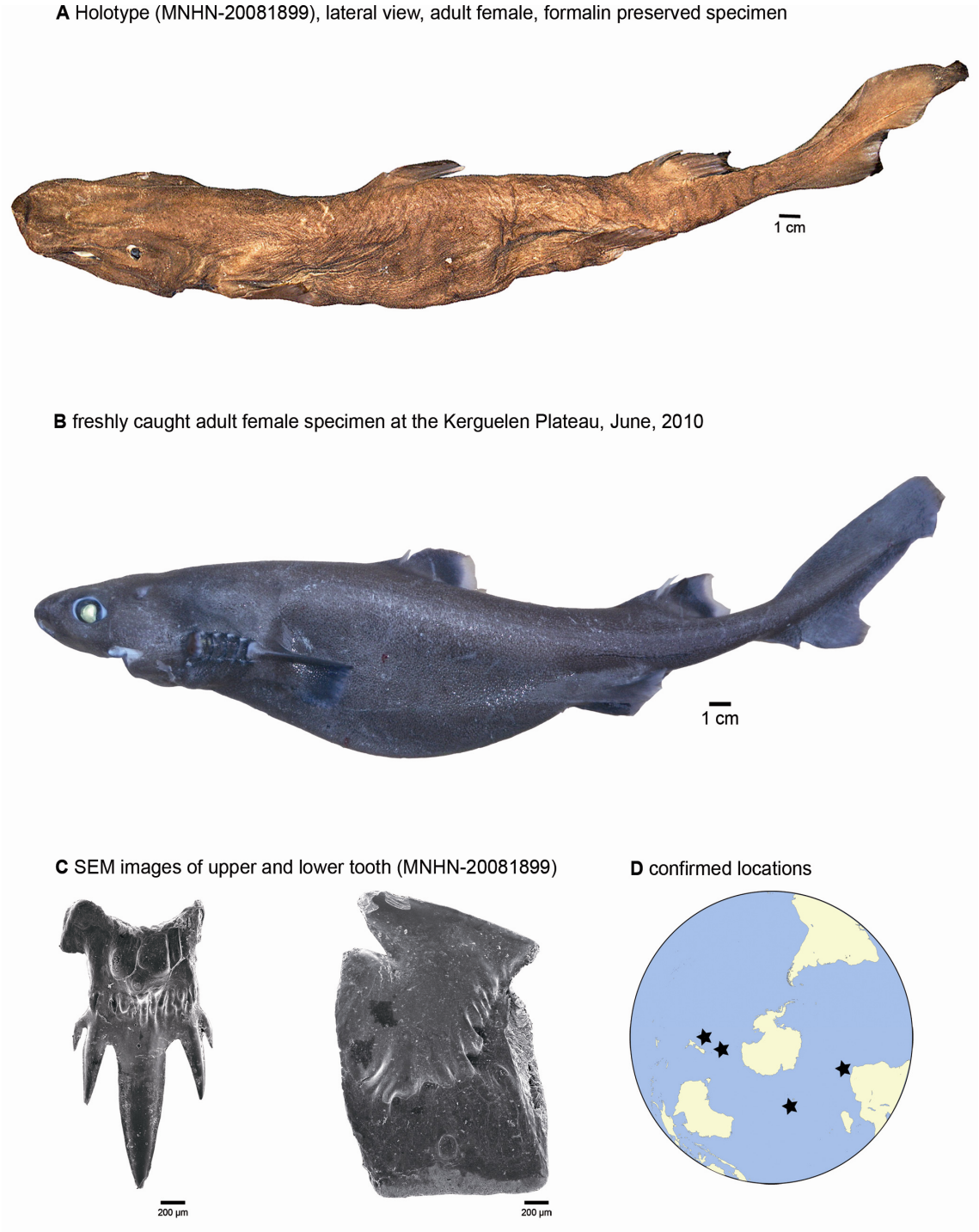

Figure 5: Overview of morphological appearance and distribution of *Etmopterus viator* sp. nov.. A= preserved holotype MNHN-20081899; B= freshly caught *E. viator* sp. nov. (Kerguelen Plateau, 06.2010); C= SEM images of upper and lower teeth extracted from holotype; D= confirmed locations for *E. viator* sp. nov..

Table I: Measurements of *Etmopterus viator* sp. nov. holotype (MNHN 20081899) and ranges of Kerguelian paratypes.

Measurement (mm)	Holotype MNHN 20081899	Range in paratypes (minimum, maximum, mean, and sd)
Total length	524.7	350.0-577.2 (457.0; 106.2)
Pre caudal fin length	415.0	280.0-440.5 (356.9; 77.2)
Pre 1st dorsal fin length	190.0	125.0-250.0 (173.0; 49.4)
Pre 2nd dorsal fin length	332.0	205.0-340.0 (270.4; 61.0)
Head length	108.0	80.74-140.0 (107.3; 25.2)
Pre branchial length	89.2	62.0-110.0 (86.3; 22.7)
Pre spiracle length	64.9	47.7-73.8 (60.3; 11.6)
Pre orbital length	34.8	26.3-43.0 (34.5; 6.6)
Pre narial length	14.9	10.7-20.0 (13.6; 3.6)
Pre oral length	45.1	36.1-59.0 (44.9; 9.2)
Eye length	28.3	17.4-32.7 (24.3; 6.6)
Spiracle length	5.8	3.1-7.0 (5.4; 1.6)
Eye spiracle distance	14.8	8.0-17.2 (12.0; 3.7)
Mouth width	43.3	16.0-45.0 (34.4; 10.23)
Nostril width	12.4	10.9-16.5 (13.2; 2.3)
Snout width	39.9	27.5-51 (39.0; 9.2)
Interorbital distance	30.5	21.8-47.0 (34.2; 9.9)
Head width	55.5	36.5-75.0 (55.2; 15.7)
Head height	36.4	25.6-48.9 (36.9; 9.5)
Pre pectoralis length	120.2	82.0-130.0 (99.6;23.3)
Pre pelvic fin length	317	19.1-317.0 (208.2; 106.4)
Pectoralis pelvic fin distance	153.5	87.0-168 (125.1; 33.1)
Interdorsal distance	99.3	61.0-125.0 (87.6; 28.1)
2nd dorsal fin to caudal fin	46.7	32.0-57.8 (44.9; 11.0)
Pelvic fin to caudal fin	83.4	53.0-93.9 (76.5; 16.2)
Pectoralis – anterior margin	48.7	33.3-60.0 (45.6; 10.3)
Pectoralis inner margin	21.6	15.5-31.0 (22.7; 6.7)
Pectoralis posterior margin	33.7	21.1-32.0 (26.4;5.3)
Pectoralis base length	28.6	15.0-30.0 (21.5;6.3)
1st dorsal fin length	49.5	36.1-61.4 (48.0;10.5)
1st dorsal fin base length	20.1	10.6-30.0 (20.4;7.7)
1st dorsal inner margin	24.0	15.0-30.3 (19.8;5.4)
1st dorsal fin height	16.5	9.5-25.0 (16.3; 5.8)
2nd dorsal fin height	48.7	37.7-73.0 (54.5; 14.4)
2nd dorsal fin base length	16.0	12.0-24.0 (17.3; 4.6)
Pelvic fin length	57.1	38.5-70.0 (54.6; 15.2)
Pelvic fin anterior margin length	36.5	16.5-46.0 (33.3; 12.4)
Caudal fin dorsal caudal margin	104.3	80.5-127.9 (100.3; 17.7)
Caudal fin pre ventral margin	58.1	42.4-76.1 (57.0; 14.5)
Caudal fin subterminal margin	100.5	66.0-120.5 (91.6;21.2)

Table II: Measurements of comparative material used for morphometric analyses.

Measurement (mm)	*Etmopterus* sp. B *sensu* Last and Stevens, 1994				*Etmopterus* cf. *granulosus* (South Africa)				*Etmopterus granulosus*				*Etmopterus litvinovi*	
													ZMH 24994	ZMH 24993
	min	max	mean	SD	min	max	mean	SD	min	max	mean	SD		
total length	325.3	672.0	476.2	127.5	270.0	665.0	524.1	103.0	212.3	742.0	493.3	128.6	440.4	404.1
pre-caudal fin length	253.0	542.0	375.4	97.9	203.0	515.0	402.9	84.1	160.5	592.0	382.1	103.4	347.5	322.9
pre-first dorsal fin length	112.0	281.5	166.8	50.1	82.1	225.0	179.6	37.6	71.2	270.0	167.7	43.4	155.8	155.8
pre-second-dorsal fin length	201.1	425.0	295.5	84.5	155.0	400.0	311.9	64.7	127.5	492.0	308.3	83.5	266.1	262.2
head length	70.0	143.6	101.9	27.1	64.2	189.5	128.1	29.8	50.7	175.0	114.1	27.0	108.7	101.6
pre-branchial fin length	49.0	109.8	77.5	19.6	53.3	129.3	101.9	21.7	42.9	126.4	94.1	21.3	88.6	87.8
pre-spiracle length	34.1	76.8	55.2	14.1	37.1	86.7	71.9	13.7	29.6	100.0	67.4	15.2	58.7	61.6
pre-orbital length	5.0	37.5	24.2	8.8	18.7	45.9	36.6	7.2	14.1	55.0	32.0	7.9	30.9	29.4
pre-oral length	24.1	59.0	36.9	10.4	27.1	61.3	50.1	8.5	22.6	65.0	48.0	10.7	39.1	39.7
eye length	9.1	31.0	19.3	7.6	17.3	35.1	29.8	4.9	11.1	38.1	28.1	6.2	27.0	26.6
distance from eye to spiracle	3.1	20.4	9.2	6.11	7.4	36.7	18.2	6.3	5.9	30.0	17.2	4.3	16.1	14.4
mouth width	18.3	65.4	38.7	14.4	23.7	72.1	51.1	12.5	19.0	85.0	48.4	15.8	47.4	37.7
snout width	21.0	54.8	35.8	11.3	23.4	55.9	44.5	8.6	20.2	73.0	44.4	9.8	44.1	40.8
interorbital distance	14.1	60.1	29.0	13.2	20.8	49.6	37.7	7.7	15.6	69.0	40.1	10.4	35.6	28.5
head width	27.7	79.0	49.5	16.8	35.2	95.6	67.3	15.3	25.4	102.0	62.3	15.7	57.9	48.0
head height	21.2	65.0	35.2	12.7	22.1	63.6	47.3	11.1	4.0	94.0	42.0	17.2	39.4	31.3
pre-pectoral fin length	68.1	148.5	101.2	26.4	62.8	155.1	126.9	26.5	12.0	173.0	113.1	32.9	113.6	102.4
pre-pelvic fin length	175.1	370.0	256.0	69.9	123.0	354.0	284.8	63.7	26.0	390.0	253.3	88.3	233.0	214.9
pectoral fin to pelvic fin distance	83.1	183.0	129.1	36.4	64.7	200.7	142.3	34.2	46.6	220.0	140.6	40.4	128.8	119.8
interdorsal distance	48.7	149.0	92.9	35.2	51.3	142.9	107.6	24.7	34.7	177.1	111.7	33.2	81.8	88.8
distance from 2nd dorsal fin to caudal fin	25.8	63.8	40.3	12.8	26.3	62.7	46.4	10.2	19.2	73.5	52.2	13.1	43.5	36.4
distance from pelvic fin to caudal fin	45.0	115.1	67.9	21.3	36.6	187.8	88.9	32.8	28.9	137.8	81.6	23.9	74.3	70.6
pectoral fin - anterior margin length	23.9	58.0	38.7	12.7	27.4	64.9	47.9	10.7	13.2	72.2	45.1	13.4	48.9	48.0
first dorsal fin - maximum length	25.0	63.0	41.5	14.7	24.4	63.7	47.3	10.2	16.0	71.0	45.6	14.6	46.3	44.5
first dorsal fin - height	2.1	18.0	9.2	5.4	8.0	22.4	15.6	3.9	8.3	26.0	17.3	4.8	15.3	14.7
second dorsal fin - maximum height	4.6	81.2	50.1	21.0	28.3	76.2	57.9	12.5	7.0	94.2	57.1	19.7	56.2	50.9
second dorsal fin - base length	5.4	27.0	14.7	7.3	10.0	27.5	19.9	4.5	2.0	32.0	20.6	7.1	20.2	19.2
pelvic fin - length	27.1	87.6	50.9	21.3	24.7	81.7	54.9	14.1	7.0	84.1	57.1	18.6	47.7	49.2
caudal fin - dorsal caudal margin	64.7	133.1	97.5	24.1	62.1	138.9	108.5	19.9	52.6	195.4	106.4	26.2	96.6	88.0
caudal fin - pre-ventral margin length	30.8	122.0	52.5	23.1	32.9	72.6	57.6	11.1	28.2	84.2	56.8	12.5	48.9	49.2
caudal fin - subterminal margin length	55.0	128.1	92.1	26.5	55.9	129.7	103.5	19.9	12.0	140.0	95.1	28.8	84.5	72.9

Table III: results from ANOVA: tests of between subject effects. TL/HFDF = ratio of total length and height of first dorsal fin; PFDL/ID = ratio of pre first dorsal fin length and interdorsal distance; HL/ID = ratio of head length and interdorsal distance.

Source	**Dependent variable**	**df**	**F**	**Significancy level**
Species	TL / FDFH	4	4.313	0.003
	PFDL/ ID	4	22.026	0.000
	HL/ID	4	13.889	0.000
Error	TL / FDFH	116	n.a.	n.a.
	PFDL/ ID	116	n.a.	n.a.
	HL/ID	116	n.a.	n.a.

Table IV: results from multiple comparisons of *Etmopterus viator* sp. nov. with congeners. TL/HFDF = ratio of total length and height of first dorsal fin; PFDL/ID = ratio of pre first dorsal fin length and interdorsal distance; HL/ID = ratio of head length and interdorsal distance.

	comparison species	**mean difference TL/HFDF**	**mean difference PFDL/ID**	**mean difference HL/ID**
***Etmopterus viator* sp. nov.**	*Etmopterus* sp. B	0.544*	-0.0422*	-0.1318*
	Etmopterus cf. *granulosus*	-0.0452*	-0.0917*	-0.0838*
	Etmopterus granulosus	-0.0131	-0.1512*	-0.2073*
	Etmopterus litvinovi	-0.0019	-0.0409	-0.0549

*= $p \leq 0.05$

Table V: results from multiple comparisons (Dunnett-test) of *Etmopterus viator* sp. nov. with congeners under the assumption that homogeneity of variance is not given. HL/IOD = ratio of head length and interorbital distance.

	comparison species	**mean difference HL/IOD**
***Etmopterus viator* sp. nov.**	*Etmopterus* sp. B	0.890*
	Etmopterus cf. *granulosus*	-0.674*
	Etmopterus granulosus	-0.0147
	Etmopterus litvinovi	-0.0606

*= $p \leq 0.05$

Article IV

IGLÉSIAS S. P., **STRAUBE N.** & SELLOS D. Y. (in preparation). Species level phylogeny of Chimaeriformes and age estimates of extant Chimaeriform diversity. Intended to be submitted to: *Molecular Phylogenetics & Evolution*.

Title: Species level molecular phylogeny of Chimaeriformes and age estimates of extant Chimaeriform diversity.

Iglésias Samuel P. **(corresponding author)**
Muséum national d'Histoire naturelle; Département Milieux et Peuplements aquatiques, USM 0405, Station de Biologie Marine de Concarneau and UMR 7208 CNRS/MNHN/IRD/UPMC, Biologie des Organismes et Ecosystèmes Aquatiques, 29182 Concarneau cedex,
France
iglesias@mnhn.fr

Straube Nicolas
Zoologische Staatssammlung München
Münchhausenstraße 21
81247 München
Germany
straube@zsm.mwn.de

Sellos Daniel Y.
Muséum national d'Histoire naturelle; Département Milieux et Peuplements aquatiques, USM 0405, Station de Biologie Marine de Concarneau and UMR 7208 CNRS/MNHN/IRD/UPMC, Biologie des Organismes et Ecosystèmes Aquatiques, 29182 Concarneau cedex,
France
sellos@mnhn.fr

Abstract

Extant Chimaeriformes are an evolutionary old group of mostly deep-sea inhabiting cartilaginous fishes (Chondrichthyes) comprising 44 described species in three families. Recent studies analysed the placement of Chimaeriformes in the overall vertebrate phylogeny and recovered major splits within the order based on total mitochondrial genomes. The focus of this study is a detailed phylogenetic analysis on genus and species level using an enhanced taxon sampling. Our dataset comprises sequence information of mitochondrial loci cytochrome oxidase I, 12s rRNA, partial 16s rRNA, $tRNA_{Val}$, and $tRNA_{Phe}$. Maximum Likelihood, Neighbor-joining, and Bayesian phylogenetic analyses recover major nodes as in previous studies. New phylogenetic insights render genera *Hydrolagus* and *Chimaera* paraphyletic, the phylogenetic placement of *Neoharriotta pinnata* is contradicting cladistics based on morphology. Node age reconstruction reveals that the extant diversity originated in the Palaeocene and implies that extant taxa are not relict taxa, which adapted to deep water refugia after the Permian Mass extinction event. Morphological apomorphies described in literature for the different taxonomic levels are largely congruent with molecular studies except for *Neoharriotta*, *Chimaera* and *Hydrolagus*.

Key Words: Chimaeras; mtDNA; molecular phylogenetics; node age estimation; deep-sea;

1 Introduction

Living Holocephali constitute a rather small group of basal marine vertebrates, the Chimaeriformes. Holocephali are phylogenetically classified as Chondrichthyes (cartilaginous fishes), also including sharks and rays (Elasmobranchii). The sister group relationship of Neoselachii (modern sharks and rays) and Chimaeriformes is undisputed and was just recently doubtlessly assessed with molecular phylogenetics based on full mitochondrial genomes (Inoue et al. 2010). The Chondrichthyan subclass Holocephali comprises the extant Chimaeriformes and a number of extinct taxa. Interestingly, the extant diversity of Holocephalans does not reflect the largest diversity in earth's history. Holocephali are already known from the Silurian (Benton & Donaghue 2007, Inoue et al. 2010) and 375 Ma years old fossils already share anatomical characters of extant species (Venkatesh et al. 2007). The largest diversity is noted for the Carboniferous (Helfman et al. 2009). The Permian mass extinction event apparently erased large parts of the Holocephalan diversity and surviving species may have adapted to deep-water refugia (Grogan & Lund 2004). This implies that Chimaeriformes are in fact living fossils with an evolutionary history of estimated 420 Ma representing one of the oldest vertebrate lineages.

Today, Chimaeriformes comprise three families and 44 described species (Eschmeyer & Fricke 2010). The different species mostly inhabit bathyal ocean regions occurring at continental shelves, seamounts, insular slopes, and abyssal plains with a depth penetration down to a maximum of 3000 meters.

Oviparous Chimaeriformes generally feed on benthic crustaceans and mollusks and reach sizes in between 1 and 2 meters total length. They are morphologically characterized by one single gill slit covered by an operculum, sharply contrasting the five to seven open gill slits in Neoselachians, large first dorsal fin spines, and up to six characteristic tooth plates. Male claspers (modified pelvic fins for internal fertilization) display morphological characters partially used for species identification. A further striking characteristic is the male "head clasper", an appendage situated on male specimens' foreheads, which detailed function remains unknown. Female egg case morphology can further provide genus or species-specific information.

The family Callorhynchidae (Elephant Fishes or Plownose Chimaeras) contains three species of the single genus *Callorhinchus*, which are restricted to the Southern Hemisphere. External morphological characteristics are serrated first dorsal

fin spines and, most striking, “hoe-shaped” snouts (Didier 1995; Last & Stevens 2009) (Fig. 1).

Rhinochimaeridae (family Spookfishes, Rabbitfishes or Longnose Chimaeras) are also characterized by the shape of their snout which is broadly elongated (Fig. 1). Spookfishes comprise three genera (*Rhinochimaera*, *Harriotta*, and *Neoharriotta*) and eight species occurring panoceanic in the deep-sea of temperate and tropical waters (Last & Stevens 2009).

The Chimaeridae (Shortnose Chimaeras or Ratfishes) display the largest diversity of Chimaeriforms including species occurring in shallower, coastal waters as e.g. *Hydrolagus colliei*. Chimaeridae lack distinct snout characteristics compared to their sister families. The snout is rounded to feebly pointed (Fig. 1).The family contains two genera only, *Chimaera* and *Hydrolagus*, with an estimated diversity of at least 35 species (Eschmeyer & Fricke 2010). Both genera are characterized by the presence (*Chimaera*) or absence (*Hydrolagus*) of an anal fin, but according to Last & Stevens (2009) this character can differ even within one species and some authors already suggested a taxonomic revision of the family (Kemper et al. 2010b). Species are partially difficult to identify (Last & Stevens 2009) and the number of newly described species from this family has recently increased (Didier 2008; Didier et al. 2008; Kemper et al. 2010a, 2010b; Luchetti et al. in press) due to expanding deep-sea commercial fisheries surfacing rare and unknown species. Chimaeriforms are partially caught as by-catch in commercial deep-sea fisheries, which led to significant catch-rate reduction as e.g. in the North Atlantic *Chimaera monstrosa*, which today is categorized as” near threatened” in the IUCN Red List of Threatened Species (2010).

Performed analyses in this study apply a phylogenetic approach to an mtDNA alignment comprising sequence data of 19 of the extant 44 species covering all families within the order. Since Inoue et al. (2010) greatly analysed the phylogenetic placement of Chimaeriformes in the overall vertebrate phylogeny and estimated major node ages, this study intends to (1) further resolve the phylogeny of extant holocephalans focusing on genus and species level by applying a larger species sampling and to (2) analyse the interspecific taxonomy of the most speciose family Chimaeridae in detail. We additionally (3) target a comparison of cladistics based on morphological data introduced by Didier (1995), and results from molecular phylogenetics in this study to discuss congruence and inconsistencies of morphological and molecular data.

Furthermore, the radiation ages of genera into the extant species diversity is estimated to (4) test the hypothesis, if the extant diversity represents relict species, which survived the Permian mass extinction event. The study also intends to (5) reveal cryptic diversity and unknown species. Today, there is the need for detailed taxonomic work on Chondrichthyes to deliver basal information for accurate management and protection efforts, which are essential in areas suffering from overfishing.

2 Material & Methods

2.1 Taxon sampling

Tissue samples were obtained from French research and commercial fisheries cruises and were extracted from freshly caught specimens. As far as possible, reference specimens were deposited in the ichthyological collection of the Museum of Natural History, Paris, France (MNHN) (Table 1). Further sequences were attained from Genbank to enrich our sampling with hitherto missing taxa. Our sampling includes five genera for the full dataset covering five mtDNA loci, all six genera (inclusion of *Neoharriotta pinnata*) are part of a smaller dataset comprising sequences of COI and partial 16s rRNA only. See Table 1 for a summary of samples used herein. Eleven Neoselachian taxa, roughly covering the Neoselachian diversity, were chosen as outgroups.

2.2 Locus sampling

Total genomic and mitochondrial DNA was extracted from muscle tissue or fin clips preserved in 96% p.a. ethanol. DNA was extracted using the QIAmp tissue kit (Qiagen®, Valencia, CA). We targeted partial fragments of the mitochondrial gene Cytochrome Oxidase I (COI, 655 bp) which is established as potential “barcoding gene” for identifying Chondrichthyan species (e.g. Ward et al., 2005, 2007; Wong et al., 2009), partial $tRNA_{Phe}$, the full 12S rRNA and partial 16S rRNA including the Valine tRNA (2606 bp when aligned). All loci were amplified using PCR following the protocol of Iglésias et al. (2005). The loci chosen for phylogenetic analyses are established for resolving phylogenies on species level in Chondrichthyans (e.g. Iglésias et al. 2005; Straube et al. 2010).

2.3 Phylogenetic Analyses

168 2.3.1 Alignment and phylogenetic signal

169 Sequences were edited using the BioEdit software version 7.0.9 (Hall 1999) and
170 aligned with MUSCLE 3.6 (Edgar 2004). Aliscore v.0.2 was used to check the 12s
171 and 16s fragments for ambiguous alignment positions (Misof and Misof, 2009). Loci
172 were aligned separately and combined afterwards with BioEdit. For analysing
173 homogeneity of base frequencies, a χ^2-test was performed with PAUP* v4b10
174 (Swofford 2003) for each locus. Phylogenetic analyses were conducted on the
175 smallest resulting sequenced fragments homologous to all taxa which match an
176 overall sequence size of 3413 bp per specimen. The first 2759 bp comprises non-
177 protein coding mtDNA fragments (combined partial $tRNA_{Phe}$, the full 12S rRNA and
178 partial 16S rRNA including the Valine tRNA). Remaining 654 bp were attained from
179 protein coding COI. To test COI against pseudogene status, sequences were
180 translated into amino acids. Ambiguous sites in sequences, attributed to double
181 peaks in the electropherogram were coded referring to IUB symbols. Transition and
182 transversion rates among third codon positions of coding gene regions were
183 examined by comparing absolute distances in PAUP* (Swofford 2003).

184 2.3.2 Tree reconstruction

185 A Bayes Factor Test was performed to test our dataset for suitable substitution
186 models and partitions using MRBAYES v3.1.2 (Huelsenbeck & Ronquist 2001) and
187 Tracer v1.5 (http://tree.bio.ed.ac.uk/software/tracer/). Results were applied to
188 Maximum Likelihood (ML) analyses as well as Bayesian phylogenetics (BP). ML
189 analyses were performed using RaxML HPC726 PTHREADS (Stamatakis 2006)
190 implemented in the RaxML GUI package. The “auto FC” command allowed for
191 estimating a suitable number of bootstrap replicates (Pattengale et al., 2009)
192 resulting in an optimal number of 100 bootstrap replicates. Several runs were
193 conducted to avoid local maxima in the space of trees. Analyses were performed for
194 single loci, i.e. COI and combined 12s, 16s, $tRNA_{Val}$, and $tRNA_{Phe}$. Results from both
195 datasets were compared in terms of tree topologies and were subsequently
196 combined. Bayesian phylogenetics were attained with MRBAYES using the same
197 data partitioning and substitution models as in ML analyses, also performing runs for
198 single loci. Runs lasted 10 million generations; trees were sampled every 1000
199 generations. After ensuring that likelihoods of Bayesian analyses reached a stable

plateau, 25% of generations were discarded as burn-in and a 50% majority rule consensus tree was generated. To compare results of previous analyses, we additionally performed Treecon v1.3.b (Van de Peer & Wachter 1994) to attain a tree topology based on neighbour-joining analysis using the Kimura 2 Parameter model. Here, an additional analysis was performed including sequence data of *Neoharriotta pinnata* to gather information on placement in the overall phylogeny. Sequences of *N. pinnata* were downloaded from Genbank (Table 1) and comprise fragments of COI (653 bp) and partial 16S rRNA (559 bp).

2.3.3 Node age reconstruction based on fossil calibration points

For estimating node ages using a relaxed molecular clock approach, Bayesian statistics implemented in BEAST v.1.6.1 (Drummond & Rambaut 2007) were performed. We adopted data partitioning and substitution models from the Bayes Factor Test. For all performed BEAST analyses, the ML tree was used as starting tree and the relaxed molecular clock was calibrated using secondary calibration. The five calibration points were attained from Inoue et al. (2010) and Straube et al. (2010). We aged the splitting of Holocephalans from Elasmobranchs to a minimum age of 410 Ma with an exponential prior distribution covering a time frame of 37 Ma. Further, we calibrated the split of sharks and rays to a minimum age of 251 Ma allowing variation of node age to a maximum of 318 Ma. The third calibration was applied to the splitting of Callorhynchidae from the rest of Chimaeriformes. The node age was dated to a minimum of 161 Ma with a maximum age of 190 Ma. The divergence of Rhinochimaeridae from Chimaeridae was used as fourth calibration point with a minimum of 98 Ma and a maximum of 146 Ma. The fifth calibration point was placed within the outgroup taxa, i.e. the split of *Trigonognathus* from *Etmopterus* was dated to a minimum age of 35.7 Ma and a maximum age of 46.0 Ma. All calibration points use exponential prior settings with a zero offset adopting minimum ages of calibration points. For a summary of calibration points see Table 2.

3. Results

3.1 Sequence characteristics

The χ^2-test revealed equally distributed base frequencies for all loci (df = 135, all p > 0.8). The COI gene shows 377 constant characters, 20 variable characters are parsimony non-informative and 258 are parsimony informative. Translation of coding

COI into amino acids showed no stop codons or improbable frame shifts. Inspection of transition and transversion rates showed no saturation for third codon positions of COI.

The 12s 16s fragment displays 1581 constant characters. Of variable characters, 215 are parsimony non-informative and 962 are parsimony informative. Aliscore detected no ambiguous loci in the alignment of non-coding loci.

3.2 Tree reconstruction

Performed phylogenetic analyses resulted in widely congruent tree topologies. Figure 1 displays an overview of attained results and Table 3 summarizes node support for the different analysing approaches for each node shown in Figure 1. Major splits are summarized as follows: monophyletic Chimaeriformes split in two major clades. The monogeneric family Callorhynchidae (*C. capensis*, *C. callorynchus*, and *C. milii*) opposes all remaining Chimaeriforms (node 1, Figure 1). The next major splitting occurs between the two genera *Rhinochimaera* and *Harriotta*, representing the family Rhinochimaeridae, from *Hydrolagus* and *Chimaera* (Chimaeridae) (node 5, Figure 1). *Hydrolagus* and *Chimaera* appear paraphyletic since both genera mix. First, three species of *Hydrolagus* (*H. mitsukurii*, *H. mirabilis*, and *H. lemures*) sister to two specimens of *Ch. phantasma* split from the remaining *Hydrolagus* and *Chimaera* species (node 8, Figure 1). Subsequently, North East Atlantic *Ch. monstrosa* constitutes a monophyletic, well-supported clade opposite to remaining *Hydrolagus* and *Chimaera* species (node 9, Figure 1). Ensuing, the next clade comprises three *Hydrolagus* species only, i.e. *H. purpurescens*, *H. affinis*, and *H. pallidus* (node 11, Figure 1). *H. purpurescens* and *H. pallidus* oppose *H. affinis* specimens within two sub clades (node 15, Figure 1). Opposite to this pure *Hydrolagus* clade, a clade comprising four species of *Chimaera* is identified (*Ch. fulva*, *Chimaera* sp. 1, *Chimaera* sp. 2, and *Ch. opalescens*), as well as the single *Hydrolagus* sp. (node 21, Figure 1).

The performed neighbour-joining analysis using a smaller dataset including sequence data of *Neoharriotta pinnata* displays congruence with the phylogenies estimated from the full dataset. *N. pinnata* creates an additional split in between the splitting of *Callorhynchidae* from remaining Chimaeriforms, i.e. *N. pinnata* is sister to all Chimaeriforms except *Callorhinchus* (Fig. 2). Bootstrap support for this node is very low, which may be caused by the shorter fragments yielding a weaker

phylogenetic signal. A subsequent ML analysis resulted in the same position of *N. pinnata*, but displayed an even lower bootstrap support value of 58% only. Due to the unsatisfying node support and ensuing phylogenetic placement of *Neoharriotta*, it was not included in subsequent node age reconstruction.

3.3 Node age estimates

Node age reconstructions performed with BEAST produced age estimates which are analogous to age estimates described in Inoue et al. 2010. The splitting of Chimaeriformes from Neoselachii (node 1, Table 4, Fig. 3) is estimated to ca. 430 (426.76 – 438.61) Ma calibrated with node ages adopted from Inoue et al. (2010). The splitting of *Raja* from remaining Elasmobranchs (node 2, Table 4, Fig. 3) is aged to 284 (279.01 – 296.46) Ma. *Callorhinchus* separates from all remaining Chimaeriforms estimated 177 (173.84 – 182.81) Ma ago (node 3, Table 4, Fig. 3). Node 4 (Table 4, Fig. 3) represents the split of genera *Harriotta* and *Rhinochimaera* from *Chimaera* and *Hydrolagus* and must have occurred some 123 (119.13 – 131.37) Ma ago. *Harriotta* separates from *Rhinochimaera* rather recently, i.e. 34 (20.4 – 50.48) Ma ago (node 5, Table 4, Fig. 3). *R. atlantica* and *R. pacifica* split approximately 16 (7.43 – 25) Ma before present (node 6, Table 4, Fig. 3). Within the mere *Chimaera*/ *Hydrolagus* clade, which is estimated to 70 (50.96 – 88.8) Ma (node 7, Table 4, Fig. 3), the age of the sub clade, containing *C. phantasma*, *H. lemures*, *H. mitsukurii*, and *H. mirabilis*, is dated to 63 (44.7 – 81.87) Ma (node 8, Table 4, Fig. 3). This sub clade radiates into different extant species in between five to 36 Ma (nodes 9, 10, and 11, Table 4, Fig. 3). North Atlantic *Ch. monstrosa* separates from remaining *Chimaera* and *Hydrolagus* species 46 (32.57 – 59.84) Ma ago (node 12, Table 4, Fig. 3), a sub clade comprising specimens of *H. pallidus* and *H. affinis* with Indian Ocean *H. purpurescens* in between, splits from remaining species 38 (27.12 – 49.83) Ma ago (node 13, Table 4, Fig. 3) and further radiates rather recently, estimated to 6 (3.6 – 9.47) Ma (node 14, Table 4, Fig. 3). Node 15 (Table 4, Fig. 3) marks the split of Indian Ocean *Chimaera* sp. 1 specimens from three remaining species and is estimated to have occurred 33 (23.25 – 43.03) Ma ago. Nodes 16, 17, and 18 (Table 4, Fig. 3) show a ladderized separation of *Ch. fulva* (29 (20.15 – 38.62) Ma) from *Chimaera* sp. 2, further split of *Hydrolagus* sp. from *Chimaera* sp. 2 (18 (11.65 – 25.28) Ma), and finally *Ch. opalescens* from *H*. sp. (12 (6.82 – 18) Ma).

297 Interestingly, the apparently phylogenetic old lineage of *Callorhinchus* radiates into its
298 extant diversity some recent 4 to 12 Ma ago (nodes 19 & 20, Table 4, Fig. 3).
299 The split of Squaliform sharks included in this analysis is estimated to have
300 occurred 162 (119.84 – 208.05) Ma (node 21, Table 4, Fig. 3) with a subsequent
301 splitting of *Squalus* from Etmopteridae at 94 (67.38 – 122.42) Ma (node 22, Table 4,
302 Fig. 3). The calibrated split of *Trigonognathus* from remaining Etmopterids is dated to
303 42 (45.16 – 51.26) Ma (node 23, Table 4, Fig. 3), with a subsequent radiation of
304 Etmopterids some 37 (31.62 – 42.52) Ma ago (node 24, Table 4, Fig. 3). *Odontaspis*
305 *ferox* separates from *Apristurus longicephalus* ca. 132 (88.68 – 184.15) Ma ago
306 (node 25, Table 4, Fig. 3).

307 ## 4 Discussion

308 ### 4.1 Phylogeny of Chimaeriformes

309 Inoue et al. (2010) mainly analysed the phylogenetic placement of
310 Chimaeriformes in the vertebrate phylogeny and identified major splits within the
311 Chimaeriform phylogeny. Therefore, Inoue et al. (2010) included several vertebrate
312 outgroups in their analyses. Here, we relinquish on such outgroups (except
313 Elasmobranch outgroups to refine the tree correctly and make use of according
314 calibration points) but focus on the radiation events of the different genera and
315 species. The estimated phylogeny in this study widely recovers major clades as
316 described in Inoue et al. (2010) although our analyses are based on a much smaller
317 dataset. Chimaeriformes constitute a monophylum sister to Elasmobranchii (sharks
318 and rays). The monogeneric family Callorhynchidae splits from remaining
319 Chimaeriforms and is therefore confirmed as the most basal family. The radiation of
320 the genus *Callorhinchus* in its extant diversity appears rather recent. Monophyletic
321 Rhinochimaeridae (genera *Harriotta* and *Rhinochimaera*) separate from
322 Chimaeridae, including paraphyletic genera *Hydrolagus* and *Chimaera* (Fig. 1). *H.*
323 *raleighana* from the South West Pacific appears as basal sister to the North Atlantic
324 and North Pacific Rhinochimaeridae and may hint to a Southern Hemisphere origin of
325 Rhinochimaeridae.
326 Our attempt to analyse the placement of *Neoharriotta* in the Chimaeriform
327 phylogeny needs to be treated with caution, since the bootstrap support and posterior
328 probabilities of nodes are weak (Fig. 2). It remains speculative, if *Neoharriotta* indeed
329 forms a distinct clade in between Callorhynchidae and Rhinochimaeridae. Didier

(1995) discusses the problematic relationships of *Harriotta* and *Neoharriotta*, which apparently do not share any synapomorphies. In our tree, *Harriotta* and *Rhinochimaera* are united in a clade. The debatable phylogenetic position of *Neoharriotta* has to be re-analysed using more specimens and additional sequence information, which should also include a number of nuclear loci. This can provide reliable estimates of its phylogenetic placement and will be analysed in the future, but for now, its position is estimated to be a sister lineage of a clade including Rhinochimaeridae and Chimaeridae, but a phylogenetic placement within Rhinochimaeridae is not unlikely, especially with regard to morphological characters shared with *Harriotta* (Didier 1995).

Generally, the resolution of clades comprising *Hydrolagus* and *Chimaera* species is unsatisfying. The first clade containing *H. mirabilis*, *H. mitsukurii*, two specimens of *Ch. phantasma*, and *H. lemures* (Fig. 1) is well supported but the radiation of the clade into different species is not. This clade already renders *Hydrolagus* and *Chimaera* paraphyletic. The largest sub clade is sister to the clade comprising *H. mirabilis*, *H. mitsukurii*, *Ch. phantasma*, and *H. lemures*. It contains all remaining *Hydrolagus* and *Chimaera* species. The first split separates North Atlantic *Ch. monstrosa* from remaining clades with high bootstrap support. *Ch. monstrosa* seems a well-defined and distinct species. The sister clade of *Ch. monstrosa* is segmented into two sister clades, one containing three species of *Hydrolagus* only (*H. purpurescens*, *H. pallidus*, and *H. affinis*, Fig. 1). Interestingly, North East Atlantic *H. pallidus* splits into two further, well-supported sub clades indicating unknown cryptic diversity. The sister clade to the mere *Hydrolagus* sub clade contains mainly *Chimaera* species with the exception of one *Hydrolagus* sp., which identity needs to be verified, but highlights the problem with identification of *Hydrolagus* and *Chimaera* species.

As described above for Rhinochimaeridae, Southern Hemisphere species are strikingly often basal to Northern Hemisphere species, i.e. *H. purpurescens* is basal sister to *H. affinis*, *Chimaera* sp. 1 (Indian Ocean), *Ch. fulva*, and *Chimaera* sp. 2 are sister to North West Pacific *Hydrolagus* sp. and North East Atlantic *Ch. opalescens*. This may imply a Southern Hemisphere origin of living taxa.

Further samples and an applied barcoding approach may be suitable to identify first population structures and support endemism of some species. *Chimaera* sp. 1 & 2 sampled in the Indian Ocean apparently represent still undescribed species and will

be described elsewhere. Unknown cryptic diversity is not astonishing since most species of the family were just recently described due to increasing commercial deep-sea fisheries in recent years (e.g. Didier 2008; Didier et al. 2008; Kemper et al. 2010a, 2010b; Luchetti et al. in press).

We additionally plotted morphological (anatomical) characters provided by Didier (1995) on our molecular tree to provide information on the congruence or inconsistency of morphological and molecular data. Didier (1995) altogether described 55 synapomorphies characterizing the different taxonomic levels in Chimaeroids. Just by simply plotting Didier's (1995) characters onto our molecular tree (Fig. 1), we are able to provide information on characters, which are or are not supported by our molecular analyses. Since the monophyly of Chimaeriformes is strongly supported in our analyses and also evidenced by Inoue et al. 2010, we suggest that all 23 morphological synapomorphies described by Didier (1995) for Chimaeriformes are suitable features (Table 5) to characterize the order. The family Callorhynchidae is characterized by nine synapomorphies, again in concordance with our molecular phylogeny (Table 5). Remaining Rhinochimaeridae and Chimaeridae share eight synapomorphies, which are supported by molecular analyses herein, too. The two synapomorphies described by Didier (1995) for Rhinochimaeridae are supported as well, whereas a comment on the apomorphies of the genus *Rhinochimaera* cannot be given due to incomplete taxon sampling of the genus in this study. All five synapomorphies of Chimaeridae are widely congruent with our phylogenetic estimates. Today, genera *Chimaera* and *Hydrolagus* are morphologically separated by the presence (*Chimaera*) or absence of an anal fin (*Hydrolagus*). Taking into account that this character can differ even within one species (Last & Stevens 2009), it is crucial to provide adequate autapomorphies for the two genera or revalidate the genera of Chimaeridae. See Table 5 and Figure 1 for a summary of synapomorphic characters provided by Didier (1995) and Last & Stevens (2009), which are supported by our molecular phylogeny estimated herein.

4.2 Node age reconstruction

Since we applied secondary calibration to the relaxed molecular clock using calibration points adopted from Inoue et al. (2010) and Straube et al. (2010), our node time estimation agrees well with those estimated by Inoue et al. (2010). Our

node age estimates further display additional information on genus and species level due to the higher number of Chimaeriform taxa included in our analyses.

According to results derived from our analyses, Chimaeriformes originated some 430 Ma ago in the Silurian and further radiated at two major events 177 and 123 Ma ago (nodes 3 & 4, Fig.3 and Table 4) into Callorhynchidae, Rhinochimaeridae, and Chimaeridae. A striking character of our estimated chronogram is the early secession of families (nodes 3 & 4, Fig. 3, Table 4) but rather recent radiations of taxa within families (nodes 7 to 20, Fig. 3 Table 4), i.e. a timeline of undetectable cladogenesis of approximately 40 Ma before the different families radiated into genera and species. Interestingly, the radiation into species clades took place in a timeframe of 59 to 18 Ma after the end-Cretaceous mass extinction event 65 Ma ago. Diversification of Chimaeroids into extant species diversity comprises nodes 9 to 18 (Fig. 3, Table 4) basically taking place from the late Paleogene on lasting until the Quaterny with a diversification peak in the Neogene. As described in Straube et al. (2010) for Lantern Sharks (Etmopteridae), a recovery phase in the Paleogene may have induced diversification of different taxa here as well. Nodes 23 and 24 (Fig. 3 and Table 4) mark the splitting of *Trigonognathus* from *Etmopterus* and further radiation within *Etmopterus* and also fall into the timeframe extrapolating radiation events in Chimaeriforms. These results partially align with the radiation of Ziphiidae (beaked whales) which show similar radiation ages (Dalebout et al. 2008) and overlap in ecological niches with Chimaeriforms.

5 Acknowledgements

SN would like to express his sincere thanks to S. Socher, M. Licht, M. Miya, B. Venkatesh, J. Schwarzer, U.K. Schliewen, G. Haszprunar, I. Stöger, M. F. Geiger, and A. Dunz.

6 References

Benton, M. J., Donoghue, P. C. J., 2007. Paleontological Evidence to Date the Tree of Life. Mol. Biol. Evol. 24 (1), 26-53.

Dalebout, M. L., Steel, D, Baker, S., 2008. Phyogeny of the Beaked Whale Genus *Mesoplodon* (Ziphiidae: Cetacea) Revealed by Nuclear Introns: Implications for the Evolution of Male Tusks. Syst. Biol. 57 (6), 857-875.

Didier, D.A., 1995. Phylogenetic Systematics of Extant Chimaeroid Fishes (Holocephali, Chimaeroidei). Am. Mus. Novit. 3119, 1-86.

Didier, D.A., 2008. Two new species of the genus *Hydrolagus* Gill (Holocephali: Chimaeridae) from Australia. In: Last, P.R., White, W.T., Pogonoski, J.J. (eds.). Descriptions of new Australian chondrichthyans. Hobart (Australia): CSIRO Publishing. p. 349–356.

Didier, D.A., Last, P.R., White, W.T., 2008. Three new species of the genus *Chimaera* Linnaeus (Chimaeriformes: Chimaeridae) from Australia. In: Last, P.R., White, W.T., Pogonoski, J.J. (eds). Descriptions of new Australian chondrichthyans. Hobart (Australia): CSIRO Publishing. p. 327–340.

Drummond, A. J., Rambaut, A., 2007. BEAST: Bayesian evolutionary analysis by sampling trees. BMC Evol. Biol. 7, 214.

Edgar, R. C., 2004. MUSCLE : multiple sequence alignment with high accuracy and high throughput. Nucleic Acids Res. 32 (5), 1792-1797.

Eschmeyer, W.N., Fricke, R. (eds.), 2010. Catalog of Fishes electronic version*:* http:// research.calacademy.org/ichthyology/catalog/fishcatsearch.

Grogan D., Lund R., 2004. The origin and relationships of early Chondrichthyes. In: Carrier, J.C., Musick, J.A., Heithanus, M.R. (eds). Biology of sharks and their relatives. London: CRC Press. p. 3–31.

Hall, T.A., 1999. BioEdit: a user-friendly biological sequence alignment editor and analysis program for Windows 95/98/NT. Nucl. Acids. Symp. Ser. 41, 95-98.

Helfman, G. S., Collette, B. B., Facey, D. E., Bowen, B. W., 2009. The diversity of fishes, 2nd ed. Oxford: Wiley-Blackwell.

Huelsenbeck, J. P., Ronquist, F., 2001. MRBAYES: Bayesian Inference of phylogenetic trees. Bioinformatics 17, 754 – 755.

Iglésias, S. P., Lecointre, G. & Sellos, D. Y., 2005. Extensive paraphylies within sharks of the order Carcharhiniformes inferred from nuclear and mitochondrial genes. Mol. Phylogenet. Evol. 34, 569-583.

Inoue, J. G., *et al*. (2010). Evolutionary Origin and Phylogeny of the Modern Holocephalans (Chondrichthyes: Chimaeriformes): A Mitogenomic Perspective. Mol. Biol. Evol. 27 (11), 2576-2586.

IUCN 2010. IUCN Red List of Threatened Species. Ver. 2010.1. http://www.iucnredlist.org.

Kemper, J.M., Ebert, D., Didier D.A., Compagno L.J.V., 2010a. Description of a new species of chimaerid, *Chimaera bahamaensis* from the Bahamas (Holocephali: Chimaeridae). Bulletin of Marine Science 86 (3), 649-659.

Kemper, J.M., Ebert, D., Compagno L.J.V., Didier D.A., 2010b. *Chimaera notafricana* sp. nov. (Chondrichthyes: Chimaeriformes: Chimaeridae), a new species of *Chimaera* from Southern Africa. Zootaxa 2532, 55-63.

466 Last, P. R., Stevens, J. D., 2009. Sharks and Rays of Australia. Harvard University
467 Press, Cambridge, 2nd edition, p. 1-554.

468 Luchetti, E. A., Iglésias, S. P. & Sellos, D. Y. (in press). *Chimaera opalescens* n. sp.,
469 a new chimaeroid (Chondrichthyes: Holocephali) from the Northeastern Atlantic. J.
470 Fish Biol.

471 Stamatakis, A., 2006. RAxML–VI-HPC: Maximum Likelihood-based phylogenetic
472 analyses with thousands of taxa and mixed models. Bioinformatics 22 (21), 2688-
473 2690.

474 Straube, N., Iglésias, S. P., Sellos, D. Y., Kriwet, J., Schliewen, U. K., 2010.
475 Molecular Phylogeny and Node Time Estimation of Bioluminescent Lantern Sharks
476 (Elasmobranchii: Etmopteridae). Mol. Phylogenet. Evol. 56, 905-917.

477 Tracer, v1.4. [http://beast.bio.ed.ac.uk/tracer]

478 Van de Peer, Y. & De Wachter, R., 1994. TREECON for Windows: a software
479 package for the construction and drawing of evolutionary trees for the Microsoft
480 Windows environment. Comput. Appl. Biosci. 10, 569-570.

481 Venkatesh B., Kirkness, E. F., Loh, Y. H., Halpern, A. L., Lee, A. P., et al. 2007.
482 Survey sequencing and comparative analysis of the elephant shark (*Callorhinchus*
483 *milii*) genome. PLoS Biology 5 (4): e 101. doi: 10.1371/journal.pbio.0050101.

484 Ward, R. D., Zemlak, T. S., Innes, B. H., Last, P. R., Hebert, D. N., 2005. DNA
485 barcoding Australia's fish species. Phil. Trans. R. Soc. Lond. B 360, 1847-1857.

486 Ward, R. D., Holmes, B. A., Zemlak, T. S., Smith, P. J., 2007. Part 12- DNA
487 barcoding discriminates spurdogs of the genus *Squalus*. In: Last, P. R., White, W. T.,
488 Pogonoski J. J. (Eds.), Descriptions of new dogfishes of the genus *Squalus*
489 (Squaloidea: Squalidae). CSIRO Marine and Atmosspheric Research Paper No. 14,
490 114-130.

491 Wong E.H.-K., Shivji M., Hanner R., 2009. Identifying sharks with DNA barcodes:
492 assessing the utility of a nucleotide diagnostic approach. Molecular Ecology
493 Resources 9 (Suppl. 1), 243–256. doi: 10.1111/j. 1755-0998.2009.02653.x

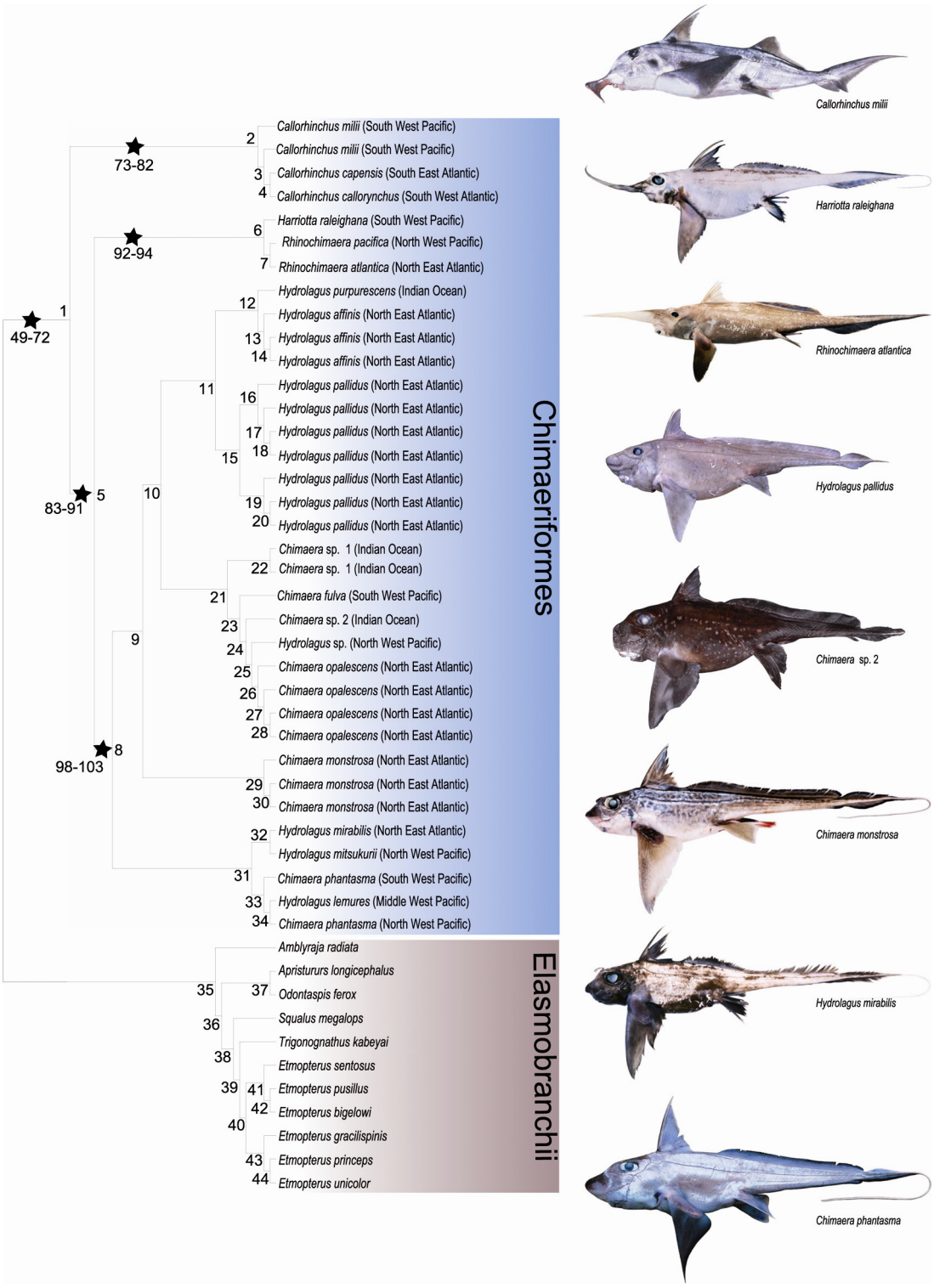

Figure 1: Phylogenetic tree reconstruction of Chimaeriformes based on five mtDNA loci and Maximum Likelihood analysis. Numbers above nodes refer to node numbers given in Table 3, which provides node support values from bootstrapping of Maximum Likelihood and neighbor-joining as well as Bayesian analyses. Stars mark morphological synapomorphies introduced by Didier (1995) and are explained in detail in Support Material 1.

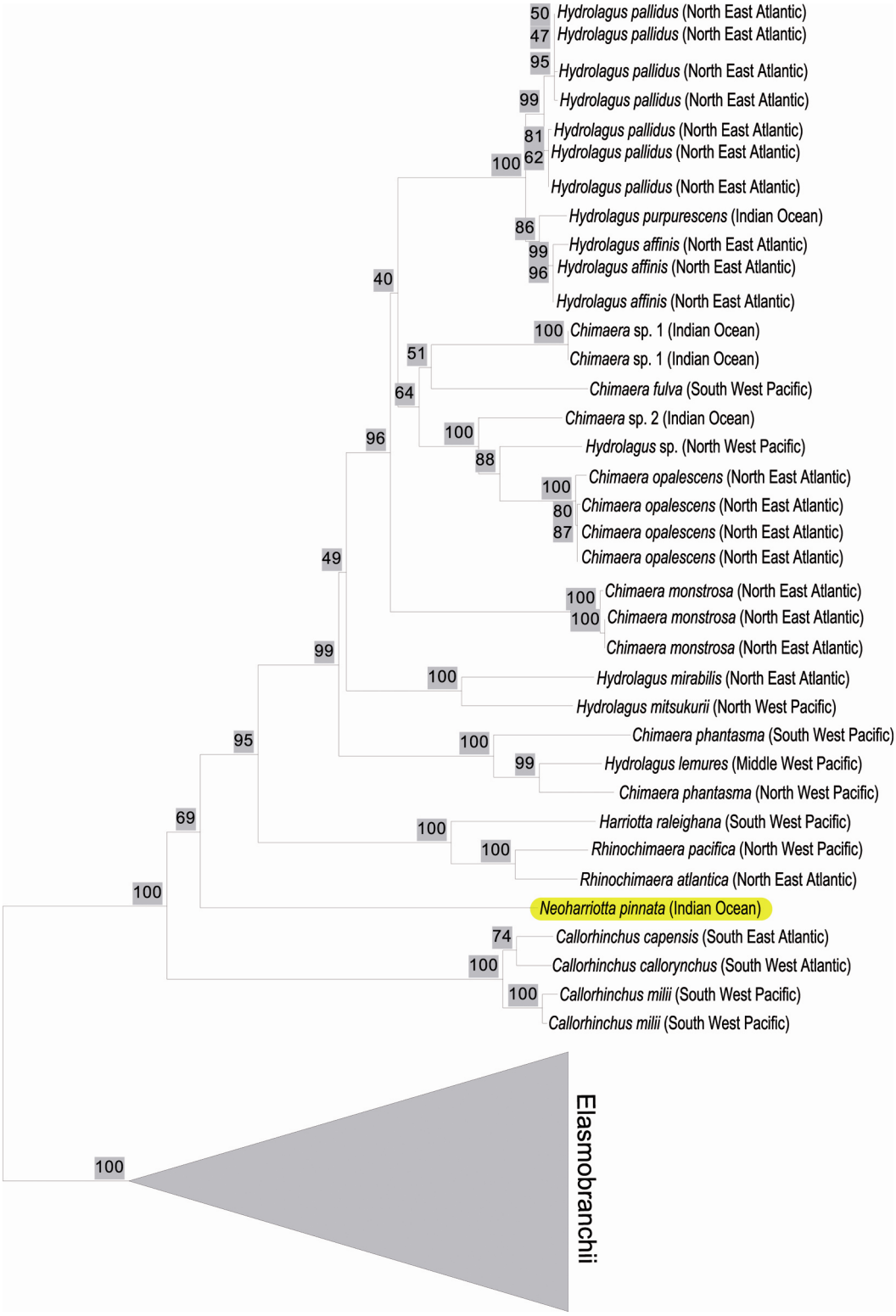

Figure 2: Phylogenetic tree reconstruction of Chimaeriformes including *Neoharriotta pinnata* based on two mtDNA loci (COI and partial 16s) and neighbor-joining analysis. Numbers above nodes indicate bootstrap support values for each node.

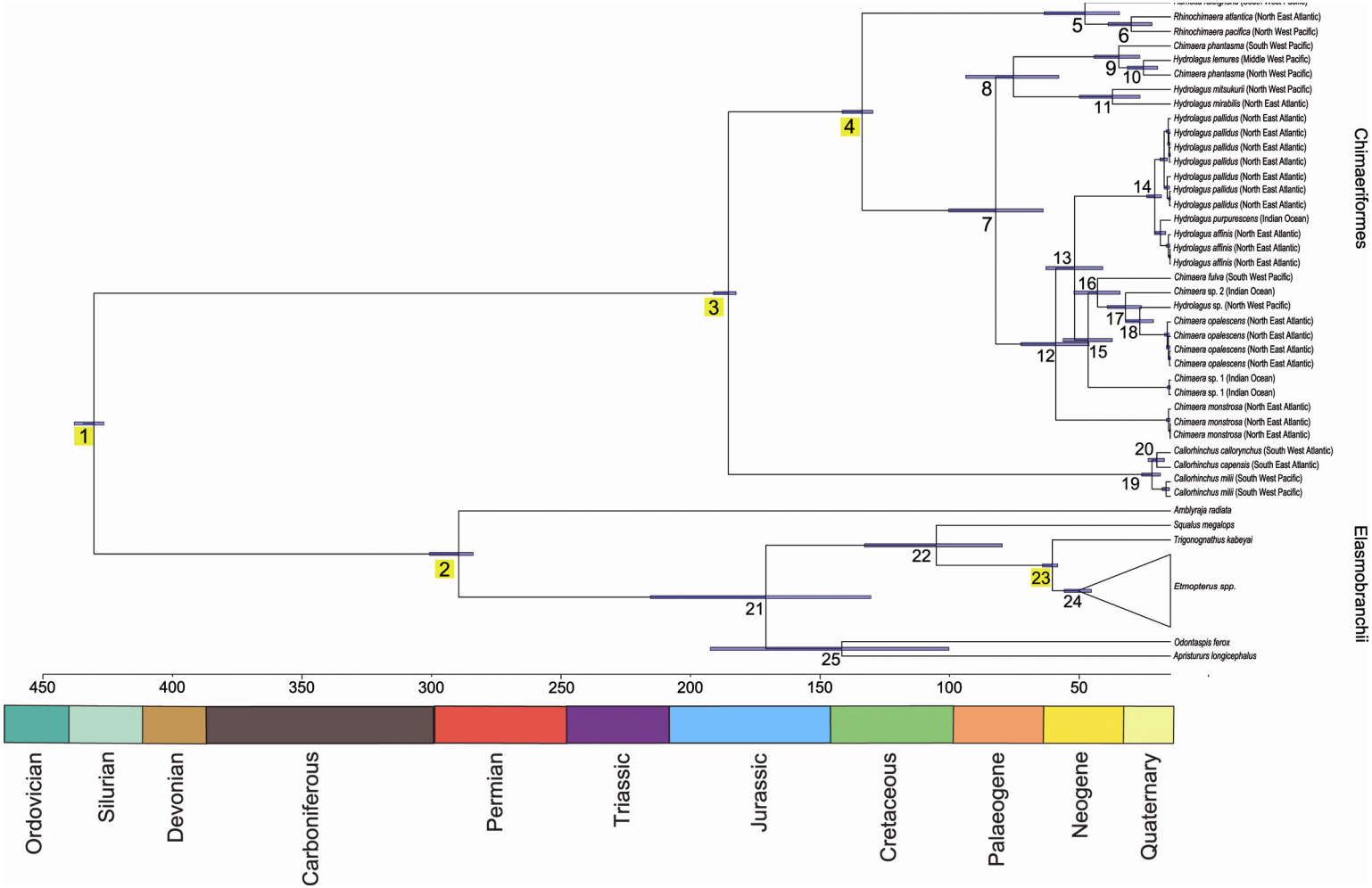

Figure 3: Chronogram of Chimaeriformes attained from Bayesian relaxed molecular clock analyses. Numbers above nodes refer to node age estimates given in Table 4. Yellow marked numbers indicate calibration points.

Table 1: Specimens used in this study.

Class	Order	Family	Genus	Species	Location	Gen Bank Accession Numbers
Neoselachii	Raiiformes	Raiidae	*Raia*	*porosa*	not recorded	AY525783
	Carcharhiniformes	Lamnidae	*Odontaspis*	*ferox*	North Atlantic	GU130600, GU130673
		Pentanchidae	*Apristurus*	*longicephalus*	South Pacific, New Caledonia	GU130599 GU130672
	Squaliformes	Squalidae	*Squalus*	*megalops*	North Pacific, Japan, off Okinawa	GU130625, GU130698
		Etmopteridae	*Trigonognathus*	*kabeyai*	North Pacific, Ensyu-Nada Sea, Japan	GU130629, GU130702
			Etmopterus	*gracilispinis*	Eastern Atlantic, off Brasil	GU130651, GU130724
				princeps	North Atlantic	GU130654, GU130727
				unicolor	North Pacific, Japan, Suruga Bay	GU130666, GU130739
				pusillus	North Pacific, Japan, Suruga Bay	GU130649, GU130722
				bigelowi	Eastern Atlantic, Golf of Mexico	GU130650, GU130723
				sentosus	Indian Ocean, South Africa/ Mozambique	GU130647, GU130720
Holocephali	Chimaeriformes	Callorhinidae	*Callorhinchus*	*callorhinchus*	South West Atlantic	HM147135
				milii	South West Pacific	HM147137
				milii	South West Pacific, Australia	to do
				capensis	South East Atlantic	HM147136
		Rhinochimaeridae	*Rhinochimaera*	*atlantica*	North West Atlantic	to do
				pacifica	North West Pacific, Japan	HM147141
			Harriotta	*raleighana*	South West Pacific	HM147140
			Neoharriotta	*pinnata*	India	HM239657, HM239670
		Chimaeridae	*Chimaera*	*monstrosa*	North West Atlantic	AJ310140
				monstrosa	North West Atlantic	NC003136, NC003136
				monstrosa	North West Atlantic	EF667482, GU244535
				phantasma	South Pacific, New Caledonia	to do
				phantasma	North Pacific, Taiwan	to do
				opalescens	North West Atlantic	EF667478, GU244531
				opalescens	North West Atlantic	EF667479, GU244532
				opalescens	North West Atlantic	EF667480, GU244533
				opalescens	North West Atlantic	EF667481, GU244534
				fulva	South West Pacific	HM147138
				sp. 2	Indian Ocean	to do
				sp. 1	Indian Ocean	to do
				sp. 1	Indian Ocean	to do
			Hydrolagus	*pallidus*	North West Atlantic	to do
				pallidus	North West Atlantic	to do
				pallidus	North West Atlantic	to do
				pallidus	North West Atlantic	to do
				pallidus	North West Atlantic	to do
				pallidus	North West Atlantic	to do
				pallidus	North West Atlantic	to do
				purpurescens	Indian Ocean	to do
				affinis	North West Atlantic	to do
				affinis	North West Atlantic	to do
				affinis	North West Atlantic	to do
				lemures	Mid-West Pacific	HM147139
				mitsukurii	North Pacific, Taiwan	to do
				mirabilis	North East Atlantic	to do
				sp.	Japan	to do

Table 2: Calibration points used for node age estimation.

Calibration point	Age (Ma)	Stage	Reference
Split Elasmobranchii/ Holocephali	421.0 (410.0-447.0)	Devonian	Inoue et al. 2010
Split rays from sharks	281.0 (251.0-318.0)	Permian	Inoue et al. 2010
Split Callorhinchidae	167.0 (161.0-190.0)	Middle Jurassic	Inoue et al. 2010
Split Rhinochimaeridae	122.0 (98.0-146.0)	Lower Cretaceous	Inoue et al. 2010
Split *Trigonognathus*/ *Etmopterus*	40.7 (35.7-46.0)	Eocene	Straube et al. 2010

Table 3: Node support from three different phylogenetic analyses referring to node numbers in Figure 1.

Node number	Bootstrap node support ML analysis (%)	Bayesian node support	Bootstrap node support NJ analysis (%)
1	100	1.0	100
2	100	1.0	100
3	55	0.9	57
4	63	-	100
5	88	1.0	100
6	100	1.0	100
7	97	1.0	100
8	93	1.0	100
9	100	1.0	100
10	53	0.7	82
11	100	1.0	100
12	94	0.9	90
13	100	1.0	100
14	99	-	95
15	94	1.0	100
16	93	1.0	97
17	71	-	63
18	37	-	37
19	89	0.96	92
20	96	-	98
21	77	0.99	46
22	100	1.0	100
23	56	0.7	65
24	100	1.0	100
25	96	1.00	86
26	100	1.0	100
27	49	1.0	92
28	77	1.0	93
29	100	1.0	100
30	99	1.0	98
31	51	0.74	92
32	95	1.0	100
33	100	1.0	100
34	88	1.0	98
35	100	1.0	100
36	96	1.0	100
37	70	0.99	80
38	100	1.0	100
39	100	1.0	100
40	100	1.0	100
41	99	1.0	100
42	100	1.0	100
43	68	0.87	58
44	68	-	100

Table 4: Mean node ages and confidence intervals attained from node age estimates with the BEAST software package. Bold numbers refer to calibrated node ages.

Node number	Node age (BEAST)	95% HPD (BEAST)
1	430.74	426.76 – 438.61
2	284.81	279.01 – 296.46
3	176.9	173.84 – 182.81
4	123.38	119.13 – 131.37
5	34.23	20.4 – 50.48
6	15.67	7.43 – 25.00
7	69.93	50.96 – 88.80
8	62.84	44.70 – 81.87
9	20.67	12.28 – 30.59
10	10.81	5.21 – 17.25
11	23.20	12.13 – 36.49
12	45.92	32.57 – 59.84
13	38.40	27.12 – 49.83
14	6.25	3.60 – 9.47
15	32.94	23.25 – 43.03
16	29.19	20.15 – 38.62
17	18.03	11.65 – 25.28
18	12.26	6.82 – 18.00
19	7.42	4.04 – 11.52
20	5.46	2.47 – 8.97
21	161.92	119.84 – 208.05
22	93.75	67.38 – 122.42
23	42.27	45.16 – 51.26
24	37.07	31.62 – 42.52
25	131.52	88.68 – 184.15

Table 5: Morphological synapomorphies of extant Chimaeriform taxa described by Didier (1995) and congruence with molecular phylogeny estimates of this study.

apomorphy	character number in Didier (1995)	congruence with molecular tree
reduction of trabecular dentine in the lateral walls of the fin spine	49	yes
scapulocoracoids are fused ventrally	50	yes
ventral lobe of the pituitary is isolated external to the cranium	51	yes
all tooth plates are composed of trabecular dentine and have hypermineralized regions (tritors) in large discontinuous patches	52	yes
a descending lamina is present on the aboral surface of the tooth plates	53	yes
morphologically complete hyoid arch that includes a pharyngohyal element present	54	yes
jaw joint is anterior to the eye with jaw muscles originating anterior to the eye	55	yes
fused pharyngo-epibranchial plate associated with 3rd, 4th, & 5th branchial arches	56	yes
the first epibranchial articulates with the hyoid arch	57	yes
presence of a fleshy operculum that is formed by the dorsal and ventral constrictor muscles and supported by an opercular cartilage and hyoid rays	58	yes
levator hyoideus originates from the suborbital shelf anterior to the otic capsule	59	yes
the presence of a hyoid arch muscle that extends anterior to the orbit	60	yes
six pairs of labial cartilages present	61	yes
prepelvic tenacula with independent cartilaginous skeleton present in both sexes	62	yes
presence of a frontal tenaculum	63	yes
fused anterior radials articulate with the propterygium of the pectoral fin	64	yes
the first two or three radials of the pelvic fin are fused with the basipterygium	65	yes
the otic capsules have a membranous median wall	66	yes
spiracle absent in adults due to ontogenetic loss	67	yes
two lateral line canals are present above the mouth	68	yes
the first three basibranchial cartilages are reduced to lumps of fibrocartilage	69	yes
large egg cases with a broad, ribbed lateral web extending around the bulbous central spindle	70	yes
at least thirteen distinct ampullary pore fields are present on the head and snout	71	yes
orbits lie dorsal to the telencephalon and are separated by a membranous interorbital septum	72	yes
calcified rings are not present in the notochordal sheath	73	yes
angular and oral canals branch separately from the infraorbital canal	74	yes
pelvic claspers are in the form of cartilaginous scrolls that lack denticles	75	yes
complex prepelvic tenacula	76	yes
the rostrum is formed into a plow shape	77	yes
Presence of superficialis muscle	78	yes
constrictor operculi dorsalis anterior	79	yes
presence of ligamentum labialis and ligamentum rostralis	80	yes
heterocercal tail	81	yes
anal fin with internal cartilaginous support	82	yes
a long, whiplike tail with supracaudal and subcaudal lobes that are almost equal in size and shape	83	yes
the absence of an anal fin with an independent cartilaginous support at its base	84	yes
loss of the prepelvic tenacula and prepelvic pouches in females	85	yes
prepelvic tenacula in males are simple denticulate blades of cartilage	86	yes
pedicular labial cartilages are absent	87	yes
anterior portion of the hyoid constrictor muscle originates from the retroarticular process	88	yes
tooth plates have hypermineralued tissue in the form of discrete rods	89	yes
the pelvic girdle articulates at the symphysis	90	yes
loss of descending lamina in the vomerine tooth plates and reduced descending lamina in the palatine and mandibular tooth plates	91	yes
presence of an elongate fleshy snout that tapers distally	92	yes
the egg cases have a constricted central spindle	93	yes
pelvic claspers are simple rods with a fleshy denticulate tip	94	Yes
loss of all hypermineralized tissue in the tooth plates	95	n a
tubercles develop on the supracaudal lobe of the tail in males	96	n a
musculus retractor mesioventralis pectoralis is not a separate muscle	97	n a
cranial lateral line canals on the rostrum are enlarged and have expanded dilations	98	yes
the blunt rostrum is supported by reduced rostral cartilages	99	yes
the egg cases are spindle-shaped with a prominent dorsal keel and lacking a lateral web	100	yes
the pelvic claspers are bifid or trifid with a shagreen of denticles	101	yes
a fleshy postanal pad is present in males and females	102	yes
vomerine tooth plates with several rows of parallel ridges exposed on the posterior face of the occlusal surface	103	yes